2014-09-24

N-terminal Regulation of L-type Calcium Channel Expression, Function and Trafficking

Simms, Brett Alan

UNIVERSITY OF CALGARY

N-terminal Regulation of L-type Calcium Channel Expression, Function and Trafficking

by

Brett Alan Simms

A THESIS

SUBMITTED TO THE FACULTY OF GRADUATE STUDIES

IN PARTIAL FULFILMENT OF THE REQUIREMENTS FOR THE

DEGREE OF DOCTOR OF PHILOSOPHY

DEPARTMENT OF NEUROSCIENCE

CALGARY, ALBERTA

SEPTEMBER 2014

Abstract

The L-type voltage-gated calcium channel Cav1.2 is important for excitation-contraction coupling in the heart, as well as CREB mediated transcription and fear conditioned learning. The ubiquitous calcium binding protein calmodulin (CaM) and its associated kinase, calmodulin dependent kinase II (CaMKII), are known to modulate calcium-dependent inactivation (CDI) and calcium dependent facilitation (CDF) of voltage-gated calcium channels (VGCCs), respectively. CDI functions to limit the amount of calcium entering through Cav1.2 channels during prolonged or repetitive membrane depolarizations, whereas a facilitative role for CaMKII can be uncovered by mutating the C-terminal PreIQ-IQ region. Here we identify a CaM interaction site in the Cav1.2 N-terminus downstream of the previously identified W52 locus that is formed by residue C106, and which functionally partakes in global CDI. We also show that the Brugada syndrome mutation A39V disrupts global CDI, but not the surface expression of neuronal Cav1.2 channels as previously described. Over the course of our research we also discovered that mutant CaM molecules alter activation properties of Cav1.2 channels in the absence of calcium and surprisingly, in a manner which can be augmented by the channel N-terminus. Finally we show that a CaMKII binding site in the N-terminus of Cav1.2 is formed by four residues (CISI) and is critical for channel expression and function. Ablation of CISI produces channels which express poorly at the surface of cells, but which also have dramatically increased channel function, which offsets the trafficking defect. Thus our data indicate that surface expression and functional regulation of Cav1.2 channels by CaM and CaMKII is more complex than previously thought, and explicitly involves the channel N-terminal domain.

Acknowledgements

This thesis would not exist if not for the belief, patience and support of Dr. Gerald Zamponi. Though my initial struggles in graduate school and then afterwards when my experiments began to work, I found out how much Gerald wanted success for me. It is one thing for a mentor to mentor, and it is quite another for a mentor to champion. Gerald left nothing to chance and helped me succeed at every opportunity. Thank you Gerald for your dedication to making my PhD the best it could be.

I would also like to thank Dr. Christophe Altier for teaching me many of the hands-on techniques I used to complete my thesis and for a being a very good friend and supporter throughout. Dr. Shalina Ousman you deserve many thanks for agreeing to be on my committee in the first place (remember the transcription stuff all those years ago), and dealing with the multiple changes in focus since then without complaint.

I would like to thank Dr. Ivana Assis Souza who has contributed immeasurably to this thesis with personal, creative and experimental assistance. Ivana has many outstanding qualities but her ability to keep things in perspective, provide solace and friendship, were her immeasurable contributions. Thank you very much Ivana (Bestchi), hopefully we can work together again soon. Ivana directly contributed to Figures: 3-2D-F, 3-5D-F, 3-6, 3-7, 5-2, 5-4, 5-5, 5-6A-C, 5-7, Appendix B 2D-E and Appendix B 3D-E.

Finally, I would like to extend thanks to all other coworkers (especially Lina Chen), colleagues (especially Dr. Corey Flynn), reviewers (especially Dr. Tuck Wah Soong and Dr. Hans Vogel), students and anyone else who I am forgetting to mention that contributed to this thesis. Lina Chen did more calcium phosphate transfections for me then I think she would care to recall and genuinely cared “how the cells were”, which I appreciated very much. Dr. Corey

Flynn gave me the valuable opportunity to teach to undergraduate Neuroscience students for four years, which dramatically improved my presentation, communication and interpersonal skills, not to mention the friendship we developed during that time.

Thank you for reading this thesis and for being a part of my PhD.

Dedication

I would like to dedicate this thesis to Renata, my parents and my immediate family. Renata and I have been through it all, and I respect and love her more than anyone else. My parents have always believed in the value of education and so for them and my immediate family (Wade and Chelsea and their families) this thesis represents what society should strive for: more knowledge, more understanding, more empathy, and more of the things that positively impact our legacy as human beings.

Table of Contents

Abstract ii
Acknowledgements iii
Dedication v
Table of Contents vi
List of Tables xi
List of Figures and Illustrations xii
List of Symbols, Abbreviations and Nomenclature xiii
Epigraph xv

CHAPTER ONE: INTRODUCTION 1

1.1 Calcium regulation in cells 1

1.2 Voltage gated calcium channel structure and function 2

1.2.1 Overview of Cavα1 subunits 2

1.2.2 Auxiliary calcium channel subunits 7

1.2.3 Determinants of Cavα1 voltage-dependent activation 9

1.2.4 Determinants of Cavα1 voltage-dependent inactivation 12

1.2.5 Determinants of Cavα1 calcium-dependent inactivation and facilitation 13

1.3 Voltage gated calcium channel trafficking 18

1.3.1 Cavβ subunit regulation of HVA Cavα1 trafficking 18

1.3.2 Calmodulin/CaM kinase regulation of Cav1.2 trafficking 21

1.4 Cav1.2 pathophysiology and Brugada Syndrome 24

1.4.1 Functional and general pathophysiology of Cav1.2 24

1.4.2 Overview of Brugada Syndrome 25

1.4.3 Brugada Syndrome mutations in Cav1.2 30

1.5 Thesis Rationale and Hypothesis 34

1.5.1 Aim 1: Identify novel N-terminal residues involved in Cav1.2 CDI....34
1.5.2 Aim 2: Decipher the pathophysiological phenotype for A39V-Cav1.2....35
1.5.3 Aim 3: Determine the function of a CaMKII site in the Cav1.2 N-terminus....35
1.5.4 Significance....36
CHAPTER TWO: MATERIALS AND METHODS....35
2.1 Molecular Biology....38
2.1.1 General methods....38
2.1.2 Donated, purchased and engineered calcium channel constructs....38
2.1.3 Cav1.2 GFP constructs....39
2.2 Transient transfection....46
2.3 Electrophysiology....47
2.3.1 General methods....47
2.3.2 Cav1.2 voltage-clamp recording solutions....47
2.3.3 Cav1.2 protocols and current analysis....48
2.4 Epifluorescence & Confocal Microscopy....49
2.4.1 Immunocytochemistry of HA-tagged channels....49
2.4.2 Live cell imaging of GFP/mCherry fusion constructs....50
2.4.3 Colocalization analysis....50
2.5 Protein Biochemistry....51

2.5.1 General methods.....51

2.5.2 Calmodulin sepharose pulldown.....52

2.5.3 Co-immunoprecipitation assays.....52

2.5.4 Cell surface biotynlation assay.....53

2.6. General Data and Statistical Analysis.....53

CHAPTER THREE: A NOVEL CALMODULIN SITE IN THE CAV1.2 N-TERMINUS REGULATES CALCIUM DEPENDENT INACTIVATION.....55

3.1 Background.....55

3.2 Results.....59

3.2.1 Refining a CaM binding site in the N-terminus of Cav1.2.....59

3.2.2 $N_{2B\text{-}II}$ binds α-CaMKII while C106 is a CaM binding residue in the proximal N-terminus of Cav1.2.....67

3.2.3 C106 modulates local Ca^{2+} mediated CDI of Cav1.2 70

3.2.4 C106 as a functional site for Cav1.2 N-lobe CDI.....77

3.3 Discussion.....80

CHAPTER FOUR: THE BRUGADA SYNDROME MUTATION A39V DOES NOT AFFECT TRAFFICKING BUT DOES AUGMENT CAV1.2 CDI AND ACTIVATION GATING BY CAM MUTANTS.....89

4.1 Background.....89

4.2 Results

4.2.1 The Brugada syndrome mutation A39V does not prevent surface expression of neuronal Cav1.2 channels.....93

4.2.2 A39V-Cav1.2 channels show normal voltage-dependent function with either cardiac or neuronal Cavβ subunits.....99

4.2.3 The Brugada syndrome mutant A39V disrupts N-lobe CDI of Cav1.2 channels but not CaM binding to the channel N-terminus.....105
4.2.4 CaM mutants differentially affect the voltage-dependence and kinetics of activation for A39V and WT-Cav1.2 channels.....113
4.3 Discussion.....119
CHAPTER FIVE: THE CAV1.2 N-TERMINUS CONTAINS A CAM KINASE SITE IMPORTANT FOR CHANNEL EXPRESSION AND FUNCTION.....123
5.1 Background.....123
5.2 Results.....124
5.2.1 A proximal CISI sequence in the N-terminus of Cav1.2 forms the α-CaMKII binding site.....124
5.2.2 Cav1.2 channels lacking an N-terminal α-CaMKII binding site have reduced surface expression but not reduced function.....129
5.2.3 Cav1.2 channels lacking an N-terminal α-CaMKII binding site can be facilitated by BayK 8644.....140
5.3 Discussion…….....…144
CHAPTER SIX: GENERAL DISCUSSION AND FUTURE DIRECTIONS.....147
6.1 Calmodulin binding and CDI of VGCCs.....147
6.2 Effects of Brugada syndrome mutations on Cav1.2 trafficking and function.....149
6.3 CaMKII as a regulator of VGCC trafficking.....149
6.4 A model incorporating A39V and Cav1.2 global CDI.....149

6.5 Closing statement.....154

REFERENCES 155

APPENDIX A: PUBLICATIONS OVER THE SPAN OF AND COPYRIGHT PERMISSIONS FOR WORK IN THIS THESIS.....176

APPENDIX B: THE AMINO TERMINUS OF HIGH VOLTAGE ACTIVATED CALCIUM CHANNELS: CAM YOU OR CAN'T YOU?.....178

List of Tables

Table 2-1: cDNA constructed for experimentation.....40

List of Figures and Illustrations

Figure 1-1: Subunit composition and transmembrane topology of voltage gated calcium channel subunits....4

Figure 1-2: Structure of CaM and CaM lobe mutants……...10

Figure 1-3: Schematic representation of possible voltage dependent inactivation (VDI) and calcium dependent inactivation (CDI) mechanisms in HVA channels....14

Figure 1-4: Forward trafficking of Cav1 and Cav2 channel complexes....22

Figure 1-5: Ion channel conductances which contribute to the five phases of the ventricular action potential (VAP)....28

Figure 1-6: The nature and location of BS mutations in VGCC subunits....31

Figure 2-1: All GFP fusion proteins of the Cav1.2 N-terminus....44

Figure 3-1: Relevant GFP fusion proteins of the Cav1.2 N-terminus....57

Figure 3-2: Ca^{2+}/CaM binding site localized to distal N_{2B} region of N-terminus....60

Figure 3-3: Binding of Nterm-GFP to CaM sepharose persists in 5mM BAPTA....62

Figure 3-4: N_1 binds weakly to Ca^{2+}/CaM and N_{2B} region does not bind CaM in 5mM EGTA by co-IP....65

Figure 3-5: C106 residue of N_{2B-I} binds CaM....68

Figure 3-6: N_{2B-II} but not N_{2B-I} colocalizes with and binds α-CaMKII....71

Figure 3-7: PreIQ-IQ-GFP colocalizes in aggregates with α-CaMKII-mCherry....73

Figure 3-8: N-terminal C106 residue plays a critical role in global CDI of Cav1.2....75

Figure 3-9: Both C106 and W52 residues modulate N-lobe CDI of Cav1.2....78

Figure 3-10: C106R-Cav1.2 lacks CDI with CaM34 in 10mM BAPTA....81

Figure 3-11: Working model for N-lobe CDI of Cav1.2....85

Figure 4-1: Sequence variation between human and rat Cav1.2 channels....91

Figure 4-2: Surface trafficking and total expression are the same for A39V-Cav1.2-HA and WT-Cav1.2-HA in the presence of Cavβ2b....95

Figure 4-3: Surface trafficking and total expression are similar for A39V-Cav1.2-HA and WT-Cav1.2-HA in the presence of neuronal Cavβ1b....97

Figure 4-4: The current voltage relation and steady-state inactivation of A39V-Cav1.2 is not significantly different from WT-Cav1.2 in the presence of Cavβ2b....100

Figure 4-5: The current voltage relation and steady-state inactivation of A39V-Cav1.2 is not significantly different from WT-Cav1.2 in the presence of Cavβ1b....103

Figure 4-6: The Brugada syndrome mutation A39V disrupts N-lobe CDI of Cav1.2 channels....106

Figure 4-7: The Brugada syndrome mutation A39V does not affect C-lobe CDI of Cav1.2 channels....109

Figure 4-8: The Brugada mutation A39V does not alter N-terminal binding to CaM.....111
Figure 4-9: CaM lobe mutants differentially shift the voltage dependence of activation for WT and A39V-Cav1.2 channels.....114
Figure 4-10: Calmodulin lobe mutants differentially affect the kinetics of activation for WT and A39V-Cav1.2 channels in the absence of calcium.....116
Figure 5-1: Relevant Cav1.2 N-terminal GFP fusion proteins.....125
Figure 5-2: α-CaMKII binding occurs within the N_{2B} region of the Cav1.2 N-terminus and causes aggregate formation in tsA-201 cells.....127
Figure 5-3: Mutagenesis of $N_{2B\text{-}II}$ identifies four residues (CISI) important for binding α-CaMKII.....130
Figure 5-4: All four residues (CISI) must be mutated to prevent co-IP with α-CaMKII.....132
Figure 5-5: mCherry-α-CaMKII requires CISI sequence for co-localization with $N_{2B\text{-}II}$-GFP in tsA-201 cells.....134
Figure 5-6: Eliminating the CISI sequence from Cav1.2 channels reduces surface expression but not current density.....137
Figure 5-7: Permeabilized tsA-201 cells have similar amounts of WT-Cav1.2 and Cav1.2$_{\text{-AAAA}}$ channels expressed.....138
Figure 5-8: Cav1.2$_{\text{-AAAA}}$ channels can be facilitated by BayK8644 but not voltage.....142
Figure 6-1 A model incorporating A39Vand Cav1.2 global CDI.....152

List of Symbols, Abbreviations and Nomenclature

Symbol	Definition
CaM	Calmodulin
CaMKII	Calmodulin Dependent Kinase II
VGCC	Voltage Gated Calcium Channel
CDI	Calcium Dependent Inactivation
CDF	Calcium Dependent Facilitation
PKC	Protein Kinase C
HVA	High Voltage Activated
LVA	Low Voltage Activated
DHP	Dihydrophyridine±±
NSCaTE	N-terminal Spatial Ca^{2+} Transforming Element
NATE	NSCaTE Associated Transduction Element
NMR	Nuclear Magnetic Resonance
ER	Endoplasmic Reticulum
VDA	Voltage Dependent Activation
Va	Half Activation Potential
VDI	Voltage Dependent Inactivation
CaBP4	Calcium Binding Protein 4
ERAD	Endoplasmic Reticulum Associated Degradation
GPCR	G Protein Coupled Receptor
VAP	Ventricular Action Potential
BS	Brugada Syndrome
SUNDS	Sudden Unexpected Nocturnal Death Syndrome
SIDS	Sudden Infant Death Syndrome
ICD	Implantable Cardioverter Defibrillator
ECG	Electrocardiograph
VF	Ventricular Fibrillation
PVT	Polymorphic Ventricular Tachycardia
V	Membrane Potential
E_{rev}	Reversal Potential
S	Slope
G_{max}	Slope conductance
Vh	Half Inactivation Potential
SCD	Sudden Cardiac Death

Epigraph

My opinion of graduate school: *It is the education you get while you are busy getting an education that matters*.

-Brett Simms

CHAPTER ONE **INTRODUCTION**

1.1 Calcium regulation in cells

The electrical activity of neurons and other excitable cells relies on a number of different types of voltage- and ligand-gated ion channels that are permeable to inorganic ions such as sodium, potassium, chloride and calcium. While the former three ions support a predominantly electrogenic role, calcium ions are different in that they can not only alter membrane potential, but also serve as important signaling entities [1]. Under normal resting conditions, intracellular calcium concentrations lie in the 100 nM range due to calcium buffering molecules and sequestration into intracellular calcium stores [1]. Opening of voltage gated calcium channels results in calcium influx along the electrochemical gradient, thus giving rise to a localized elevation of intracellular calcium into the high micromolar range [2]. This in turn triggers a wide range of calcium-dependent processes that include gene transcription, muscular contraction, neurotransmitter release, hormone secretion, neurite outgrowth, and the activation of calcium dependent enzymes, such as, calmodulin-dependent protein kinase II (CaMKII) and protein kinase C (PKC) [3-7]. On the other hand, prolonged elevation of intracellular calcium levels is cytotoxic [8], and as a result, the activities of voltage-gated and other types of calcium permeable channels are tightly regulated both by intrinsic gating processes, as well as by cell signaling pathways that control channel activity and trafficking to and from the plasma membrane [9]. Dysregulation of these processes and associated alterations in calcium channel activity have been linked to various types of disorders, including epilepsy, migraine, cardiac arrhythmias and chronic pain [10-12]. Therefore, voltage gated calcium channels are important pharmacological targets for these and other conditions [13]. Here, we will provide an overview of voltage gated calcium channels and discuss aspects of their structure, function, and subcellular trafficking.

Throughout the introduction the L-type calcium channel Cav1.2 will be highlighted, since the N-terminus of this channel is the focus of this thesis. Where ever possible we will highlight critical background literature and explain why this information is relevant to our work with Cav1.2. The introduction will close by addressing the pathophysiology of the idiopathic cardiac disease, Brugada Syndrome as it relates to a specific N-terminal mutation in this calcium channel.

1.2 Voltage gated calcium channel structure and function

1.2.1 Overview of Cavα1 subunits

Prior to the advent of molecular cloning techniques, our understanding of voltage gated calcium channels was derived primarily from electrophysiological characterization of voltage gated calcium currents in neurons and heart cells. Based on biophysical characteristics, voltage gated calcium channels were divided into two major families – high voltage activated (HVA) channels that open in response to large membrane depolarizations, and low voltage activated (LVA) channels that are activated by smaller voltage changes [14, 15] near typical neuronal resting membrane potentials. The HVA family can be further subdivided by their pharmacological properties into L-, N-, P-, Q- and R-types [16]. L-type channels display slow voltage-dependent gating characteristics and are sensitive to a number of different dihydropyridine (DHP) antagonists and agonists [17]. N-type type channels are selectively inhibited by ω-conotoxins GVIA and MVIIA that are isolated from the venom of marine fish hunting mollusks *Conus geographus* and *Conus magus*, respectively [18, 19]. P-and Q-type channels are both blocked (albeit with different affinities) by ω-agatoxin IVA – a peptide isolated from American funnel web spider venom [20]. The term "R-type" channel was assigned originally due to the "resistance" of these channels to the aforementioned inhibitors [17], but SNX-482, a peptide

from *Hyristocrates Gigas* Tarantula venom, has since been used to isolate these channels [21, 22]. In addition to their rapid gating kinetics and low voltage threshold for activation, LVA channels (also known as T-type channels) can be distinguished by their sensitivity to nickel, and relative resistance to block by cadmium ions which block all HVA channels in the low micromolar range [23].

A much greater understanding of calcium channel diversity arose from biochemical and molecular analyses [24]. We now know that HVA channels are heteromultimeric protein complexes that are formed through the co-assembly of a pore forming Cavα1 subunit, plus ancillary Cavβ and Cavα2δ subunits, whereas LVA channels appear to lack these ancillary subunits [25]. The Cavα1 subunit is the key determinant of calcium channel subtype. There are three major families of Cavα1 subunits (termed Cav1, Cav2 and Cav3), each of which have several members [25]. The Cav1 channel family encodes three L-type channels (termed Cav1.2, Cav1.3 and Cav1.4) plus a skeletal muscle specific isoform, Cav1.1 [26-29]. I reiterate that the N-terminus of L-type calcium channel Cav1.2 is the focus of this thesis. Cav2 channels include Cav2.1 which, through alternative splicing, gives rise to P- and Q-type channels [30], Cav2.2 which encodes N-type channels [31, 32], and Cav2.3 which corresponds to R-types [33]. There are three types of Cav3 channels (Cav3.1, Cav3.2 and Cav3.3) all of which represent T-type calcium channels [34-36]. All ten Cavα1 subunits share a common transmembrane topology of four major transmembrane domains, each of which contain six membrane spanning helices (termed S1-S6), a positively charged S4 segment that controls voltage-dependent activation [37], and a re-entrant p-loop motif between S5 and S6 that forms the permeation pathway (Figure 1-1).

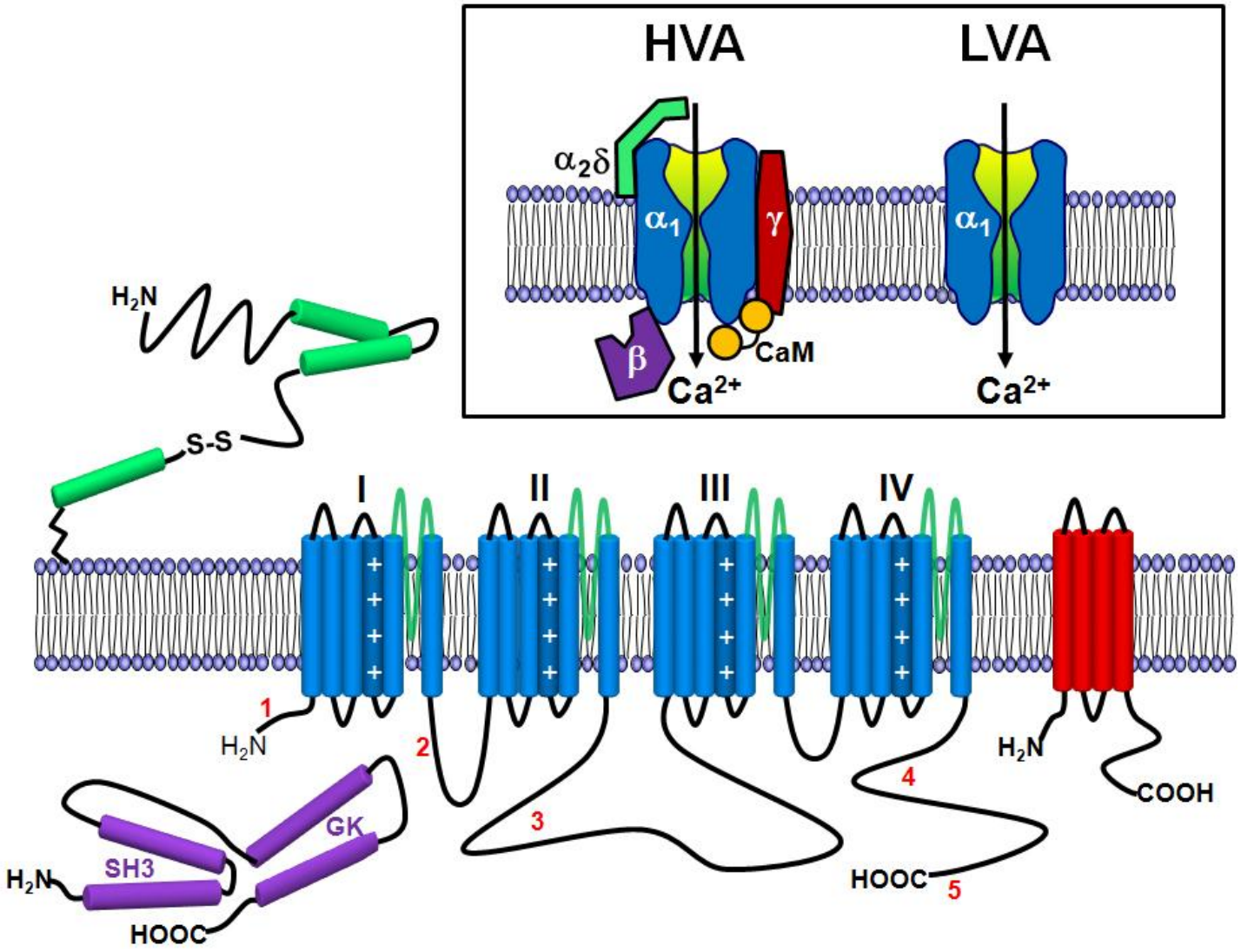
HVA
LVA
α2δ
α1
γ
β
CaM
Ca2+
Ca2+
H2N
S-S
I
II
III
IV
1
H2N
2
3
4
5
H2N
COOH
HOOC
GK
SH3
H2N
HOOC

Figure 1-1

Figure 1-1: **Subunit composition and transmembrane topology of voltage gated calcium channel subunits**. HVA channels are heteromultimers comprised of a pore forming Cavα1 subunit that coassembles with ancillary Cavβ, Cavα2δ and possibly Cavγ subunits, plus calmodulin (CaM), LVA channels on the other hand function as Cavα1 subunit monomers. The Cavα1 subunit (blue) is comprised of four major transmembrane domains (I-IV) that are connected by cytoplasmic linkers. Each of these domains contains 6 membrane spanning helices, plus a re-entrant pore loop (shown in green). The fourth transmembrane segment in each domain contains positively charged amino acids in every third position and forms the voltage sensor. Key protein interaction sites with the Cavα1 subunits are indicated by numbers: 1- N-terminal calmodulin association sites in L-type channels (i.e. NSCaTE & NATE to be discussed later), 2 – Cavβ interaction domain in all HVA channels, 3- synaptic protein interaction site (synprint) present in Cav2 channels, 4- pre-IQ (PCI-1/2) and IQ motifs in Cav1 and Cav2 channels that associate with calmodulin, 5 – scaffolding protein interaction sites in Cav2 channels. The Cavα2δ subunit (green) is attached to the extracellular leaflet of the plasma membrane via a GPI anchor. The Cavβ (purple) subunit contains conserved interacting GK and SH3 domains that are separated by regions that are more variable among different Cavβ subunit isoforms. The Cavγ subunit contain four membrane spanning helices, CaM has been omitted from the bottom depiction for simplicity.

Each of the p-loop regions contain highly conserved negatively charged amino acid residues (in the case of HVA channels, glutamic acids) that cooperate to form a pore that is highly selective for permeant cations such as calcium [38-40], barium and strontium [41], and which interact with non-permeant divalents such as cadmium [42]. Interestingly, despite the conservation of the key glutamate residues, different types of calcium channels display different single channel conductances that vary over one order of magnitude, with Cav1.4 channels showing the smallest conductance [43-45]. By contrast Cav1.2 channels have the largest single channel conductance [44, 46] which becomes particularly relevant in Chapter 5 when we discuss the phenotype of a N-terminal CaMKII mutant. Therefore, the fact that single channel conductance differs among channel subtypes suggests the involvement of other pore lining amino acid residues in ion permeation [47]. The major membrane domains are connected by large cytoplasmic linker regions, and are bracketed by cytoplasmic N- and C-termini [25]. These cytoplasmic regions show the greatest sequence variation among channel subtypes and are important not only for second messenger regulation of channel function, but also contain important sites for protein-protein interactions with regulatory elements, such as G-proteins and protein kinases [48-50]. Each of the known Cavα1 subunits can undergo alternate splicing, which may occur in a tissue and age dependent manner, thus giving rise to additional functional diversity [51, 52].

The majority of structure/function information about voltage gated calcium channels has been deduced from site mutagenesis and generation of chimeric calcium channel subunits. However, several homology models of Cavα1 subunits based on the crystal structures of potassium channels, have been constructed and used to model drug interactions, in particular with L-type channels [53-55]. Cryo-EM structures have revealed crude structural information about this channel subtype [56-59], however, not at a resolution high enough to gain insights into

the structural basis of channel function. Unlike for potassium and bacterial sodium channels, it has not yet been possible to obtain crystal structure information of entire mammalian Cavα1 subunits. HVA and LVA Cavα1 subunits share a common architecture which produces membrane spanning proteins with calcium conducting pore structures.

1.2.2 Auxiliary calcium channel subunits

Voltage gated calcium channel ancillary subunits include Cavβ, Cavα2δ, Cavγ and calmodulin (CaM). There are four known genes that encode Cavβ subunits (Cavβ1-4), again with multiple alternate splice transcripts [60]. Cavβ2b is considered the cardiac isoform and its dysfunction is linked to Brugada Syndrome [61], a congenital arrhythmic disorder discussed in Section 1.5. Cavβ subunits are cytoplasmic proteins that contain conserved GK and SH3 domains and associate with the Cavα1 subunit at the domain I-II linker [62-64] (Figure 1-1). Crystal structures of the Cavβ subunit bound to a fragment of the Cavα1 subunit I-II linker have been solved by multiple groups [63-65]. Functionally, Cavβ subunits alter the gating properties of Cavα1, and perhaps more importantly, increase cell surface trafficking which will discussed in depth later (Section 1.3.1) [60, 66].

There are also four different types of Cavα2δ subunits (Cavα2δ1-4) that are each transcribed and translated as a single protein, post-translationally cleaved and then re-connected by a disulfide bond [67]. It was originally thought that the Cavδ portion spanned the plasma membrane, but more recent evidence indicates that the entire Cavα2δ subunit is attached to the extracellular leaflet of the plasma membrane via a glycophosphatidylinositol (GPI) anchor [68, 69] (Figure 1-1**)**. While there appears to be only a small effect of Cavα2δ on channel function [70], its coexpression typically results in increased channel cell surface density. These changes in

channel cell surface density critically dependent on a metal ion binding site located within a von Willebrand factor domain of the α2 portion of this subunit [71]. In neurons, increased expression of Cavα2δ results in improved synaptic targeting of voltage gated calcium channels and enhanced release probability, which occurs independently of the trafficking effect [72]. Recent evidence indicates that Cavα2δ subunits act as thrombospondin receptors and it is possible that interactions with thrombospondin are involved in the aforementioned modulation of synaptic release [73].

Skeletal muscle L-type channels (Cav1.1) also contain an ancillary Cavγ subunit that is constructed of four transmembrane helices [74, 75]. As many as seven potential Cavγ isoforms have been identified in neuronal tissue, including Cavγ2 which is also known as "*stargazin*" [76, 77]. While certain types of Cavγ subunits can have profound effects on whole cell current density, it is not clear whether they should be considered true neuronal calcium channels subunits [78, 79]. This is because *stargazin* is associated with other cellular functions outside of calcium channels, such as AMPA receptor trafficking [80-82].

There is considerable evidence, however that all HVA channels associate with CaM, suggesting CaM should be considered as the fourth calcium channel subunit [83]. Furthermore, co-crystal structures of calmodulin bound to the C-terminus of Cav1.2 and Cav2.1 have been reported [84-87], as has an NMR structure for the Cav1.2 N-terminus with CaM [88]. CaM modulates gating of various Cavα1 channels in a calcium sensitive manner, which is of particular importance to our work, and will introduced at length in Section 1.2.5. Briefly here, calmodulin (CaM_{WT}) is a ubiquitously expressed, 17 kDa calcium sensing protein capable of many calcium sensitive conformations [89-92]. These conformations are possible because of four EF-hands which bind calcium, two in the N-lobe (low affinity) and two in the C-lobe (high affinity) of

CaM [93, 94] (Figure 1-2). Mutant CaM molecules, on the other hand, were created as an experimental tool in the early 1990's [95, 96] and display a different set of basic conformations [39, 97]. These mutants were created by changing calcium-stabilizing aspartic acid residues in the EF hand of corresponding lobes to alanine. For the N-lobe mutant of CaM (CaM_{12}), EF-hands 1 and 2 were ablated- the C-lobe mutant is therefore CaM_{34} and the double lobe mutant CaM_{1234} [95]. Calmodulin mutants remain the gold standard for evaluating channel inactivation in calcium, however these mutant molecules impart unintended functional effects on Cav1.2 channels (see Section 4.2.4), cautioning the over interpretation of calcium inactivation data.

Given the importance of ancillary subunits for the trafficking and function of HVA channels, it is surprising that Cav3 channels functional perfectly as monomers [23]. Whether T-type channels include specific membrane targeting motifs that are absent in HVA channels, or lack ER retention and proteasomal targeting motifs remains to be determined. With that said, auxiliary subunits remain important for HVA Cavα1 trafficking to the cell membrane and modulation of channel function at the surface.

1.2.3 Determinants of Cavα1 voltage dependent activation

As discussed previously all Cavα1 subunits activate in response to depolarizing voltages because of positively charged arginine residues in their S4 segments (voltage sensors) which lever the channel pore open under depolarizing influence [37]. This process is called voltage dependent activation (VDA) and in fact, reduced voltage sensor movement by mutations such as R1262G in Cav2.1 channels reduces channel conductance in an ataxic mouse [98]. Therefore, how effectively the voltage sensors "sense" depolarization determines what percentage of a population of channels will be open at a given potential.

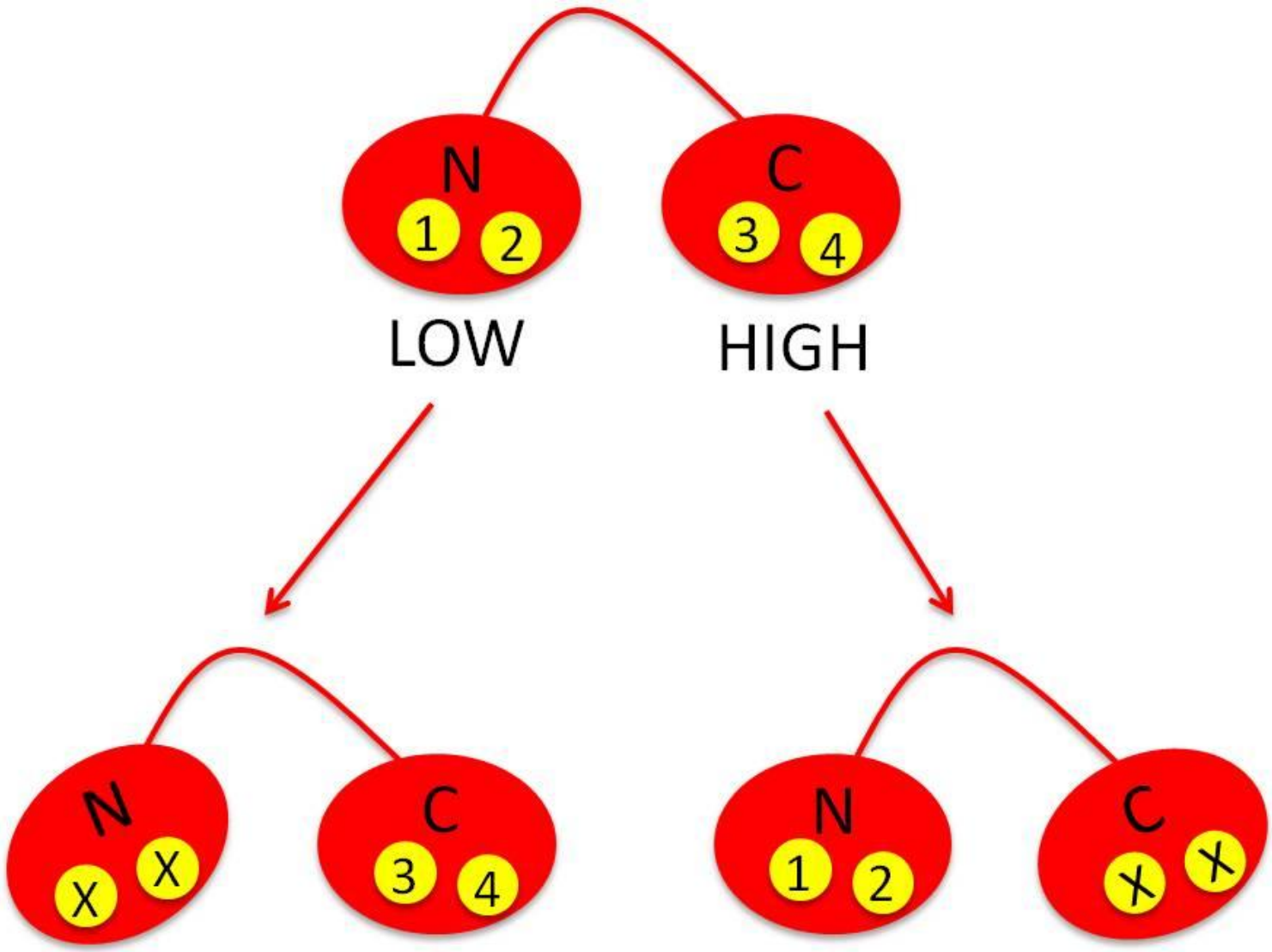

Figure 1-2

Figure 1-2: Structure of Calmodulin and CaM Lobe Mutants. A cartoon depiction of CaM molecules whose structure consists of two calcium sensing lobes (N & C) spaced by a flexible linker. The C-lobe of CaM has a high affinity for calcium (nM), whereas the N-lobe does not (uM). Each lobe of CaM has two EF-hand motifs which are numbered sequentially by lobe (1/2 for N and 3/4 for C) and which stabilize calcium ion binding at aspartic acid residues. Mutating these aspartic acid residues to alanine generates CaM mutants which are unable to bind calmodulin in that particular EF-hand. For example, CaM_{34} on the bottom right of the figure has a functional N-lobe, but the EF-hands in the C-lobe (3/4) no longer bind calcium. Compared to wildtype CaM, mutant CaM molecules demonstrate differential structural configurations because of these EF-hand mutations. This phenomenon is represented above by the tilting of mutant lobes in CaM_{12} and CaM_{34} relative to wildtype CaM.

As a further example of this concept, LVA calcium channels "sense" small depolarizations more effectively than HVA calcium channels and thus a greater percentage of LVA calcium channels will be open at more negative potentials, when compared to their HVA counterparts.

When discussing activation gating characteristics of voltage gated ion channels, two functional properties are important: 1) the voltage at which half of the channel population is open, termed Va, or the voltage-dependence of activation and 2) how quickly channels reach maximal conductance after opening (kinetics of activation). There is good evidence that Cavβ subunits modulate both activation parameters of HVA calcium channels [99-103] while Cavα2δ subunits modulate only kinetics of activation [104].

In Chapter 4 we describe a process whereby CaM mutants regulate the voltage dependence and kinetics of Cav1.2 activation in a manner which depends on the channel N-terminus.

1.2.4 Determinants of Cavα1 voltage dependent inactivation

To prevent calcium overload in response to prolonged membrane depolarization, voltage-calcium channels have developed voltage- and/or calcium-dependent inactivation mechanisms. Voltage dependent inactivation (VDI) is a property that is common to all voltage-gated calcium channels subtypes, although the extent of voltage dependent inactivation varies with calcium channel isoform, and is potently modulated in HVA channels by the Cavβ subunit [105]. Unlike in voltage gated potassium and sodium channels where there is clear evidence of a pore blocking, inactivation gating particle (i.e., "ball and chain" and "hinged-lid" inactivation mechanisms) [106, 107], it has proven somewhat more difficult to identify the mechanistic basis of VDI in HVA calcium channels.

Numerous studies have identified amino acids residues that appear to modulate inactivation, and many of them are found in either the domain I-II linker region, or in the S6 regions of the major transmembrane domains [108-111]. Based on extensive mutagenesis and chimeric work on HVA channels [112-114] our lab proposed a model in which the S6 segments undergo structural rearrangement in response to prolonged membrane depolarization (Figure1-3). This then may expose a docking site for the domain I-II linker to act as a hinged-lid- like gating particle [105]. Further evidence for a hinged-lid type of mechanism was derived from mutagenesis studies on Cav1.3 channels which revealed an additional inhibitory element (termed inactivation shield) that can modulate the docking of the inactivation gate [115]. These findings can be reconciled with our model by a mechanism in which the S6 helices are coupled to the inactivation shield. Ultimately, NMR and/or crystal structure information will be required to gain precise insights into how calcium channels inactivate in response to voltage.

Cav1.2 VDI is not directly studied in this thesis but is used as a reference point for any additional channel closing imposed by calcium dependent inactivation. When studying VDI it is common practice to record currents in barium as opposed to calcium, as the latter ion promotes additional acceleration of inactivation kinetics (see Section 1.2.5).

1.2.5 Determinants of Cavα1 calcium dependent inactivation and facilitation

A much more complete picture has emerged in the area of calcium-dependent inactivation (CDI), although it is by no means less complicated. In Chapter 3 we extend knowledge of a specific type of CDI for Cav1.2 channels, which involves the N-terminus and the N-lobe of CaM. As eluded to above the process of CDI only becomes apparent when comparing channel current kinetics in

the presence of barium (VDI) to that of calcium, with the latter charge carrier imparting pronounced speeding of current decay kinetics [116].

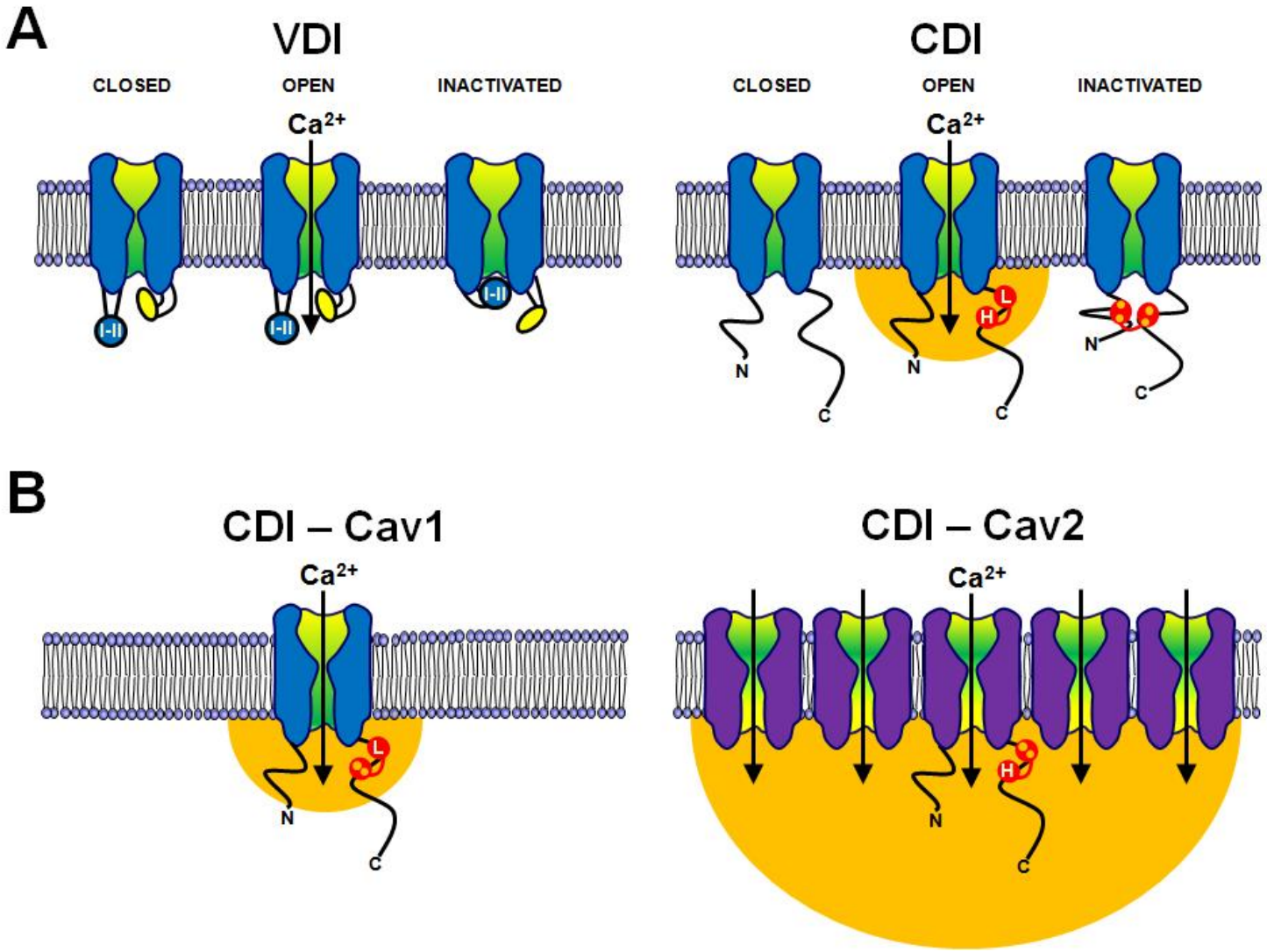
A
VDI
CLOSED
OPEN
INACTIVATED
Ca2+
I-II
CDI
CLOSED
OPEN
INACTIVATED
Ca2+
L
H
N
C
B
CDI – Cav1
Ca2+
CDI – Cav2
Ca2+

Figure 1-3

Figure 1-3: **Schematic representation of possible voltage dependent inactivation (VDI) and calcium dependent inactivation (CDI) mechanisms in HVA channels**. A. Left: Membrane depolarizations trigger a conformational change (leveraging by voltage sensors, not shown) in the channel that results in a transition from the closed to an open (i.e. calcium conducting state). Prolonged membrane depolarization triggers a further change in channel conformation (potentially mediated by the S6 segments in the four membrane domains, not shown). This then repositions a channel structure termed an "inactivation shield" (yellow), thus exposing a docking site for the inactivation gate that is formed by the domain I-II linker (blue ball like structure). The inactivation gate then physically obstructs calcium entry. Right panel: Calcium influx upon membrane depolarization also created a calcium domain near the inner mouth of the pore. Calmodulin (CaM, indicated by dumbbell structure in red with its high (H) affinity and low (L) affinity calcium binding sites) that is preassociated with the C-terminus of the Cav1 channel binds calcium, which in turn causes molecular repositioning of CaM in the C-terminus region and additional interactions with sites in the N-terminus region of the channel when fully loaded with calcium (small orange dots). This leads to an inactivated (non-conducting) conformation of the channel. B. Calcium influx though an individual Cav1 channels creates a calcium nanodomain that is sufficient to activate the high affinity sites on calmodulin, which in turn goes on to cause CDI (this process is EGTA insensitive). In contrast, for Cav2 channels, a concerted opening of multiple channels gives rise to a calcium microdomain that activates the low affinity binding sites of CaM to trigger CDI (this can be blocked by EGTA).

This effect is critically dependent on CaM, and blocked by overexpressing a dominant–negative mutant of CaM (called CaM_{1234}) that lacks the ability to bind calcium in both its N-lobe (CaM_{12}) and C-lobe (CaM_{34}) [117-119]. From a mechanistic standpoint it is believed that calcium-free CaM is pre-associated or anchored to the C-terminus of the channel at several sites including an "IQ" and "pre-IQ" domain [120] (Figure 1-3). Upon a rise in intracellular calcium, channel anchored CaM binds calcium which in turn promotes a conformational change in the C-terminus/CaM complex and gives rise to CDI [121-123] (Figure 1-3). For many years CDI was thought to only occur with L-type channels because no calcium-induced speeding of current decay kinetics was observed with native, or cloned N-, R-, or T-type channels. However, whole cell recordings during this era were typically performed with 10 mM EGTA in the patch pipette which produces significant reduction in intracellular calcium. The fact that CDI persists for L-type channels under these conditions indicates that L-type CDI involves the two high affinity (C-lobe) calcium binding sites on CaM. On the other hand, when intracellular calcium buffering is made less stringent with 0.5 mM EGTA, CDI also becomes apparent for the three members of the Cav2 channel family [124], meaning CDI of Cav2 channels occurs because of the low affinity (N-lobe) calcium binding sites of CaM. In other words, CDI of Cav1.2 and Cav1.3 channels is supported by a local rise in calcium near the inner mouth of the pore, or rather, calcium entry through an individual channel is sufficient to mediate its own CDI [125]. In contrast, CDI of Cav2 channels requires a global rise in intracellular calcium, which is supported by the concerted calcium influx of a population of channels, hence explaining the EGTA sensitivity of this process [123, 125]. Crystal structure information reveals that CaM interacts with the Cav2.1C-terminus in an opposite orientation compared to Cav1.2, and although the

functional importance of this finding is unclear, it could possibly explain why Cav1 and Cav2 channel families exhibit differing CDI mechanisms [85].

There are several additional twists to CDI: first, although Cav1.4 channels can bind calmodulin, they lack CDI [126], the latter because of an autoinhibitory domain in the distal C-terminus that occludes upstream CaM binding sequences [127, 128]. This resistance to inactivation is likely necessary because these channels support tonic glutamate release in photoreceptor synapses [129] and must therefore show sustained activity at depolarized potentials. Second, there is a curious absence of CDI for native Cav1.3 currents in auditory hair cells. This absence appears to be due to calcium-binding protein 4 (CaBP4), a CaM homolog with reduced calcium binding ability which is expressed in these cells and antagonizes the CDI process [130]. Competition between CaBP4 and CaM for the C-terminus of Cav1.2 supports a role for the disruption of CDI by CaBP [131, 132]. Third, recent evidence shows that CDI of Cav1.2 channels requires two different CaM molecules bound to the C-terminus [86]. Fourth, Cav1.3 shows distinct modes of CDI that differentially depend on the high (C-lobe) and low (N-lobe) affinity calcium binding sites of CaM [133]. Cav1 channel CDI that depends on the high affinity C-lobe of CaM appears to require only C-terminal regions of the channel, while low affinity, N-lobe CDI involves interactions of CaM with the N-terminus, as well as the C-terminus [134] (Figure 1-3). In Chapter 3 we show that Cav1.2 has a second N-terminal site (C106) which participates in N-lobe CDI. Our data suggests that the N-terminus of Cav1.2 promotes CDI by propagating the signal for inactivation into domain I of the Cavα1 subunit [135].

Finally, Cav2.1 channels show a second form of calcium regulation (calcium-dependent facilitation, or CDF) that involves the high affinity sites on CaM [136, 137]. Single channel recording demonstrate that unlike CDI of these channels which requires global calcium increase,

calcium entry through an individual Cav2.1 channel is sufficient to promote CDF [138]. Furthermore, this example highlights how Cav2.1 channels can be differentially regulated by two opposing calcium-dependent processes, while using the same calcium sensor, CaM. Interestingly, L-type channels can exhibit CDF but only with substantial C-terminal mutations in the same region which natively promotes CDF of Cav2 channels [118, 139]. Whether CDF and CDI are mediated by distinct binding conformations, or orientations of CaM, or by separate CaM molecules bound at different regions of Cav1 and Cav2 channels, remains to be determined. Nevertheless, CDI and CDF are important processes that limit excessive calcium entry into the cytosol. While VDI is intrinsic to the channel and only depends on voltage, CDI is a tunable process that provides feedback inhibition in response to rising intracellular calcium levels.

1.3 Voltage gated calcium channel trafficking

1.3.1 Cavβ subunit regulation of HVA Cavα1 trafficking

The ability of Cavβ subunits to promote membrane expression of HVA calcium channels is well established. Early experiments revealed that antisense knockdown of β subunits reduced HVA plasma membrane expression in dorsal root ganglion neurons [100], and that whole cell currents carried by various HVA calcium channels in transient expression systems such as *Xenopus* oocytes and tsA-201 cells were dramatically reduced in the absence of co-expressed β subunits, albeit not completely eliminated [140, 141]. This Cavβ subunit dependent increase in plasma membrane expression levels could be in principle due to a number of different mechanisms, including an upregulation of Cavα1 subunit transcription, enhanced export of the channels from the ER, or an increase in channel stability once the channels have reached the plasma membrane. Bichet and colleagues showed that CD8 receptor fusion constructs of the Cav2.1 I-II linker

region were retained in the ER unless coexpressed with a β subunit [142]. Furthermore, deletion of a portion of the channel domain I-II linker resulted in increased ER export in the absence of the Cavβ subunit. Based on these findings, the authors suggested that one of the major roles of the Cavβ subunit is to occlude an ER retention motif on the domain I-II linker of the channel. The ER retention mechanism is also supported by experiments showing that a single point mutation in the region that binds Cavβ can prevent plasma membrane translocation of Cav1.2 and Cav2.2 channels even in the presence of Cavβ subunits [143, 144] and it is therefore unlikely that the Cavβ subunit acts as a transcription factor for Cavα1.

Nevertheless, the molecular details by which Cavβ subunits promote ER export appear to vary with calcium channel subtype. Using an approach similar to that used by Bichet and colleagues, our lab showed that the domain I-II linkers of Cav1.2 and Cav2.2 are not retained in the ER, but that instead the C-terminus region of these two channel subtypes may be responsible for the ER retention [9]. Because the Cavβ subunit does not bind to the C-terminus region of these channels, this suggests that the Cavβ subunit could perhaps indirectly (i.e., sterically or allosterically) mask these retention motifs when Cavβ is bound to the domain I-II linker. Such a mechanism was explored recently in an elegant study by Fang and Colecraft [145] who swapped intracellular regions between L-type and T-type calcium channels to examine structural determinants of L-type channel membrane expression. Based on the expression of these constructs in the absence and the presence of the Cavβ subunit, the authors concluded that the ancillary subunit promotes rearrangements of the major intracellular loops of the channel which ultimately result in the obfuscation of multiple ER retention motifs contained within these linkers. Interestingly, the authors also showed that the domain I-II linker in fact contains an ER-export motif whose function is compromised by Cavβ subunit coexpression. While the net effect

of Cavβ subunit coexpression is an overall enhancement of channel trafficking, this ER export motif may perhaps explain the ability of some Cavβ-free channels to escape the ER. Altogether it appears as if the Cavβ subunit is able to overcome intrinsic ER retention properties of at least three of the major HVA channel subtypes, albeit perhaps by channel subtype specific mechanisms.

What happens to channels that remain associated with the ER? We recently showed that Cav1.2 channels are tonically ubiquitinated, and that the degree of both mono and poly-ubiquitination is increased in the absence of the Cavβ subunit [9]. Furthermore, we were able to show that RFP2, an ER associated ubiquitin ligase, was responsible for this effect. We were then able to demonstrate that in the absence of the Cavβ subunit, an interaction occurs between the channel and p97/Derlin-1, two proteins associated with the ER Associated Protein Degradation (ERAD) system. The end result is channel retrotranslocation and proteasomal degradation in the cytosol (Figure 1-4) [146, 147]. Consistent with this model, treatment of cells with the proteasomal inhibitor MG132 resulted in increased cell surface expression of Cav1.2 channels lacking the Cavβ subunit. The proteasomal inhibitor MG132 has also been reported to enhance trafficking of N-type calcium channels expressed in sympathetic neurons [148].

Altogether, these findings suggest that the Cavβ subunit acts as a switch that diverts channels away from a proteasomal degradation pathway to allow channel export to the plasma membrane via reduced ER retention. In Chapter 4 we describe an updated phenotype for the Brugada syndrome mutant A39V (background discussed in Section 1.4) which in the rat brain isoform of Cav1.2 traffics normally to the cell surface.

1.3.2 Calmodulin/CaM kinase regulation of Cav1.2 trafficking

Although calmodulin is a ubiquitous calcium sensing protein with numerous cellular functions, the fact that it is associated with every type of HVA calcium channel has led to suggestions this protein is a de facto calcium channel subunit. In the context of voltage-gated calcium channels calmodulin and CaM kinase are recognized mainly for contributions to CDI and CDF which was discussed earlier (Section 1.2.5) [124, 149].

Contribution of CaM and CaM kinase to trafficking of HVA calcium channels is controversial. Data from HEK-293 cells suggests CaM has no additive effect to Cavα1.2 surface expression in either the presence, or the absence of Cavβ/Cavα2δ subunits [150]. It has also been shown in tsA-201 cells that deleting the C-terminal IQ domain and a portion of the pre-IQ sequence is sufficient to completely abolish surface expression of Cav1.2 in the presence of β2a [151]. It is interesting to note that this pre-IQ region not only binds CaM, but also CaMKII [139] implicating that at least one of these proteins may be involved in trafficking of Cav1.2 to the cell surface.

As noted above in Section 1.3.1, our laboratory identified the C-terminal domain of Cav1.2 as having multiple ER retention regions [9]. The two retained portions of Cavα1.2 contain the EF-hand motif as well as a downstream IQ domain. Our observation that this downstream region of Cav1.2 spans the CaM binding IQ domain supports literature that suggests this region of the channel has a role in surface expression [151]. In COS1 cells which are believed to be devoid of all VGCC auxiliary subunits, exogenous CaM increased surface expression and recovered activity of Cavα2δ-free, and what were believed to be functionally silent Cav1.2/Cavβ2d channel complexes [152].

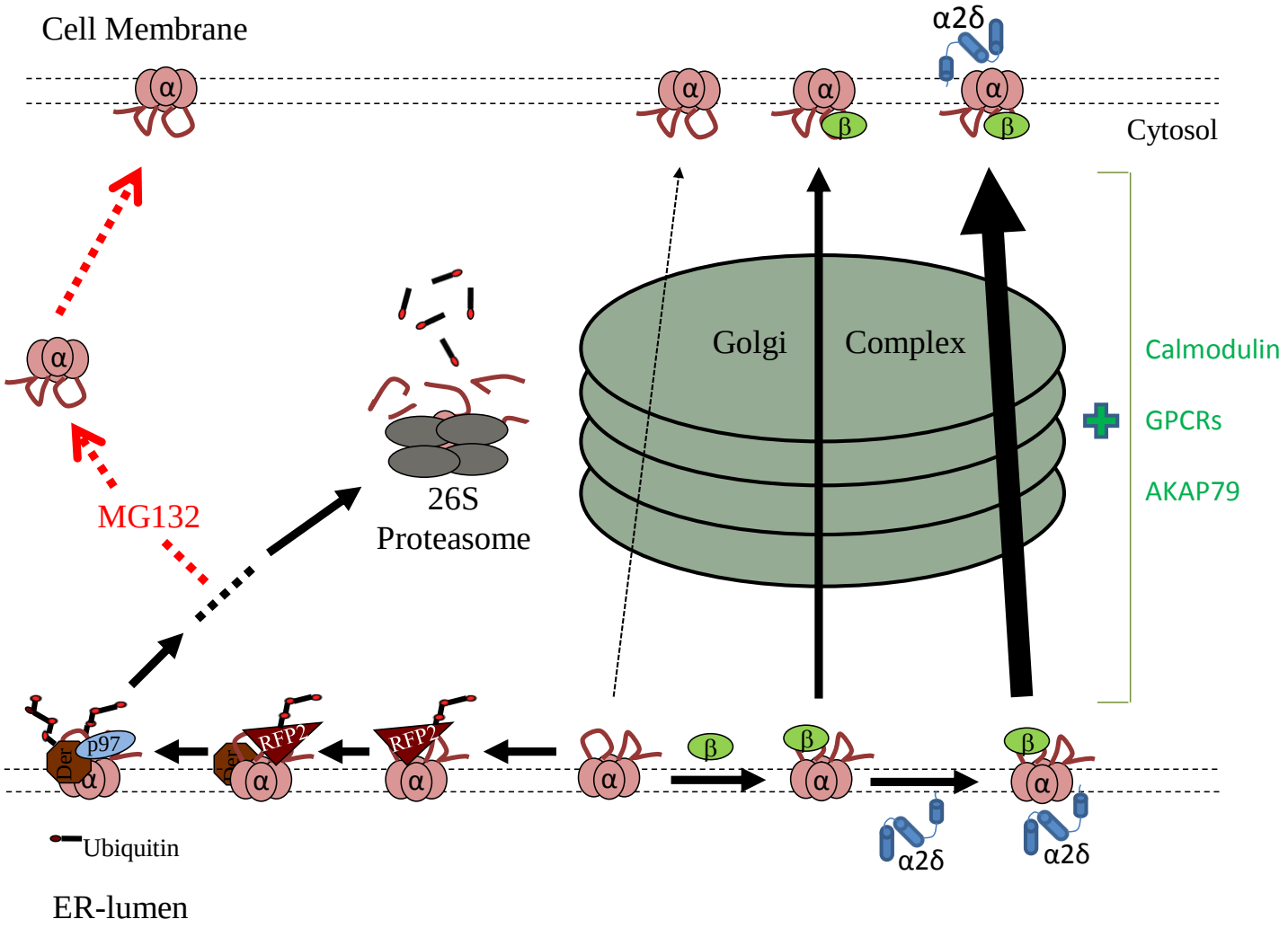
Cell Membrane
α2δ
α
β
Cytosol
Golgi
Complex
Calmodulin
GPCRs
AKAP79
MG132
26S
Proteasome
Der
p97
RFP2
Ubiquitin
ER-lumen

Figure 1-4

Figure 1-4: Forward trafficking of Cav1 and Cav2 channel complexes. Cavα1 can traffic to the surface without auxiliary subunits, but Cavβ and Cavα2δ subunits dramatically and additively increase the proportion of channels in the cell membrane. This increased surface expression is achieved by promoting ER export and increasing overall channel stability. Calmodulin, AKAP79 and GPCRs can augment forward trafficking of calcium channel complexes. The Cavβ subunit protects Cav1.2 and Cav2.2 from ER associated proteasomal degradation (ERAD). The Cavβ subunit protects Cav1.2 from ERAD by interfering with the ubiquitin ligase activity of RFP2. RFP2 ubiquitination leads to Derlin and p97 association with the calcium channel complex and retrotranslocation of the poly-ubiquitinated channels. Poly-ubiquitinated channels in the cytosol move on to the 26S proteasome for degradation. Proteasomal inhibitors such as MG132 are able to rescue some of the retrotranslocated channels.

Previous studies have also shown that mutations in the C-terminal EF-hand domain of Cav1.2 channels can drastically alter current density [121, 153, 154]. While it is possible that these mutations affect channel function rather than cell surface targeting [155, 156] it is probable that the lack of whole cell currents carried by some of these mutants arises from disruption of a CaM, or CaM kinase dependent cell surface trafficking mechanisms. In hippocampal neurons, Cav1.2 trafficking to the distal dendrites is accelerated by the presence of Ca^{2+}/CaM, but not CaM_{1234} [157]. The idea that CaM can influence the spatial and temporal distribution of channels, rather than just cell surface trafficking, is an intriguing possibility that requires further exploration.

In Chapter 5 we show that the N-terminal α-CaMKII site in Cav1.2 may have a role in silencing WT-Cav1.2 channels, or at least a significant proportion of them. This feature is absent from mutant channels of this site. This N-terminal α-CaMKII site also appears to augment forward trafficking of the Cav1.2 channel complexes, which is interesting because it was shown previously that removal of the N-terminus increases abundance of channels at the surface of COS1 cells [158, 159].

1.4 Cav1.2 pathophysiology and Brugada Syndrome

1.4.1 Function and general pathophysiology of Cav1.2

The L-type calcium channel Cav1.2 is important in neuronal tissue at the cellular level for CREB mediated transcription and neurite outgrowth, and also for fear conditioned learning as illustrated by conditional hippocampus/cortex knockout mice [154, 160, 161]. These mice also demonstrate impairment of spatial memory [162] and produces anxiety like behavior [163]. It makes sense then, that mild Cav1.2 dysfunction in humans is linked to various psychiatric (i.e. Schizophrenia

and major depressive disorder) and learning abnormalities such as autism [164-167]. Moreover, a congenital form of Cav1.2 dysfunction called Timothy syndrome produces debilitating disease symptoms of which include mental retardation, lethal cardiac arrhythmias, and severe developmental abnormalities [168, 169]. Many Timothy syndrome mutations effect the domain I-II linker region of Cav1.2 which interferes with both VDI and CDI and abnormally increases channel activity [170, 171].

Despite the physiological importance of Cav1.2 in the brain, expression of this channel in the heart is absolutely critical for life. Cav1.2 null mice die *in utero* at day 14.5 *post coitum* as this calcium channel subtype is essential for the ventricular action potential (VAP) and therefore cardiac muscle contraction [172]. Just as Timothy syndrome patients develop lethal arrhythmias because of excessive Cav1.2 conductance [173] diminished Cav1.2 function also produces cardiac arrhythmia. In this case however arrhythmia results from reduced depolarizing influence and weaker ventricular contraction, manifesting as early repolarization of the VAP. The congenital form of this abnormality is called Brugada Syndrome and will be discussed next.

1.4.2 Overview of Brugada Syndrome

Brugada Syndrome (BS) is an inherited cardiac illness characterized by a defect in repolarization of the right ventricular outflow tract, leading to phase 2 (discussed below) reentry and polymorphic ventricular tachycardia [174]. Brugada Syndrome has a an estimated prevalence of 1/10000- 5/10000 in Europe, and 12/10000 in Southeast Asia [175-177]. Men account for 80% of BS patients, with most arrhythmic events occurring between the ages of 40-45 years and typically after large meals, in periods of rest, or during sleep [178-180]. BS is responsible for 4% of all sudden deaths and 20% of sudden deaths in people without structural heart problems

[179]. Emerging clinical evidence suggests that sudden unexpected nocturnal death syndrome (SUNDS) and sudden infant death syndrome (SIDS) may in fact be an infant forms of BS [181]. The most common gene mutated in BS patients is *SCN5A* (Nav1.5), which is also aberrant in several SUNDS and sudden infant death syndrome (SIDS) patients [182, 183].

Brugada Syndrome was first described by Pedro and Josep Brugada who recognized a previously undiagnosed patient population with structurally normal hearts, and who exhibited idiopathic ventricular fibrillation [184]. Mutations in several ion channel genes including: voltage-gated sodium (*SCN5A*/*SCN1B*/*SCN3B*), potassium (*KCND3*/*KCNE3*/*MiRP2*/*KCNJ8*), hyperpolarization activated cation (*HCN4*), and voltage-gated calcium channel subunits (*CACNA1C* /*CACNB2b*/ *CACNA2D1*) have been linked to BS [61, 185-191]. Pharmacological treatment therefore targets some of these channels, but direct block of voltage-dependent calcium channels (VGCCs) is contraindicative for BS [192]. Only the implantable cardioverter defibrillator (ICD)- an electrical impulse generator designed to detect and correct arrhythmias- is considered an effective long term treatment for Brugada Syndrome [193].

Brugada Syndrome is an electrical disease of the ventricles and therefore it is worth revisiting the ventricular action potential (VAP) to understand how ion channels contribute to the VAP, and how a VAP is displayed on an electrocardiograph (ECG). Figure 1-5 illustrates the five phases of the VAP. An inward rush of sodium through Nav1.5 gives the initial peak of VAP depolarization (Phase 0), which is recessed by the exit of potassium through Kv4.3 channels and voltage dependent inactivation (VDI) of Nav1.5 (Phase 1) [194, 195]. The plateau (Phase 2) of the VAP is maintained by the opening and prolonged influx of calcium through Cav1.2 channels, and efflux of potassium by the delayed rectifier hERG (I_{Kr}) [195-197]. Cav1.2 conductance during the VAP provides the initial influx of calcium necessary to trigger calcium release from

the sarcorplasmic reticulum causing muscle fibres in the heart to physically contract, in other words excitation-contraction coupling [198] (for reviews see [199, 200]). During repolarization of the VAP (Phase 3) Cav1.2 channels close limiting depolarization, while the slow outward rectifier KCNQ1 (I_{Ks}) opens, driving the membrane potential down toward resting levels [201]. The fourth phase of the VAP is the maintenance of resting membrane potential by Kir2.1 (I_{K1}) an inward rectifying potassium channel [202].

The current criteria for diagnosis of BS includes an elevated ST segment of the right precordial leads in the presence, or absence of a sodium channel blocker with one of the following: ventricular fibrillation (VF), inducibility of VT with programmed electrical stimulation, polymorphic ventricular tachycardia (PVT), a family history of sudden cardiac death under the age of 45, or syncope [179]. This lengthy definition for Brugada Syndrome is necessary clinically because of related of J-wave syndromes with similar electrical characteristics [203]. BS patients can present with one of two types of elevated ST segment differentially characterized by shape and degree of elevation. The first type displays a coved ST elevation (>2mm) followed by a negative T-wave, the second an elevated ST segment (>1mm) with a saddleback appearance and a positive, or bi-phasic T wave [204, 205].

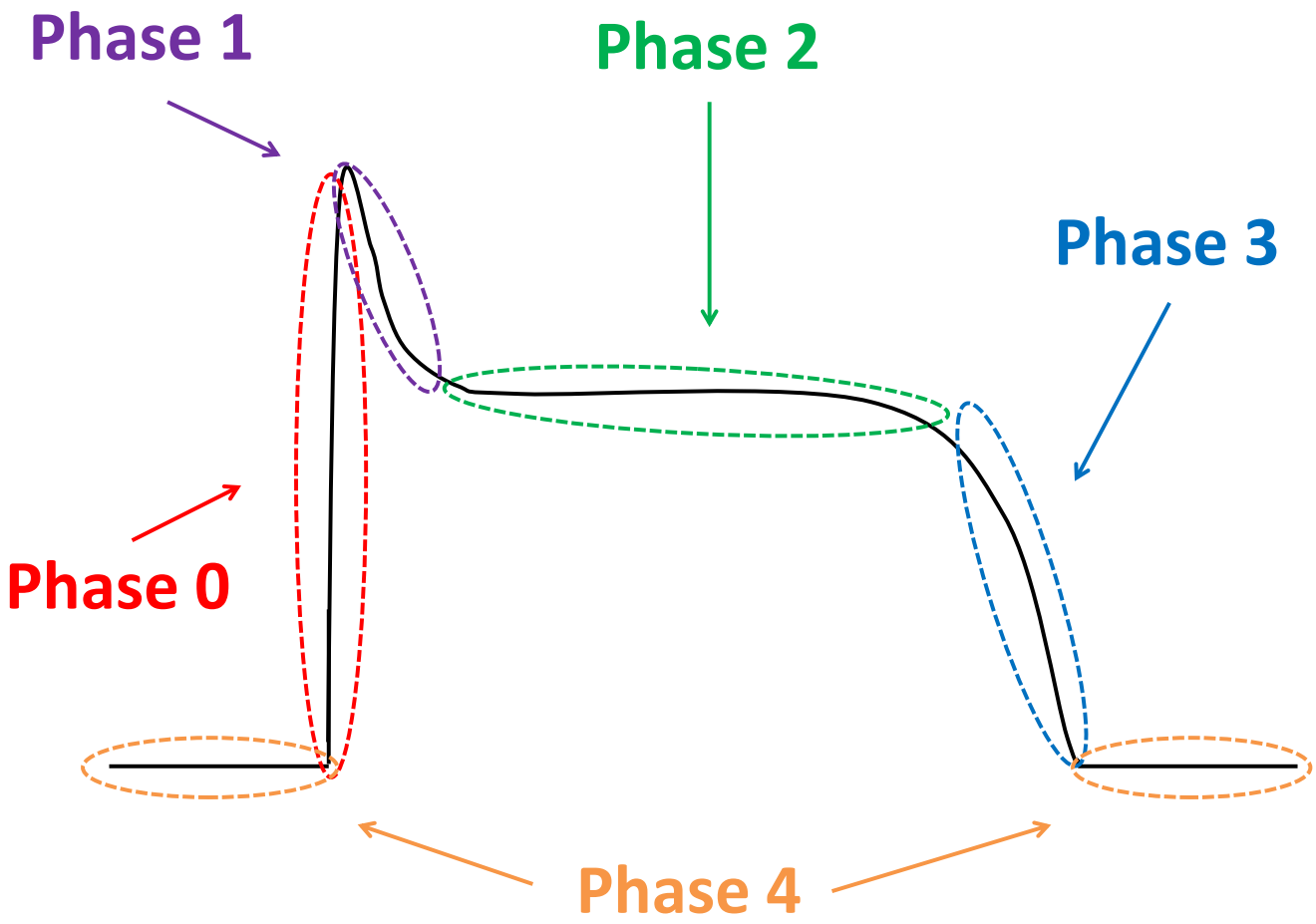

Figure 1-5

Figure 1-5: Ion channel conductances which contribute to the five phases of the ventricular action potential (VAP). The VAP begins with Phase 0 (red) which is the rapid inward current carried by Nav1.5 (I_{Na}) leading to immediate depolarization of the ventricles. In Phase 1(purple) partial repolarization of the ventricles occurs as Nav1.5 channels close and Kv4.3 (I_{TO}) open, permitting potassium to exit. During Phase 2 (green) sustained inward calcium via Cav1.2 (I_{Ca}) and outward delayed potassium currents through hERG maintain the VAP plateau. Phase 3 (blue) leads to complete repolarization of the VAP as Cav1.2 channels close, and slow outward potassium currents (KCNQ1) activate. Phase 4 (orange) is maintenance of the resting membrane potential by inward rectifying Kir2.1 channels.

1.4.3 Brugada Syndrome Mutations in Cav1.2

L-type calcium channels were first found to contribute to BS by Fish and colleagues who showed that block of these channels dramatically increased ST segment elevation in dissociated ventricular myocytes [7]. The first genetic evidence linking BS to calcium channel subunits came four years later when A39V/G490R mutations were identified in Cav1.2 after screening several BS patients for polymorphisms [61]. Since that time the number of BS mutations in VGCC subunits has increased to nine for Cav1.2, ten for Cavβ2b and four for Cavα2δ1 [185, 206]. Figure 1-6 depicts the location of known BS mutations in these channel subunits.

Typically BS mutations in Cav1.2 elicit disease phenotype (decreased conductance) by reducing surface expression of the channel, or by augmenting channel gating. For example, G490R-Cav1.2 (located in domain I-II linker) was characterized as having reduced current density in COS cells [61]. Given the location of G490R in the channel, reduced current density could reflect decreased surface expression, or alternatively augmented voltage-dependent gating– this remains unsolved [145, 207]. Much like G490R-Cav1.2 the mechanism for why a duplication of five amino acids in the distal C-terminus of Cav1.2 (E1829_Q1833-dup-Cav1.2) produces severely reduced current is unknown [185]. The C-terminus of Cav1.2 contains critical trafficking and ER retention motifs in various regions including the residues in and around E1829-Q1833 suggesting one possible explanation [9, 145]. As with the domain I-II linker however, the C-terminus of Cav1.2 is intimately tied to channel function and so, whether E1829_Q1833-Cav1.2 is a BS mutation because of aberrant trafficking or function remains to be determined [122, 158, 208].

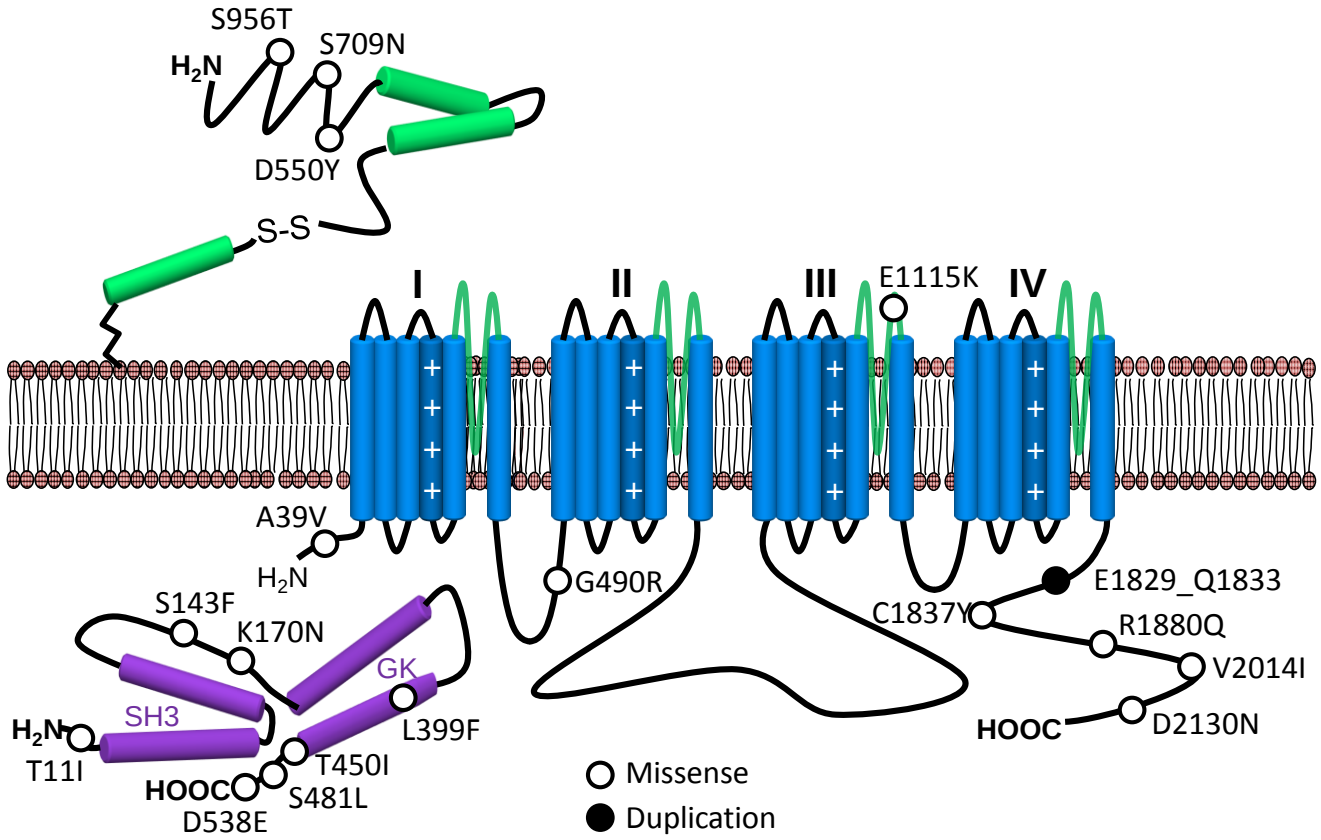
S956T
S709N
H2N
D550Y
S-S
I
II
III
E1115K
IV
A39V
H2N
G490R
S143F
K170N
GK
SH3
H2N
T11I
L399F
T450I
S481L
HOOC
D538E
E1829_Q1833
C1837Y
R1880Q
V2014I
HOOC
D2130N
Missense
Duplication

Figure 1-6

Figure 1-6: The nature and location of BS mutations in VGCC subunits

The Cav1.2 pore forming subunit (blue) has four domains (DI-IV), each with six transmembrane segments (S1-S6). The Cavβ2 subunit is displayed in purple with its SH3 and GK-like domains highlighted. The Cavα2δ subunit (green) is cleaved after translation into α2 and δ components, which are then disulfide linked (vertical black lines) in the intact protein. All currently known BS mutations are shown in this diagram with missense mutations (open circles) and a duplication event (dark circle) noted. This figure is modeled after Burashnikov et al (2010) [185] Figure 3.

VGCCs preferentially pass calcium because of sequence specific pore loops or calcium selectivity filters which are located between S5-S6 of each domain [6, 38]. A single point mutation in a p-loop residue for instance can transform a calcium selective channel into one which prefers sodium [209]. The BS mutation E1115K-Cav1.2 has reduced calcium flux through its pore because of such an aberration [185]. The E1115K mutation does not alter voltage or calcium dependent gating of the channel, but strictly reduces single channel conductance of calcium tending to prefer monovalent cations. Extrapolating this cellular phenotype to hearts of BS patients suggests how a loss of a calcium preference of E1115K-Cav1.2 result in elevated ST segments on ECG.

The BS mutation of interest in this thesis is A39V, an N-terminal mutation which was initially reported to cause Cav1.2 channels to distribute in a peri-nuclear manner, or in other words, prevent Cav1.2 trafficking to the cell surface [61]. Binding of Cavβ auxiliary subunits to the domain I-II linker of all HVA calcium channels dramatically increases surface expression, yet A39V-Cav1.2 was unique in the fact that an N-terminal mutation could prevent successful trafficking of the channel [9, 61, 142]. In a follow up paper however, we were unable to duplicate a lack of surface expression for A39V when expressed in the rat brain isoform of Cav1.2, thus creating some confusion for the phenotype of this mutant [210]. In Chapter 4 we describe a novel means by which Ca^{2+}/CaM modulates voltage-dependent activation of Cav1.2 and how A39V-Cav1.2 channels resist this new form of functional regulation. We believe this loss of functional regulation is the true phenotype for patients afflicted with A39V-Cav1.2.

Brugada syndrome is inherited loss-of-function disease for Cav1.2 channels which manifests as early repolarization of the ventricles, arrhythmia and in some cases sudden death.

1.5 Thesis Rationale and Hypothesis

Voltage-gated calcium channels regulate electrical properties and calcium signalling of many different cell types. Mutations in calcium channels typically disturb sub-cellular trafficking, or channel function, which then typically result in pathology. The L-type calcium channel Cav1.2 modulates emotional learning and maintains the VAP. A loss of function of Cav1.2- such as in the inherited disorder Brugada syndrome- results in early repolarization of the ventricles, which can lead to arrhythmia and sudden cardiac death. Understanding the molecular underpinnings of Cav1.2 sub-cellular trafficking and function are therefore of the utmost importance. Given the recent discovery that the N-terminus of Cav1.2 participates in CDI as well as, the peculiar location and phenotype of the Brugada syndrome mutation A39V, I was pertinent to study the N-terminus of this channel. *We therefore hypothesized that the N-terminus contains elements, or residues that regulate the function and sub-cellular trafficking of Cav1.2 channels.*

1.5.1 Aim 1: Identify novel N-terminal residues involved in Cav1.2 CDI

The N-terminus of Cav1.2 was recently shown to participate in global CDI, or in other words, in a manner which depends on the low affinity N-lobe of CaM. The first residue attributed to this function was W52 and is located mid-way through the N-terminus. With this said, precise residues were never identified for a proximal N-terminus region which bound the CaM homolog, calcium binding protein (CaBP) [211]. CaBP cannot participate in CDI because two of its calcium binding EF hands are inactive, but plausibly this second more proximal region might also bind CaM and participate in Cav1.2 CDI. *We therefore hypothesized that additional residues in the N-terminus of Cav1.2 modulate global CDI*. Chapter 3 describes how the N-terminal residue C106, or the region we term NATE (NSCaTE Associated Transduction

Element) biochemically and functionally couples to CaM to modulate global CDI of Cav1.2 channels.

1.5.2 Aim 2: Decipher the pathophysiological phenotype for A39V-Cav1.2

The literature initially characterized the Brugada syndrome mutant A39V-Cav1.2 as having a surface expression defect which was Cavβ insensitive [61]. This was surprising considering the N-terminal location of A39V and fact that Cavβ dependent channel trafficking depends on an interaction with the domain I-II linker, and not the N-terminus. We therefore attempted to repeat this finding (see Chapter 4) and could not with the rat neuronal isoform, suggesting there could be an alternate phenotype for A39V-Cav1.2 in brain. Given our prior interest with the N-terminus of Cav1.2 and CDI *we then hypothesized that A39V-Cav1.2 has augmented calcium dependent channel gating which may explain the loss-of-function phenotype.* Chapter 4 describes how A39V-Cav1.2 channels demonstrate augmented CDI and differentially shifted voltage-dependence and kinetics of channel activation when expressed with mutant CaM molecules in the absence of calcium.

1.5.3 Aim 3: Determine the function of a CaMKII site in the N-terminus of Cav1.2

The N-terminus was first shown to contain a CaMKII binding site nearly 10 years ago [139], but the precise location of the site, and its function were never characterized. While working with CaM sepharose pull-downs for Aim 1 it became apparent that a calcium insensitive interaction in the proximal N-terminus of Cav1.2 existed, which is not characteristic of most CaM binding sites. *We therefore hypothesized that the proximal region of the N-terminus contains a CaMKII binding site which is involved in trafficking or functional regulation of Cav1.2*. Chapter 5

describes the offsetting trafficking and functional phenotype of Cav1.2 channels lacking this N-terminal CaMKII site.

1.5.4 Significance

The work in this thesis describes how the N-terminus of Cav1.2 contributes significantly to surface expression and gating of the channel. Structure/function analysis of the N-terminus of calcium channels has picked up recently and our work adds to this growing body of evidence which has far reaching implications for how we understand emotional learning and heart function.

CHAPTER TWO **MATERIALS AND METHODS**

2.1 Molecular Biology

2.1.1 General methods

All restriction enzymes used herein were obtained from New England BioLabs. Hot start TAQ used for traditional polymerase chain reaction (PCR) was obtained from Agilent Technologies while site directed mutagenesis was conducted using the enzyme PFU and the QuickChange mutagenesis kit produced by Promega. PCR reactions were conducted in a volume of 50ul in a BioRad DNA Engine DYAD thermal cycler. All oligonucleotide primers were generated by UCDNA Services DNA/RNA Synthesis Laboratory, while PCR products and other DNA fragments of interest were run on agarose gel, and appropriately sized bands extracted using the QIAquick Gel Extraction Kit (Qiagen). Ligations were carried out overnight at 4°C in a final volume of 20ul using T4 DNA ligase (Promega). All DNA clones were transformed using the heat shock method into DH5α cells (Life Technologies). DNA was isolated from transformed bacteria using either Qiagen Plasmid Mini, or Maxi kits (Qiagen) and clone fidelity was verified by the University of Calgary Genetic Analysis Laboratory.

2.1.2 Donated, purchased and engineered calcium channel constructs

Wild type (WT) rat calcium channel subunit cDNAs encoding Cav1.2, Cavβ1b, Cavβ2a and Cavα2δ1 subunits, as well as the pMT2 vector were generously donated by Dr. Terry Snutch (University of British Columbia, Vancouver, BC). Rat brain Cav1.2 has a polymorphism (glycine at amino acid position 57) which is not present in the human cardiac isoform. To facilitate comparison with previous work [61] we mutated rat Cav1.2 at position 57 to aspartic

acid (Table 2-1). We refer to this channel throughout as WT-Cav1.2. A39V-Cav1.2 was created by site-directed mutagenesis of WT-Cav1.2. W52A, C106R, W52A-C106R, and Cav1.2-$_{AAAA}$ channels were created by cloning their respective synthesized sequences (Genscript) into the original clones using ClaI/BsrGI. The HA tagged version of Cav1.2 has been previously described [212] and all channel clones mentioned above were constructed in non-tagged and extracellularly, HA-tagged versions. The Cavβ2b clone was generously donated by Dr. Henry Colecraft (Columbia University, New York, USA). Wild type (CaM_{WT}) and the CaM mutant with four mutated EF hands (CaM_{1234}) were a gift from Dr. John Adelman (University of Heath and Science, Oregon). CaM mutants with EF hands 3 and 4 mutated (CaM_{34}), or EF hands 1 and 2 mutated (CaM_{12}) were constructed by swapping homologous domains of CaM_{WT} and CaM_{1234} in pcDNA3 via common EcoRI sites. Xpress-CaM was made by PCR from wild type CaM which was then cloned downstream of His/Xpress tags in pcDNA3.1HisB (Invitrogen) with BamHI/XhoI. Cherry-α-CaMKII was a gift from Dr. Paul De Konnick (Universite of Laval, Quebec) and has been previously described [213] GenBank™ accession numbers, or origins of the clones used in thesis are as follows: Cav1.2 [M67515], Cavβ1b [NM017346], Cavβ2a [214] Cavβ2b [AF423193.1], Cavα2δ1 [AF286488], CaM [NP_114175.1] and α-CaMKII [NM_012920.1].

2.1.3 Cav1.2 GFP constructs

All Cav1.2 N-terminal GFP fusion proteins (Figure 2-1), as well as the C-terminal PreIQ-IQ segment were cloned into N1-GFP, or N1-mCherry (Clontech) using BamHI/XhoI (Table 2-1). PCR of Cav1.2 channels followed by restriction digestion and cloning yielded the following GFP fusion constructs: PreIQ-IQ, Nterm, W52A-Nterm, C106R-Nterm, W52A-C106R-Nterm, $N_{1\text{-}EX}$

Table 2-1: cDNA constructed for experimentation

cDNA	Vector	PCR primers/Cloning sites
WT-Cav1.2	pMT2	GGCAGGCAGCCATCGACGCCGCCCGGCAGGCC/ GGCCTGCCGGGCGGCGTCGATGGCTGCCTGCC
A39V-Cav1.2	pMT2	AATGCAGCTGCAGGACTTGTCCCCGAGCACATCCCTACTCC/ GGAGTAGGGATGTGCTCGGGGACAAGTCCTGCAGCTGCATT
W52A-Cav1.2	pMT2	ClaI/BsrGI
C106R-Cav1.2	pMT2	ClaI/BsrGI
W52A-C106R-Cav1.2	pMT2	ClaI/BsrGI
$Cav1.2_{-AAAA}$	pMT2	ClaI/BsrGI
His-Express-CaM	pcDNA3.1-HisB	TTAAGGATCCTATGGCTGACCAACTGAC/ AATTCTCGAGTCACTTCGCTGTCATCAT
CaM_{12}	pcDNA3.1	EcoRI
CaM_{34}	pcDNA3.1	EcoRI
PreIQ-IQ-GFP	N1-GFP	ATATCTCGAGATGAACATGCCTCTGAACAG/ TATAGGATCCCCGGAGGCAGCAGACACTGC

Nterm-GFP, A39V-Nterm-GFP W52A-Nterm-GFP, C106R-Nterm-GFP & W52A-C106R-Nterm-GFP	N1-GFP	ATATCTCGAGATGGTCAATGAAAACACG/ TATAGGATCCCCTTTCCATTCAACAATGC
N_1-GFP, A39V-N_1-GFP, W52A-N_1-GFP	N1-GFP	ATATCTCGAGATGGTCAATGAAAACACG/ ATATGGATCCCCCTTGGCCTGCCGGGC
$N_{1\text{-}EX}$-GFP, A39V-$N_{1\text{-}EX}$-GFP, W52A-$N_{1\text{-}EX}$-GFP	N1-GFP	ATATCTCGAGATGGTCAATGAAAACACG/ TATAGGATCCCCGGGCGGCCGTGTGGCAGTTGTGC
$N_{1\text{-}MID}$-mCherry	N1-mCherry	TCGAGATGGGTTCCAACTATGGGAGCCCACGCCCAGCTCATGCCAACATGAATG CCAATGCAGCTGCAGGACTTGCCCCCGAGCACATCCCTACTCCAGGGGCAGGG/ GATCCCCTGCCCCTGGAGTAGGGATGTGCTCGGGGGCAAGTCCTGCAGCTGCAT TGGCATTCATGTTGGCATGAGCTGGGCGTGGGCTCCCATAGTTGGAACCCATC
A39V-$N_{1\text{-}MID}$-mCherry	N1-mCherry	TCGAGATGGGTTCCAACTATGGGAGCCCACGCCCAGCTCATGCCAACATGAATG CCAATGCAGCTGCAGGACTTGTCCCCGAGCACATCCCTACTCCAGGGGCAGGG/ GATCCCCTGCCCCTGGAGTAGGGATGTGCTCGGGGACAAGTCCTGCAGCTGCAT TGGCATTCATGTTGGCATGAGCTGGGCGTGGGCTCCCATAGTTGGAACCCATC
N_2-GFP	N1-GFP	ATATCTCGAGATGTTAATGGGCAGTGCTGG/

		TATAGGATCCCCTTTCCATTCAACAATGC
N_{2A}-GFP	N1-GFP	ATATCTCGAGATGTTAATGGGCAGTGCTGG/ TATACGGTGGATCCCCCTTGGGTTTCCCATACTGC
N_{2B}-GFP	N1-GFP	ATATCTCGAGATGAAGCAGGGGGGCACAACTGC/ TATAGGATCCCCTTTCCATTCAACAATGC
N_{2B-I}-GFP	N1-GFP	ATATCTCGAGATGAAGCAGGGGGGCACAACTGC/ TATAGGATCCCCCAGGCAGAGCAGAGCC
C106R-N_{2B-I}-GFP	N1-GFP	TCGAGATGAAGCAGGGGGGCACAACTGCCACACGGCCGCCCCGGGCTCCGCCCCGCCTGGGG/ GATCCCCCAGGCGGGGCGGAGCCCGGGGCGGCCGTGTGGCAGTTGTGCCCCCCTGCTTCATC
N_{2B-II}-GFP	N1-GFP	TCGAGATGACTCTGAAGAACCCCATCAGGAGGGCATGCATCAGCATTGTTGAATGGAAAGGG/ GATCCCCTTTCCATTCAACAATGCTGATGCATGCCCTCCTGATGGGGTTCTTCAGAGTCATC
$N_{2B-II-R}$-GFP	N1-GFP	TCGAGATGACTCTGAAGAACCCCATCAGGAGGGCACGCATCAGCATTGTTGAATGGAAAGGG/

		GATCCCCTTTCCATTCAACAATGCTGATGCGTGCCCTCCTGATGGGGTTCTTCAG AGTCATC
$N_{2B\text{-}II\text{-}RR}$-GFP	N1-GFP	TCGAGATGACTCTGAAGAACCCCATCAGGAGGGCACGCATCCGCATTGTTGAAT GGAAAGGG/ GATCCCCTTTCCATTCAACAATGCGGATGCGTGCCCTCCTGATGGGGTTCTTCAG AGTCATC
$N_{2B\text{-}II\text{-}RARA}$-GFP	N1-GFP	TCGAGATGACTCTGAAGAACCCCATCAGGAGGGCACGCGCCCGCGCTGTTGAAT GGAAAGGG/ GATCCCCTTTCCATTCAACAGCGCGGGCGCGTGCCCTCCTGATGGGGTTCTTCAG AGTCATC
$N_{2B\text{-}II\text{-}AAAA}$-GFP	N1-GFP	TCGAGATGACTCTGAAGAACCCCATCAGGAGGGCAGCTGCCGCAGCTGTTGAAT GGAAAGGG/ GATCCCCTTTCCATTCAACAGCTGCGGCAGCTGCCCTCCTGATGGGGTTCTTCAG AGTCATC

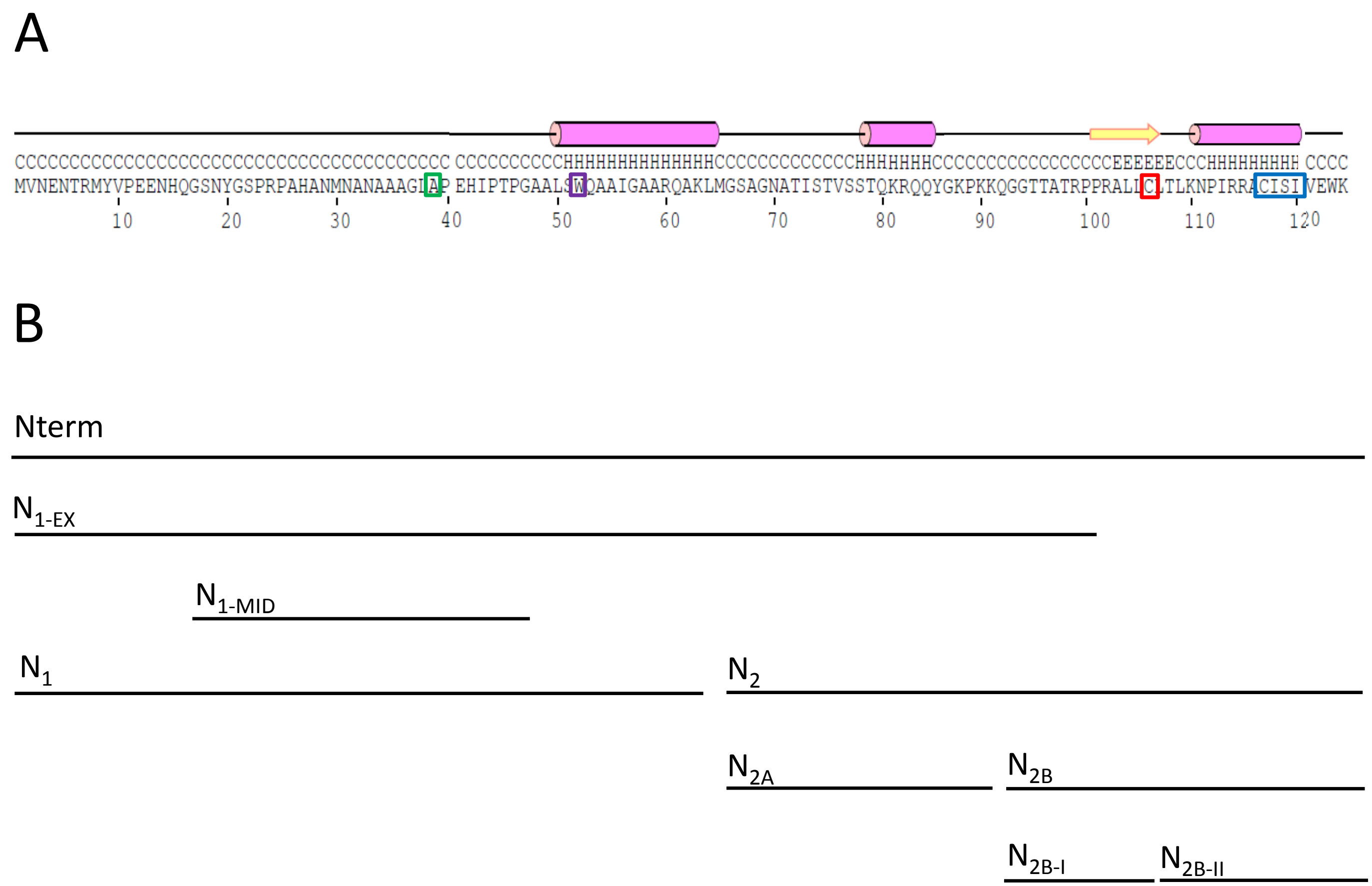
A
CCCCCCCCCCCCCCCCCCCCCCCCCCCCCCCCCCCCCCCC CCCCCCCCCCHHHHHHHHHHHHHHCCCCCCCCCCCCHHHHHHHCCCCCCCCCCCCCCCCEEEEEECCCHHHHHHHHH CCCC
MVNENTRMYVPEENHQGSNYGSPRPAHANMNANAAAGLAP EHIPTPGAALSWQAAIGAARQAKLMGSAGNATISTVSSTQKRQQYGKPKKQGGTTATRPPRALLCLTLKNPIRRACISIVEWK
10 20 30 40 50 60 70 80 90 100 110 120
B
Nterm
N1-EX
N1-MID
N1
N2
N2A
N2B
N2B-I
N2B-II

Figure 2-1

Figure 2-1: All GFP fusion proteins of the Cav1.2 N-terminus. A) Predicted secondary structure (PSIPRED http://bioinf.cs.ucl.aIt c.uk/psipred/) of the Cav1.2 N-terminus. The green box highlights the location of the Brugada syndrome mutation (A39V), the purple box a residue important for N-lobe CDI of Cav1 channels (W52), while C106 (red box) and the CISI element (blue box) are important for binding Ca^{2+}/CaM and CaMKII, respectively, and are functionally described herein. The residue W52 was *NSCaTE* by Dick and colleagues (2008) for *N*-terminal *S*patial Ca^{2+} *T*ransforming *E*lement. Consequently we later named C106, *NATE* for *NSCaTE* *A*ssociated *T*ransduction *E*lement. B) Map of Cav1.2 N-terminal GFP fusion proteins used in this thesis.

, A39V-$N_{1\text{-}EX}$, W52A-$N_{1\text{-}EX}$, N_1, W52A-N_1, N_2, N_{2A}, N_{2B}, and $N_{2B\text{-}I}$. Annealing reactions (95 degrees for 10 mins, followed by cooling to 20 degrees over a 25 min period) of complimentary primers (20pmol/primer) followed by cloning (BaMHI/XhoI) were used to generate the following Cav1.2 GFP fusion constructs : $N_{1\text{-}MID}$, A39V-$N_{1\text{-}MID}$, C106R-$N_{2B\text{-}I}$, $N_{2B\text{-}II}$, $N_{2B\text{-}II\text{-}R}$, $N_{2B\text{-}II\text{-}RR}$, $N_{2B\text{-}II\text{-}RARA}$, and $N_{2B\text{-}II\text{-}AAAA}$.

2.2 Tissue culture and transient transfection

Human embryonic kidney tsA-201 cells were cultured and transiently transfected using the calcium phosphate method as described previously [215]. For immunocytochemistry of channel GFP/ mCherry fusion proteins, or mCherry-CaMKII, 250ng of each construct was transfected per 35 mm dish (MatTek). For immunocytochemistry of HA-tagged calcium channels 500ng each of the Cavα, Cavβ and Cavα2δ1 subunits were transfected per 35mm dish. For immunoblotting 3ug of each cDNA was transfected per 10 cm plate. For electrophysiology experiments 3ug of each Cavα subunit and 3ug of Cavβ and Cavα2δ1 subunits were transfected per 10 cm plate. In addition, 125ng of GFP was included in each electrophysiology transfection to identify transfected cells. In order to increase current magnitude 6ug of each Cavα subunit were transfected for barium/calcium exchange experiments and 750ng of one of CaM_{WT}, CaM_{12}, CaM_{34}, or CaM_{1234}. For immunoblot and immunocytochemistry experiments, cells were grown at 37°C for 48-72 hours (75-85% confluence), while cells for electrophysiology were kept to low confluence and were grown for 72 hours at 28°C.

2.3 Electrophysiology

2.3.1 General methods

Whole cell patch clamp recordings were performed in voltage-clamp mode using an Axopatch 200B amplifier (Axon Instruments) linked to a personal computer with pCLAMP software version 9.2. Series resistance was compensated by 85%, leak currents were negligible, and the data were filtered at 5 kHz. Micro-electrode patch pipettes were pulled and polished using a DMZ- Universal Puller (Zeitz Instruments GmbH) to a typical resistance of 3–5 MΩ. All electrophysiological data were analyzed using Clampfit version 9.2 (Axon Instruments) and plotted in Origin 7/9 (Origin Lab Corporation). Statistical analyses for electrophysiological data were carried out using Origin 7/9.

2.3.2 Cav1.2 voltage-clamp recording solutions

Seventy-two hours post-transfection glass cover slips carrying cells containing WT or mutant Cav1.2 channels were transferred to a 1.5ml recording chamber containing an external recording solution consisting of 20 mM $BaCl_2$, 1 mM $MgCl_2$, 10 mM HEPES, 10 mM Glucose and 136 mM CsCl (pH 7.4 adjusted with CsOH). For barium/calcium exchange experiments (i.e. CDI) 20mM $BaCl_2$ was substituted for 20mM $CaCl_2$ in the external solution. The internal pipette solution used in the initial A39V-Cav1.2 paper [210] consisted of 110 mM CsCH3SO3, 20 mM TEA-Cl, 10 mM EGTA, 2 mM MgCl2 and 10 mM HEPES (pH 7.2 adjusted with CsOH). The internal pipette solution used for all experiments afterwards lacked TEA-Cl as this potassium channel blocker can affect Cav1.2 channel currents when present intracellularly [112]. The low calcium buffering internal pipette solution used throughout this thesis consisted of 141 mM $CsCH_3SO_3$, 0.5 mM EGTA, 4 mM $MgCl_2$ and 10 mM HEPES (pH 7.2 adjusted with CsOH).

The high calcium buffering internal solution was prepared in the same manner however less $CsCH_3SO_3$ (131mM) was used to offset the increase in calcium buffer concentration (10 mM BAPTA). Added daily to both internal solutions was 5mM Di-Tris-Creatine Phosphate, 2 mM Tris-ATP and 0.5mM Na-GTP.

2.3.3 Cav1.2 protocols and current analysis

Individual pEGFP expressing cells were held at either -100mV before recording. An IV protocol was used to for both current density and barium/calcium exchange experiments whereby voltage clamped cells were stepped from holding potential to 10mV incremental steps for 1 sec beginning at -60mV and ending at +50mV. Individual sweeps were separated by 15 s to allow complete channel recovery from VDI. For steady state inactivation curves, we applied 4.5 s conditioning depolarizations, followed by a test pulse to +10 mV for 0.5 s. Individual sweeps were separated by 15 s once more. All stable cells with detectable inward current at 0 mV were used to calculate current density.

Only those cells whose whole cell current voltage relationships could be fit with the modified Boltzmann equation, $I = (1/(1 + \exp^{(-(Va-V)/S))})*(V-E_{rev})*G_{max}$, where 'I' is current, 'V_a' is half-activation potential, 'V' is membrane potential, 'E_{rev}' is reversal potential, S is the slope factor, and 'G_{max}' is slope conductance, were used for determination of voltage-dependent properties. As well, only cells whose steady-state inactivation could be fit by the Boltzmann equation, $I/I_{max} = A_2 + A_1/(1 + \exp^{((V-Vh)/S)})$, where '$I/I_{max}$' is normalized current, 'A_2' is the non-inactivating fraction, 'A_1' is inactivating fraction, 'V' is membrane potential, S is the slope factor, and 'V_h' is half inactivation potential, were used to calculate voltage-dependent properties of steady-state inactivation.

For CDI experiments only cells with > 100pA of Ba^{2+} current proceeded to recordings in Ca^{2+} this is necessary because Cav1.2 calcium currents are typically 30-60% the magnitude of paired barium recordings. In order to quantify CDI we used a previously described method of paired analysis [149]. In this method the fraction of current remaining at 300ms (r300) in Ca^{2+} is subtracted from the current fraction remaining at 300ms in Ba^{2+}. The difference obtained between the two charge carriers represents additional inactivation promoted by Ca^{2+} (f_{300}), or rather CDI. Because Ca^{2+} conductance in the solutions used was maximal at 10mV, the -100 to 10mV (1sec) pulse was used for determining degree of CDI.

2.4 Epifluorescence & Confocal Microscopy

2.4.1 Immunocytochemistry of HA-tagged channels

Seventy two hours after transfection cells containing WT, or mutant HA-tagged Cav1.2 channels were fixed with 4% paraformaldehyde and immunostained with rat anti-HA (1/1000, Roche) or mouse anti-HA antibody (1/1000, Covance). Either Alexa Fluor 594-conjugated goat α-rat IgG antibody (Molecular Probes, 1/1000) or Alexa Fluor 488- conjugated goat α-mouse IgG antibody (Molecular Probes, 1/1000) were used as the secondary antibodies. Cells were imaged using a Zeiss LSM-510 Meta confocal microscope with either a 40 × 1.2NA water immersion, or a 63X 1.4NA oil immersion lens in the inverted position. The AF-594 antibody was visualized by excitation with a HeNe laser (543 nm) and emission detected using a 585–615-nm band pass filter. The Alexa Fluor 488 antibody was visualized by excitation with an Argon laser (488 nm) and emission detected using a 515-530-nm band pass filter. Image acquisition was performed with identical gain, contrast, laser excitation, pinhole aperture (fully open for epiflorescence

quantification, or as appropriate for confocal slice), scan size and laser scanning speed for all samples. Where necessary, quantification of fluorescent signal was done following offline threshold adjustment with Image J. To obtain values for fluorescence/cell the total fluorescence per image was divided by the number of cells above threshold in that image.

2.4.2 Live cell imaging of GFP/mCherry fusion constructs

For live cell imaging of GFP and mCherry fusion proteins, tsA-201 cells were grown for 48 hours post-transfection, and then placed in HBSS. Images were acquired with a Zeiss LSM-510 Meta confocal microscope using a 63X 1.4NA oil immersion lens in the inverted position. Co-localization experiments using GFP and mCherry constructs were performed using dual excitation (488 and 543) and emission filters BP505-530 and LP650. Detector gain, pinhole aperture, laser excitation and scanning speed were left unchanged from sample to sample unless otherwise indicated.

2.4.3 Colocalization analysis

Colocalization was determined using the ICQ analysis pioneered by Li et al [216]. For all colocalization analysis we selected relevant ROIs. To summarize this analysis briefly, the ICQ plug-in for Image J determines if fluorescent pixels from one channel (i.e. GFP) exactly overlap with pixels from another channel (i.e. mCherry), which if so yields an ICQ value of 0.5 and reflects perfect co-localization. Alternatively an ICQ value of -0.5 reflects perfect segregation of pixels, and an ICQ value of 0 equates to a random overlap of pixels.

2.5 Protein Biochemistry

2.5.1 General methods

Cultured tsA-201 cells were transiently transfected as described earlier and were lysed with a modified RIPA buffer (in mM; 50 Tris, 130 NaCl, 0.2% triton X-100, 0.2% NP-40, 5 EGTA, or 0.5 Ca^{2+}, pH 7.4). Lysis was carried out on ice for 15 min after which cells were centrifuged at 13,000 rpm for 5 min at 4°C. Samples were dissolved in loading buffer containing 100mM Tris, 4% SDS, 0.02% bromophenol blue, 20% glycerol, 100mM 2-mercaptoethanol, pH 6.8 and were denatured by heating to either 55, 100ºC for 10 min. All experiments were run on tris-glycine denaturing gels and transferred via a wet transfer apparatus to 0.45 polyvinylidene difluoride (PVDF) membranes (Millipore). Samples were run through the gel (35-70mA) and proteins were transferred on ice at 250mA for 60 min. All membranes were incubated with primary antibody dissolved in PBS and 2-5% milk for 1 hour at room temperature. Membranes were washed 3x 15 min each with PBS/0.1% tween-20 (PBS-T) and incubated with secondary antibody (1/5000 GE-Healthcare horseradish peroxidase-linked secondary antibodies recognizing rabbit, rat, or mouse) in PBS (2-5% milk) for 35 min at room temperature. Membranes were washed 3x 15 min and were visualized with ECL reagent or SuperSignal West Dura Chemiluminescent Substrate (Thermo Scientific) by exposure of X-ray film (Kodak). Where necessary, Image J (National Institute of Health) was used to quantify the integrated density of protein on immunoblots. For each blot the background signal was subtracted from experimental integrated densities to obtain sample values.

2.5.2 Calmodulin sepharose pulldown

Supernatants prepared as in Section 2.5.1 were transferred to two sets of new tubes with CaM Sepharose 4B beads (GE Healthcare Life Sciences) which were used for pull-down assays overnight, while tumbling at 4°C. All CaM Sepharose pull-down assays proceeded in 0.5mM calcium, until the following morning where one matching set of pull-downs was washed with 0.5mM calcium and the other with 5mM EGTA lysis buffer. Samples of lysate (2.5%) were also run to verify protein expression. Immunoblot of CaM Sepharose pull-downs were performed using 1/1000 anti-GFP (Santa-Cruz-8334).

2.5.3 Co-immunoprecipitation assays

Supernatants prepared as in Section 2.5.1 were transferred to new tubes and solubilized proteins were incubated overnight at 4ºC with 1 µg of one of the following antibodies for immunoprecipitation: anti-HA (Roche), anti-calmodulin (Epitomics-5197-1), anti-Xpress (Life Technologies R910-25), or anti-GFP (Abcam-ab1218). After incubation with antibodies, 50 µl of Protein G, or A Sepharose beads (GE Healthcare Life Sciences) were added to the samples and incubated at 4°C for one hour. Co-immunoprecipitates were washed with either the 0.5mM calcium, or 5mM EGTA lysis buffer, experiment depending. Immunoblot of co-immunoprecipitation experiments, or inputs were performed using one of the following: 1/1000 anti-actin (Sigma), 1/1000 anti-GFP (Santa-Cruz-8334), 1/1000 anti-mCherry (Abcam-1C51), 1/2000 anti-CaM (Epitomics-5197-1) or 1/1000 α-CaMKII (Santa Cruz-9035). Membranes were then stripped for 10mins at 55°C in the following buffer in order to re-probe for immunoprecipitates: 2.5mM Tris, 2% SDS and 0.78% Beta-mercapto-ethanol.

2.5.4 Cell surface biotynlation assay

Cells transfected with HA-tagged channels were washed and incubated with cold HBSS on ice for 20 min to stop trafficking of proteins. Surface proteins were biotinylated with 1 mg/ml EZ-Link Sulfo-NHS-SS-Biotin (Thermo Scientific) for 1 hour on ice. The biotinylation reaction was quenched with cold 100mM glycine in HBSS for 15 min, following that cells were washed with HBSS and lysed in modified RIPA buffer (5mM EGTA) for 15 min. Protein concentration of lysates was measured using the BioRad protein assay and so 100 µl of Neutravidin beads (Thermo Scientific) were added per 1100 µg of lysate. After incubation for 1.5h at 4^{o}C, beads were washed 4 times with lysis buffer and biotinylated proteins eluted with sample buffer. Biotinylated and non-biotinylated fractions as well as lysates were resolved by SDS-PAGE followed by western blot analysis.

2.6 General Data and Statistical Analysis

All electrophysiological data were analyzed using Clampfit version 10.2 (Axon Instruments) and fit in Origin 7/9 (Origin Lab Corporation). Statistical analyses for data was carried out using Origin 7/9. All sample means are reported +/− SEM. Statistically significant differences between means were assessed using student's *t*-test, paired *t*-test, or one-way ANOVA at 95% confidence level as appropriate.

CHAPTER THREE: **A NOVEL CALMODULIN SITE IN THE CAV1.2 N-TERMINUS**

3.1 Background

Calcium ions are important signaling molecules and regulate a myriad of intracellular processes, however excessive calcium entry is cytotoxic to cells. To limit calcium entry during prolonged periods of electrical activity, HVA channels undergo two distinct inactivation processes VDI and CDI (Section 1.2.4 & 1.2.5, respectively). The type of calcium-dependent inactivation imparted by CaM differs across HVA calcium channel families [217]. Cav2 calcium channels exhibit CDI in response to a global calcium rise, a feature regulated by the low affinity N-lobe of CaM [149, 218], whereas Cav1 channels inactivate, predominantly, because of increasing local calcium- this process is regulated by the high affinity C-lobe of CaM [117, 118, 219].

Much research on CDI of HVA channels has focused on the C-terminal tail of the pore forming Cavα1 subunit largely because of the presence of an IQ domain – a CaM binding consensus motif that is present in all HVA channel C-termini [118, 220, 221]. This region binds the Ca^{2+} free version of CaM, called apoCaM [122, 208, 222], thus anchoring CaM to the channel where it is in a prime position to interact with calcium ions and modulate channel activity. Several groups have elaborately shown how multiple CaM molecules interact with the C-terminus and how RNA editing modulates the IQ domain, and consequently CDI [84, 86, 223-226]. The current functional model of CDI proposes that apoCaM associates with both the IQ domain and upstream sequences, referred to as the *P*roximal *C*alcium *I*nactivation (PCI) domain, at rest. Upon calcium increase, the C-lobe of CaM then migrates further upstream in the

PCI region (immediately adjacent the EF-hand) initiating local CDI, which is exclusively a C-terminal process [133].

The N-terminus of Cav1 channels has also been implicated in CDI, but N-lobe CDI, as it involves the low affinity calcium binding domain of CaM [134]**.** Dick and colleagues (2008) [134] used a chimeric approach to demonstrate that the N-termini of L-type (Cav1.2 & Cav1.3) channels could confer L-type calcium channel-like CDI characteristics onto N-type (Cav2.2) channels, which otherwise only show global CDI. They went on to demonstrate that a tryptophan residue in the N-terminus (W82 in cardiac and W52 in neuronal Cav1.2 splice variants) completed a CaM binding site that modulated N-lobe CDI for L-type calcium channels (Figure 3-1A, green box) [134]. This particular CaM site was named NSCaTE for *N*-terminal *S*patial Ca^{2+} *T*ransforming *E*lement- we refer to NSCaTE throughout as W52 for simplicity. What makes W52 an ideal CaM site for global CDI is its low affinity for the N-lobe of CaM (approximate K_d for Ca^{2+}/CaM in the micromolar range) [88]. This is in contrast to the nanomolar CaM affinity of the IQ domain [222, 227]. W52 is conserved from invertebrates to humans, and its ability to bind CaM has been verified independently, emphasizing its importance in Cav1-related channels [228, 229].

While W52 is clearly important for N-lobe CDI of L-type channels, there is evidence that there may be other regions within the Cav1.2 N-terminus that partake in calcium-dependent feedback regulation. First, a CaM homolog, calcium binding protein (CaBP) [211, 230] was found to bind the proximal N-terminus of Cav1.2 (Figure 3-1A, red box) and modulate function [230, 231] and second, the N-terminus of Cav1.2 is thought to contain a CaM kinase binding site [139] which suggests the possibility of adjacent CaM interaction sites, as has been observed for the C-terminus of the channel [232, 233]. We use several biochemical approaches, paired with

electrophysiology to show that there is a second N-terminal CaM site which works cooperatively with W52 to modulate N-lobe CDI of Cav1.2 channels.

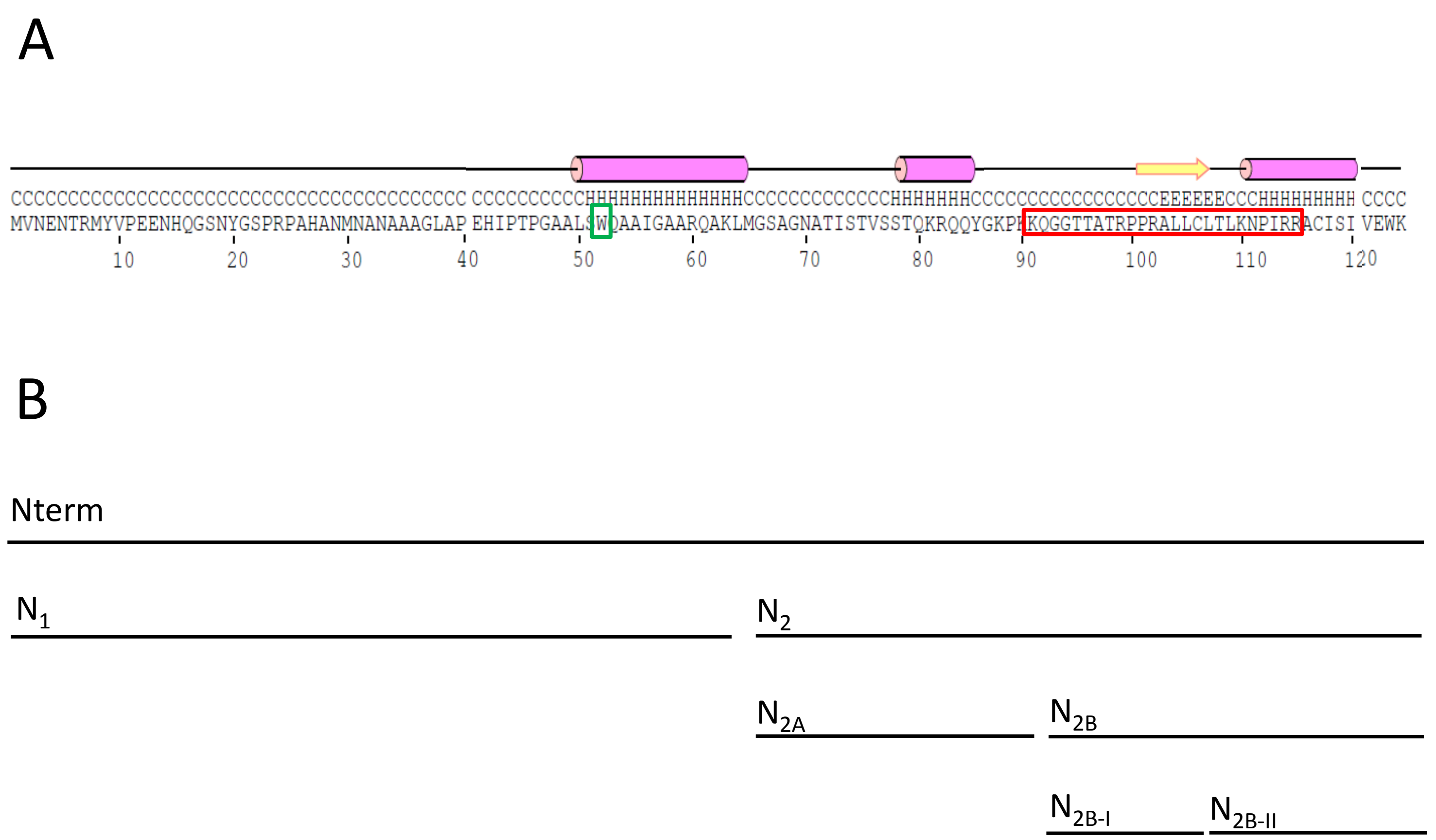
A
CCCCCCCCCCCCCCCCCCCCCCCCCCCCCCCCCCCCCCCC CCCCCCCCCCHHHHHHHHHHHHHHHCCCCCCCCCCCCCHHHHHHHCCCCCCCCCCCCCCCCCCEEEEEECCCHHHHHHHHHH CCCC
MVNENTRMYVPEENHQGSNYGSPRPAHANMNANAAAGLAP EHIPTPGAALSWQAAIGAARQAKLMGSAGNATISTVSSTQKRQQYGKPKKQGGTTATRPPRALLCLTLKNPIRRACISI VEWK
10
20
30
40
50
60
70
80
90
100
110
120
B
Nterm
N1
N2
N2A
N2B
N2B-I
N2B-II

Figure 3-1

Figure 3-1: Relevant GFP fusion protein of the Cav1.2 N-terminus. A) Predicted secondary structure (PSIPRED http://bioinf.cs.ucl.aIt c.uk/psipred/) of the Cav1.2 N-terminus. Residue W52 (in green box) has been previously demonstrated to bind Ca^{2+}/CaM and regulate N-lobe CDI of Cav1.2. The red box shows the region known to bind CaBP. B) Map of Cav1.2 N-terminal GFP fusion proteins (GFP is C-terminal to channel sequences).

3.2 Results

3.2.1 Refining a CaM binding site in the N-terminus of Cav1.2

The distal N-terminus of L-type calcium channels, specifically a tryptophan residue (W82 in cardiac and W52 in neuronal Cav1.2 splice variants), has been identified as a CaM binding site. W52 functions to inactivate L-type calcium channels in response to a local Ca^{2+} increase and is unique to the Cav1 family of calcium channels [134, 229] (Figure 3-1, green box). The current model for N-lobe CDI of Cav1.2 depicts CaM bridging the C- and N-termini of the channel during inactivation, which is reasonable considering that the two termini are likely in close proximity in the holochannel. However, what is not know is how the interaction of the CaM N-lobe with the Cav1.2 N-terminus alters channel gating, and it is thus possible that there may be a CDI transduction element that has not yet been found.

To scan for candidate CaM binding sites we constructed GFP fusion proteins of the Cav1.2 N-terminus (Figure 3-1B) and designed these fusion proteins based on predicted secondary structure (PSIPRED http://bioinf.cs.ucl.ac.uk/psipred/) rather than primary sequence. Scanning the N-terminus for CaM binding motifs did not identify an obvious consensus sequence. We then screened for CaM interactions by pulling down Cav1.2 N-terminal-GFP fusion proteins with CaM Sepharose, in calcium (0.5mM) (Figure 3-2). As shown in Figure 3-2A, the full N-terminus, N_2 and N_{2B} portions of Cav1.2 all bound readily to CaM Sepharose in calcium, but also unexpectedly, in the absence of free calcium (5mM EGTA) (Figure 3-2B and C). An analogous set of experiments involving 5mM BAPTA washes (Figure 3-3) revealed that binding of the N-terminus to CaM Sepharose persisted irrespective of the type of buffer used.

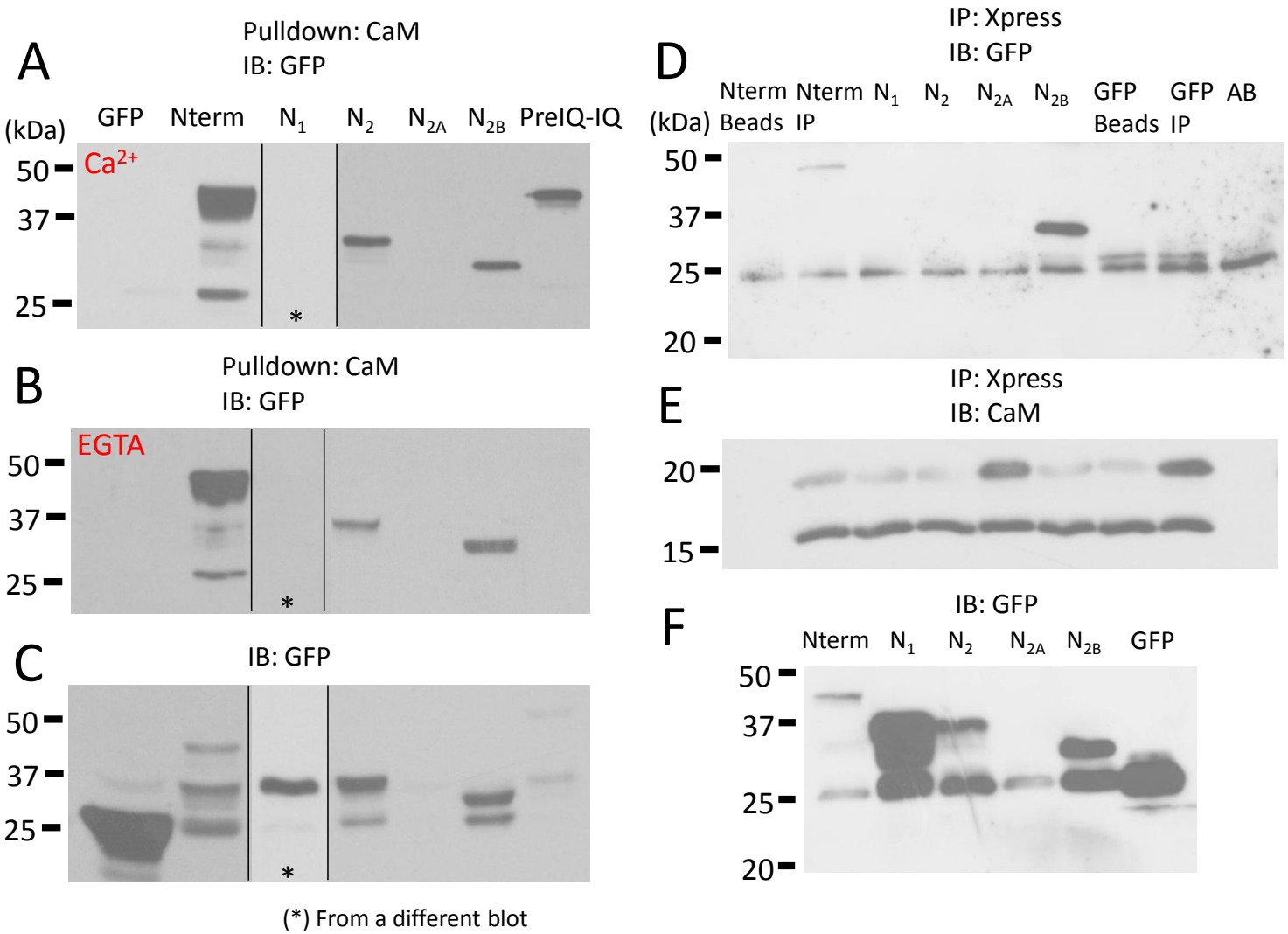
A
Pulldown: CaM
IB: GFP
(kDa)
GFP
Nterm
N1
N2
N2A
N2B
PreIQ-IQ
50
37
25
Ca2+
*
B
Pulldown: CaM
IB: GFP
EGTA
50
37
25
*
C
IB: GFP
50
37
25
*
(*) From a different blot
D
IP: Xpress
IB: GFP
(kDa)
Nterm Beads
Nterm IP
N1
N2
N2A
N2B
GFP Beads
GFP IP
AB
50
37
25
20
E
IP: Xpress
IB: CaM
20
15
F
IB: GFP
Nterm
N1
N2
N2A
N2B
GFP
50
37
25
20

Figure 3-2

Figure 3-2: Ca^{2+}/CaM binding site localized to distal N_{2B} region of N-terminus. A) CaM pulldown experiments of N-terminal GFP fusion proteins lysed in 0.5mM Ca^{2+}. The PreIQ-IQ segment of the Cav1.2 C-terminus was included as a control for Ca^{2+} sensitivity of CaM Sepharose. Pull downs of fusion proteins were washed with 0.5mM Ca^{2+}, or 5mM EGTA (B), and run on SDS-PAGE with corresponding lysates (C) and blotted for GFP. D) Co-immunoprecipitation experiments of CaM and N-terminal GFP fusion proteins (0.5mM Ca^{2+}). Immunoprecipitates of Xpress-CaM and controls (antibody (AB) or beads) were run on SDS-PAGE and blotted for GFP. E) Membranes were then stripped and re-probed for CaM. F) Western blot of GFP lysate. All pulldowns shown in the figure are a representative example of at least three experiments, co-IPs were done at least twice by Dr. Ivana Assis-Souza.

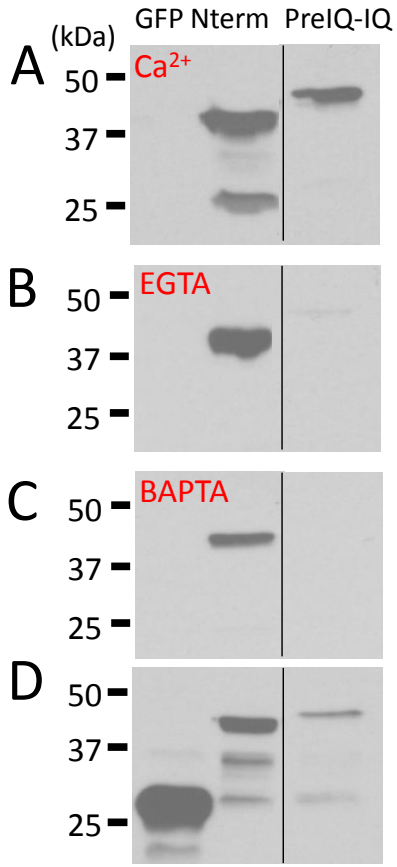

Duplicate samples removed from
between Nterm-GFP and PreIQ-IQ-GFP

Figure 3-3

Figure 3-3: Binding of Nterm-GFP to CaM sepharose persists in 5mM BAPTA. A) CaM pulldown experiments of N-term-GFP lysed in 0.5mM Ca^{2+}. The PreIQ-IQ segment of the Cav1.2 C-terminus was included as a control for Ca^{2+} sensitivity of CaM Sepharose. Pull downs of fusion proteins were washed with 0.5mM Ca^{2+}, or 5mM EGTA (B), or 5mM BAPTA (C) and run on SDS-PAGE with corresponding lysates (D) and blotted for GFP.

The efficacy of the buffers was also verified using a PreIQ-IQ-GFP construct, which lost its ability to interact with CaM beads in the presence of EGTA or BAPTA (Figure 3-2B and Figure 3-3 B/C). Although surprising for CaM, or CaM related proteins, calcium insensitive binding has been shown previously in the N_{2B} portion of Cav1.2 which binds CaBP in the absence of calcium [211].

To validate our findings, we performed standard co-immunoprecipitation (co-IP) experiments with N-terminal GFP fusion proteins with either wild type CaM, or Xpress tagged CaM. Figure 3-2D illustrates a co-IP between Xpress-CaM and $Nterm_{-GFP}$, as well as $N_{2B\text{-}GFP}$ in 0.5mM Ca^{2+} consistent with our findings obtained with CaM sepharose. On the other hand, $N_{2\text{-}GFP}$ did not appear to interact with CaM under these conditions in contrast with the CaM sepharose pull down. Furthermore, $N_{1\text{-}GFP}$ (containing W52) did not strongly bind to CaM Sepharose nor did we detect appreciable immunoprecipitation with CaM (Figure 3-4A). Weaker than expected binding between N_1 and CaM can be explained by a difference in N-terminal fusion proteins used in this study compared with previous work based on FRET measurements [134]. Careful comparison suggests that sequences following N_1 may increase the fidelity of a W52/CaM interaction. Alternatively FRET assays may be more sensitive and preserve more delicate interactions with CaM.

Interestingly, the calcium insensitivity seen with CaM pull downs was not observed in CaM co-IP experiments which were never successful in the presence of 5 mM EGTA (Figure 3-4C).

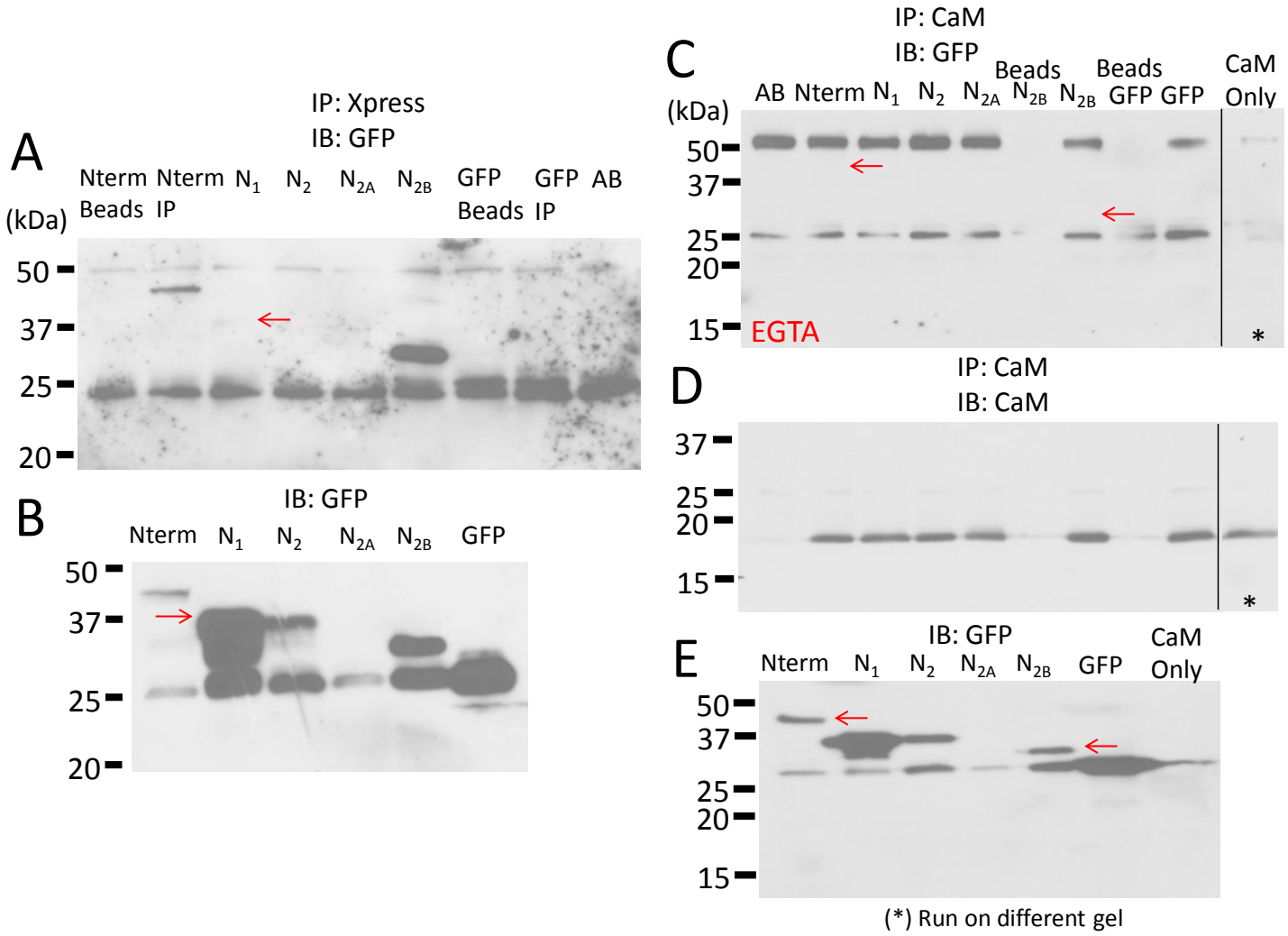
A
IP: Xpress
IB: GFP
Nterm Beads
Nterm IP
N1
N2
N2A
N2B
GFP Beads
GFP IP
AB
(kDa)
50
37
25
20
B
IB: GFP
Nterm
N1
N2
N2A
N2B
GFP
50
37
25
20
C
IP: CaM
IB: GFP
AB
Nterm
N1
N2
N2A
Beads N2B
Beads N2B
GFP
GFP
CaM Only
(kDa)
50
37
25
20
15
EGTA
*
D
IP: CaM
IB: CaM
37
25
20
15
*
E
IB: GFP
Nterm
N1
N2
N2A
N2B
GFP
CaM Only
50
37
25
20
15
(*) Run on different gel

Figure 3-4

Figure 3-4: N_1 binds weakly to Ca^{2+}/CaM and N_{2B} region does not bind CaM in 5mM EGTA by co-IP. A) Overexposed co-IP blot from Figure 2D showing very weak binding of N_1 segment to CaM (0.5mM Ca^{2+}). B) N-terminal-GFP fusion protein lysates from Figure 2F duplicated for ease of reference. Red arrows denote expected band size. C) Co-immunoprecipitation experiments of CaM and N-terminal GFP fusion proteins (5mM EGTA). Immunoprecipitates of CaM and controls (antibody (AB) or beads) were run on SDS-PAGE and blotted for GFP. D) Membranes were then stripped and re-probed for CaM. E) Western blot of GFP lysate.

A possible reason for this difference is that interactions in live cells may be more sensitive than what is reflected by an *in vitro* pulldown where a very high concentration of CaM is presented to target proteins. Hence, the higher calcium sensitivity in the co-IPs likely presents a more physiologically relevant scenario.

3.2.2 $N_{2B\text{-}II}$ binds α-CaMKII while C106 is a CaM binding residue in the proximal N*-terminus of Cav1.2*

Next, we further narrowed down the channel structural determinants of CaM binding by separating the beta fold ($N_{2B\text{-}I}$) from the remaining alpha-helix ($N_{2B\text{-}II}$) (see Figure 3-1). We then carried out CaM pull down experiments as described above. As shown in Figure 3-5 (A-C) both $N_{2B\text{-}I}$ and $N_{2B\text{-}II}$ were subject to pull-down with CaM Sepharose. $N_{2B\text{-}I}$ contains a conspicuous cysteine residue at position 106 which we targeted. When replaced with arginine, the co-immunoprecipitation of the $N_{2B\text{-}I}$ region with CaM in 0.5mM Ca^{2+} was ablated (Figure 3-5D). This is recapitulated in Figure 3-5A with CaM pull downs. Furthermore, co-IP of CaM with $N_{2B\text{-}I}$-GFP was reproducibly inhibited by 5mM EGTA washes (data not shown) indicating that Ca^{2+} is critical for the interaction of $N_{2B\text{-}I}$ with CaM.

At a first glance, our findings shown in Figure 3A-5 would indicate that the proximal N-terminus of Cav1.2 may contain two separate CaM interaction sites. However, it is equally possible that one or both of these regions may interact with a CaM binding protein rather than CaM *per se*, such as for example, CaMKII. Indeed, there are examples in the literature in which CaM sepharose was used to purify CaM kinase [234] due to its high affinity for CaM [235].

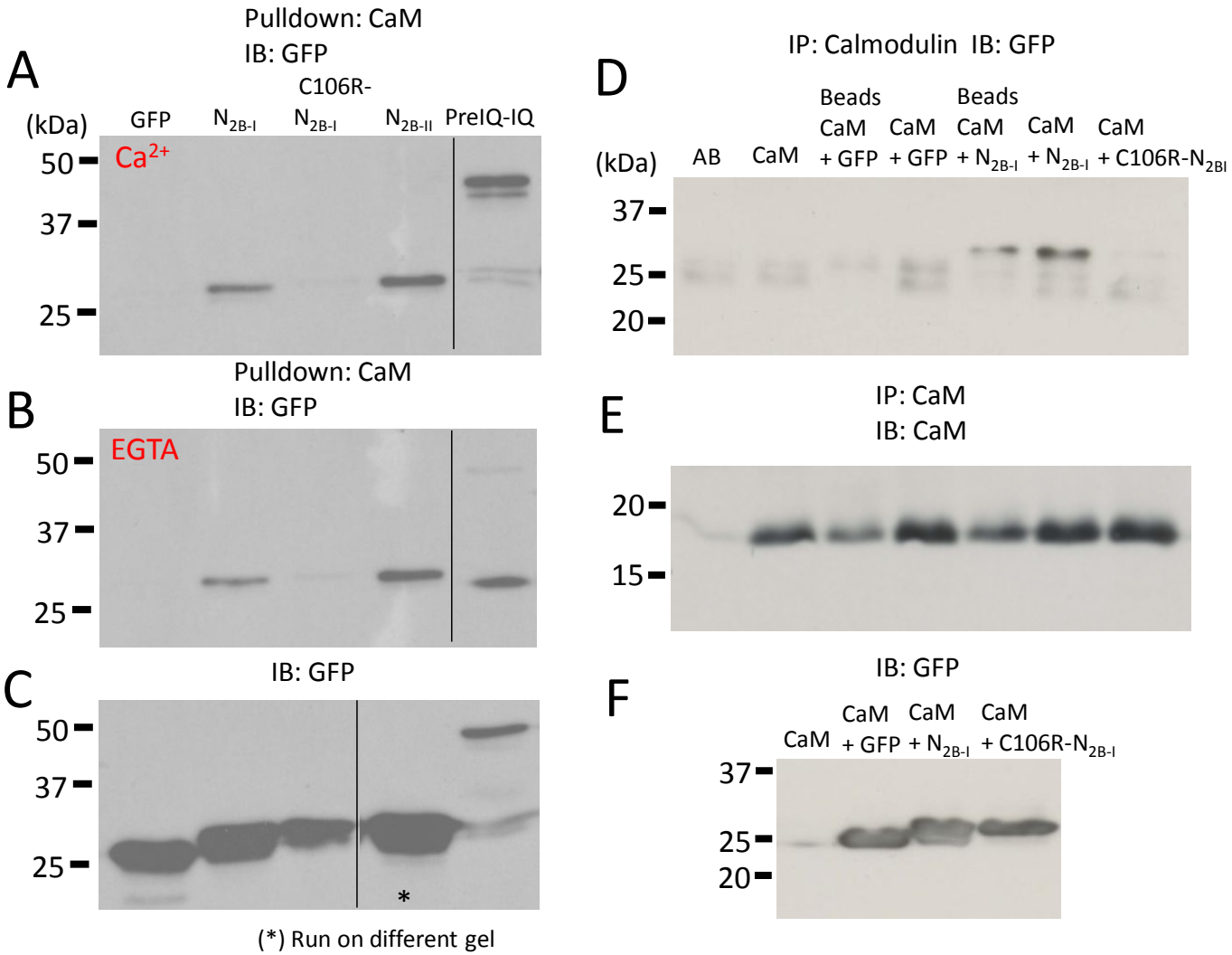
A
Pulldown: CaM
IB: GFP
(kDa)
GFP
N2B-I
C106R-N2B-I
N2B-II
PreIQ-IQ
50
37
25
Ca2+
B
Pulldown: CaM
IB: GFP
EGTA
50
37
25
C
IB: GFP
50
37
25
*
(*) Run on different gel
D
IP: Calmodulin IB: GFP
(kDa)
AB
CaM
Beads CaM + GFP
CaM + GFP
Beads CaM + N2B-I
CaM + N2B-I
CaM + C106R-N2BI
37
25
20
E
IP: CaM
IB: CaM
20
15
F
IB: GFP
CaM
CaM + GFP
CaM + N2B-I
CaM + C106R-N2B-I
37
25
20

Figure 3-5:

Figure 3-5: C106 residue of N_{2B-I} binds CaM. A) CaM pulldown experiments of $N_{2B-I/II}$ GFP fusion proteins lysed in 0.5mM Ca^{2+}. The PreIQ-IQ segment of the Cav1.2 C-terminus was included as a control for Ca^{2+} sensitivity of CaM Sepharose. Pull downs of fusion proteins were washed with 0.5mM Ca^{2+}, or 5mM EGTA (B), and run on SDS-PAGE with corresponding lysates (C) and blotted for GFP. All pulldowns shown in the Figure are a representative example of at least three experiments. D) Co-immunoprecipitation experiments of N_{2B-I}, or C106R-N_{2B-I}-GFP with CaM carried out in 0.5mM Ca^{2+}. Immunoprecipitates of calmodulin and controls (antibody (AB)/beads alone) were run on SDS-PAGE and blotted for GFP. E) Membranes were then stripped and re-probed for CaM. (E) Western blot for GFP in lysate (F). Note lysates for IPs and controls are from the same sample and not shown in duplicate. The co-IP is a representative example of at least two independent experiments performed by Dr. Ivana Assis Souza.

To determine whether this may be the case, we co-expressed a fluorescently tagged α-CaMKII with N_{2B-I}-GFP and N_{2B-II}-GFP and then examined the subcellular distributions of the fluorescence signals. As shown in Figure 3-6A and B, N_{2B-II}-GFP formed large aggregates that perfectly co-localized with α-CaMKII-mCherry (ICQ value = 0.34 ± 0.03, n=4 $p \leq 0.001$ by student's *t*-test), but not mCherry (ICQ value= -0.21 ± 0.03, n=4). Colocalization was also observed with a GFP-tagged version of a known CaMKII interaction motif (i.e., PreIQ-IQ-GFP [139], Figure 3-7). In contrast, no colocalization was observed between α-CaMKII-mCherry and either GFP, or the N_{2B-I}-GFP constructs (Figure 3-6C/D). These data suggest that N_{2B-II} may interact with CamKII, and that the pulldown of N_{2B-II} with CaM sepharose may occur indirectly via CamKII. A follow up co-IP with α-CaMKII-mCherry in 5mM EGTA verified that N_{2B-II}-GFP (Figure 3-6E) co-immunoprecipitated with CaM kinase whereas GFP or N_{2B-I}-GFP did not. We note that N_{2B-II}-GFP formed clusters even in the absence of coexpressed α-CaMKII-mCherry, presumably because of the formation of dodecameric complexes of endogenous CamKII (for review see [236]), whereas N_{2B-I}-GFP did not (Figure 3-6B/E). Altogether, our data suggest that while the N_{2B-II} region appears to form a CaMKII interaction domain, N_{2B-I} may in fact be a bona fide CaM interaction site. Because CDI is linked to CaM [117, 237] rather than CaMKII [223], we thus focused further attention on the N_{2B-I} site.

3.2.3 C106 modulates local Ca^{2+} mediated CDI of Cav1.2

To determine the functional role of the C106 site, we carried out whole cell patch clamp recordings. To isolate local Ca^{2+} signaling all experiments in Figure 3-8 were performed in 10mM BAPTA, which restricts Ca^{2+} signals to the immediate vicinity of the channel, or channel nano-domain [238].

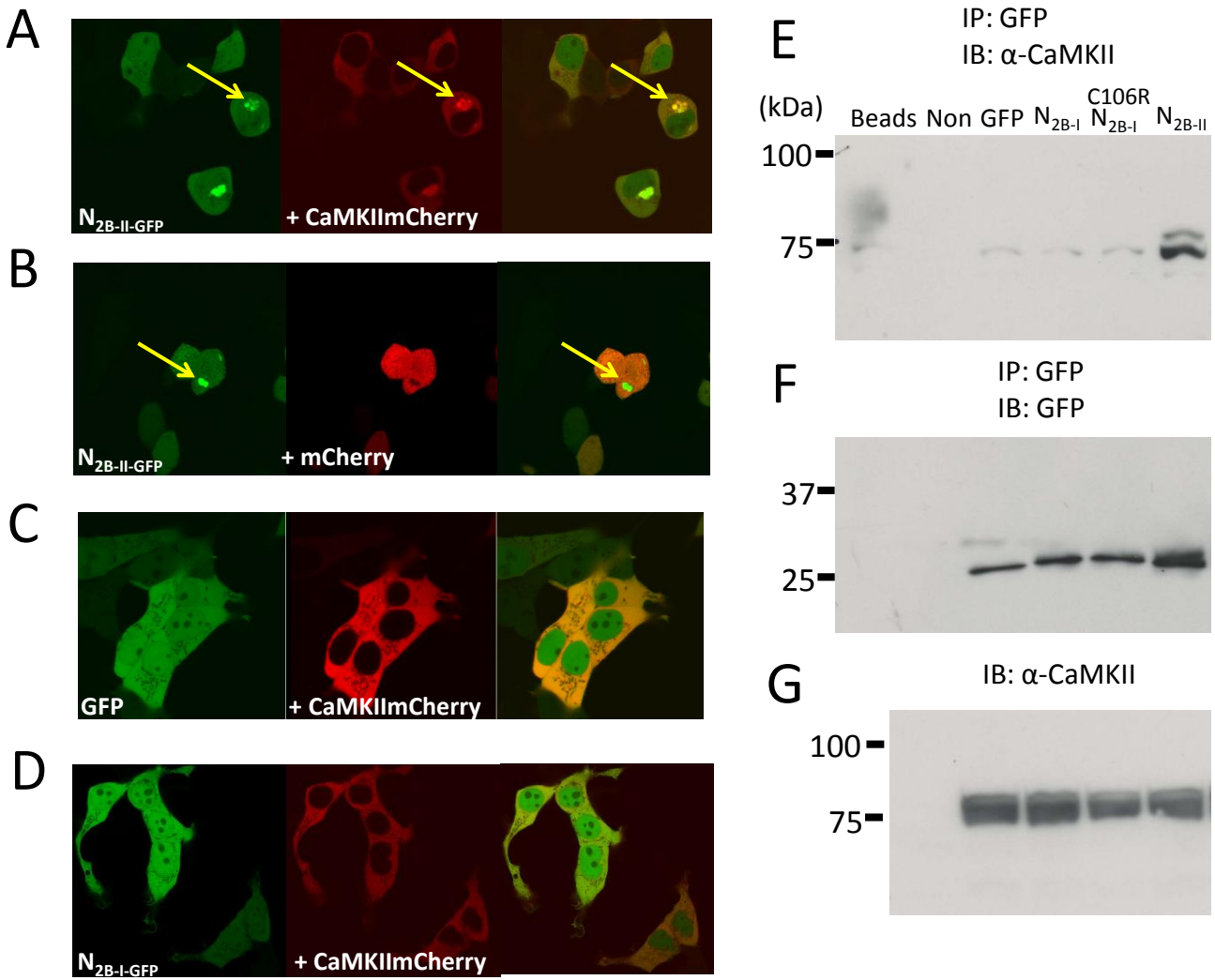
A
N2B-II-GFP
+ CaMKIImCherry
B
N2B-II-GFP
+ mCherry
C
GFP
+ CaMKIImCherry
D
N2B-I-GFP
+ CaMKIImCherry
E
IP: GFP
IB: α-CaMKII
(kDa)
Beads
Non GFP
N2B-I
C106R N2B-I
N2B-II
100
75
F
IP: GFP
IB: GFP
37
25
G
IB: α-CaMKII
100
75

Figure 3-6

Figure 3-6: $N_{2B\text{-}II}$ but not $N_{2B\text{-}I}$ colocalizes with and binds α-CaMKII. A) Confocal images of live tsA-201 cells expressing mCherry-α-CaMKII and $N_{2B\text{-}II}$-GFP, or mCherry and $N_{2B\text{-}II}$-GFP (B), or mCherry-α-CaMKII and GFP (C), or mCherry-α-CaMKII and $N_{2B\text{-}I}$-GFP (D). Yellow arrows highlight co-localization. Note that the gain in panels A and D was reduced relative to panel C because of the brightness of the aggregates, and hence the dimmer mCherry signal does not represent less expression. E) Co-immunoprecipitation experiments of mCherry-α-CaMKII and $N_{2B\text{-}I}$, C106R-$N_{2B\text{-}I}$ and $N_{2B\text{-}II}$ GFP. Immunoprecipitates of GFP and controls (IgG only & beads alone) were run on SDS-PAGE and blotted for α-CaMKII. F) Membranes were then stripped and re-probed for GFP. G) Western blot of α-CaMKII in lysate. All co-IPs are representative examples of multiple independent experiments performed by Dr. Ivana Assis Souza.

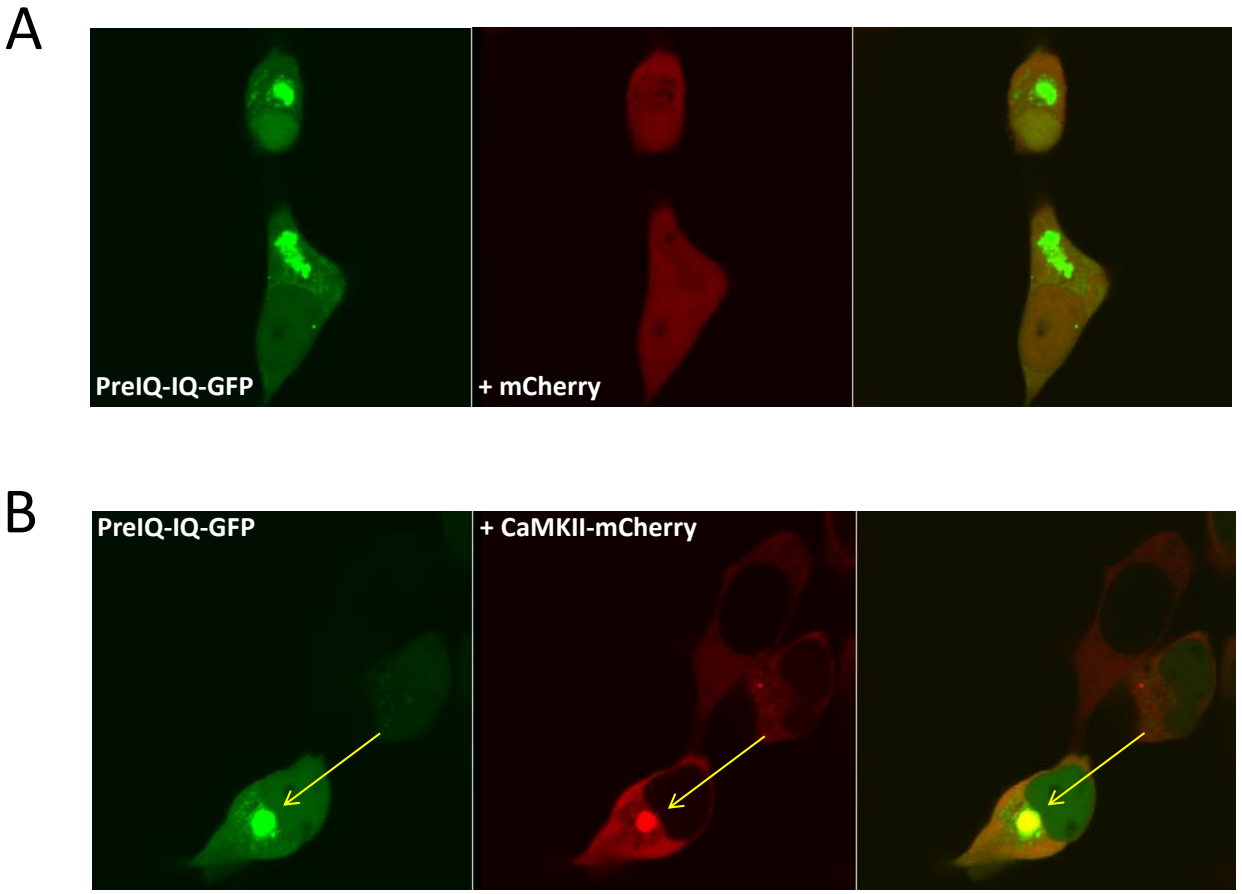

Figure 3-7

Figure 3-7: PreIQ-IQ-GFP colocalizes in aggregates with α-CaMKII-mCherry. A) Confocal images of live tsA-201 cells expressing mCherry and PreIQ-IQ-GFP, or mCherry-α-CaMKII and PreIQ-IQ-GFP (B). Yellow arrows highlight co-localization. Images gathered by Dr. Ivana Assis-Souza.

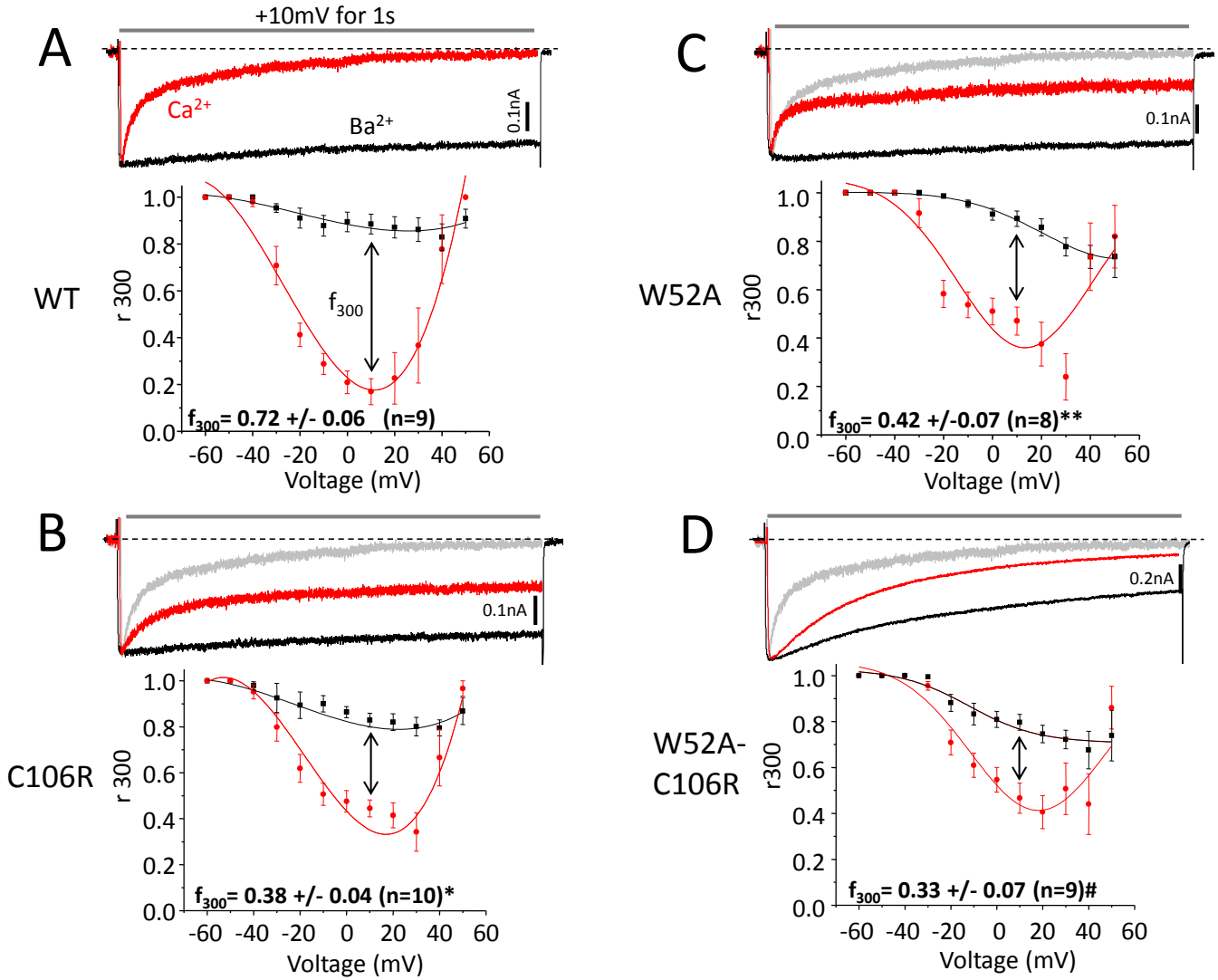
A
+10mV for 1s
Ca2+
Ba2+
0.1nA
WT
r 300
f300
f300= 0.72 +/- 0.06 (n=9)
Voltage (mV)
B
0.1nA
C106R
f300= 0.38 +/- 0.04 (n=10)*
C
0.1nA
W52A
r300
f300= 0.42 +/-0.07 (n=8)**
D
0.2nA
W52A-
C106R
f300= 0.33 +/- 0.07 (n=9)#

Figure 3-8

Figure 3-8: N-terminal C106 residue plays a critical role in global CDI of Cav1.2. A) Representative Ba^{2+} (black) and Ca^{2+} (red) traces of WT-Cav1.2 channels expressed with Cavβ2a/Cavα2δ in the presence of high calcium buffering internal solution (10mM BAPTA). Note that the peak of the Ba^{2+} trace is normalized to that of Ca^{2+} and that average CDI (f_{300}) of WT-Cav1.2 is displayed in the graph. B) C106R-Cav1.2 has significantly less CDI than WT-Cav1.2 (*$p \leq 0.05$ by one-way ANOVA). For reference the WT-Cav1.2 Ca^{2+} trace is displayed in grey. C) W52A-Cav1.2 has significantly less CDI than WT-Cav1.2, but not significantly less than C106R-Cav1.2 (**$p \leq 0.05$ by one-way ANOVA). D) The double mutant W52A-C106R-Cav1.2 has significantly less CDI than WT-Cav1.2 (# $p \leq 0.05$ by one-way ANOVA), but not less than W52A, or C106R-Cav1.2 channels.

Figure 3-8A shows a representative set of paired traces from WT-Cav1.2 channels recorded in Ba^{2+} (black) and then Ca^{2+} (red). The Ca^{2+} trace shows significant CDI over the duration of a 1 second pulse to +10mV, whereas the Ba^{2+} trace shows very little inactivation. Plotted in the graph below the traces is the fractional inactivation at 300ms (r300) in Ba^{2+} (black) and Ca^{2+} (red) across the various test potentials. Subtracting the additional inactivation imposed by Ca^{2+} on the channel, compared to Ba^{2+}at 300 ms, yields an f_{300} value (black arrow) that is a direct reflection of CDI. As shown in Figure 3-8A**,** WT-Cav1.2 channels demonstrate dramatic CDI and as a consequence have a large f_{300} value of 0.72 ± 0.06. By comparison C106R-Cav1.2 (Figure 3-8B) has a significantly reduced f_{300} value of 0.38 ± 0.04 (* $p \leq 0.05$ by ANOVA) when compared to WT-Cav1.2. Similar reductions in CDI are observed with W52A-Cav1.2 (Figure 3-8C) (f_{300}= 0.42 ± 0.07, * $p \leq 0.05$ by ANOVA) and the double-mutant W52A-C106R-Cav1.2 (Figure 3-8D) (f_{300}= 0.33 ± 0.07, * $p \leq 0.05$ by ANOVA). The fact that W52A-Cav1.2, C106R-Cav1.2 and W52A-C106R-Cav1.2 do not have statistically different f_{300} values, suggests that W52 and C106 are likely involved in the same, local CDI process.

3.2.4 C106 as a functional site for Cav1.2 N-lobe CDI

As C106 appears to contribute to local CDI of Cav1.2 channels, we tested whether mutants of CaM deficient for binding Ca^{2+} in their C-lobe (CaM_{34}), could alter N-lobe CDI for C106R-Cav1.2. All traces in Figure 3-9 were recorded in 0.5mM EGTA in order to provide the N-lobe of CaM (in this case CaM_{34}) with the abundance of Ca^{2+} needed to function. Figure 3-9A shows that WT-Cav1.2 channels (f_{300}= 0.45 ± 0.07) exhibit significant N-lobe CDI when expressed with CaM_{34} and recorded in Ca^{2+} (red trace), when compared to Ba^{2+} (black trace).

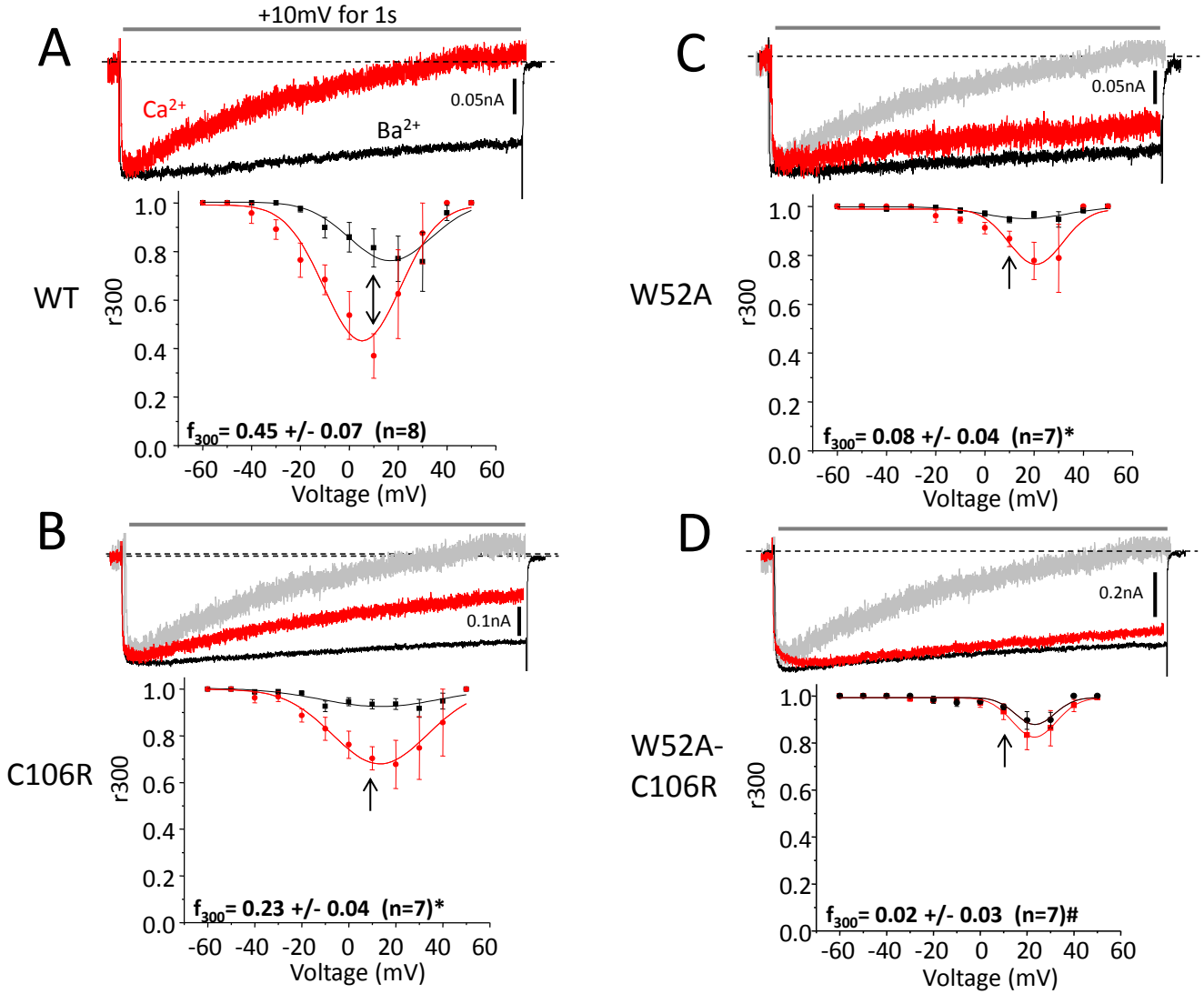
A
+10mV for 1s
Ca2+
Ba2+
0.05nA
WT
r300
1.0
0.8
0.6
0.4
0.2
0.0
f300= 0.45 +/- 0.07 (n=8)
-60 -40 -20 0 20 40 60
Voltage (mV)
C
0.05nA
W52A
f300= 0.08 +/- 0.04 (n=7)*
B
0.1nA
C106R
f300= 0.23 +/- 0.04 (n=7)*
D
0.2nA
W52A-
C106R
f300= 0.02 +/- 0.03 (n=7)#

Figure 3-9

Figure 3-9: Both C106 and W52 residues modulate N-lobe CDI of Cav1.2. A) Representative Ba^{2+} (black) and Ca^{2+} (red) traces of WT-Cav1.2 channels expressed with Cavβ2a/Cavα2δ in the presence of low calcium buffering (0.5 EGTA). Note that the peak of the Ba^{2+} trace is normalized to that of Ca^{2+} and that average CDI (f_{300}) of WT-Cav1.2 is displayed below in the graph. B) C106R-Cav1.2 display significantly less CDI than WT-Cav1.2 (*$p \leq 0.05$ by one-way ANOVA). For reference the WT-Cav1.2 Ca^{2+} trace is displayed in grey. C) W52A-Cav1.2 has significantly less CDI than WT-Cav1.2 (*$p \leq 0.05$ by one-way ANOVA), but not less than C106R-Cav1.2. D) The double mutant W52A-C106R-Cav1.2 has significantly less CDI than both WT-Cav1.2 and C106R-Cav1.2 (# $p \leq 0.05$ by one-way ANOVA), but not W52A-Cav1.2.

Compared with WT-Cav1.2 Ca^{2+} (grey trace), C106R-Cav1.2 (f_{300}=0.23 ± 0.04, *p≤0.05 by ANOVA) shows significantly reduced N-lobe CDI, as does W52A-Cav1.2 (f_{300}=0.08 ± 0.04, *p≤0.05 by ANOVA) and W52A-C106R-Cav1.2 (f_{300}=0.02 ± 0.03, #p≤0.05 by ANOVA) (Figure 3-9B-D). Furthermore the double mutant W52A-C106R-Cav1.2 has significantly less CDI than C106R-Cav1.2, but not W52A-Cav1.2. Altogether, these data suggest that W52 is the dominant residue involved in Cav1.2 N-lobe CDI, but also that C106 is intimately tied to W52 in function. Figure 3-10 verifies that the C-lobe of CaM_{34} is non-functional in our experiments, as 10 mM BAPTA suffices to remove any difference in N-lobe CDI for WT-Cav1.2 (f_{300}=0.08 ± 0.03, p≥0.05 by ANOVA), C106R-Cav1.2 (f_{300}=0.1 ± 0.03, p≥0.05 by ANOVA), W52A-Cav1.2 (f_{300}=0.07 ± 0.05, p≥0.05 by ANOVA) and W52A-C106R-Cav1.2 (f_{300}=0.02 ± 0.04, p≥0.05 by ANOVA).

3.3 Discussion

CaM is an important functional regulator of CDI and recently the N-terminus of L-type channels has been shown to modulate this process [134]. Here, we show that N-lobe CDI for Cav1.2 channels involves a second N-terminal CaM interaction site at residue C106 that contributes to this process. We also identified a CaMKII interaction domain adjacent to this CaM interaction site which we did not further explore here. It is however interesting to note that the CaMKII interacting peptides formed aggresomal clusters in tsA-201 cells – a property that could potentially be exploited as a screen for CaMKII interacting peptides in live cells.

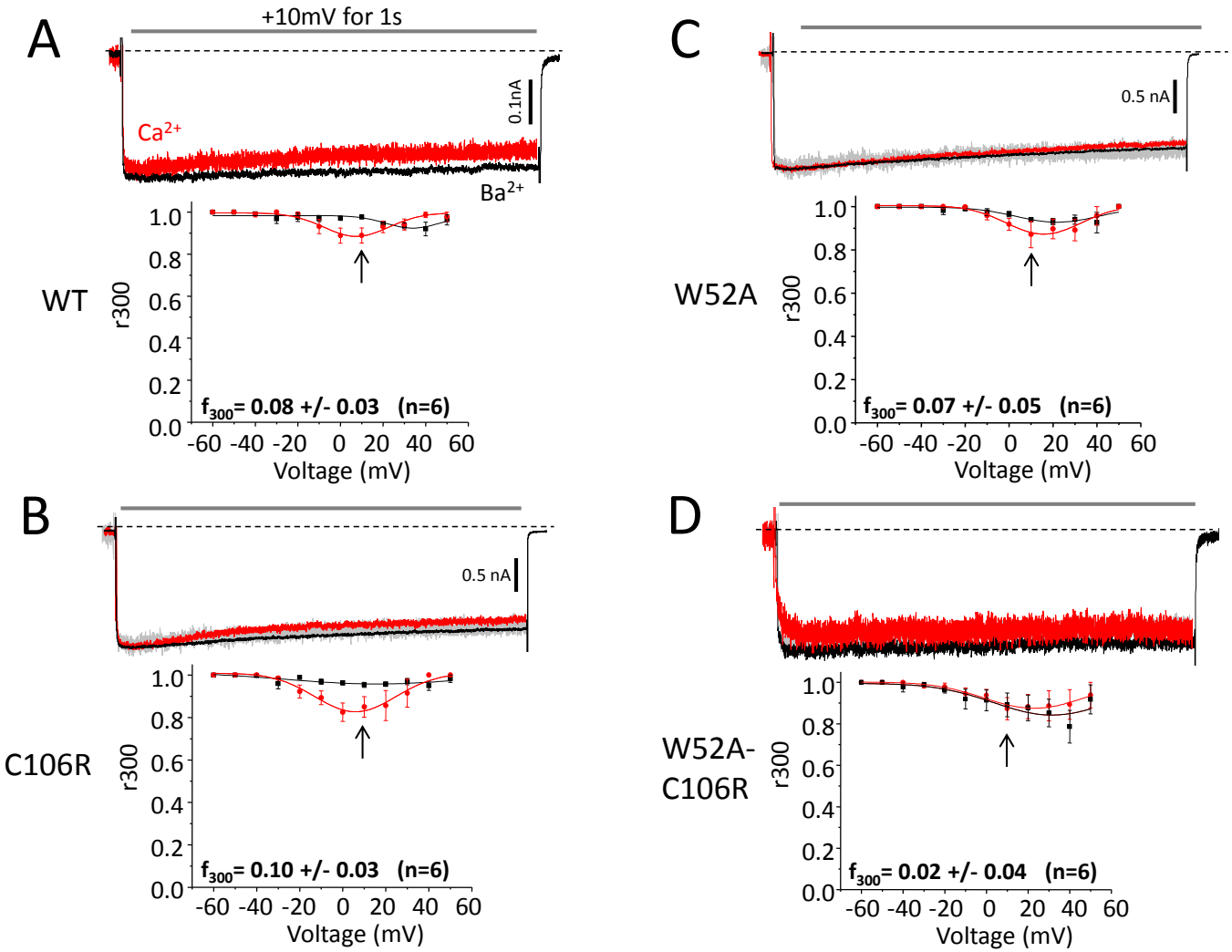
A
+10mV for 1s
0.1nA
Ca2+
Ba2+
WT
r300
1.0
0.8
0.6
0.4
0.2
0.0
f300= 0.08 +/- 0.03 (n=6)
-60 -40 -20 0 20 40 60
Voltage (mV)
B
0.5 nA
C106R
f300= 0.10 +/- 0.03 (n=6)
C
0.5 nA
W52A
f300= 0.07 +/- 0.05 (n=6)
D
W52A-
C106R
f300= 0.02 +/- 0.04 (n=6)

Figure 3-10

Figure 3-10: C106R-Cav1.2 lacks CDI with CaM_{34} in 10mM BAPTA. A) Representative Ba^{2+} (black) and Ca^{2+} (red) traces of WT-Cav1.2 channels expressed with Cavβ2a/Cavα2δ/ CaM34 in the presence of high calcium buffering (10mM BAPTA). Note that the peak of the Ba^{2+} trace is normalized to that of Ca^{2+}.The average CDI (f_{300}) of WT-Cav1.2 is displayed below in the graph. Arrows point to +10mV, r300 values used for f_{300} calculation. B) C106R-Cav1.2 displays CDI not significantly different from WT-Cav1.2 ($p \geq 0.05$ by one-way ANOVA). For reference the WT-Cav1.2 Ca^{2+} trace is displayed in grey. C) W52A-Cav1.2 has CDI not significantly different from WT-Cav1.2, as does the double mutant W52A-C106R-Cav1.2 ($p \geq 0.05$ by one-way ANOVA) (D).

Our biochemical data are consistent with C106 forming a calcium sensitive CaM binding site, or alternatively that removing C106 destabilizes CaM binding with neighboring hydrophobic leucines (i.e. L104/5) which are considered canonical for CaM binding [239]. CaM does not contain a cysteine residue therefore disulfide bonding with C106 is unlikely, yet palmitoylation of C106 could sterically or allosterically regulate CaM association: to the best of our knowledge we are unaware of such an example in the literature. Furthermore if palmitoylation of C106 were to regulate CaM binding we would also expect GFP constructs containing palmitoylated C106 to traffic to the cell membrane [240]- as per one of the functions of this modification- which they do not appear to do in our hands. Our electrophysiological analysis suggests that C106 is an important site for local CDI (without overexpressed CaM), and more specifically, N-lobe CDI of Cav1.2 as evident from our results with CaM_{34}. Our data indicate that W52 and C106 participate in the same CDI process with W52 dominating N-lobe CDI. That said W52 and C106 mutations reduced CDI compared to WT-Cav1.2, suggesting that both residues are functionally important.

So how do our data fit with current thinking about the mechanisms of Cav1.2 CDI? Figure 3-11A shows a cartoon of N-lobe CDI for Cav1.2 channels whereby a C-terminal CaM molecule, upon global Ca^{2+} rise, releases its N-lobe from the channel C-terminus. The N-lobe then binds N-terminus which inactivates the channel. The observed Ca^{2+}/CaM sensitivity of CaM binding to W52 and C106 suggests that neither residue is capable of providing an CaM anchoring site under resting channel conditions (i.e., under conditions where calcium concentration is low). Hence, pre-association of apo-CaM is unlikely to occur in the N-terminus, and instead requires the C-terminal region of the channel [122, 133, 208] (i.e. PCI-2-IQ) and so therefore this aspect remains essential to the model. The addition of C106 to this model suggests

that the N-terminus must be folded during CDI such that both W52 and C106 can bind the N-lobe of CaM. The N-terminus has been previously shown to regulate channel gating [158, 241], and it is thus possible that e function of the region near C106 is to transmit, or transduce CDI from the dominant CaM binding residue W52 through to domain I. In such a model, the region near C106 would act as an *N*SCaTE *A*ssociated *T*ransduction *E*lement (NATE) that transduces the binding of CaM into a change in channel function.

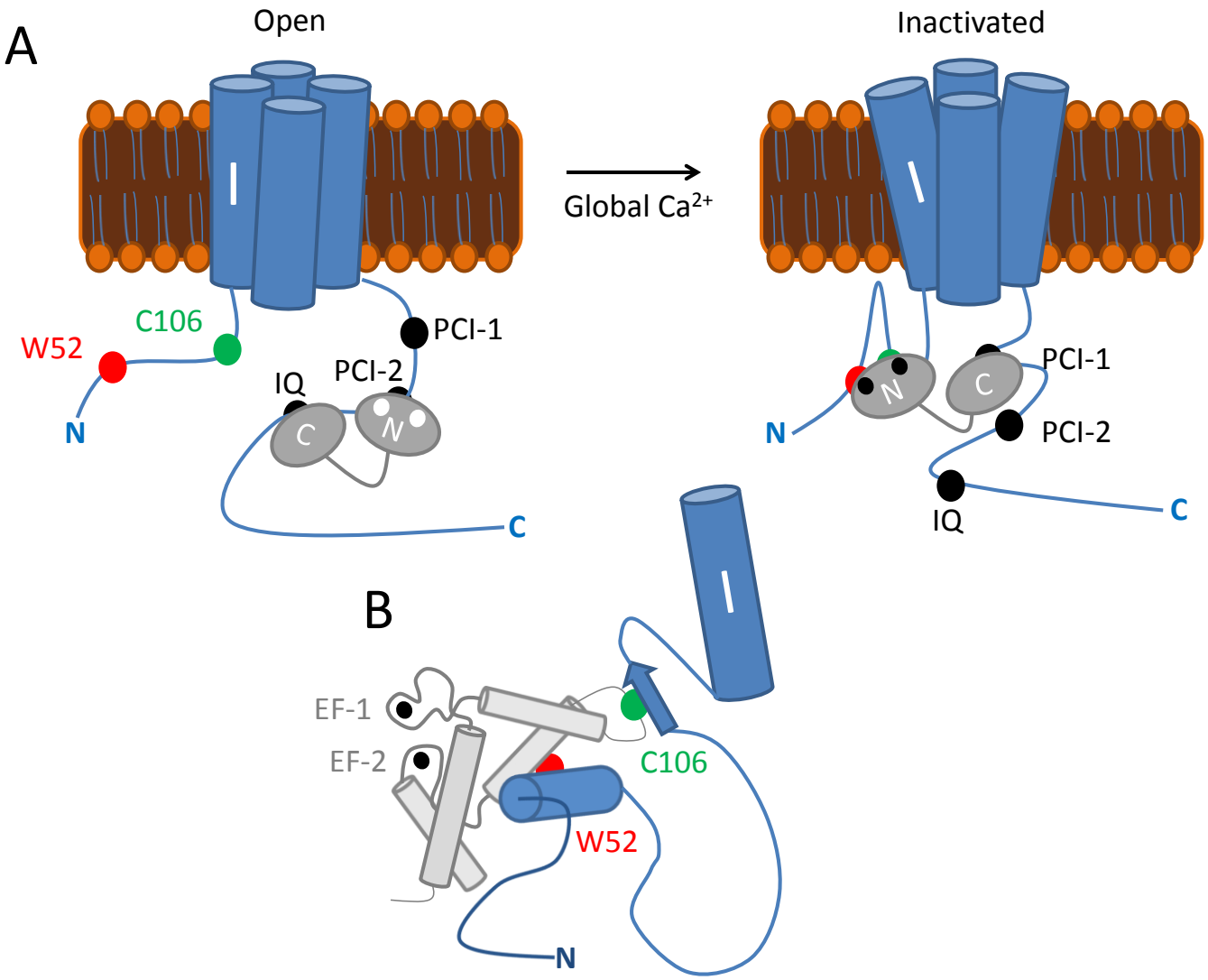
A
Open
Inactivated
Global Ca2+
I
C106
W52
N
IQ
PCI-2
PCI-1
C
N
C
N
PCI-1
PCI-2
IQ
C
B
I
EF-1
EF-2
C106
W52
N

Figure 3-11

Figure 3-11: Working model for N-lobe CDI of Cav1.2. A) The working model of N-lobe CDI for Cav1.2 channels whereby CaM bridges the C and N-termini in response to global calcium increase and inactivates the channel. At rest CaM is anchored on the C-terminus at the IQ domain and PCI-2. Note also that the N-lobe lacks calcium (white circles) at rest. Upon a global calcium increase the N-lobe binds two Ca^{2+} ions (black circles) and forms a tripartite N-terminal association with both W52 (NSCaTE) and C106 (NATE). The C-lobe of CaM remains associated with the C-terminus, but shifts from PCI-2 to PCI-1. B) A hypothetical cartoon for the association of NSCaTE and NATE with the N-lobe of CaM during CDI. The N-lobe of CaM (grey) interacts with W52 (red) which is located in the NSCaTE alpha helix via its own EF-hand alpha helix. Note both EF-hands are occupied with calcium (black circles). This then creates an interaction site for C106 (green) within the NATE beta fold, which allosterically modulates channel gating.

Given that some CDI is observed for C106R-Cav1.2 with CaM_{34}, but virtually none is with W52A-Cav1.2 or W52A-C106R-Cav1.2 under the same condition we propose that W52 may be the *sensor* for N-lobe CDI and C106 the *transducer* of that signal.

Figure 3-11B illustrates how the NATE sequence may interact with NSCaTE. NSCaTE resides in an alpha-helical structure and interacts favorably with an EF-hand helix in the N-lobe of CaM [242]. NATE conversely is predicted to be part of a β-fold structure (Figure 3-1). Most CaM binding interactions with ion channels involve alpha helices [84, 85] (and for review see [243]) but CaM has also been shown to bind beta strands [244]. Hence, we suggest that the low affinity N-lobe of CaM interacts with NSCaTE as proposed by Liu and colleagues [88]. We envision that the NATE motif would then associate with this CaM/NSCaTE complex, thus transducing the NSCaTE/CaM binding into a change in channel function. Mutations in either residue W52 or C106 would disrupt the overall N-lobe CDI mechanism.

Such intra-region interactions are seen with other parts of L-type channels. For example, the PCI-2 region and IQ domain are separated by over 70 amino acids and yet come close enough to support apoCaM binding at rest. Functionally, PCI-1 (adjacent EF-hand motif) and the IQ domain have been shown to work in concert and transduce CDI signals up the C-terminus to the channel [121, 221], which is not unlike what we are proposing for NSCaTE and NATE. The C-terminus of Cav1.4 channels illustrates another example of intra-linker interaction which effect CDI. For Cav1.4 channels the very distal C-terminus is able to fold back and interact with the PCI-1 region of the channel (over 440a.a. of separation), thus preventing successful transduction of CDI [127, 245] and a sustained conductance needed in the retina. These examples of intra-linker interactions suggest that NSCaTE and NATE could be interacting similarly with CaM to promote global CDI of Cav1.2.

In conclusion, our data expand current thinking about the mechanism of N-lobe CDI for L-type calcium channels. We have shown that C106 is an important residue in this process and that functionally NSCaTE and NATE cooperatively regulate N-lobe CDI of Cav1.2 channels. It appears then, that N-lobe CDI of Cav1.2 is more complicated and involves a larger portion of the N-terminus than previously thought.

CHAPTER FOUR: **THE BRUGADA SYNDROME MUTATION A39V DOES NOT AFFECT TRAFFICKING BUT DOES AUGMENT CAV1.2 CDI AND ACTIVATION GATING BY CAM MUTANTS**

4.1 Background

Extensive alternate splicing of Cav1.2 channels between neuronal and cardiac backgrounds alters channel structure and function, as does the type of Cavβ subunit that is expressed in a given tissue [60, 246-248]. A loss of Cav1.2 function can give rise to a heart specific disorder termed Brugada syndrome whose phenotype consists of a shortened Q-T interval, ventricular fibrillation and sudden cardiac death (SCD) [174]. How exactly reduced Cav1.2 function selectively affects the heart and not the brain is unknown, but may be explained by tissue-specific splice isoforms of the channel. Recent reports of splice isoform specific effects of mutations in Cav2 and Cav3 VGCCs [249, 250] suggest that the tissue selective effect of Brugada syndrome mutations could be related to Cav1.2 channel sequences which are specific to the heart.

Recently a point mutation in the N-terminus of Cav1.2 (A39V) was identified in a patient with Brugada syndrome. This mutation resulted in a striking loss-of-function by way of disabled surface trafficking of the L-type channel complex [61]. The defective surface expression of A39V-Cav1.2 persisted upon coexpression of the cardiac Cavβ2b subunit, indicating that the effects of the mutation dominated over the well documented protective effect of Cavβ. This may be due to the possibility that intracellular linkers other than the I-II linker modulate surface expression of Cav1.2 and alternate splicing in the amino terminus of the channel can alter cell surface trafficking [145, 158, 246]. In addition an N-terminal splice variant specific to the heart termed the ‘long variant’, imparts PKC regulation upon the channel, while another shorter variant found in both heart and brain does not [241, 251]. What is more important is that this

second N-terminal variant is common to both the brain isoform used in our study and the cardiac channel used to test A39V-Cav1.2 previously. Other key sequence differences between cardiac and neuronal Cav1.2 variants do exist however, as do differences between human and rat channels, which are approximately 95% homologous (Figure 4-1).

The fact remains that the patient carrying A39V-Cav1.2 did not present with neurological symptoms raising the possibility that this mutation does not affect the sub-cellular trafficking of neuronal Cav1.2 channels. To test this hypothesis we introduced the A39V mutation into rat brain Cav1.2 channels and examined its functional consequences in tsA-201 cells. Unlike in previous work with cardiac Cav1.2, we show that neuronal A39V-Cav1.2 retains Cavβ2b-dependent increases in surface expression, as well as total expression.

With trafficking ruled out as a phenotypical explanation for A39V-Cav1.2 we turned to electrophysiology to probe for changes in channel function. As shown in Chapter 3, excessive calcium influx through wild type Cav1.2 (WT-Cav1.2) channels is limited by the ubiquitous calcium sensing protein calmodulin (CaM), which promotes calcium-dependent inactivation (CDI) [117, 118, 220]. Deciphering Ca^{2+}/CaM dependent gating of various ion channels [95, 252-254], including the complexities of Cav1.2 CDI [133-136, 255] and trafficking [49], has benefited greatly from the use of CaM molecules with mutated low-affinity (N-lobe), or high affinity (C-lobe) calcium binding sites. To reiterate, each lobe of CaM has two EF-hand motifs which when mutated (CaM_{12} is the N-lobe mutant and CaM_{34} is the C-lobe mutant) prevent the binding of calcium. What is interesting to note now is that CaM mutants unable to bind calcium have different structural properties [39, 97] from those of wild type CaM molecules [89-92], suggesting that these conformational changes might affect channel gating independently of their ability, or inability to bind calcium.


A
Human Z34815 MVNENTRMYIPEENHQGSNYGSPRPAHANMNANAAAGLAPEHIPTPGAALSWQAAIDAARQAKLMG
Human AJ224873 MVNENTRMYIPEENHQGSNYGSPRPAHANMNANAAAGLAPEHIPTPGAALSWQAAIDAARQAKLMG
Rat M67515 MVNENTRMYVPEENHQGSNYGSPRPAHANMNANAAAGLAPEHIPTPGAALSWQAAIGAARQAKLMG
Human Z34815 SAGNATISTVSSTQRKRQQYGKPKKQGSTTATRPPRALLCLTLKNPIRRACISIVEWK
Human AJ224873 SAGNATISTVSSTQRKRQQYGKPKKQGSTTATRPPRALLCLTLKNPIRRACISIVEWK
Rat M67515 SAGNATISTVSSTQRKRQQYGKPKKQGGTTATRPPRALLCLTLKNPIRRACISIVEWK
B
Human Z34815 (8a) VNDAVGRDWPWIYFVTLIII
Human AJ224873 (8) MQDAMGYELPWVYFVSLVIF
Rat M67515 (8) MQDAMGYELPWVYFVSLVIF
C
Human Z34815 IAVDNLADAESLTSAQKEEEEEKERKKLAR---TASPEKKQELVEKPAVGESKEEKIELKSITADG
Human AJ224873 IAVDNLADAESLTSAQKEEEEEKERKKLAR---TASPEKKQELVEKPAVGESKEEKIELKSITADG
Rat M67515 IAVDNLADAESLTSAQKEEEEEKERKKLARPARTASPEKKQEVMEKPAVEESKEEKIELKSITADG
D
Human Z34815 LSPAIRVQEVAWKLSSNRCHSRESQAAMAGQEETSQDETYEVKMNHDTEACSEPSLLSTEMLSYQD
Human AJ224873 LSPAIRVQEVAWKLSSNRCHSRESQAAMAGQEETSQDETYEVKMNHDTEACSEPSLLSTEMLSYQD
Rat M67515 LSPAVRVQEAAWKLSSKRCHSRESQGATVSQDMFPDETRSSVRLSEEVEYCSEPSLLSTDILSYQD

Figure 4-1

Figure 4-1: Sequence variation between human and rat Cav1.2 channels. A) Sequence alignment of the N-terminus of the two human A39V-Cav1.2 variants used in previous work [61] (accessions Z34815 & AJ224873) and the rat short N-terminus used in this study (M67515). Polymorphisms between rat and human channels are denoted by an 'X' below the amino acid position. Note however that the polymorphism (in red) present in the rat clone was mutated back to aspartic acid to match the human channels (Section 2.1.2). Both studies used short N-terminal splice variants of Cav1.2, which incorporate exon 1b. B) Sequence alignment of the exon 8/8a segment of Cav1.2 used in each study. Note that YFP-containing exon 8a Cav1.2 was used for trafficking experiments in previous work [61], while exon 8 containing Cav1.2 was used in our study. Exon 8 (in red) is identical between human and rat. Polymorphisms detected between exon 8/8a are denoted by an 'X' below the amino acid position. C) Sequence alignment of a portion of the II-III intracellular linker of the two human variants used in previous work [61] and the rat Cav1.2 channel used in our work. Note the inclusion of an inserted sequence in the rat channel which has been previously reported [256]. D) Sequence alignment of the most divergent portion of the C-terminus of the two human cardiac sequences used in previous work [61] and the rat brain isoform used in our study.

While investigating effects on global CDI for a Cav1.2 N-terminal point mutant (A39V) linked to Brugada syndrome [61, 210] we observed that CaM_{WT} differentially affected the kinetics and voltage-dependence of activation for Cav1.2 when compared to CaM lobe mutants. We also show that these effects occur in the absence of calcium and that they can be modulated by the N-terminal A39V mutation, indicating that the N-terminus of the channel can be involved in CaM-dependent modulation of Cav1.2 activation.

Altogether our work with the Brugada syndrome mutation A39V demonstrate that this residue does not promote the loss of trafficking of neuronal Cav1.2 channels to the cell surface, but does reduce the amount of global CDI. A39V-Cav1.2 does however affect how these channels open in a CaM mutant dependent fashion.

4.2 Results

4.2.1 The Brugada syndrome mutation A39V does not prevent surface expression of neuronal Cav1.2 channels

It was shown previously that a point mutation (A39V) in the N-terminus of a cardiac isoform of Cav1.2 severely limited membrane expression of the channel even upon coexpression of the ancillary Cavβ2b subunit [61]. This is unexpected considering that the Cavβ subunit promotes ER export and surface trafficking of the channel by binding the intracellular linker connecting domains I and II of the calcium channel Cavα1 subunit [142, 145]. Given that Brugada syndrome does not involve compromised brain function, we wondered if the A39V mutation might trigger a similar loss-of-trafficking phenotype in neuronal Cav1.2 channels.

We first examined whether cell surface expression of A39V-Cav1.2 was different from that of WT-Cav1.2 by staining for an external HA epitope on the channel in non-permeablized

tsA-201 cells. We found that in the rat brain channel, surface expression of A39V-Cav1.2-HA (Figure 4-2A) was visible and that Cavβ2b significantly increased surface expression. Quantification of A39V-Cav1.2-HA fluorescence determined that the signal per cell (i.e., the surface pool of channels per cell), was significantly increased upon co-expression of a Cavβ subunit (Figure 4-2B). We found that WT-Cav1.2-HA and A39V-Cav1.2-HA were not differentially expressed at the cell surface (7064 ± 1211 and 6298 ± 785 ALUs, respectively). Coexpression of Cavβ2b significantly increased the surface pools of both WT-Cav1.2-HA (13087 ± 964 ALUs, $p \leq 0.05$ ANOVA) and A39V-Cav1.2-HA (12715 ± 1291 ALUs $p \leq 0.05$ ANOVA). Cavβ1b was able to significantly increase the surface pool of WT-Cav1.2-HA (10145 ± 790 ALUs, p=<0.05 ANOVA), and there was a strong trend towards increased surface expression of A39V-Cav1.2 (10109 ± 842 ALUs), however, this effect did not reach statistical significance (also see Supplementary Figure 1). Altogether, Figure 4-2A and B show that A39V-Cav1.2 is able to traffic to the cell membrane as well as WT-Cav1.2, and that the cardiac Cavβ2b subunit significantly increases surface expression of A39V-Cav1.2 in a neuronal background. Since previous work showed that Cavβ2b was unable to traffic the cardiac isoform of A39V-Cav1.2 to the cell membrane [61], the robust Cavβ-dependent trafficking observed in our experiments implies isoform specific effects for the A39V mutation. Splice variants of the Cav1.2 N-terminus have been shown to regulate cell surface expression of Cav1.2 in smooth muscle cells, indicating that this region of the channel may be involved in subcellular trafficking [246].

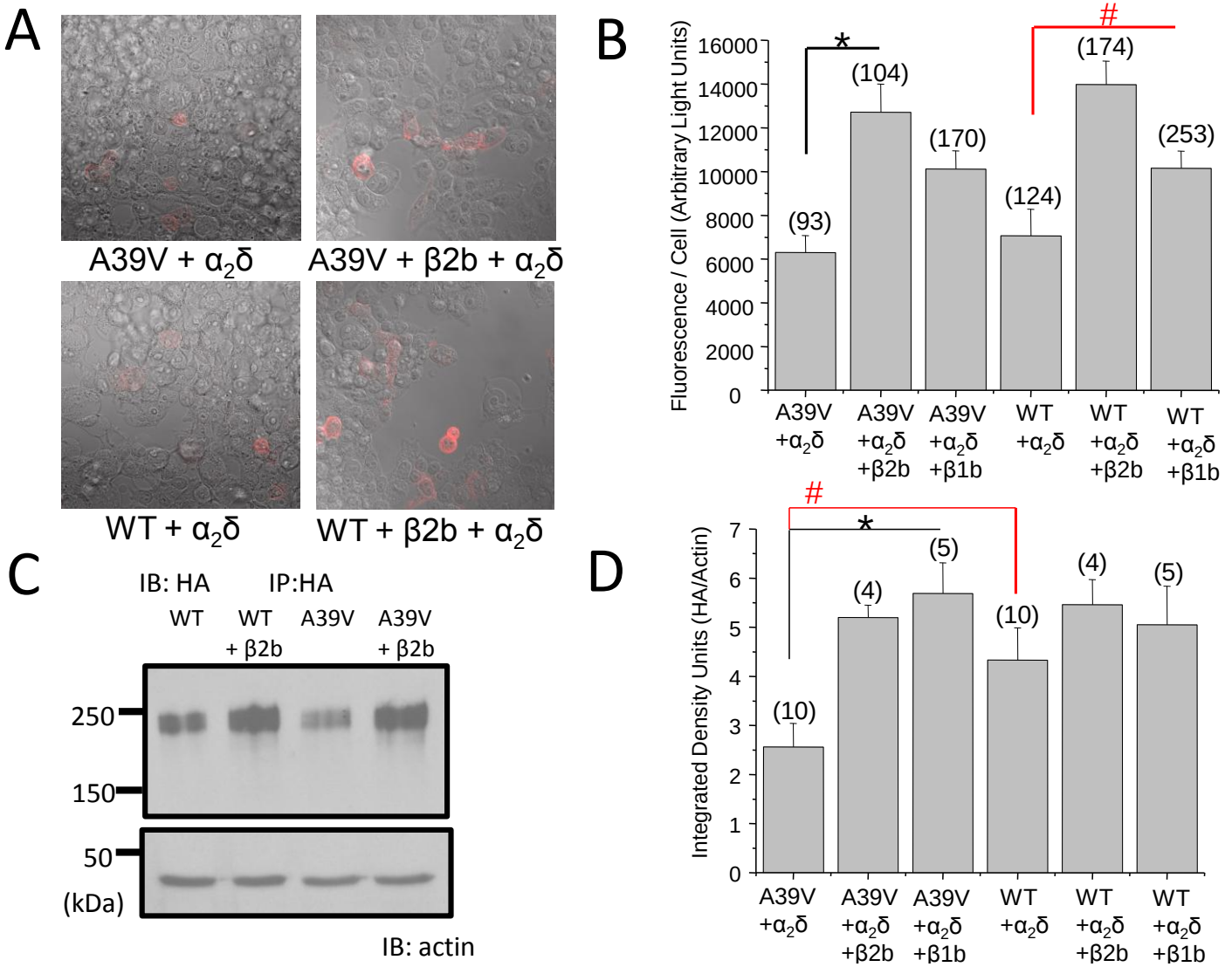
A
A39V + α2δ
A39V + β2b + α2δ
WT + α2δ
WT + β2b + α2δ
B
Fluorescence / Cell (Arbitrary Light Units)
16000
14000
12000
10000
8000
6000
4000
2000
0
(93)
(104)
(170)
(124)
(174)
(253)
*
#
A39V +α2δ
A39V +α2δ +β2b
A39V +α2δ +β1b
WT +α2δ
WT +α2δ +β2b
WT +α2δ +β1b
C
IB: HA
IP:HA
WT
WT + β2b
A39V
A39V + β2b
250
150
50
(kDa)
IB: actin
D
Integrated Density Units (HA/Actin)
7
6
5
4
3
2
1
0
(10)
(4)
(5)
(10)
(4)
(5)
*
#
A39V +α2δ
A39V +α2δ +β2b
A39V +α2δ +β1b
WT +α2δ
WT +α2δ +β2b
WT +α2δ +β1b

Figure 4-2

Figure 4-2: Surface trafficking and total expression are the same for A39V-Cav1.2-HA and WT-Cav1.2-HA in the presence of cardiac Cavβ2b. A) Cavβ2b significantly increases the surface trafficking of A39V-Cav1.2-HA and WT-Cav1.2-HA in nonpermeablized tsA-201 cells. B) Quantification of HA surface pool displayed as fluorescence per cell (arbitrary light units). Cavβ2b and Cavβ1b (Figure 4-3A) significantly increase the fluorescence per cell of WT-Cav1.2-HA, while only Cavβ2b significantly increased the surface fluorescence of A39V-Cav1.2-HA (* $p \leq 0.05$ and # $p \leq 0.05$ by one-way ANOVA). Cavβ1b does not significantly increase the fluorescence per cell of A39V-Cav1.2 ($p \geq 0.05$ by one-way ANOVA). C) Total protein expression of A39V-Cav1.2-HA and WT-Cav1.2-HA from tsA-201 cell lysates expressed with and without Cavβ2b. D) Quantification of A39V-Cav1.2-HA and WT-Cav1.2-HA total expression (integrated density units) with and without Cavβ2b/β1b (Figure 4-3B). The data is expressed as a ratio of HA/α-actin. Both Cavβ2b and Cavβ1b significantly increase the expression of A39V-Cav1.2 (*$p \leq 0.05$ by one-way ANOVA). A39V-Cav1.2 shows less expression than WT-Cav1.2 in the absence of Cavβ (# $p = 0.04$ student's t-test).

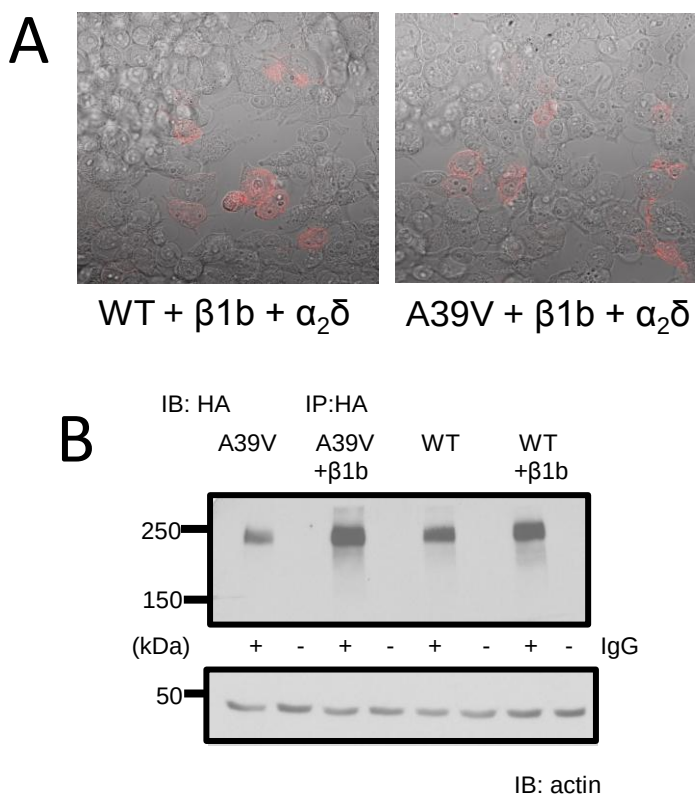
A
WT + β1b + α2δ
A39V + β1b + α2δ
B
IB: HA
IP:HA
A39V
A39V +β1b
WT
WT +β1b
250
150
(kDa)
+ - + - + - + -
IgG
50
IB: actin

Figure 4-3

Figure 4-3: Surface trafficking and total expression are similar for A39V-Cav1.2-HA and WT-Cav1.2-HA in the presence of neuronal Cavβ1b. A) Cavβ1b increases the fluorescence per cell of WT-Cav1.2-HA ($p \leq 0.05$ by one-way ANOVA), but not A39V-Cav1.2-HA ($p \leq 0.05$ by one-way ANOVA). B) Cavβ1b significantly increases the total protein expression of A39V-Cav1.2-HA ($p \leq 0.05$ by ANOVA), but not WT-Cav1.2-HA.

The Cavβ subunit has been shown to increase total expression of Cav1.2 by binding to the I-II intracellular linker of the channel and preventing ER associated degradation (ERAD) [9]. We therefore tested whether A39V-Cav1.2-HA total protein was increased upon coexpression of Cavβ2b and whether A39V-Cav1.2-HA expressed like WT-Cav1.2-HA without a Cavβ subunit (Figure 4-2C). Immunoprecipitation of the channels combined with semi-quantification against alpha-actin yield demonstrated that, in the absence of a Cavβ subunit, the integrated density of A39V-Cav1.2-HA (2.56 ± 0.48 IDUs) was significantly less than WT-Cav1.2-HA (4.33 ± 0.66 IDUs, $p = 0.04$ by students *t*-test) (Figure 4-2D). Therefore, A39V-Cav1.2 is either produced to a lesser extent, or degraded more effectively than WT-Cav1.2. Since both Cav1.2 constructs were transfected identically and driven by the same constitutive promoter, the latter of these two possibilities appears more likely. Our data also reveal that coexpression of either Cavβ2b (5.20 ± 0.25 IDUs) (Figure 4-2C) or Cavβ1b (5.69 ± 0.62 IDUs) (Figure 4-3B), results in a significant increase in A39V-Cav1.2-HA protein levels ($p \leq 0.05$ by ANOVA) (Figure 4-2D). This confirms that the protective role of the Cavβ subunit is maintained in the A39V-Cav1.2 channel. Interestingly, total WT-Cav1.2-HA protein levels were increased upon coexpression of Cavβ1b (5.05 ± 0.79 IDUs), but to a lesser degree than described by our lab previously for a Cav1.2. We attribute this to a different amino acid sequence in the N-terminus of the channel [9], perhaps suggesting that the N-terminus is involved in regulating Cav1.2 channel stability.

4.2.2 A39V-Cav1.2 channels show normal voltage-dependent function with either cardiac or neuronal Cavβ subunits

We next evaluated whether the A39V mutation could alter the functional properties of the neuronal Cav1.2 isoform.

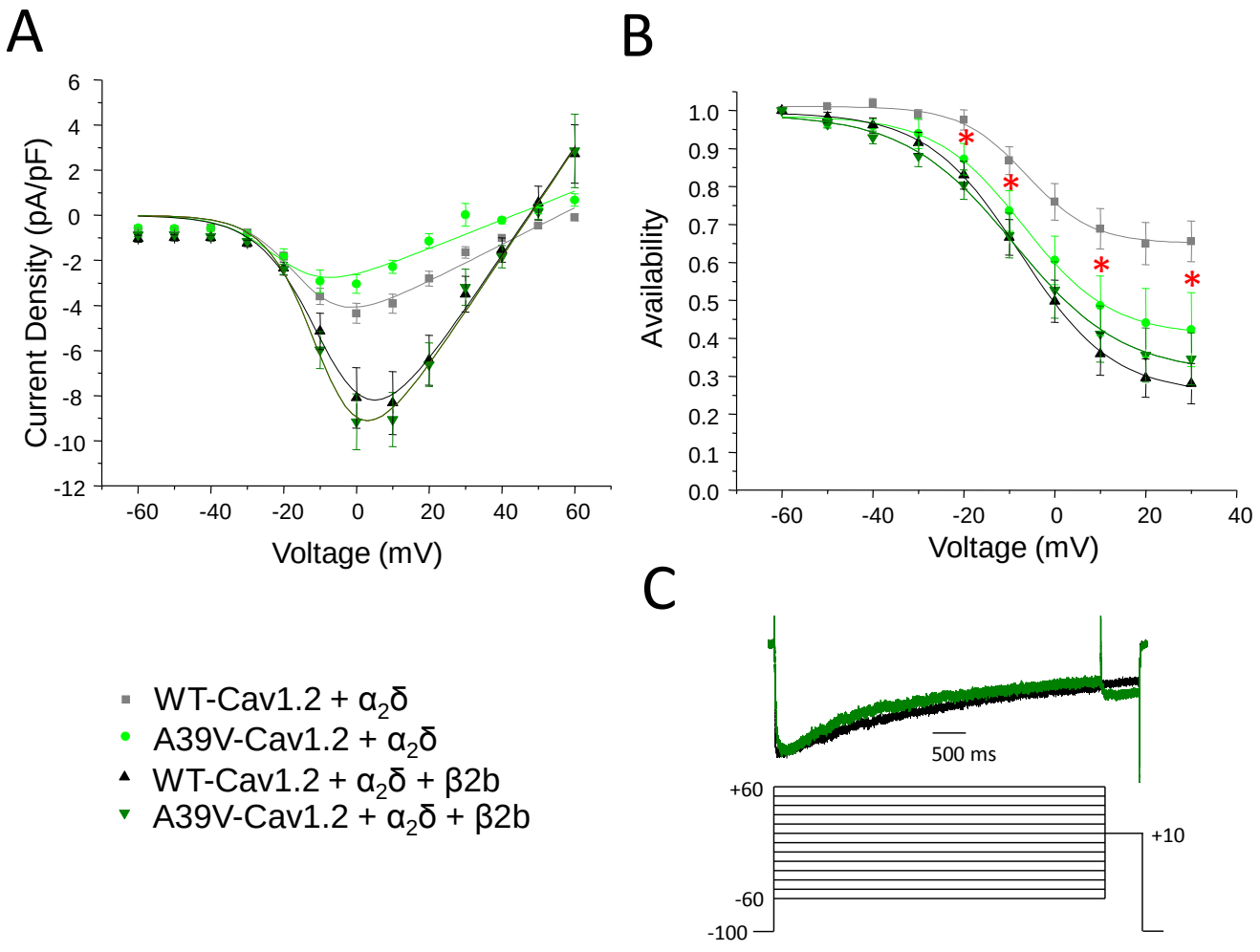
A
Current Density (pA/pF)
Voltage (mV)
B
Availability
Voltage (mV)
C
500 ms
+60
+10
-60
-100
WT-Cav1.2 + α2δ
A39V-Cav1.2 + α2δ
WT-Cav1.2 + α2δ + β2b
A39V-Cav1.2 + α2δ + β2b

Figure 4-4

Figure 4-4: The current voltage relation and steady-state inactivation of A39V-Cav1.2 is not significantly different from WT-Cav1.2 in the presence of Cavβ2b. A) The IV relationships of WT and A39V-Cav1.2 with and without Cavβ2b. There is no significant difference in current density, or voltage-dependent properties when comparing WT-Cav1.2 (grey) and A39V-Cav1.2 (light green); or WT-Cav1.2 (black) and A39V-Cav1.2 (dark green) with Cavβ2b. Cavβ2b does significantly increase the current density of both WT and A39V-Cav1.2 ($p \leq 0.05$ by one-way ANOVA). Cavβ1b also significantly increased current density of A39V-Cav1.2 ($p \leq 0.05$ by one-way ANOVA) (Figure 4-5). B) Steady-state inactivation plots of WT and A39V-Cav1.2 with and without Cavβ2b. There is no significant difference in the steady-state of inactivation between WT-Cav1.2 and A39V-Cav1.2 in the presence of Cavβ2b or Cavβ1b (Figure 4-5). The slope of steady state inactivation is increased for A39V-Cav1.2 when compared to WT-Cav1.2 in the absence of the Cavβ subunit which significantly reduces the percentage of channels available at marked voltages (*) when compared to WT ($p = 0.05$ by students *t*-test). (C) Voltage clamp protocol for inactivation curves, and sample traces of WT-Cav1.2 and A39V-Cav1.2 with Cavβ2b. Normalized traces of WT-Cav1.2 (black) and A39V-Cav1.2 (dark green) with Cavβ2b illustrating no significant difference in the time course of inactivation. Currents were evoked from a holding potential of -100mV to various 4.5 s long conditioning potentials (ranging from -60mV through +60mV in 10mV increments), followed by a test pulse to +10mV, for 0.5 seconds.

In the absence of the Cavβ subunit WT-Cav1.2 exhibits a peak current density of -4.4 ± 0.5, pA/pF at a test potential of 0 mV. As expected, co-expression of either Cavβ2b (-9.1 ± 1.4 pA/pF, $p \leq 0.05$ ANOVA), or Cavβ1b (-10.6 ± 1.1 pA/pF, $p \leq 0.05$ ANOVA) significantly increases the peak current density of WT-Cav1.2. The current-voltage relationship of A39V-Cav1.2 is not statistically different from WT-Cav1.2 in the presence of either Cavβ2b (Figure 4-4A), or Cavβ1b (see Figure 4-5A). The A39V-Cav1.2 construct shows a peak current density of -3.3 ± 0.5, pA/pF which does not differ from that of the WT channel and which is increased upon coexpression of Cavβ2b (-9.5 ±1.6 pA/pF, $p \leq 0.05$ by ANOVA), or Cavβ1b (-8.3 ± 1.0 pA/pF, $p \leq 0.05$ by ANOVA). Altogether, these data fit with our biochemical analysis in Figure 4-2. Moreover, the time course of inactivation (Figure 4-4C) was not statistically different between A39V-Cav1.2 and WT-Cav1.2, with or without Cavβ subunit co-expression at all potentials tested between -10mV and +30mV (data not shown).

It has been demonstrated that mutations in the cardiac Cavβ2b subunit can affect inactivation of Cav1.2 in order to produce a Brugada phenotype [206]. Furthermore, the N-terminus of Cav1.2 has been shown to affect inactivation of the channel in a manner dependent on the Cavβ subunit [158]. We therefore tested whether the steady-state inactivation properties of A39V-Cav1.2 were different from those of WT-Cav1.2 in the presence of a Cavβ subunit. In the presence of either Cavβ2b (Figure 4-4B), or Cavβ1b (Figure 4-5B) the steady-state inactivation properties of A39V-Cav1.2 were not significantly different from WT-Cav1.2. However, in the absence of the Cavβ subunit, A39V-Cav1.2 displays a significant increase in the slope of the inactivation curve (11.8 ± 1.4 mV) which is significant when compared to WT-Cav1.2 (6.9 ± 0.6 mV, $p = 0.01$ students *t*-test).

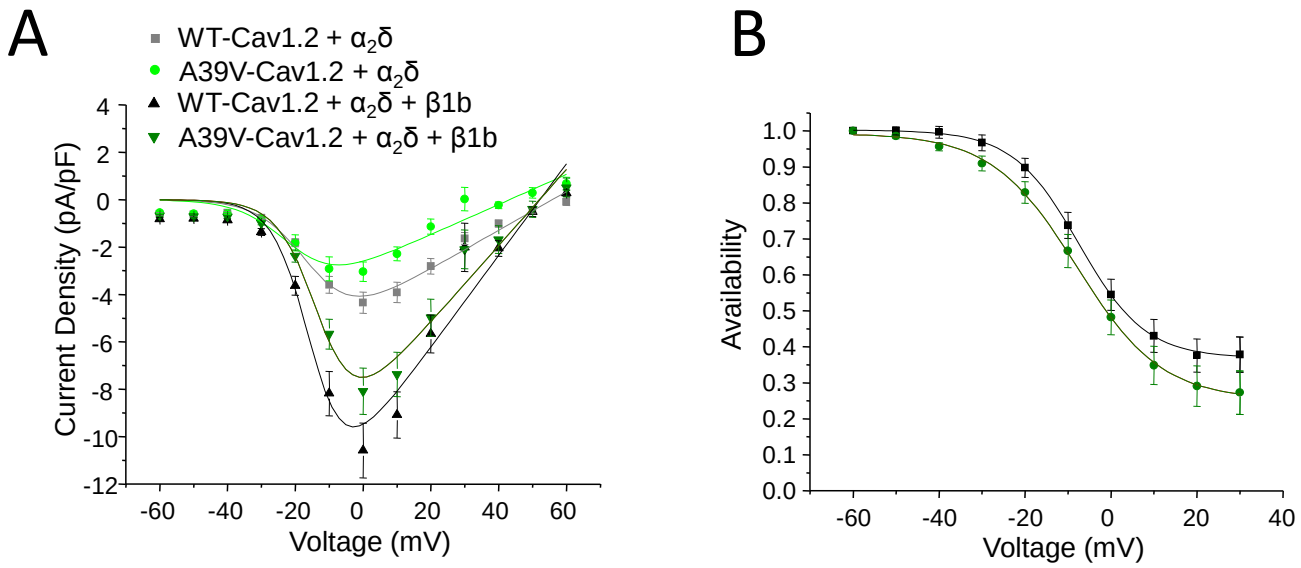
A
WT-Cav1.2 + α2δ
A39V-Cav1.2 + α2δ
WT-Cav1.2 + α2δ + β1b
A39V-Cav1.2 + α2δ + β1b
Current Density (pA/pF)
Voltage (mV)
B
Availability
Voltage (mV)

Figure 4-5

Figure 4-5: The current voltage relation and steady-state inactivation of A39V-Cav1.2 is not significantly different from WT-Cav1.2 in the presence of Cavβ1b A) Cavβ1b significantly increases current density of WT and A39V-Cav1.2 ($p \leq 0.05$ one-way ANOVA). (D). Steady-state inactivation properties of A39V-Cav1.2 are the same as WT in the presence of Cavβ1b.

Furthermore, the A39V-Cav1.2 channel underwent a greater extent of total inactivation compared to the WT channel as denoted by red asterisks in Figure 4-4B (test potentials of -20,-10, +10, and +30mV, $p \leq 0.05$ by students *t*-test). This behavior of A39V-Cav1.2 could in principle be interpreted as a loss-of-function; however, as this occurs only in the absence of Cavβ, this effect will not likely manifest itself in native cells.

Our results indicate that in the neuronal channel background A39V does not impart a Cavβ dependent trafficking defect onto Cav1.2, nor does the point mutation dramatically effect overall expression and function of the channel in the presence of neuronal or cardiac Cavβ subunits.

4.2.3 The Brugada syndrome mutant A39V disrupts N-lobe CDI of Cav1.2 channels but not CaM binding to the channel N-terminus

We have shown in the previous section that the Cav1.2 point mutant A39V linked to Brugada syndrome, does not elicit a trafficking defect in the neuronal isoform of the channel or major effects on voltage-dependent activation and inactivation in the presence of Cavβ [210]. Recently Dick and colleagues [134] and our group (Chapter 3) [135] have shown that the N-terminus of L-type calcium channels participates in a type of CDI which occurs when intracellular levels of calcium elevate globally – it is therefore termed global CDI.

Because of the documented role of the Cav1.2 N-terminus in CDI, we tested whether the Brugada syndrome mutant A39Vmay affect this process.

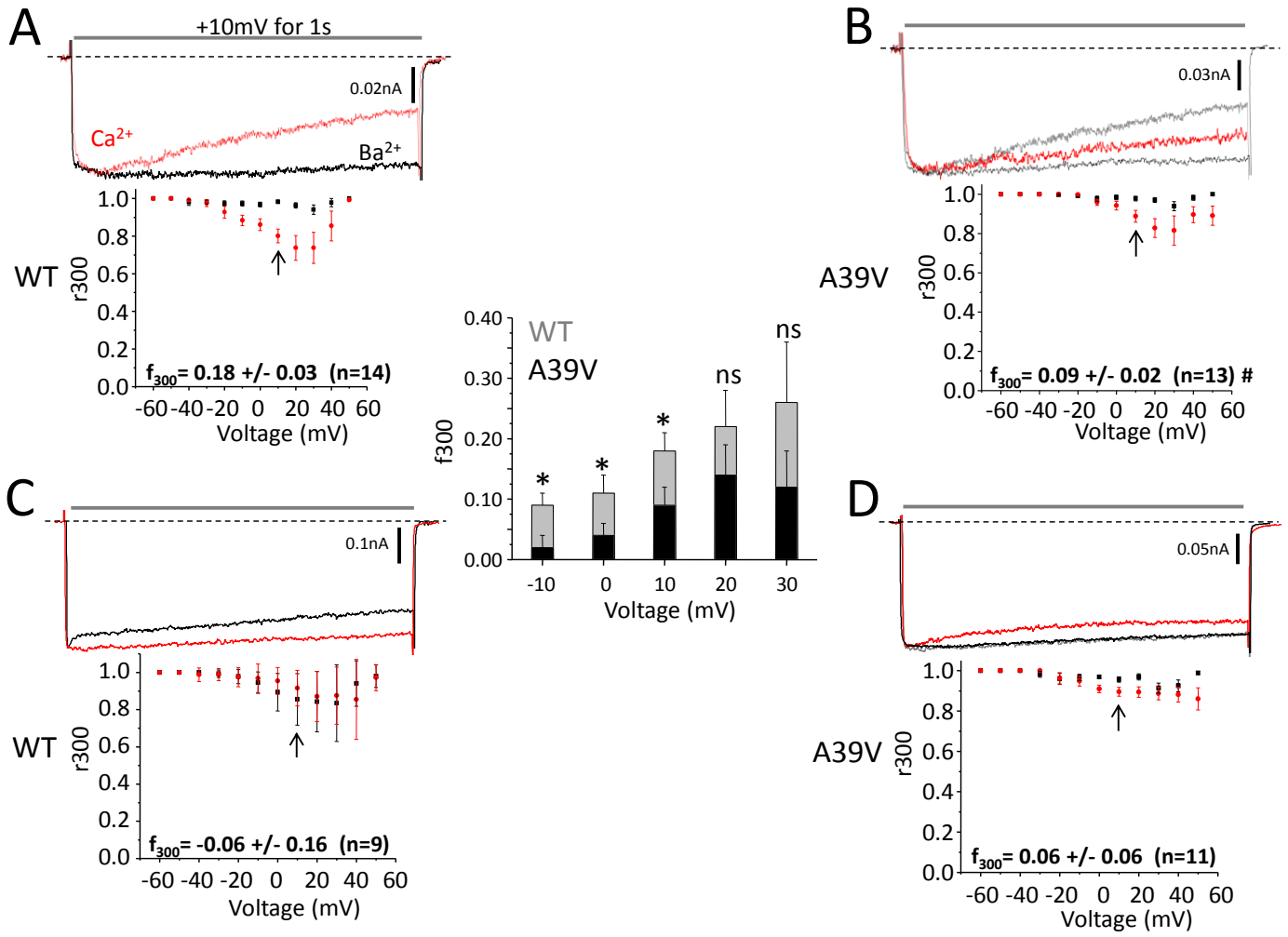
A
+10mV for 1s
0.02nA
Ca2+
Ba2+
WT
r300
f300= 0.18 +/- 0.03 (n=14)
Voltage (mV)
B
0.03nA
A39V
f300= 0.09 +/- 0.02 (n=13) #
Voltage (mV)
WT
A39V
f300
ns
Voltage (mV)
C
0.1nA
WT
f300= -0.06 +/- 0.16 (n=9)
Voltage (mV)
D
0.05nA
A39V
f300= 0.06 +/- 0.06 (n=11)
Voltage (mV)

Figure 4-6

Figure 4-6: The Brugada syndrome mutation A39V disrupts N-lobe CDI of Cav1.2 channels. A) Representative Ba^{2+} (black) and Ca^{2+} (red) traces of WT and A39V-Cav1.2 channels (B) expressed with Cavβ2a/Cavα2δ in the presence of low calcium buffering (0.5mM EGTA) and CaM_{34}. Note that the peak of the Ba^{2+} trace is normalized to that in the presence of Ca^{2+}. For reference the WT-Cav1.2 Ca^{2+} trace is displayed in grey in (B). The plots shown below the current traces reflect average CDI (f_{300}) which is quantified by the fraction of current remaining after 300ms (r300) in calcium, and is then subtracted from the fraction of current remaining in barium at the same time point. The f_{300} value at 10mV (arrows) is significantly less for A39V, than WT-Cav1.2 (# $p \leq 0.04$ by student's *t*-test). The inset bar graph displays additional f_{300} values over a potential range from -10mV to +30mV. A significant difference is observed in the f_{300} values between WT-Cav1.2 and A39V-Cav1.2 at -10, 0 and +10mV ($p \leq 0.05$ by student's *t*-test), but not at +20 ($p = 0.28$ by student's *t*-test) or +30mV ($p = 0.26$ by student's *t*-test). C) Under high calcium buffering (10mM BAPTA) conditions WT-Cav1.2 channels expressed as in (A) no longer exhibit N-lobe CDI. D) A39V-Cav1.2 does not show significant N-lobe CDI compared to WT-Cav1.2 in high calcium buffering at +10mV (arrows). For reference the WT-Cav1.2 Ca^{2+} trace (C) is displayed in grey.

This was done by overexpressing CaM_{34} and buffering intracellular calcium with 0.5mM EGTA. Figure 4-6A shows that WT-Cav1.2 channels show little voltage-dependent inactivation (VDI) in barium (black trace) but significant N-lobe CDI upon exposure to calcium (red trace), in agreement with our previous work [135]. A +10mV test depolarization was used for comparison in Figure 1 because this test potential corresponds to the peak of the IV curve in 20mM external barium. Quantification of the amount of N-lobe CDI is reflected in the f_{300} value (i.e. the fraction of channels which are inactivated after 300 ms) at +10mV, which equals 0.18 ± 0.03 (n=14) for WT-Cav1.2 and CaM_{34}. Figure 4-6B shows that A39V-Cav1.2 channels have significantly reduced N-lobe CDI at +10mV (f_{300} = 0.09 ± 0.02, n=13, # $p \leq 0.04$ by student's *t*-test) with CaM_{34} compared to WT-Cav1.2 channels under the same conditions. To facilitate comparison the WT-Cav1.2 calcium trace is shown in grey in Figure 4-6B. The inset bar graph in Figure 1 shows that in addition to +10mV, A39V-Cav1.2 shows significantly less CDI than WT-Cav1.2 at -10 and 0mV ($p \leq 0.05$ by student's *t*-test). A similar trend was seen +20 and +30mV, but did not reach statistical significance ($p = 0.28$ and $p = 0.26$ by student's *t*-test, respectively), presumably because there is an increasing contribution of VDI at these potentials. To facilitate comparison the WT-Cav1.2 calcium trace is shown in grey in Figure 4-6B. Repeating the experiment with 10 mM BAPTA intracellularly to significantly increase calcium buffering verified that both WT-Cav1.2 (f_{300} = -0.06 ± 0.16, n=9) (Figure 4-6C) and A39V-Cav1.2 (f_{300} = 0.06 ± 0.06, n=11) (Figure 4-6D) channels were indeed undergoing N-lobe CDI, which is also supported by the flattened red traces in Figures 4-6C/D.

We next tested whether A39V-Cav1.2 channels exhibited augmented C-lobe CDI by expressing the channels with CaM_{12}.

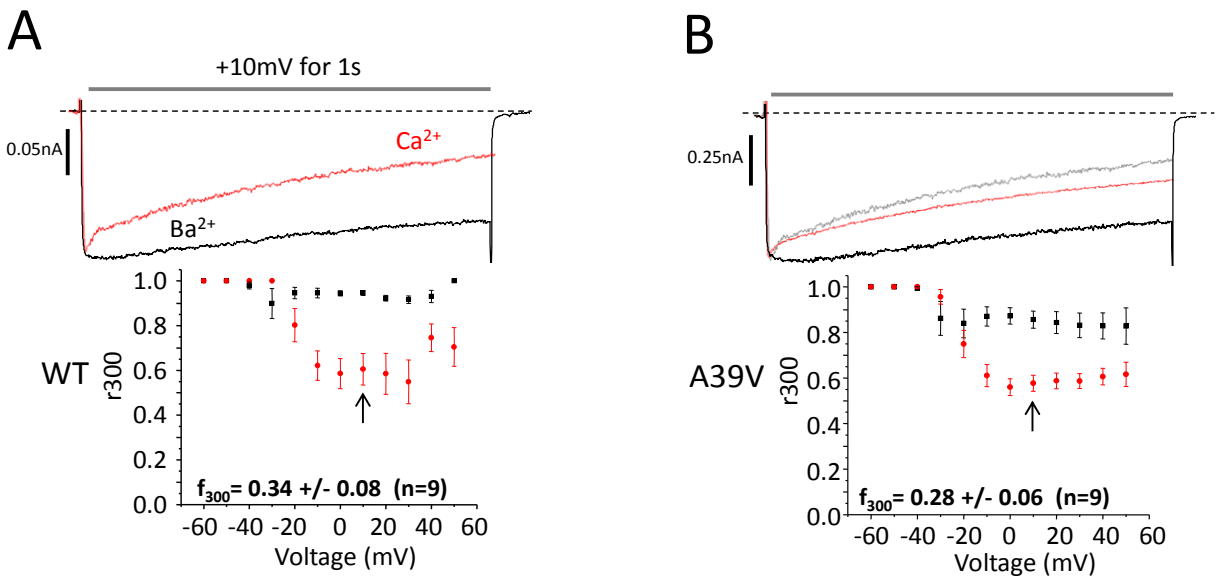
A
+10mV for 1s
0.05nA
Ca2+
Ba2+
WT
r300
1.0
0.8
0.6
0.4
0.2
0.0
f300= 0.34 +/- 0.08 (n=9)
-60 -40 -20 0 20 40 60
Voltage (mV)
B
0.25nA
A39V
r300
1.0
0.8
0.6
0.4
0.2
0.0
f300= 0.28 +/- 0.06 (n=9)
-60 -40 -20 0 20 40 60
Voltage (mV)

Figure 4-7

Figure 4-7: The Brugada syndrome mutation A39V does not affect C-lobe CDI of Cav1.2 channels. A) Representative Ba^{2+} (black) and Ca^{2+} (red) traces of WT-Cav1.2 channels expressed with Cavβ2a/Cavα2δ and CaM_{12} in the presence of high calcium buffering (10 mM BAPTA). Note that the peak of the Ba^{2+} trace is normalized to that in the presence of Ca^{2+} and that average CDI (f_{300}) of WT-Cav1.2 is displayed below in the graph. B) A39V-Cav1.2 channels expressed with Cavβ2a/Cavα2δ and CaM_{12} in the presence of high calcium buffering (10mM BAPTA). Inset graphs show average CDI (f_{300}) which is not statistically different ($p \leq 0.55$ by student's *t*-test), between the two channel types.

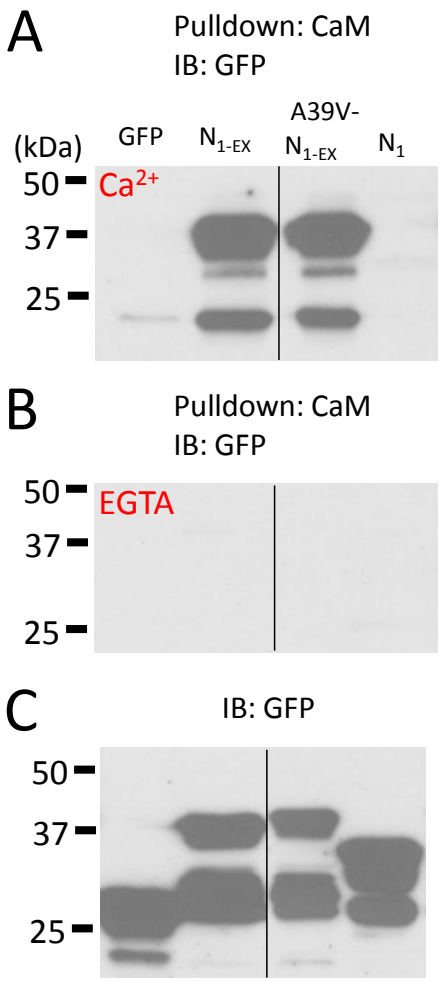
A
Pulldown: CaM
IB: GFP
(kDa)
GFP
N1-EX
A39V-
N1-EX
N1
50
37
25
Ca2+
B
Pulldown: CaM
IB: GFP
50
37
25
EGTA
C
IB: GFP
50
37
25

Figure 4-8

Figure 4-8: The Brugada mutation A39V does not alter N-terminal binding to CaM. A) CaM sepharose pull-down experiments of $N_{1\text{-}EX}$, A39V-$N_{1\text{-}EX}$ and N_1 GFP fusion proteins in 0.5mM Ca^{2+}, or 5mM EGTA (B) run on SDS-PAGE with corresponding lysates (C) and blotted for GFP. Black lines mark where the gel picture was cut and irrelevant samples removed. These experiments were performed twice each.

Figure 4-7A shows that WT-Cav1.2 channels show substantial C-lobe CDI in the presence of calcium (f_{300} = 0.34 ± 0.08, n=9) which agrees with the literature [124, 134]. Figure 4-7B shows also that A39V-Cav1.2 also exhibits considerable C-lobe CDI (f_{300} = 0.28 ± 0.06, n=9) which is not statistically different from WT-Cav1.2 channels. Overall, our data reveal a reduction in N-lobe CDI for A39V-Cav1.2, which implies a gain of function effect of this mutation. This is unexpected as Brugada syndrome is considered a loss-of-function disorder in the context of Cav1.2 channels [61, 179].

As N-lobe CDI was affected in the A39V mutant, we tested whether this was due to altered binding of CaM to the Cav1.2 N-terminus. We used CaM sepharose pulldowns to test whether CaM could differentially bind to fusion proteins of the distal N-terminus (methionine 1 to proline 101) of the channel. Figure 4-8A shows that both $N_{1\text{-}EX}$ and A39V-$N_{1\text{-}EX}$ GFP fusion proteins bound readily to CaM sepharose in 0.5mM calcium. This binding was completely removed with 5 mM EGTA washes (Figure 4-8B). The smaller N_1-GFP fusion protein (methonine 1 to lysine 63) did not bind CaM and agrees with our previous findings [135]. Altogether, these biochemical measurements show that A39V does not change the binding of CaM to the distal portion of the N-terminus. It is therefore unlikely that differential CaM binding explains the changes in N-lobe CDI observed for A39V-Cav1.2 channels.

4.2.4 CaM mutants differentially affect the voltage-dependence and kinetics of activation for A39V and WT-Cav1.2 channels

During the course of our experiments, we noticed that CaM lobe mutants affected the voltage-dependence of activation of Cav1.2 channels when bathed in extracellular barium solution.

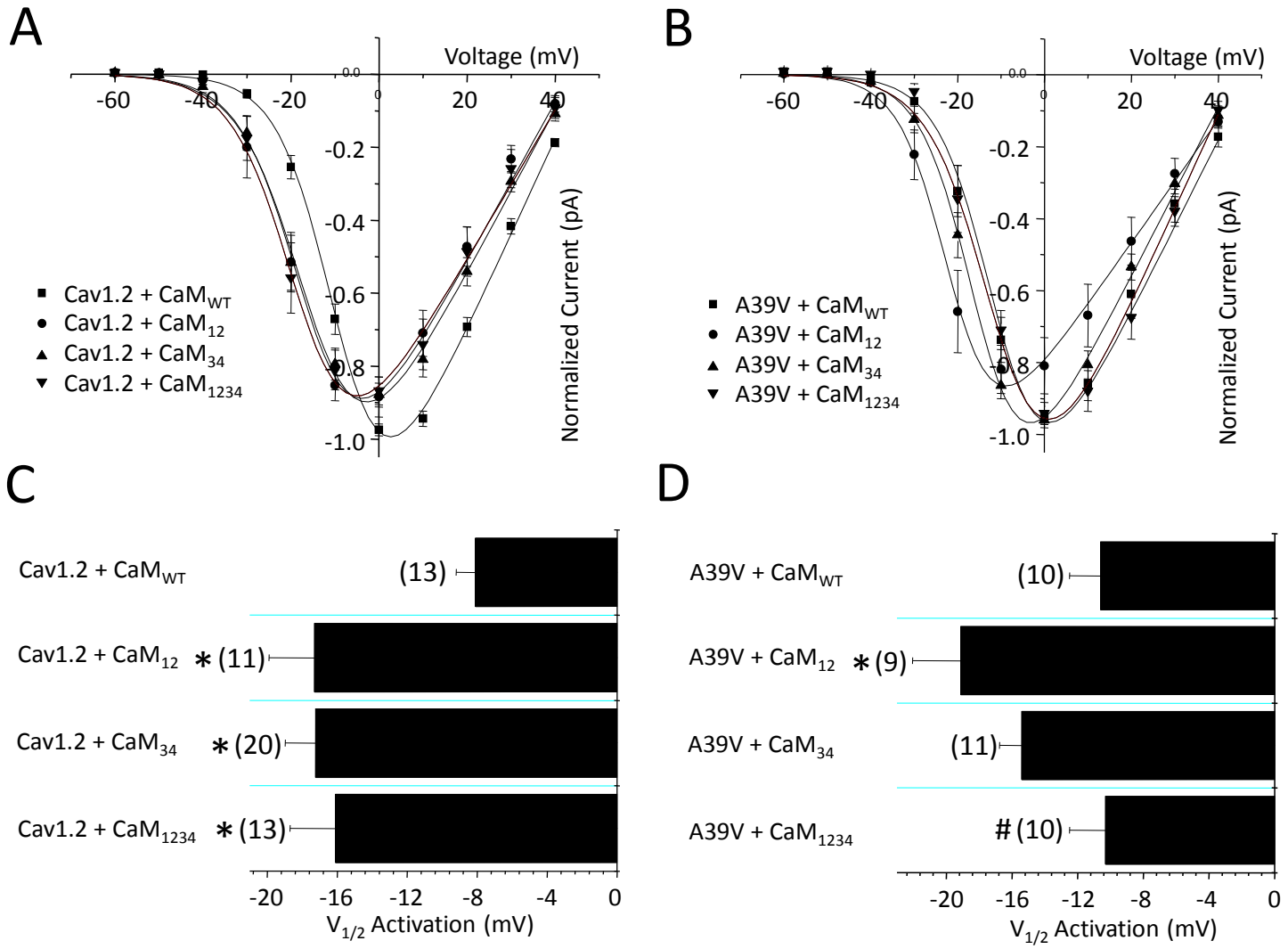
A
Voltage (mV)
-60
-40
-20
0
20
40
0.0
-0.2
-0.4
-0.6
-0.8
-1.0
Normalized Current (pA)
Cav1.2 + CaM$_{WT}$
Cav1.2 + CaM$_{12}$
Cav1.2 + CaM$_{34}$
Cav1.2 + CaM$_{1234}$
B
Voltage (mV)
A39V + CaM$_{WT}$
A39V + CaM$_{12}$
A39V + CaM$_{34}$
A39V + CaM$_{1234}$
Normalized Current (pA)
C
Cav1.2 + CaM$_{WT}$ (13)
Cav1.2 + CaM$_{12}$ * (11)
Cav1.2 + CaM$_{34}$ * (20)
Cav1.2 + CaM$_{1234}$ * (13)
-20
-16
-12
-8
-4
0
V$_{1/2}$ Activation (mV)
D
A39V + CaM$_{WT}$ (10)
A39V + CaM$_{12}$ * (9)
A39V + CaM$_{34}$ (11)
A39V + CaM$_{1234}$ # (10)
V$_{1/2}$ Activation (mV)

Figure 4-9

Figure 4-9: CaM lobe mutants differentially shift the voltage dependence of activation for WT and A39V-Cav1.2 channels. A) Current voltage relationships for WT-Cav1.2 channels expressed transiently in tsA-201 cells with Cavβ2a/Cavα2δ and recorded in barium with one of four CaM conditions: CaM_{WT}, CaM_{12}, CaM_{34}, or CaM_{1234}. All experiments were recorded with high calcium buffering intracellularly (10mM BAPTA). B) Current-voltage relationships for A39V-Cav1.2 channels expressed as in (A) with one of four CaM conditions: CaM_{WT}, CaM_{12}, CaM_{34}, or CaM_{1234}. C) A bar graph displaying the half activation potentials for Cav1.2 channels recorded in barium. WT-Cav1.2 channels recorded with any CaM mutant have a significant leftward shift in the voltage-dependence of activation in barium compared to CaM_{WT} (*$p \leq 0.05$ by one-way ANOVA). D) A bar graph displaying the voltage dependence of activation for A39V-Cav1.2 channels recorded in barium. A39V-Cav1.2 channels recorded with CaM_{12} have a significant leftward shift in the voltage-dependence of activation in barium compared to CaM_{WT} (*$p \leq 0.05$ by one-way ANOVA), and CaM_{1234} (# $p \leq 0.05$ by one-way ANOVA).

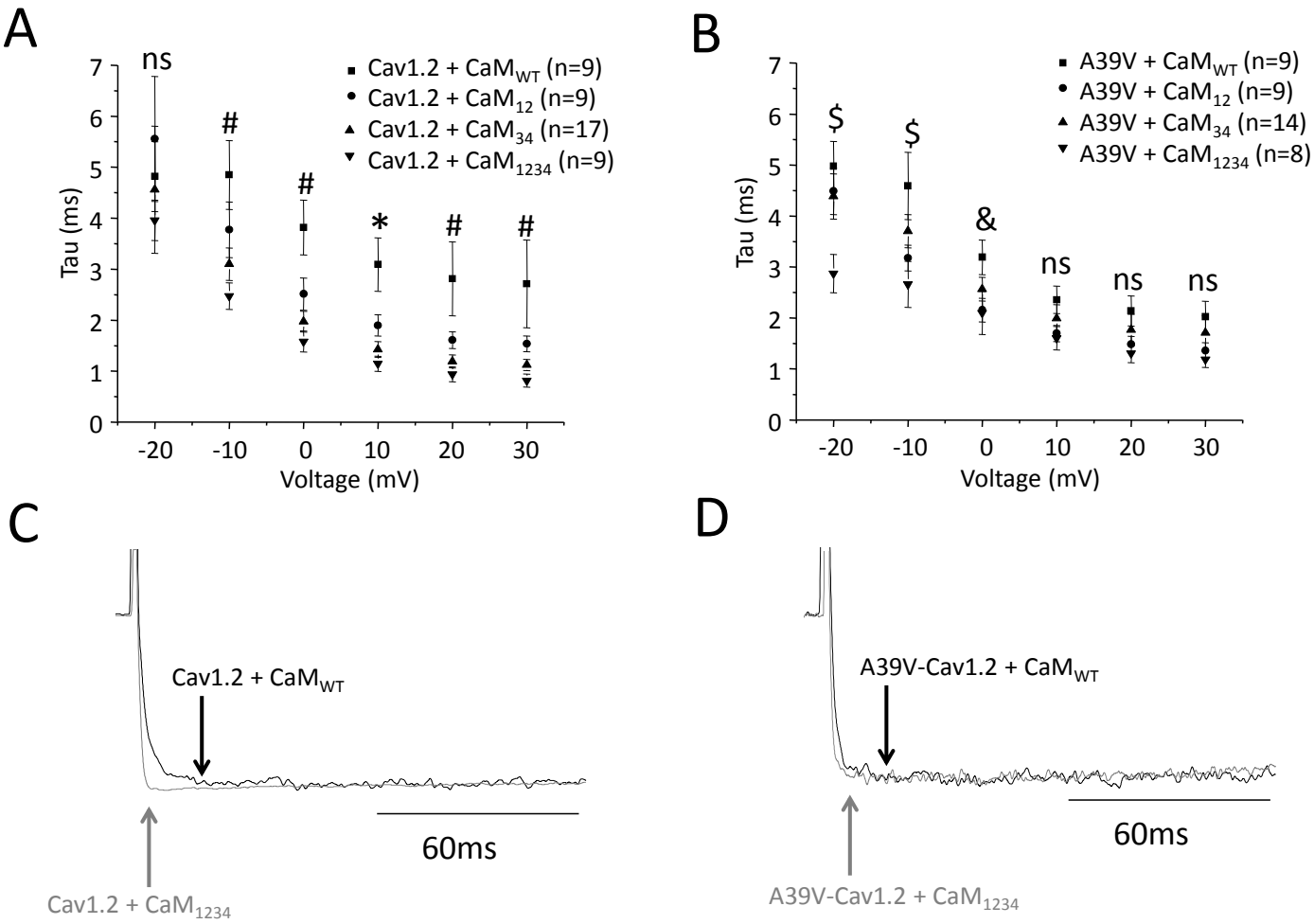
A
ns
#
#
*
#
#
Cav1.2 + CaM$_{WT}$ (n=9)
Cav1.2 + CaM$_{12}$ (n=9)
Cav1.2 + CaM$_{34}$ (n=17)
Cav1.2 + CaM$_{1234}$ (n=9)
Tau (ms)
Voltage (mV)
B
$
$
&
ns
ns
ns
A39V + CaM$_{WT}$ (n=9)
A39V + CaM$_{12}$ (n=9)
A39V + CaM$_{34}$ (n=14)
A39V + CaM$_{1234}$ (n=8)
Tau (ms)
Voltage (mV)
C
Cav1.2 + CaM$_{WT}$
60ms
Cav1.2 + CaM$_{1234}$
D
A39V-Cav1.2 + CaM$_{WT}$
60ms
A39V-Cav1.2 + CaM$_{1234}$

Figure 4-10

Figure 4-10: Calmodulin lobe mutants differentially affect the kinetics of activation for WT and A39V-Cav1.2 channels in the absence of calcium. A) Plot illustrating the time to maximum activation (Tau) at various voltages for WT-Cav1.2 channels expressed transiently in tsA-201 cells with Cavβ2a/Cavα2δ and recorded in barium with one of CaM_{WT}, CaM_{12}, CaM_{34} or CaM_{1234} and with 10mM BAPTA intracellular. Voltages for which all mutant CaMs differ significantly from the CaM_{WT} condition (* $p \leq 0.05$ by one-way ANOVA), and where CaM_{34} and CaM_{1234} differ from CaM_{WT} condition (# $p \leq 0.05$ by one-way ANOVA). B) Plot for the kinetics of activation of A39V-Cav1.2 channels expressed as in (A). Voltages for which CaM_{1234} differs significantly from the CaM_{WT} condition ($ $p \leq 0.05$ by one-way ANOVA), and where CaM_{12} and CaM_{1234} differ from CaM_{WT} condition (& $p \leq 0.05$ by one-way ANOVA). C) Sample traces of WT-Cav1.2 channels expressed with CaM_{WT} and CaM_{1234} at 10mV. Note that the CaM_{1234} trace has been normalized to that of CaM_{WT} and that the arrows denote peak of activation for WT-Cav1.2 with either CaM_{WT} (black) or CaM_{1234} (grey). D) Sample traces of A39V-Cav1.2 channels expressed with CaM_{WT} and CaM_{1234} at 10mV. Note that the CaM_{1234} trace has been normalized to that of CaM_{WT} and that the arrows denote peak of activation for A39V-Cav1.2 with either CaM_{WT} (black) or CaM_{1234} (grey).

Figure 4-9A displays current-voltage (IV) relationships for WT-Cav1.2 channels expressed with Cavβ2a/Cavα2δ and either CaM_{WT}, or one of CaM_{12}, CaM_{34}, or CaM_{1234}. WT-Cav1.2 channels expressed with CaM_{WT} display a right-shifted IV relationship compared to all CaM mutants. Figure 4-9B displays the IV relationship for A39V-Cav1.2 under the same conditions, but in this instance, only the CaM_{12} condition shows an appreciable leftward shift relative to CaM_{WT}. The bar graph in Figure 4-9C displays the half-activation potential (Va) for WT-Cav1.2 channels and reveals that all CaM mutants show a hyperpolarizing shift in the voltage-dependence of activation relative to the CaM_{WT} condition ($p \leq 0.05$ by one-way ANOVA).

For A39V-Cav1.2 only CaM_{12} shows a hyperpolarizing shift in Va compared to CaM_{WT} ($p \leq 0.05$, one-way ANOVA) (Figure 4-9D). Altogether, these data indicate that alterations in CaM structure due to the functional elimination of either the N- or C-lobe EF hand motifs produce direct effects on Cav1.2 channel gating. These effects are present in the absence of calcium and can be modulated by the N-terminus of the channel as the A39V-Cav1.2 data indicates. We next examined whether the kinetics of Cav1.2 activation was affected by CaM mutants. Figure 4-10A shows that WT-Cav1.2 channels recorded with Cavβ2a/Cavα2δ and CaM_{WT} reach peak current amplitude much more slowly than all CaM mutants at 10 mV ($p \leq 0.05$ by one-way ANOVA), and slower than CaM_{34} and CaM_{1234} at 0, 20 and 30 mV ($p \leq 0.05$ by one-way ANOVA). This data indicates that mutating the C-lobe of CaM causes WT-Cav1.2 channels to open much quicker than they would otherwise at physiological depolarizations. Throughout our analysis we used a single exponential equation to fit the rapid rising phase of channel activation. In rare occasions, (1 cell out of 9 at +10mV, for WT-Cav1.2), a second slower activation component was observed, but only in conditions with WT channels and CaM_{WT}. We focused on our analysis only on the fast activation time constant.

As with the voltage-dependence of activation data, A39V-Cav1.2 channels behave differently than wild type channels with regards to their kinetics of activation in the presence of CaM mutants (Figure 4-10B). Specifically, at depolarized potentials A39V-Cav1.2 channels have similar kinetics of activation in the presence of wild type or mutant CaMs ($p \geq 0.05$ by one-way ANOVA). This is also illustrated in the form of whole cell current traces depicted in Figures 5-10C and D at a test depolarization of +10 mV.

Altogether, the results of this section reveal a previously unrecognized functional effect of CaM lobe mutants on Cav1.2 channel activation that can involve the N-terminus of the channel.

4.3 Discussion

We have identified a novel effect of the pathophysiological mutation (A39V) through its reduction of N-lobe CDI of Cav1.2. Furthermore, our data reveal that mutant CaM molecules change activation gating of the channel in the absence of calcium, and that A39V does not affect Cavβ-dependent trafficking of neuronal Cav1.2 channels. The concept of channel isoform-dependent effects of disease causing mutations is not without precedent [249, 250] and in the case of the Brugada mutation A39V may perhaps explain why patients afflicted with this mutation do not exhibit a neuronal phenotype.

Contrary to previous work on the cardiac isoform of Cav1.2 showing a loss of cell surface trafficking of A39V-Cav1.2 in the presence of Cavβ2b, we find that both cardiac Cavβ2b and neuronal Cavβ1b equally regulate the neuronal forms of mutant and WT Cav1.2 channels, and that the mutation does not alter the behavior of the neuronal channel in the absence of the Cavβ subunit. The N-terminus of the Cav1.2 isoform used herein has the same exon1b/2

composition as the channel construct used in previous work with A39V-Cav1.2 [61], and hence N-terminal variations cannot account for the observed differences between our findings and those reported previously. Several sequence differences between brain and cardiac isoforms do exist, however, one of which is a sequence insertion in the II-III intracellular linker of the brain isoform that has been hypothesized to augment protein binding in this region of the channel [256] (see Figure 4-1). Moreover, the study by Antzelevitch and colleagues [61] utilized YFP tagged Cav1.2 channels containing exon 8a, whereas the Cav1.2 channels used in our experiments contained exon 8. It is possible that such splice isoform specific differences, or the attachment of a large YFP epitope could contribute to the observed differences in our findings compared to those reported previously. In our hands, A39V-Cav1.2 was able to traffic to the cell membrane as well as WT-Cav1.2, and the cardiac Cavβ2b subunit significantly increased surface expression of A39V-Cav1.2 in tsA-201 cells.

The observation that the A39V mutation reduced N-lobe CDI of Cav1.2 is surprising because Brugada syndrome is thought to involve a loss-of-function of these channels [61, 179], rather than the gain of function observed here. To reiterate cDNA construct used in our studies corresponds to the neuronal form of the channel, and it is possible that the observed gain of function is specific to neuronal channels. Importantly, A39V is only thirteen residues away from a key amino acid residue that has been implicated in N-lobe CDI (W52). Indeed, Dick and colleagues [134] suggested that during N-lobe CDI, CaM leaves a C-terminal anchoring site upon calcium elevation to then interact directly with the N-terminal residue W52, which in turn promotes CDI. Our recent work (Chapter 3) has expanded this idea so that CaM binds W52 and a second more proximal residue C106, which then transduces the CDI signal into domain I of the channel, promoting closure. The observation that A39V does not affect CaM binding to the N-

terminus of Cav1.2 (Figure 4-8) suggests that this residue may somehow be allosterically coupled to the CDI process. This could perhaps occur by partial immobilization of the N-terminus of Cav1.2, or by promoting additional intramolecular interactions within the N-terminus, or channel regions. For example, the N-terminus of Cav2.2 channels is capable of binding both the intracellular I-II linker and C-terminus [257]. As hydrophobic residues are often the anchor points for protein-protein interactions, it is possible that the A39V mutation may create a potential hydrophobic anchor.

How CaM molecules that are deficient in their ability to bind calcium affect Cav1.2 activation, is particularly interesting. Figure 4-10 shows that the kinetics of Cav1.2 activation is altered by mutant CaMs. The immediacy of this kinetic change suggests that CaMs which participate in this process must be pre-bound to the channel. Because all of our experiments were performed in barium and with 10mM BAPTA to buffer intracellular calcium, it is very unlikely that calcium has any role whatsoever in this effect. There is substantial evidence in the literature that in the absence of calcium CaM is tethered, or anchored to the C-terminus of VGCCs, specifically to the IQ domain [117, 118] and upstream PCI region [133]. It is known that CaM_{WT} is capable of many conformations, most of which are calcium sensitive [89-92]. Conversely, CaM_{1234} (and potentially CaM_{12} and CaM_{34}) display a different set of basic conformations [39, 97] that may differ from calcium-free CaM_{WT}. It is thus possible that the voltage-dependence and kinetics of Cav1.2 activation may be exquisitely sensitive to subtle changes in CaM structure. It is interesting to note that Cav1.2 channels have an EF-hand motif in the proximal C-terminus which has been proposed to be involved in the transduction of CDI signals in the holo channel [121, 221, 258]. Immediately downstream of the EF-hand region is the PCI region which anchors the N-lobe of CaM in the absence of calcium [133]. The EF-hand of Cav1.2 has

also been shown to modulate the voltage-dependence of activation with changing magnesium concentrations, a process which occurs also in the absence of calcium [155, 156]. We propose that the inherent conformational differences of CaM mutants leverage the EF-hand region differently than CaM_{WT} and perhaps in a manner analogous to magnesium occupancy. The observation that this effect was abrogated in the A39V mutant may then indicate that this region may be functionally coupled to the C-terminus/CaM complex.

However, irrespective of the underlying molecular mechanisms, our data reveal that widely used CaM mutant constructs may exert effects on ion channel function that are independent of the inability of these proteins to bind calcium. This should be taken into consideration when interpreting data that rely on these CaM mutants.

CHAPTER FIVE: **THE CAV1.2 N-TERMINUS CONTAINS A CAM KINASE SITE IMPORTANT FOR CHANNEL EXPRESSION AND FUNCTION**

5.1 Background

Cav1.2 is essential for emotional learning through its activity in the amygdala and anterior cingulated cortex [161, 259]. Not dissimilar from Cav1.2 channels, the calcium activated cascade comprising calmodulin kinase (CaMK) and calmodulin kinase kinase (CaMKK) participates in emotional learning [260, 261].

At the molecular level neuronal Cav1.2 channels and CaMKII regulate CREB activation following brief depolarizations in a manner which is intimately tied to open probability of the channel [4]. For the Cav2 family of voltage-gated calcium channels calmodulin (CaM) and CaM kinase modulate a process known as calcium dependent facilitation (CDF), which functions to upregulate channel conductance in low intracellular calcium, but which is in competition with calcium dependent inactivation (CDI) when levels of calcium rise [136, 262]. For L-type calcium channels two different types of CDI are evident [134, 226, 259] and although CaMK is involved in facilitating these channels, CDF is only possible when the C-terminal IQ region of the channel is mutated [118]. Nevertheless, in the presence of the IQ mutation, removal of CaMKII binding from the neighboring PreIQ-IQ region quells frequency dependent facilitation of Cav1.2 channels in calcium, thus suggesting that under certain conditions CaMKII may modulate Cav1.2 CDF [139]. It is from the work of Hudmon and colleagues (2005) that the presence of an N-terminal CaMKII site in Cav1.2 was first demonstrated through the use of GST pulldowns, although no function was ever described [139]. While exploring CDI of Cav1.2 channels in a

recent study, we narrowed the site of CaMKII interaction to the proximal N-terminus of the channel. Here using a combination of biochemistry, immunocytochemistry and electrophysiology we identify the precise location of this N-terminal CaMKII site and describe its effects on sub-cellular trafficking and function of the Cav1.2 channel.

5.2 Results

5.2.1 A proximal CISI sequence in the N-terminus of Cav1.2 forms the α-CaMKII binding site

Several intracellular linkers including the N-terminus of Cav1.2 have been shown to bind CaMKII with unknown functional consequence [139]. In previous work (Chapter 3) we narrowed the site of α-CaMKII binding to the proximal N-terminus of Cav1.2, but did not explore this interaction further [135]. Because CaMK is important for CDF of Cav2 [136, 137], and CREB dependent gene transcription of both Cav1 [263] and Cav2 channels [4, 264], we focused on further understating the physiological role of this novel CaMKII site.

Using coimmunoprecipitation experiments and live cell imaging of GFP fusion proteins of the Cav1.2 N-terminus (Figure 5-1) we first verified the existence of the proximal N-terminus α-CaMKII interaction site. Figure 5-2A-C show that all N-terminal constructs containing the proximal N_{2B} portion (i.e. Nterm, N_2 and N_{2B}) of Cav1.2 coimmunoprecipitate mCherry- α-CaMKII, as does the positive control PreIQ-IQ-GFP. Live cell imaging in tsA-201 cells (Figures 5-2D-H) shows that N_{2B} containing GFP fusion proteins (i.e. Nterm and N_{2B}) form aggregates, while all other N-terminal fusion proteins do not. Our previous work [135] has attributed this aggregation of N-terminal fusion proteins to an association with CaMK, thus providing a useful assay to examine CaMK interactions in live cells.

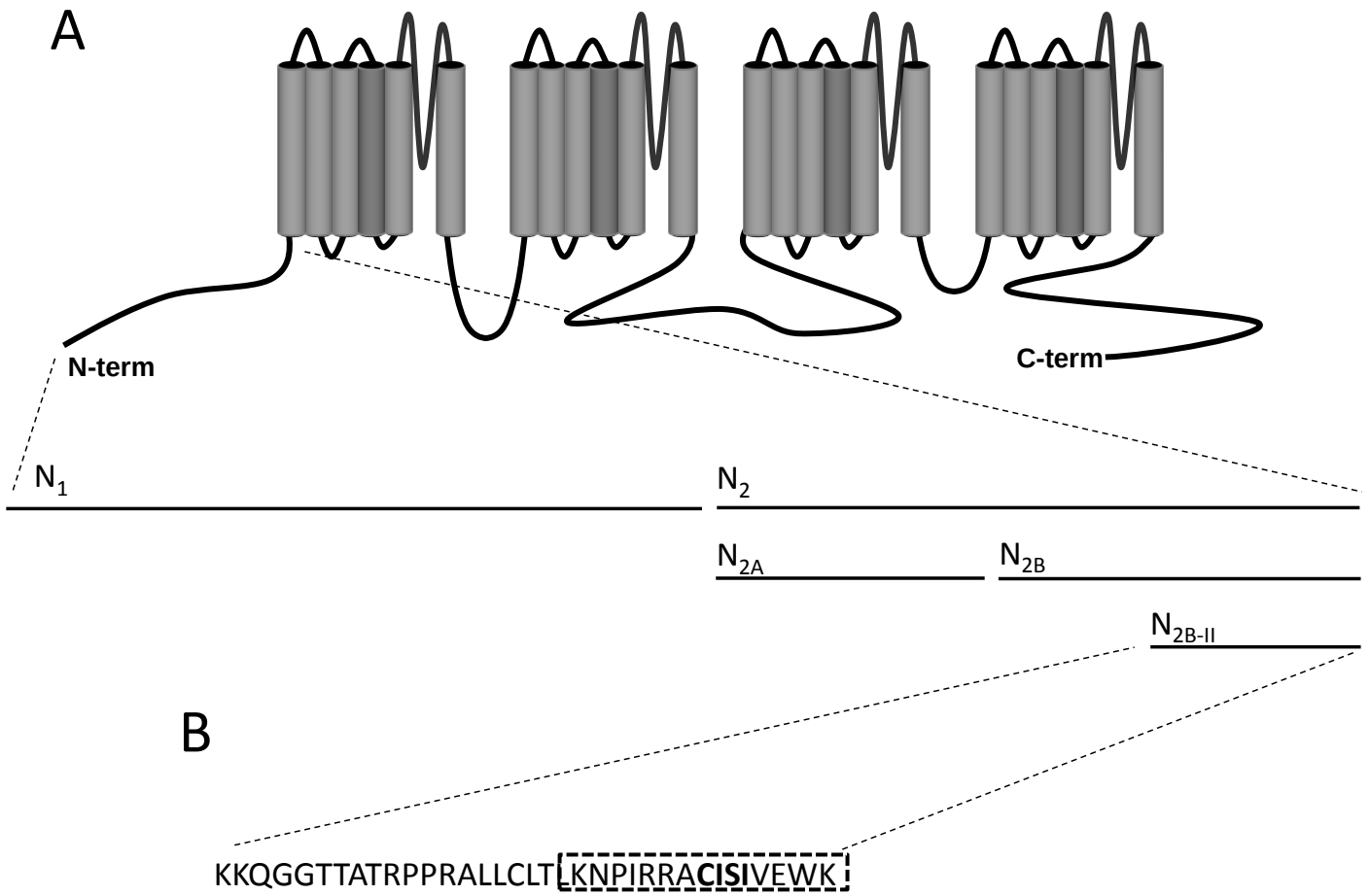
A
N-term
C-term
N1
N2
N2A
N2B
N2B-II
B
KKQGGTTATRPPRALLCLTLKNPIRRACISIVEWK

Figure 5-1

Figure 5-1: Relevant Cav1.2 N-terminal GFP fusion proteins A) Cartoon of the four domain Cav1.2 structure highlighting N-terminal GFP fusion proteins used. GFP is C-terminal to channel sequence in these constructs. B) The primary amino acid sequence of the $N_{2B\text{-}II}$ portion of the Cav1.2 N-terminus. The hatched box denotes the approximate location of the α-CaMKII interaction site mapped by our previous work. Bolded residues highlight the α-CaMKII interaction site identified here.

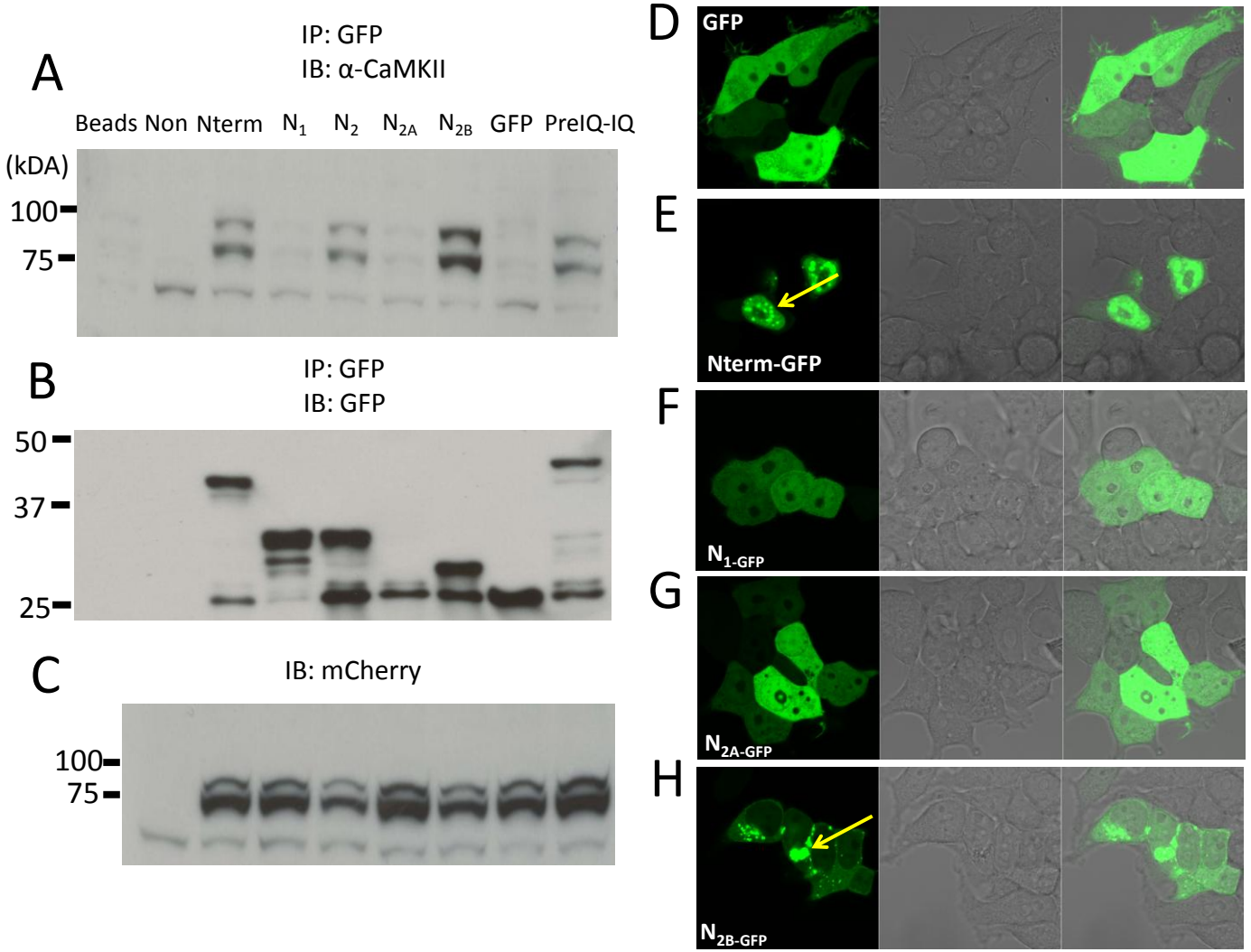
A
IP: GFP
IB: α-CaMKII
Beads Non Nterm N1 N2 N2A N2B GFP PreIQ-IQ
(kDA)
100
75
B
IP: GFP
IB: GFP
50
37
25
C
IB: mCherry
100
75
D
GFP
E
Nterm-GFP
F
N1-GFP
G
N2A-GFP
H
N2B-GFP

Figure 5-2

Figure 5-2: α-CaMKII binding occurs within the N_{2B} region of the Cav1.2 N-terminus and causes aggregate formation in tsA-201 cells A) Co-immunoprecipitation experiments of mCherry-α-CaMKII and N-terminal GFP fusion proteins or PreIQ-IQ positive control. Immunoprecipitates of GFP and controls (nontransfected/beads alone) were run on SDS-PAGE and blotted for α-CaMKII. B) Membranes were then stripped and re-probed for GFP. C) Western blot of α-CaMKII in lysate. D) Confocal images of live tsA-201 cells expressing GFP, Nterm-GFP (E), N_1-GFP (F), N_{2A}-GFP (G) and N_{2B}-GFP (H). Each experiment is representative of three successful attempts and yellow arrows highlight co-localization. Images and co-IPs performed by Dr. Ivana Assis Souza.

We next focused on pinpointing the exact residues by which α-CaMKII binds the proximal N-terminus of Cav1.2. Figure 5-3 demonstrates that replacing four sequential residues cysteine-isoleucine-serine-isoleucine (CISI, 117-120a.a.) with alanines, prevents binding of $N_{2B\text{-}II}$-GFP to mCherry-α-CaMKII. A single mutant C117R or double mutant C117R/S119R version of $N_{2B\text{-}II}$-GFP both retain binding to α-CaMKII, necessitating mutation of the adjacent isoleucines (Figure 5-4**)**. It is interesting to note that disruption of α-CaMKII binding to the PreIQ-IQ region of the C-terminus of Cav1.2 also requires multiple mutations (TVGKFY-AAAAAA), suggesting that channel interactions with α-CaMKII are inherently resilient [139]. Nevertheless, given the loss of mCherry-α-CaMKII binding to $N_{2B\text{-}II\text{-}AAAA}$-GFP we expected that the latter fusion protein would no longer aggregate in live tsA-201 cells. Indeed, as shown in Figure 5-5B, $N_{2B\text{-}II}$-GFP aggregates and co-localizes with mCherry-α-CaMKII in live cells whereas $N_{2B\text{-}II\text{-}AAAA}$-GFP does not (Figure 5-5D). Altogether, our biochemical and immunocytochemical results illustrate that four residues in the proximal N-terminus of Cav1.2 bind and promote co-localization with α-CaMKII.

5.2.2 Cav1.2 channels lacking an N-terminal α-CaMKII binding site have reduced surface expression but not reduced function

In order to determine the function of the α-CaMKII site in the N-terminus of Cav1.2 we applied a combination of surface protein biotinylation, confocal imaging and electrophysiological analysis. Figure 5-6A shows that externally tagged WT-Cav1.2 channels, in the presence of auxiliary subunits, express well both at the cell surface and intracellularly (Figure 5-7A).

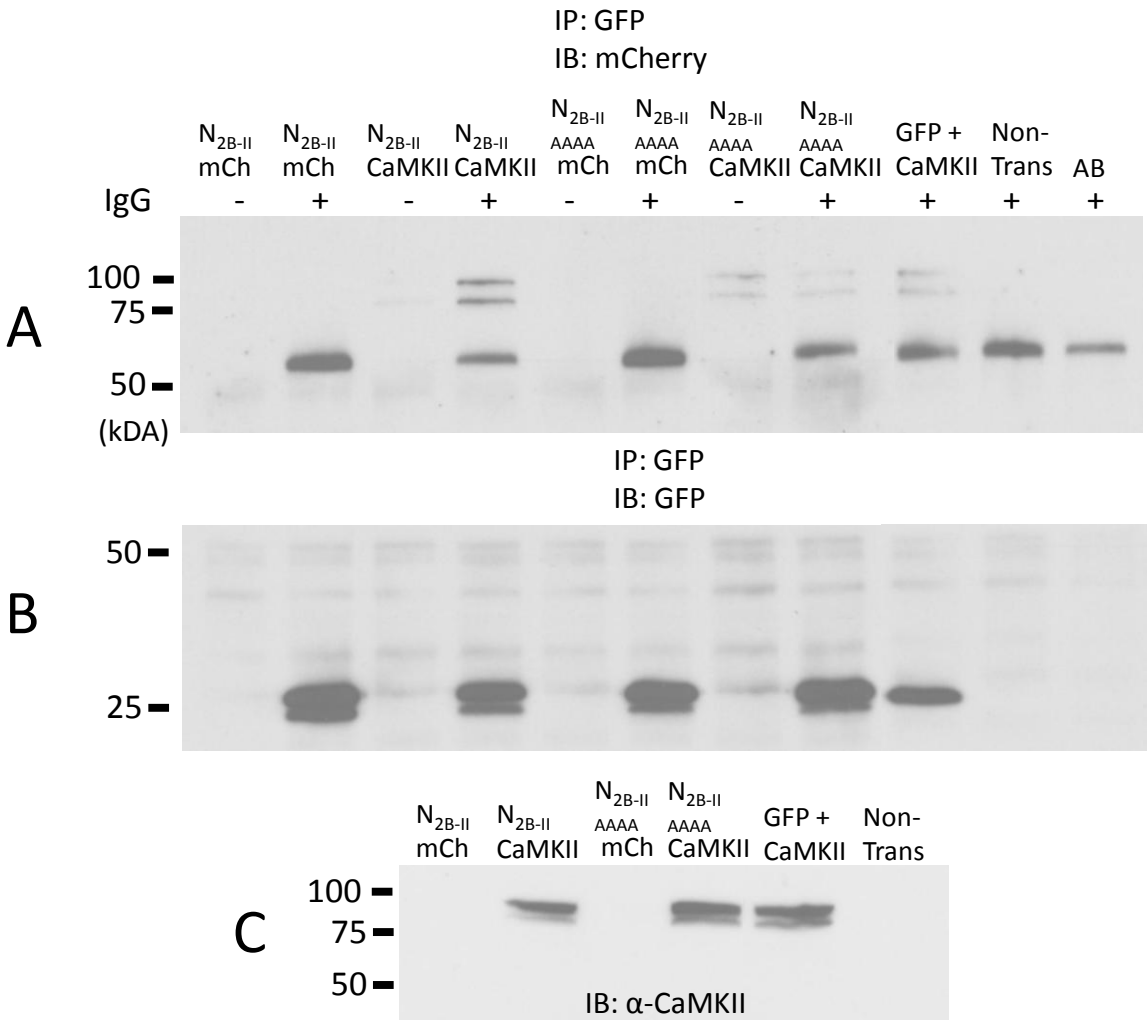
IP: GFP
IB: mCherry
N2B-II mCh
N2B-II mCh
N2B-II CaMKII
N2B-II CaMKII
N2B-II AAAA mCh
N2B-II AAAA mCh
N2B-II AAAA CaMKII
N2B-II AAAA CaMKII
GFP + CaMKII
Non-Trans
AB
IgG - + - + - + - + + + +
A
100
75
50
(kDA)
IP: GFP
IB: GFP
B
50
25
N2B-II mCh
N2B-II CaMKII
N2B-II AAAA mCh
N2B-II AAAA CaMKII
GFP + CaMKII
Non-Trans
C
100
75
50
IB: α-CaMKII

Figure 5-3

Figure 5-3: Mutagenesis of $N_{2B\text{-}II}$ identifies four residues (CISI) important for binding α-CaMKII A) Co-immunoprecipitation experiments of mCherry (mCh), or mCherry-α-CaMKII with one of $N_{2B\text{-}II}$-GFP, or $N_{2B\text{-}II\text{-}AAAA}$-GFP (AAAA). Immunoprecipitates of GFP constructs and controls (nontransfected, or antibody [AB]) were run on SDS-PAGE and blotted for mCherry. B) Membranes were then stripped and re-probed for GFP. C) Western blot of α-CaMKII in lysate. This experiment is representative of two successful experiments.

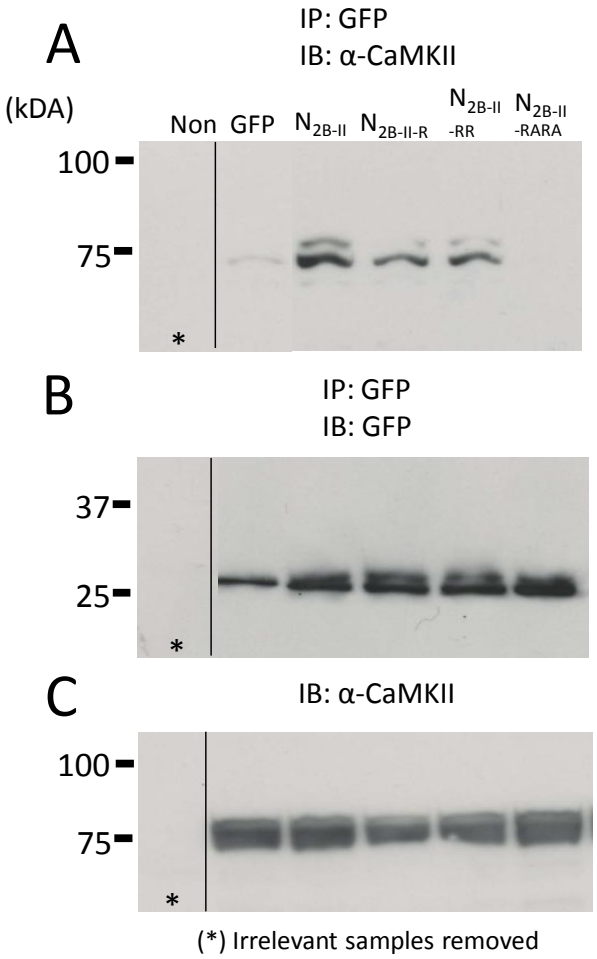
A
IP: GFP
IB: α-CaMKII
(kDA)
Non
GFP
N2B-II
N2B-II-R
N2B-II -RR
N2B-II -RARA
100
75
*
B
IP: GFP
IB: GFP
37
25
*
C
IB: α-CaMKII
100
75
*
(*) Irrelevant samples removed

Figure 5-4

Figure 5-4: All four residues (CISI) must be mutated to prevent co-IP with α-CaMKII A) Co-immunoprecipitation experiments of mCherry-α-CaMKII and either GFP, or $N_{2B\text{-}II}$-GFP fusion proteins with the following point mutations: $N_{2B\text{-}II\text{-}R}$ (C117R), $N_{2B\text{-}II\text{-}RR}$ (C117R/S119R) and $N_{2B\text{-}II\text{-}RARA}$ (C117R/I118A/S119R/I120A). Immunoprecipitates of GFP or nontransfected control were run on SDS-PAGE and blotted for α-CaMKII. B) Membranes were then stripped and re-probed for GFP. C) Western blot of α-CaMKII in lysate. This experiment is representative of two successful experiments performed by Dr. Ivana Assis Souza.

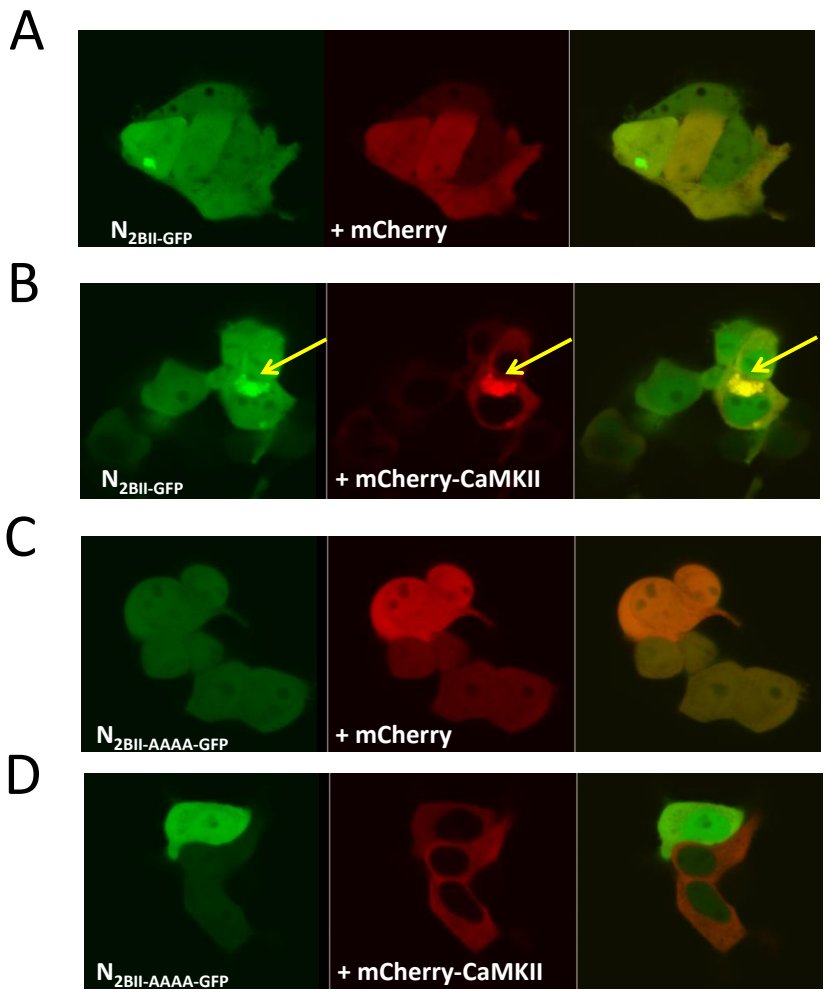
A
N2BII-GFP
+ mCherry
B
N2BII-GFP
+ mCherry-CaMKII
C
N2BII-AAAA-GFP
+ mCherry
D
N2BII-AAAA-GFP
+ mCherry-CaMKII

Figure 5-5

Figure 5-5: mCherry-α-CaMKII requires CISI sequence for co-localization with $N_{2B\text{-}II}$ in tsA-201 cells A) Confocal images of live tsA-201 cells expressing mCherry and $N_{2B\text{-}II}$-GFP, mCherry-α-CaMKII and $N_{2B\text{-}II}$-GFP (B), mCherry and $N_{2B\text{-}II\text{-}AAAA}$-GFP (C), mCherry-α-CaMKII and $N_{2B\text{-}II\text{-}AAAA}$-GFP (D). Yellow arrows highlight co-localization. This experiment is representative of two successful experiments which were performed by Dr. Ivana Assis Souza.

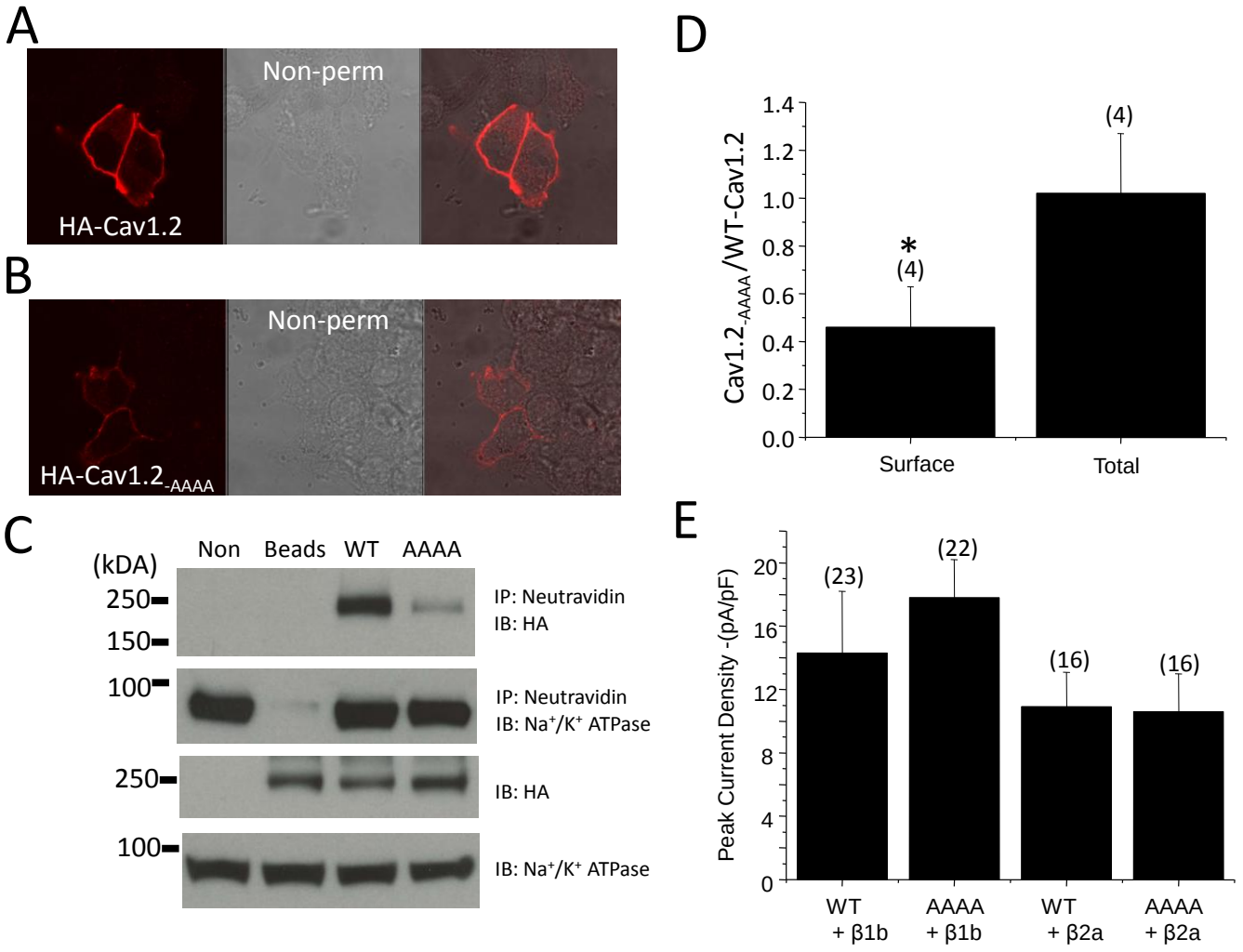
A
Non-perm
HA-Cav1.2
B
Non-perm
HA-Cav1.2-AAAA
C
(kDA)
Non
Beads
WT
AAAA
250
150
100
250
100
IP: Neutravidin
IB: HA
IP: Neutravidin
IB: Na+/K+ ATPase
IB: HA
IB: Na+/K+ ATPase
D
Cav1.2-AAAA/WT-Cav1.2
1.4
1.2
1.0
0.8
0.6
0.4
0.2
0.0
*
(4)
(4)
Surface
Total
E
Peak Current Density -(pA/pF)
20
16
12
8
4
0
(23)
(22)
(16)
(16)
WT + β1b
AAAA + β1b
WT + β2a
AAAA + β2a

Figure 5-6

Figure 5-6: Eliminating the CISI sequence from Cav1.2 channels reduces surface expression but not current density. A) Non-permeabilzed tsA-201 cells expressing Cavβ1b/Cavα2δ with externally tagged HA-Cav1.2 (Alexa 594) or HA-Cav1.2$_{-AAAA}$ channels (B). C) Biotinylation of HA tagged Cav1.2 (WT) and Cav1.2-$_{AAAA}$ channels (AAAA) expressed with Cavβ1b/α2δ in transfected tsA-201 cells and below, the same biotinylation stripped and reprobed for Na^+/K^+ ATPase. Controls are non-transfected and beads only. The third blot shows 100ug of lysates probed for HA and below this, the same blot stripped and reprobed for Na^+/K^+ ATPase. D) Normalized quantification of biotinylated channels from (C) which shows that Cav1.2$_{-AAAA}$ channels express significantly less (0.46 ± 0.17, *p = 0.02 by students *t*-test) at the cell surface compared to WT-Cav1.2. E) A bar graph displaying peak current density of non-tagged Cav1.2 and Cav1.2$_{-AAAA}$ channels transiently expressed in tsA-201 cells with either Cavβ1b, or Cavβ2a and Cavα2δ. There is no significant difference in the current density of WT-Cav1.2 (-14.3 ± 3.9 pA/pF) and Cav1.2$_{-AAAA}$ (-17.8 ± 2.4 pA/pF) channels with Cavβ1b, or between WT-Cav1.2 (-10.9 ± 2.2 pA/pF), and Cav1.2$_{-AAAA}$ (-10.6 ± 2.4 pA/pF) with Cavβ2a. Biotynlation performed by Dr. Ivana Assis Souza.

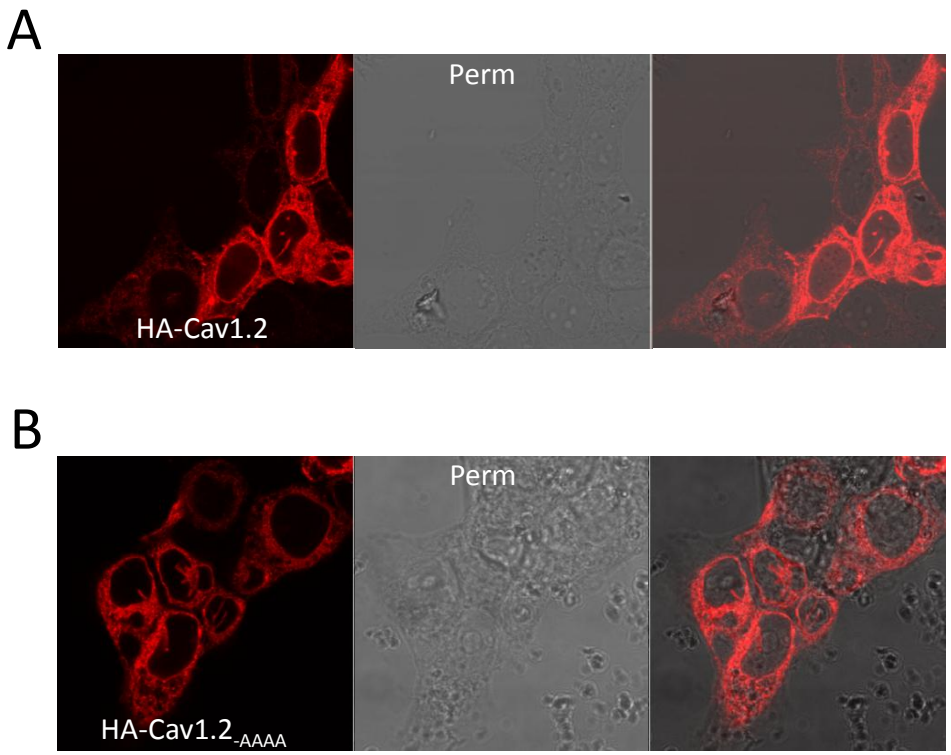

Figure 5-7

Figure 5-7: Permeabilized tsA-201 cells have similar amounts of WT-Cav1.2 and Cav1.2$_{-AAAA}$ channels expressed. A) Permeabilized tsA-201 cells expressing Cavβ1b/Cavα2δ with externally tagged HA-Cav1.2 (Alexa 594) or HA-Cav1.2$_{-AAAA}$ channels (B). Images gathered by Dr. Ivana Assis Souza.

Externally tagged HA-Cav1.2$_{-AAAA}$ channels on the other hand, have much lower surface expression under the same conditions (non permeabilized cells, Figure 5-6B), but show robust total protein expression (permeabilized cells, Figure 5-7B). Surface protein biotinylation studies support these observations and demonstrate that Cav1.2$_{-AAAA}$ expresses much less than WT-Cav1.2 channels in the surface pool (Figure 5-6C). Normalized quantification of channel biotinylations illustrates that Cav1.2$_{-AAAA}$ (0.46 ± 0.17, *p = 0.02 by students *t*-test) expresses significantly less at the cell surface compared to WT-Cav1.2 channels. This data strongly suggest that α-CaMKII may regulate the sub-cellular trafficking of Cav1.2 channels.

We next used electrophysiology to test whether Cav1.2$_{-AAAA}$ whole cell current density was altered by the reduction in the surface pool of channels. Unexpectedly, Cav1.2$_{-AAAA}$ current density was not statistically different from WT-Cav1.2 channels in the presence of either Cavβ1b, or Cavβ2a auxiliary subunits (Figure 5-6E). This surprising result suggests that Cav1.2$_{-AAAA}$ channels exhibit augmented single channel function which offsets their poor surface expression.

5.2.3 Cav1.2 channels lacking an N-terminal α-CaMKII binding site can be facilitated by BayK 8644

The observation that whole cell current densities of the quadruple alanine mutant were not different from those of wild type channels suggest that Cav1.2$_{-AAAA}$ channels either have an augmented single channel amplitude, or alternatively an increased open probability. The former possibility is highly unlikely given that the CaMK site is located far from the selectivity filter, leaving an increase in maximum open probability as a more likely scenario. To further explore

the gating behavior of the mutant channels, we examined their facilitation by either voltage, or BayK 8644. As CaM kinase is linked to voltage-dependent facilitation (VDF) of L-type calcium channels [262], we first considered the possibility that Cav1.2$_{-AAAA}$ channels might be tonically facilitated. Figure 5-8A shows that Cavβ2a promotes a minimal 20% increase in VDF of WT channels which is consistent with previous reports [265, 266]. Mutant channels showed voltage facilitation that was indistinguishable from that of WT with Cavβ2a. In contrast, Cavβ1b prevented facilitation of both channels in our hands, in contrast with previous studies [267, 268]. Altogether, the results in Figure 5-8A indicate that Cav1.2$_{-AAAA}$ is not in a tonically facilitated state.

Next we tested whether Cav1.2$_{-AAAA}$ could be facilitated by application of BayK 8644 which is known to increases the open probability of L-type calcium channels [269-271]. Indeed, exogenous calcium insensitive CaMKII has also been shown to promote increased open probability of L-type calcium channels in ventricular myocytes, in analogy with the effects of BayK 8644 [264]. Figure 5-8B displays the current-voltage relationship for WT-Cav1.2 and Cav1.2$_{-AAAA}$ channels treated with 1μM BayK 8644. Although both channels displayed increased whole cell current density upon treatment, Cav1.2$_{-AAAA}$ showed a much greater BayK 8644 - mediated increase (239 ± 28 % at peak, *p = 0.04 by student's *t*-test) in current density compared to WT-Cav1.2 channels (139 ± 16%). These data suggest that the inability of the mutant channel to bind CaMKII renders the channel more susceptible to the effects of BayK-8644, suggesting that CaMKII deficient channels can be opened more effectively.

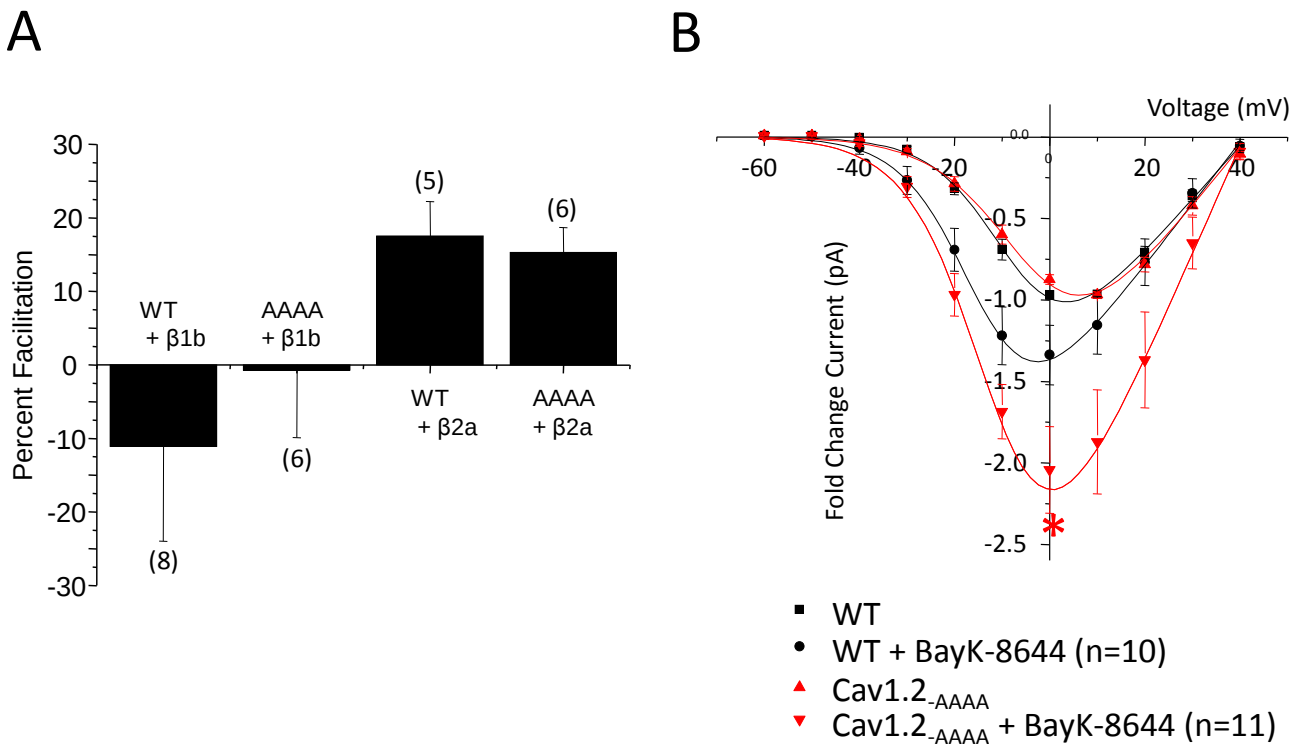
A
B
Percent Facilitation
30
20
10
0
-10
-20
-30
WT
+ β1b
AAAA
+ β1b
WT
+ β2a
AAAA
+ β2a
(8)
(6)
(5)
(6)
Voltage (mV)
Fold Change Current (pA)
-60
-40
-20
20
40
-0.5
-1.0
-1.5
-2.0
-2.5
WT
WT + BayK-8644 (n=10)
Cav1.2-AAAA
Cav1.2-AAAA + BayK-8644 (n=11)

Figure 5-8

Figure 5-8: Cav1.2-$_{AAAA}$ channels can be facilitated by BayK 8644 but not voltage. A) A bar graph displaying percent change for voltage-dependent facilitation of non-tagged Cav1.2 and Cav1.2$_{-AAAA}$ channels transiently expressed in tsA-201 cells with Cavα2δ and either Cavβ1b or Cavβ2a. There is no significant difference in the percent facilitation by voltage for WT, or Cav1.2$_{-AAAA}$ channels with either Cavβ subunit. B) Current voltage relationships of non-tagged Cav1.2, or Cav1.2$_{-AAAA}$ channels expressed with Cavβ1b/ Cavα2δ with and without 1uM ± BayK-8644. Cav1.2$_{-AAAA}$ channels show significantly more facilitation of peak current (red asterisks) by ± BayK-8644 (239 ± 28%, * $p \leq 0.04$ by student's *t*-test) compared to WT-Cav1.2 channels (139 ± 16%).

5.3 Discussion

Cav1.2 and CaM kinase are important components of neuronal calcium signaling pathways. CaM kinase can associate with the C-terminus of Cav1.2 and modulate CDF [139], but only when the IQ domain which anchors CaM is ablated [118]. We recently narrowed the position of an N-terminal CaMKII site in Cav1.2 [135] and in this work, have localized it to four residues (CISI) proximal to domain I of the channel. Strictly speaking we are unable to conclude whether removing CISI from the N-terminus, or replacing CISI with four alanine residues- propensity to induce α-helices and alter secondary structure- ablates binding to CaM kinase. It also remains possible that by performing this mutation CaMKII binding may have been lost via a competitive gain-of-binding of another protein. Nevertheless, full length channels lacking this CISI element ($Cav1.2_{-AAAA}$) display a significant reduction in surface expression, yet as well, an unexpected increase in function which offsets the trafficking defect. To our knowledge there is no prior evidence in the literature for a role of CaM kinase in calcium channel trafficking, however it is worth noting that CaMKII does regulate trafficking of potassium channels to the cell membrane [272-274]. Also, removal of the Cav1.2 N-terminus has been shown to increase surface expression of these channels in *Xenopus* oocytes indicating this region of the channel can participate in subcellular trafficking [159].

The compensatory increase we observe in the functional properties of $Cav1.2_{-AAAA}$ could in principle be due to two mechanisms. On the one hand it is possible that $Cav1.2_{-AAAA}$ channels have a larger single channel conductance than WT-Cav1.2. However, given that the pool of $Cav1.2_{-AAAA}$ channels in the membrane is less than half of that of WT-Cav1.2 (Figure 5-6D) this would imply that the single channel conductance of the $Cav1.2_{-AAAA}$ would need to double to

account for the reduction in surface expression. This seems unlikely given that only the p-loops and outer vestibules of the pore (i.e. membrane spanning regions S5-S6 regions) have been shown to strongly impact selectivity [38] and permeation [46, 192, 275], whereas the N-terminal region, and more specifically, the CISI site we describe, is far from these loci.

The possibility of an increase in maximum open probability of Cav1.2$_{-AAAA}$ is therefore the more likely scenario, and is supported by a number of considerations: First, we have previously measured the open probability of Cav1.2 channels at the single channel level and found it to be 0.07 at the peak of the current–voltage relation 0 mV [44], leaving considerable room for increase in the open probability of mutant channels. Second, deletion of the first 46 amino acids in the N-terminus of the cardiac Cav1.2 channel have been previously shown to affect maximum open probability without affecting the voltage-dependence of gating (note that the voltage-dependence of activation was not visibly affected by the alanine substitutions, see Figure 5-8B) [241], suggesting the possibility that this stretch of residues might perhaps functionally interact with the newly identified CaMKII site. Finally, it is worth noting that a portion of the Cav1.2 C-terminus which contains the C-terminal CaMKII site has been shown to regulate both channel trafficking and single channel open probability [276]. Although voltage-dependent facilitation was not different between the mutant and WT channels, BayK8644 appeared to more effectively augment the CaMKII binding deficient mutant channel. This implies that Cav1.2$_{-AAAA}$ may be susceptible to even greater increases in maximum open probability compared to wild type channels. Altogether our results suggest that the N-terminal CaMKII site is linked allosterically to the activation gating machinery of the channel.

At this point it is unclear whether CaMKII modulation of native channels parallels our observations in tsA-201 cells, although it is tempting to speculate about the physiological significance of offsetting effects on channel trafficking and function. The resultant effect of course is the same net Cav1.2 whole cell current. One key function of neuronal Cav1.2 channels is the activation of calcium-dependent gene transcription events that are dependent on CaM interactions with the channel and downstream activation of CaMKII [264]. Importantly, this process is critically dependent on the open probability of individual channels [4]. A switch to fewer channels with increased open probability would therefore result in more effective excitation transcription coupling, without producing a net rise in calcium influx, and thus in increased risk of calcium toxicity [1]. In this regard CaMKII could act as a negative feedback regulator that reduces open probability upon association with the channel. This possibility will need to be explored experimentally in future studies.

Altogether, our data reveal a CaMKII site in the N-terminus of Cav1.2 is formed by four proximal residues (CISI). In the full length Cav1.2 channel removal of CISI results in a decrease in surface expression, but an offsetting functional increase presumably due to an increase in maximum open probability. These data thus implicate a role for CaMKII in both channel trafficking and function.

CHAPTER SIX: **GENERAL DISCUSSION AND FUTURE DIRECTIONS**

This thesis focuses on how the N-terminus of Cav1.2 regulates channel trafficking, expression and function. We chose to study the N-terminus of Cav1.2 because of a surprising lack of surface expression reported for the Brugada syndrome mutation A39V in cardiac Cav1.2 channels [61]. We show here that this was a tissue specific effect, as A39V has no such trafficking defect in neuronal Cav1.2 channels and that A39V can functionally regulate the channel in a CaM dependent fashion. Because A39V is proximal to a residue (W52) recently shown to modulate Cav1.2 global CDI [134], we investigated whether other N-terminal CaM binding sites were involved in this process, indeed we found A39V does alter CDI, but not CaM binding. We also show that the Cav1.2 N-terminus has two proximal channel sequences ($N_{2B\text{-}I}$ and $N_{2B\text{-}II}$) which bind CaM and α-CaMKII, respectively. $N_{2B\text{-}I}$ contains the residue C106 which binds CaM and works in cooperation with W52 to regulate global CDI of Cav1.2 channels. $N_{2B\text{-}II}$ contains four residues (C117, I118, S119 and I120) that anchor α-CaMKII, and which regulate surface expression and functional silencing of Cav1.2 channels in an offsetting manner. We believe our contribution to the field of Cav1.2 structure/function to be substantial and yet with every answer comes further questions. The following sections address potential future directions for the field. We conclude by proposing how the Brugada mutation A39V integrates into the model of global CDI proposed in Chapter 3.

6.1 Calmodulin binding and CDI of VGCCs

We were able to show by two seperate biochemical methods that CaM binds the N-terminus of Cav1.2 at C106, and that this binding regulates global CDI. Much like the NMR work recently

reported for the CaM binding residue W52 [88], it would be interesting to know exactly how CaM associates with C106, or rather how CaM can participate in binding of both W52 and C106. Studying such interactions by NMR or crystallography, would compliment the various crystal structures already gathered for C-terminal/CaM interactions [84-87] and extend our understanding of VGCC CDI.

Recall Figure 4-1A and the sequence alignment of human and rat clones of Cav1.2. In order to better match the human sequences, we mutated G57 to aspartic acid in the rat clone. During this thesis we worked for a period of time on a epigenetics project which implicated codon 57 in age and tissue dependent RNA editing. We do not present the data here because it is incomplete, but it appeared that in younger rats (p0-p18) this codon was edited to produce a glycine a position 57 in brain, but not heart tissue. Moreover in adult rats (4 months) RNA editing had ceased at this position, thus constituitvely producing aspartic acid. It is conspicuous that G57 exists only five residues away from the critical CDI residue W52, and is present in the same alpha-helical region called NSCaTE (see Figure 3-11). We do not have evidence yet that this potential RNA edit impacts global CDI, but recent papers have shown that RNA editing of the C-terminal IQ domain alters local CDI [225, 226]. It would be interesting to uncover if glycine at position 57 is an RNA edit specifically designed to tune Cav1.2 conductance in fetal brain tissue.

A domain I-II linker CaM binding site has been reported multiple times for Cav1.2, but never functionally characterized [221, 277]. Considering that the domain I-II linker and Cavβ subunit compose a portion of the channel inactivation machinery [105], it seems plausible that a domain I-II linker/CaM interaction exists to modulate CDI of Cav1.2 channels, perhaps acting as a focal point for N-terminal and C-terminal CDI processes. Given that Cav2.2 channels can

partake in intralinker binding (i.e. N-terminus can bind I-II linker, or C-terminus) [257] it seems plausible that a domain I-II linker CaM interaction may exist for Cav1.2 channels in order to consolidate spatially distinct CDI proceses into a unified channel closing mechanism.

6.2 Effects of Brugada syndrome mutations on Cav1.2 trafficking and function

We have shown that the Brugada syndrome mutation A39V does not produce a trafficking defect in the neuronal isoform of Cav1.2. As discussed briefly in Section 4.3 the N-terminus of Cav1.2 channels has three, tissue specific, first exons (1a, 1b, 1c). Our cDNA of Cav1.2 contains the brain splice variant (exon 1b) [256], whereas cardiac tissue contains (exon 1a) [278] and smooth arterial myocytes (exon 1c) [279]. It remains to be tested whether A39V produces trafficking or CDI defects in Cav1.2 channels possessing exon 1a. Why is this the case? The group that screens patients and reports Brugada syndrome mutations in *CACNA1C* [61, 185] functionally analyzes their clones in a mixed cDNA background (see Figure 4-1) which does not include the cardiac specific exon 1a. It seems pertinent then that A39V be functionally studied in an pure cardiac Cav1.2 channel in order to compliment the neuronal studies we have done here. Moreover, many Brugada syndrome mutations in VGCC subunits [185] have not been functionally characterized, and so a wealth of work awaits in this field.

6.3 CaMKII as a regulator of VGCC trafficking

This thesis concludes with a chapter that identifies a α-CaMKII site in the proximal N-terminus of Cav1.2. We identified this site because of calcium insensitive pulldowns of N-terminal proteins on CaM sepharose beads. We also noted that GFP fusion proteins containing these calcium insensitive sites formed aggregates in cells, which vanished when co-IP with α-CaMKII,

or pulldown on CaM sepharose ceased. What we have identified therefore, is a means of quickly screening for α-CaMKII binding sites in proteins of interest, which of course must later be verified by co-IP with the kinase. The advantage to our screening method is that co-IPs are often finiky and unreliable, whereas CaM sepharose pulldowns and fluorsecent aggregates in cells are immediately apparent. With this in mind Hudmon and colleagues showed that all Cav1.2 intracellular linkers can associate with α-CaMKII, but the exact binding sites were not identifed, that is, with the exception of the C-terminal IQ domain site [139] and the N-terminal site we have characterized. These other intracellular sites can now be easily identified using our CaM sepharose pulldown/ live cell aggregate assay.

In Appendix B we use this very technique to pinpoint a probable α-CaMKII binding site in the N-terminus of Cav2.1. Because this thesis focuses on Cav1.2 we did not include this data in previous chapters yet the data in Appendix B shed light on what may be conservered CaM binding sites in the N-terminus of all HVA VGCCs.

6.4 A model incorporating A39V and Cav1.2 global CDI

In Chapter 3 we expand on the model of global CDI and propose that the inactivation signal imparted by CaM binding toW52 (NSCaTE) and C106 (NATE) propagates through these motifs and into domain I of the channel, promoting closure (Figure 3-11). In Chapter 4 we describe how the Brugada syndrome mutation A39V augments the activation of Cav1.2 and as well, global CDI of the channel in a manner which does not effect N-terminal CaM binding. How can the model of global CDI described in Chapter 3 incorporate this new data?

Figure 6-1A shows WT-Cav1.2 channels in three states: closed, open and during global CDI (inactivated). In Figure 6-1A CaM does not associate (closed and open states) with the N-

terminus at W52 and C106 until calcium rises sufficiently to induce global CDI (inactivated) of the channel. The red arrow in Figure 6-1A illustrates that in the WT condition all of the global CDI signal produced by CaM binding to NSCaTE/NATE is transduced into domain I of the channel. Figure 6-1B proposes that an abberant intralinker binding event occurs between the N-terminus and proximal C-terminus of the channel near the PCI 1 region. This of course is a result of the Brugada mutation A39V. Although we have not tested this scenario biochemically, several lines of functional data support this idea. First, in the absence of calcium A39V augments both the voltage-dependence (Figure 4-9) and kinetics (4-10) of Cav1.2 activation differently than WT-Cav1.2 channels expressed with either CaM_{WT}, or CaM_{1234}. As discussed in the introduction the only channel linker known to possess a calcium free CaM binding site is the C-terminus (i.e. PCI2 and IQ regions). If we assume all CaMs (CaM_{WT}, CaM_{1234} etc) are tethered to the C-terminus in the absence of calcium, then the fact that A39V immediately affects channel activation kinetics suggests that the N-terminus of Cav1.2 is impeding function of the C-terminus where the tethered CaMs reside.

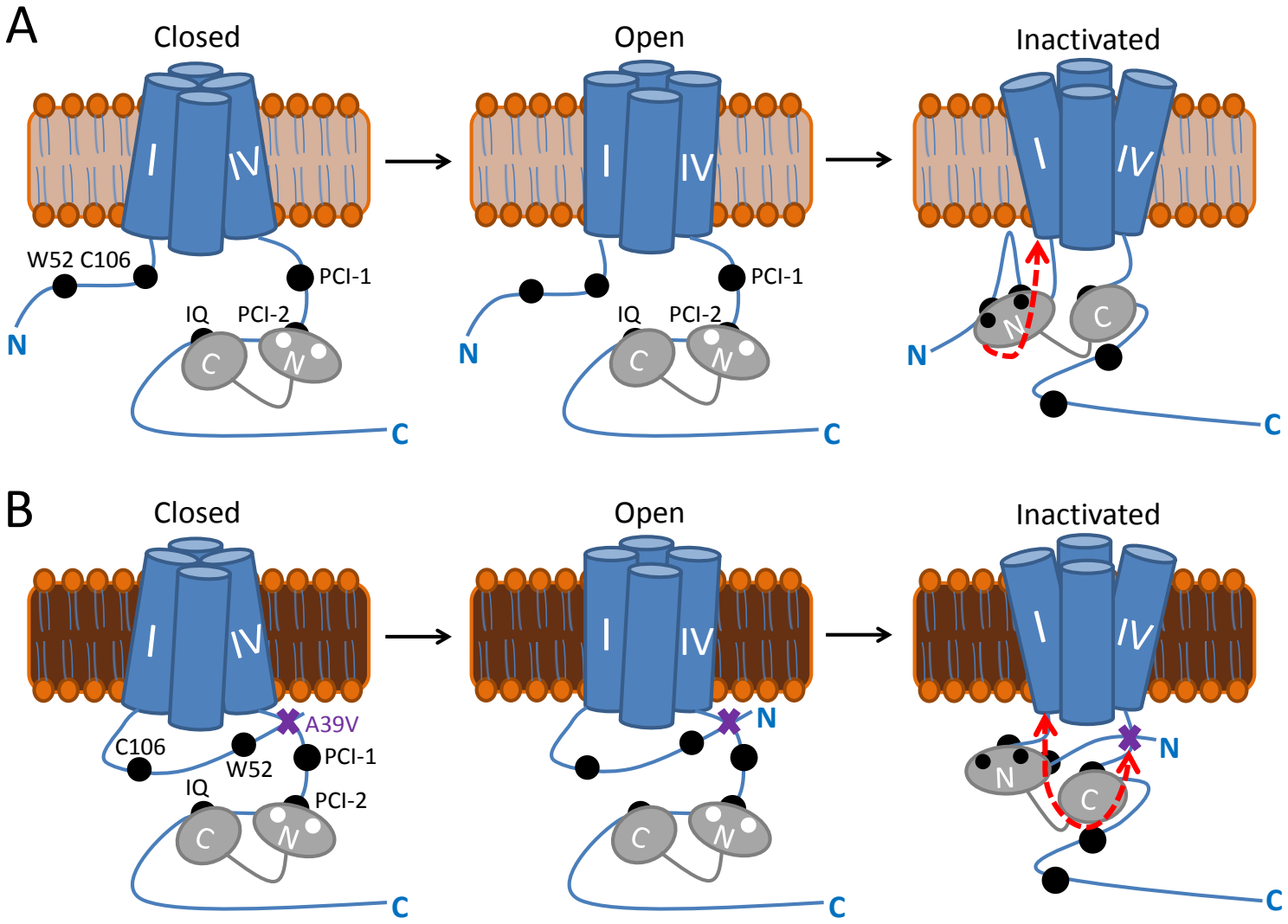
A
Closed
Open
Inactivated
I
IV
W52 C106
PCI-1
IQ
PCI-2
N
C
B
Closed
Open
Inactivated
A39V
C106
W52
PCI-1
IQ
PCI-2
N
C

Figure 6-1

Figure 6-1: A model incorporating A39V and Cav1.2 global CDI. A) WT-Cav1.2 channels in closed, open and inactivated (global CDI) states. When the channel is closed, and until calcium levels rise sufficiently once open, CaM is anchored to the C-terminus of Cav1.2 at the IQ domain and PCI-2 region. Note also that the N-lobe of CaM (grey) lacks calcium (white circles) while the channel is closed and before calcium rises sufficiently. Upon a global calcium increase of ample concentration the N-lobe of CaM binds two Ca^{2+} ions (black circles) and forms a tripartite N-terminal association with both W52 (NSCaTE) and C106 (NATE). The maximum amount of global CDI signal (red arrow) is therefore transduced into domain I of Cav1.2, promoting channel closure. The C-lobe of CaM remains associated with the C-terminus during global CDI, but shifts from PCI-2 to PCI-1. B) A39V-Cav1.2 channels in closed, open and inactivated states. Note that the Brugada mutation (purple X) has caused aberrant intralinker binding between the N-terminus and proximal C-terminus. Following a sufficient increase in calcium some NSCaTE/NATE/CaM binding and therefore global CDI persists for A39V-Cav1.2, but it is less efficient (bidirectional red arrow) than for WT-Cav1.2. We propose that the reduction in global CDI caused by A39V occurs because this mutation has either disrupted C-terminal CaM interactions which then affect N-terminal CaM interactions and N-lobe CDI, or because transduction of the global CDI signal is reduced by N-terminal immobilization.

Second, A39V disrupts global CDI (Figure 4-6) in a manner which does not alter N-terminal CaM binding (Figure 4-8). Therefore, we must assume that W52 and C106 retain CaM binding in the intact A39V-Cav1.2 channel, yet the transduction of global CDI is incomplete. This is represented by the bidirectional red arrow in Figure 6-1B which shows that because the N-terminus is anchored to a C-terminal portion of the channel, it is unable to transduce global CDI as effectively to domain I. Note that this model does not eliminate the possibility that A39V could be disrupting a C-terminal CaM interaction, which then affects global CDI at the channel N-terminus. Regardless of whether A39V disrupts C-terminal CaM binding, or successful global CDI signal transduction in the N-terminus, or both, it seems plausible that A39V augments Cav1.2 function by aberrant intralinker binding.

6.5 Closing statement

We have made significant contributions to the structure/function literature of neuronal Cav1.2 channels. We show that the N-terminus of this channel contributes to various aspects of function, as well as surface and total channel expression. Bottom line: L-type calcium channels are important.

References:

1. Clapham, D.E., *Calcium signaling.* Cell, 2007. **131**(6): p. 1047-58.
2. Wadel, K., E. Neher, and T. Sakaba, *The coupling between synaptic vesicles and Ca2+ channels determines fast neurotransmitter release.* Neuron, 2007. **53**(4): p. 563-75.
3. Wheeler, D.B., A. Randall, and R.W. Tsien, *Roles of N-type and Q-type Ca2+ channels in supporting hippocampal synaptic transmission.* Science, 1994. **264**(5155): p. 107-11.
4. Wheeler, D.G., C.F. Barrett, R.D. Groth, P. Safa, and R.W. Tsien, *CaMKII locally encodes L-type channel activity to signal to nuclear CREB in excitation-transcription coupling.* J Cell Biol, 2008. **183**(5): p. 849-63.
5. Wheeler, D.G., R.D. Groth, H. Ma, C.F. Barrett, S.F. Owen, P. Safa, and R.W. Tsien, *Ca(V)1 and Ca(V)2 channels engage distinct modes of Ca(2+) signaling to control CREB-dependent gene expression.* Cell, 2012. **149**(5): p. 1112-24.
6. Catterall, W.A., *Structure and regulation of voltage-gated Ca2+ channels.* Annu Rev Cell Dev Biol, 2000. **16**: p. 521-55.
7. Fish, J.M. and C. Antzelevitch, *Role of sodium and calcium channel block in unmasking the Brugada syndrome.* Heart Rhythm, 2004. **1**(2): p. 210-7.
8. Stanika, R.I., I. Villanueva, G. Kazanina, S.B. Andrews, and N.B. Pivovarova, *Comparative impact of voltage-gated calcium channels and NMDA receptors on mitochondria-mediated neuronal injury.* J Neurosci, 2012. **32**(19): p. 6642-50.
9. Altier, C., A. Garcia-Caballero, B. Simms, H. You, L. Chen, J. Walcher, H.W. Tedford, T. Hermosilla, and G.W. Zamponi, *The Cavbeta subunit prevents RFP2-mediated ubiquitination and proteasomal degradation of L-type channels.* Nat Neurosci, 2011. **14**(2): p. 173-80.
10. Cain, S.M. and T.P. Snutch, *Voltage-gated calcium channels and disease.* Biofactors, 2011. **37**(3): p. 197-205.
11. Hedley, P.L., P. Jorgensen, S. Schlamowitz, J. Moolman-Smook, J.K. Kanters, V.A. Corfield, and M. Christiansen, *The genetic basis of Brugada syndrome: a mutation update.* Hum Mutat, 2009. **30**(9): p. 1256-66.
12. Hsiao, P.Y., H.C. Tien, C.P. Lo, J.M. Juang, Y.H. Wang, and R.J. Sung, *Gene mutations in cardiac arrhythmias: a review of recent evidence in ion channelopathies.* Appl Clin Genet, 2013. **6**: p. 1-13.
13. Belardetti, F. and G.W. Zamponi, *Calcium channels as therapeutic targets.* Wiley Interdisciplinary Reviews: Membrane Transport and Signaling, 2012. **1**(4): p. 433-451.
14. Armstrong, C.M. and D.R. Matteson, *Two distinct populations of calcium channels in a clonal line of pituitary cells.* Science, 1985. **227**(4682): p. 65-7.
15. Bean, B.P., *Two kinds of calcium channels in canine atrial cells. Differences in kinetics, selectivity, and pharmacology.* J Gen Physiol, 1985. **86**(1): p. 1-30.
16. Zhang, J.F., A.D. Randall, P.T. Ellinor, W.A. Horne, W.A. Sather, T. Tanabe, T.L. Schwarz, and R.W. Tsien, *Distinctive pharmacology and kinetics of cloned neuronal Ca2+ channels and their possible counterparts in mammalian CNS neurons.* Neuropharmacology, 1993. **32**(11): p. 1075-88.
17. Randall, A. and R.W. Tsien, *Pharmacological dissection of multiple types of Ca2+ channel currents in rat cerebellar granule neurons.* J Neurosci, 1995. **15**(4): p. 2995-3012.

18. McCleskey, E.W., A.P. Fox, D.H. Feldman, L.J. Cruz, B.M. Olivera, R.W. Tsien, and D. Yoshikami, *Omega-conotoxin: direct and persistent blockade of specific types of calcium channels in neurons but not muscle.* Proc Natl Acad Sci U S A, 1987. **84**(12): p. 4327-31.
19. Olivera, B.M., L.J. Cruz, V. de Santos, G.W. LeCheminant, D. Griffin, R. Zeikus, J.M. McIntosh, R. Galyean, J. Varga, W.R. Gray, and et al., *Neuronal calcium channel antagonists. Discrimination between calcium channel subtypes using omega-conotoxin from Conus magus venom.* Biochemistry, 1987. **26**(8): p. 2086-90.
20. Adams, M.E., R.A. Myers, J.S. Imperial, and B.M. Olivera, *Toxityping rat brain calcium channels with omega-toxins from spider and cone snail venoms.* Biochemistry, 1993. **32**(47): p. 12566-70.
21. Newcomb, R., B. Szoke, A. Palma, G. Wang, X. Chen, W. Hopkins, R. Cong, J. Miller, L. Urge, K. Tarczy-Hornoch, J.A. Loo, D.J. Dooley, L. Nadasdi, R.W. Tsien, J. Lemos, and G. Miljanich, *Selective peptide antagonist of the class E calcium channel from the venom of the tarantula Hysterocrates gigas.* Biochemistry, 1998. **37**(44): p. 15353-62.
22. Bourinet, E., S.C. Stotz, R.L. Spaetgens, G. Dayanithi, J. Lemos, J. Nargeot, and G.W. Zamponi, *Interaction of SNX482 with domains III and IV inhibits activation gating of alpha(1E) (Ca(V)2.3) calcium channels.* Biophys J, 2001. **81**(1): p. 79-88.
23. Perez-Reyes, E., *Molecular physiology of low-voltage-activated t-type calcium channels.* Physiol Rev, 2003. **83**(1): p. 117-61.
24. Curtis, B.M. and W.A. Catterall, *Purification of the calcium antagonist receptor of the voltage-sensitive calcium channel from skeletal muscle transverse tubules.* Biochemistry, 1984. **23**(10): p. 2113-8.
25. Catterall, W.A., E. Perez-Reyes, T.P. Snutch, and J. Striessnig, *International Union of Pharmacology. XLVIII. Nomenclature and structure-function relationships of voltage-gated calcium channels.* Pharmacol Rev, 2005. **57**(4): p. 411-25.
26. Tanabe, T., H. Takeshima, A. Mikami, V. Flockerzi, H. Takahashi, K. Kangawa, M. Kojima, H. Matsuo, T. Hirose, and S. Numa, *Primary structure of the receptor for calcium channel blockers from skeletal muscle.* Nature, 1987. **328**(6128): p. 313-8.
27. Mikami, A., K. Imoto, T. Tanabe, T. Niidome, Y. Mori, H. Takeshima, S. Narumiya, and S. Numa, *Primary structure and functional expression of the cardiac dihydropyridine-sensitive calcium channel.* Nature, 1989. **340**(6230): p. 230-3.
28. Williams, M.E., D.H. Feldman, A.F. McCue, R. Brenner, G. Velicelebi, S.B. Ellis, and M.M. Harpold, *Structure and functional expression of alpha 1, alpha 2, and beta subunits of a novel human neuronal calcium channel subtype.* Neuron, 1992. **8**(1): p. 71-84.
29. Bech-Hansen, N.T., M.J. Naylor, T.A. Maybaum, W.G. Pearce, B. Koop, G.A. Fishman, M. Mets, M.A. Musarella, and K.M. Boycott, *Loss-of-function mutations in a calcium-channel alpha1-subunit gene in Xp11.23 cause incomplete X-linked congenital stationary night blindness.* Nat Genet, 1998. **19**(3): p. 264-7.
30. Bourinet, E., T.W. Soong, K. Sutton, S. Slaymaker, E. Mathews, A. Monteil, G.W. Zamponi, J. Nargeot, and T.P. Snutch, *Splicing of alpha 1A subunit gene generates phenotypic variants of P- and Q-type calcium channels.* Nat Neurosci, 1999. **2**(5): p. 407-15.
31. Williams, M.E., P.F. Brust, D.H. Feldman, S. Patthi, S. Simerson, A. Maroufi, A.F. McCue, G. Velicelebi, S.B. Ellis, and M.M. Harpold, *Structure and functional expression*

of an omega-conotoxin-sensitive human N-type calcium channel. Science, 1992. **257**(5068): p. 389-95.
32. Dubel, S.J., T.V. Starr, J. Hell, M.K. Ahlijanian, J.J. Enyeart, W.A. Catterall, and T.P. Snutch, *Molecular cloning of the alpha-1 subunit of an omega-conotoxin-sensitive calcium channel.* Proc Natl Acad Sci U S A, 1992. **89**(11): p. 5058-62.
33. Soong, T.W., A. Stea, C.D. Hodson, S.J. Dubel, S.R. Vincent, and T.P. Snutch, *Structure and functional expression of a member of the low voltage-activated calcium channel family.* Science, 1993. **260**(5111): p. 1133-6.
34. Perez-Reyes, E., L.L. Cribbs, A. Daud, A.E. Lacerda, J. Barclay, M.P. Williamson, M. Fox, M. Rees, and J.H. Lee, *Molecular characterization of a neuronal low-voltage-activated T-type calcium channel.* Nature, 1998. **391**(6670): p. 896-900.
35. Cribbs, L.L., J.H. Lee, J. Yang, J. Satin, Y. Zhang, A. Daud, J. Barclay, M.P. Williamson, M. Fox, M. Rees, and E. Perez-Reyes, *Cloning and characterization of alpha1H from human heart, a member of the T-type Ca2+ channel gene family.* Circ Res, 1998. **83**(1): p. 103-9.
36. Lee, J.H., A.N. Daud, L.L. Cribbs, A.E. Lacerda, A. Pereverzev, U. Klockner, T. Schneider, and E. Perez-Reyes, *Cloning and expression of a novel member of the low voltage-activated T-type calcium channel family.* J Neurosci, 1999. **19**(6): p. 1912-21.
37. Catterall, W.A., *Ion channel voltage sensors: structure, function, and pathophysiology.* Neuron, 2010. **67**(6): p. 915-28.
38. Yang, J., P.T. Ellinor, W.A. Sather, J.F. Zhang, and R.W. Tsien, *Molecular determinants of Ca2+ selectivity and ion permeation in L-type Ca2+ channels.* Nature, 1993. **366**(6451): p. 158-61.
39. Ellinor, P.T., J. Yang, W.A. Sather, J.F. Zhang, and R.W. Tsien, *Ca2+ channel selectivity at a single locus for high-affinity Ca2+ interactions.* Neuron, 1995. **15**(5): p. 1121-32.
40. Tang, L., T.M. Gamal El-Din, J. Payandeh, G.Q. Martinez, T.M. Heard, T. Scheuer, N. Zheng, and W.A. Catterall, *Structural basis for Ca2+ selectivity of a voltage-gated calcium channel.* Nature, 2014. **505**(7481): p. 56-61.
41. Bourinet, E., G.W. Zamponi, A. Stea, T.W. Soong, B.A. Lewis, L.P. Jones, D.T. Yue, and T.P. Snutch, *The alpha 1E calcium channel exhibits permeation properties similar to low-voltage-activated calcium channels.* J Neurosci, 1996. **16**(16): p. 4983-93.
42. Lansman, J.B., P. Hess, and R.W. Tsien, *Blockade of current through single calcium channels by Cd2+, Mg2+, and Ca2+. Voltage and concentration dependence of calcium entry into the pore.* J Gen Physiol, 1986. **88**(3): p. 321-47.
43. Fox, A.P., M.C. Nowycky, and R.W. Tsien, *Single-channel recordings of three types of calcium channels in chick sensory neurones.* J Physiol, 1987. **394**: p. 173-200.
44. Doering, C.J., J. Hamid, B. Simms, J.E. McRory, and G.W. Zamponi, *Cav1.4 encodes a calcium channel with low open probability and unitary conductance.* Biophys J, 2005. **89**(5): p. 3042-8.
45. Weber, A.M., F.K. Wong, A.R. Tufford, L.C. Schlichter, V. Matveev, and E.F. Stanley, *N-type Ca2+ channels carry the largest current: implications for nanodomains and transmitter release.* Nat Neurosci, 2010. **13**(11): p. 1348-50.

46. Dirksen, R.T., J. Nakai, A. Gonzalez, K. Imoto, and K.G. Beam, *The S5-S6 linker of repeat I is a critical determinant of L-type Ca2+ channel conductance.* Biophys J, 1997. **73**(3): p. 1402-9.
47. Feng, Z.P., J. Hamid, C. Doering, S.E. Jarvis, G.M. Bosey, E. Bourinet, T.P. Snutch, and G.W. Zamponi, *Amino acid residues outside of the pore region contribute to N-type calcium channel permeation.* J Biol Chem, 2001. **276**(8): p. 5726-30.
48. Zamponi, G.W., E. Bourinet, D. Nelson, J. Nargeot, and T.P. Snutch, *Crosstalk between G proteins and protein kinase C mediated by the calcium channel alpha1 subunit.* Nature, 1997. **385**(6615): p. 442-6.
49. Hall, D.D., S. Dai, P.Y. Tseng, Z. Malik, M. Nguyen, L. Matt, K. Schnizler, A. Shephard, D.P. Mohapatra, F. Tsuruta, R.E. Dolmetsch, C.J. Christel, A. Lee, A. Burette, R.J. Weinberg, and J.W. Hell, *Competition between alpha-actinin and Ca(2)(+)-calmodulin controls surface retention of the L-type Ca(2)(+) channel Ca(V)1.2.* Neuron, 2013. **78**(3): p. 483-97.
50. Dai, S., D.D. Hall, and J.W. Hell, *Supramolecular assemblies and localized regulation of voltage-gated ion channels.* Physiol Rev, 2009. **89**(2): p. 411-52.
51. Lipscombe, D., A. Andrade, and S.E. Allen, *Alternative splicing: functional diversity among voltage-gated calcium channels and behavioral consequences.* Biochim Biophys Acta, 2013. **1828**(7): p. 1522-9.
52. Lipscombe, D., *Neuronal proteins custom designed by alternative splicing.* Curr Opin Neurobiol, 2005. **15**(3): p. 358-63.
53. Lipkind, G.M. and H.A. Fozzard, *Molecular modeling of interactions of dihydropyridines and phenylalkylamines with the inner pore of the L-type Ca2+ channel.* Mol Pharmacol, 2003. **63**(3): p. 499-511.
54. Zamponi, G.W., S.C. Stotz, R.J. Staples, T.M. Andro, J.K. Nelson, V. Hulubei, A. Blumenfeld, and N.R. Natale, *Unique structure-activity relationship for 4-isoxazolyl-1,4-dihydropyridines.* J Med Chem, 2003. **46**(1): p. 87-96.
55. Huber, I., E. Wappl, A. Herzog, J. Mitterdorfer, H. Glossmann, T. Langer, and J. Striessnig, *Conserved Ca2+-antagonist-binding properties and putative folding structure of a recombinant high-affinity dihydropyridine-binding domain.* Biochem J, 2000. **347 Pt 3**: p. 829-36.
56. Serysheva, II, S.J. Ludtke, M.R. Baker, W. Chiu, and S.L. Hamilton, *Structure of the voltage-gated L-type Ca2+ channel by electron cryomicroscopy.* Proc Natl Acad Sci U S A, 2002. **99**(16): p. 10370-5.
57. Wolf, M., A. Eberhart, H. Glossmann, J. Striessnig, and N. Grigorieff, *Visualization of the domain structure of an L-type Ca2+ channel using electron cryo-microscopy.* J Mol Biol, 2003. **332**(1): p. 171-82.
58. Walsh, C.P., A. Davies, M. Nieto-Rostro, A.C. Dolphin, and A. Kitmitto, *Labelling of the 3D structure of the cardiac L-type voltage-gated calcium channel.* Channels (Austin), 2009. **3**(6): p. 387-92.
59. Walsh, C.P., A. Davies, A.J. Butcher, A.C. Dolphin, and A. Kitmitto, *Three-dimensional structure of CaV3.1: comparison with the cardiac L-type voltage-gated calcium channel monomer architecture.* J Biol Chem, 2009. **284**(33): p. 22310-21.
60. Buraei, Z. and J. Yang, *The Beta subunit of voltage-gated Ca2+ channels.* Physiol Rev, 2010. **90**(4): p. 1461-506.

61. Antzelevitch, C., G.D. Pollevick, J.M. Cordeiro, O. Casis, M.C. Sanguinetti, Y. Aizawa, A. Guerchicoff, R. Pfeiffer, A. Oliva, B. Wollnik, P. Gelber, E.P. Bonaros, Jr., E. Burashnikov, Y. Wu, J.D. Sargent, S. Schickel, R. Oberheiden, A. Bhatia, L.F. Hsu, M. Haissaguerre, R. Schimpf, M. Borggrefe, and C. Wolpert, *Loss-of-function mutations in the cardiac calcium channel underlie a new clinical entity characterized by ST-segment elevation, short QT intervals, and sudden cardiac death.* Circulation, 2007. **115**(4): p. 442-9.
62. Pragnell, M., M. De Waard, Y. Mori, T. Tanabe, T.P. Snutch, and K.P. Campbell, *Calcium channel beta-subunit binds to a conserved motif in the I-II cytoplasmic linker of the alpha 1-subunit.* Nature, 1994. **368**(6466): p. 67-70.
63. Opatowsky, Y., C.C. Chen, K.P. Campbell, and J.A. Hirsch, *Structural analysis of the voltage-dependent calcium channel beta subunit functional core and its complex with the alpha 1 interaction domain.* Neuron, 2004. **42**(3): p. 387-99.
64. Van Petegem, F., K.A. Clark, F.C. Chatelain, and D.L. Minor, Jr., *Structure of a complex between a voltage-gated calcium channel beta-subunit and an alpha-subunit domain.* Nature, 2004. **429**(6992): p. 671-5.
65. Chen, Y.H., M.H. Li, Y. Zhang, L.L. He, Y. Yamada, A. Fitzmaurice, Y. Shen, H. Zhang, L. Tong, and J. Yang, *Structural basis of the alpha1-beta subunit interaction of voltage-gated Ca2+ channels.* Nature, 2004. **429**(6992): p. 675-80.
66. Brice, N.L. and A.C. Dolphin, *Differential plasma membrane targeting of voltage-dependent calcium channel subunits expressed in a polarized epithelial cell line.* J Physiol, 1999. **515 (Pt 3)**: p. 685-94.
67. Dolphin, A.C., *The alpha2delta subunits of voltage-gated calcium channels.* Biochim Biophys Acta, 2013. **1828**(7): p. 1541-9.
68. Davies, A., I. Kadurin, A. Alvarez-Laviada, L. Douglas, M. Nieto-Rostro, C.S. Bauer, W.S. Pratt, and A.C. Dolphin, *The alpha2delta subunits of voltage-gated calcium channels form GPI-anchored proteins, a posttranslational modification essential for function.* Proc Natl Acad Sci U S A, 2010. **107**(4): p. 1654-9.
69. Kadurin, I., A. Alvarez-Laviada, S.F. Ng, R. Walker-Gray, M. D'Arco, M.G. Fadel, W.S. Pratt, and A.C. Dolphin, *Calcium currents are enhanced by alpha2delta-1 lacking its membrane anchor.* J Biol Chem, 2012. **287**(40): p. 33554-66.
70. Yasuda, T., L. Chen, W. Barr, J.E. McRory, R.J. Lewis, D.J. Adams, and G.W. Zamponi, *Auxiliary subunit regulation of high-voltage activated calcium channels expressed in mammalian cells.* Eur J Neurosci, 2004. **20**(1): p. 1-13.
71. Canti, C., M. Nieto-Rostro, I. Foucault, F. Heblich, J. Wratten, M.W. Richards, J. Hendrich, L. Douglas, K.M. Page, A. Davies, and A.C. Dolphin, *The metal-ion-dependent adhesion site in the Von Willebrand factor-A domain of alpha2delta subunits is key to trafficking voltage-gated Ca2+ channels.* Proc Natl Acad Sci U S A, 2005. **102**(32): p. 11230-5.
72. Hoppa, M.B., B. Lana, W. Margas, A.C. Dolphin, and T.A. Ryan, *alpha2delta expression sets presynaptic calcium channel abundance and release probability.* Nature, 2012. **486**(7401): p. 122-5.
73. Eroglu, C., N.J. Allen, M.W. Susman, N.A. O'Rourke, C.Y. Park, E. Ozkan, C. Chakraborty, S.B. Mulinyawe, D.S. Annis, A.D. Huberman, E.M. Green, J. Lawler, R. Dolmetsch, K.C. Garcia, S.J. Smith, Z.D. Luo, A. Rosenthal, D.F. Mosher, and B.A.

Barres, *Gabapentin receptor alpha2delta-1 is a neuronal thrombospondin receptor responsible for excitatory CNS synaptogenesis.* Cell, 2009. **139**(2): p. 380-92.
74. Sharp, A.H. and K.P. Campbell, *Characterization of the 1,4-dihydropyridine receptor using subunit-specific polyclonal antibodies. Evidence for a 32,000-Da subunit.* J Biol Chem, 1989. **264**(5): p. 2816-25.
75. Arikkath, J. and K.P. Campbell, *Auxiliary subunits: essential components of the voltage-gated calcium channel complex.* Curr Opin Neurobiol, 2003. **13**(3): p. 298-307.
76. Chen, R.S., T.C. Deng, T. Garcia, Z.M. Sellers, and P.M. Best, *Calcium channel gamma subunits: a functionally diverse protein family.* Cell Biochem Biophys, 2007. **47**(2): p. 178-86.
77. Chu, P.J., H.M. Robertson, and P.M. Best, *Calcium channel gamma subunits provide insights into the evolution of this gene family.* Gene, 2001. **280**(1-2): p. 37-48.
78. Letts, V.A., R. Felix, G.H. Biddlecome, J. Arikkath, C.L. Mahaffey, A. Valenzuela, F.S. Bartlett, 2nd, Y. Mori, K.P. Campbell, and W.N. Frankel, *The mouse stargazer gene encodes a neuronal Ca2+-channel gamma subunit.* Nat Genet, 1998. **19**(4): p. 340-7.
79. Rousset, M., T. Cens, S. Restituito, C. Barrere, J.L. Black, 3rd, M.W. McEnery, and P. Charnet, *Functional roles of gamma2, gamma3 and gamma4, three new Ca2+ channel subunits, in P/Q-type Ca2+ channel expressed in Xenopus oocytes.* J Physiol, 2001. **532**(Pt 3): p. 583-93.
80. Tomita, S., H. Adesnik, M. Sekiguchi, W. Zhang, K. Wada, J.R. Howe, R.A. Nicoll, and D.S. Bredt, *Stargazin modulates AMPA receptor gating and trafficking by distinct domains.* Nature, 2005. **435**(7045): p. 1052-8.
81. Bats, C., L. Groc, and D. Choquet, *The interaction between Stargazin and PSD-95 regulates AMPA receptor surface trafficking.* Neuron, 2007. **53**(5): p. 719-34.
82. Matsuda, S., W. Kakegawa, T. Budisantoso, T. Nomura, K. Kohda, and M. Yuzaki, *Stargazin regulates AMPA receptor trafficking through adaptor protein complexes during long-term depression.* Nat Commun, 2013. **4**: p. 2759.
83. Minor, D.L., Jr. and F. Findeisen, *Progress in the structural understanding of voltage-gated calcium channel (CaV) function and modulation.* Channels (Austin), 2010. **4**(6): p. 459-74.
84. Van Petegem, F., F.C. Chatelain, and D.L. Minor, Jr., *Insights into voltage-gated calcium channel regulation from the structure of the CaV1.2 IQ domain-Ca2+/calmodulin complex.* Nat Struct Mol Biol, 2005. **12**(12): p. 1108-15.
85. Kim, E.Y., C.H. Rumpf, Y. Fujiwara, E.S. Cooley, F. Van Petegem, and D.L. Minor, Jr., *Structures of CaV2 Ca2+/CaM-IQ domain complexes reveal binding modes that underlie calcium-dependent inactivation and facilitation.* Structure, 2008. **16**(10): p. 1455-67.
86. Kim, E.Y., C.H. Rumpf, F. Van Petegem, R.J. Arant, F. Findeisen, E.S. Cooley, E.Y. Isacoff, and D.L. Minor, Jr., *Multiple C-terminal tail Ca(2+)/CaMs regulate Ca(V)1.2 function but do not mediate channel dimerization.* Embo J, 2010. **29**(23): p. 3924-38.
87. Mori, M.X., C.W. Vander Kooi, D.J. Leahy, and D.T. Yue, *Crystal structure of the CaV2 IQ domain in complex with Ca2+/calmodulin: high-resolution mechanistic implications for channel regulation by Ca2+.* Structure, 2008. **16**(4): p. 607-20.
88. Liu, Z. and H.J. Vogel, *Structural basis for the regulation of L-type voltage-gated calcium channels: interactions between the N-terminal cytoplasmic domain and Ca(2+)-calmodulin.* Front Mol Neurosci, 2012. **5**: p. 38.

89. Finn, B.E., J. Evenas, T. Drakenberg, J.P. Waltho, E. Thulin, and S. Forsen, *Calcium-induced structural changes and domain autonomy in calmodulin.* Nat Struct Biol, 1995. **2**(9): p. 777-83.
90. Chou, J.J., S. Li, C.B. Klee, and A. Bax, *Solution structure of Ca(2+)-calmodulin reveals flexible hand-like properties of its domains.* Nat Struct Biol, 2001. **8**(11): p. 990-7.
91. Wriggers, W., E. Mehler, F. Pitici, H. Weinstein, and K. Schulten, *Structure and dynamics of calmodulin in solution.* Biophys J, 1998. **74**(4): p. 1622-39.
92. Gariepy, J., T.A. Mietzner, and G.K. Schoolnik, *Peptide antisera as sequence-specific probes of protein conformational transitions: calmodulin exhibits calcium-dependent changes in antigenicity.* Proc Natl Acad Sci U S A, 1986. **83**(23): p. 8888-92.
93. Heizmann, C.W., *Intracellular calcium-binding proteins: structure and possible functions.* J Cardiovasc Pharmacol, 1986. **8 Suppl 8**: p. S7-12.
94. Kilhoffer, M.C., J. Haiech, and J.G. Demaille, *Ion binding to calmodulin. A comparison with other intracellular calcium-binding proteins.* Mol Cell Biochem, 1983. **51**(1): p. 33-54.
95. Xia, X.M., B. Fakler, A. Rivard, G. Wayman, T. Johnson-Pais, J.E. Keen, T. Ishii, B. Hirschberg, C.T. Bond, S. Lutsenko, J. Maylie, and J.P. Adelman, *Mechanism of calcium gating in small-conductance calcium-activated potassium channels.* Nature, 1998. **395**(6701): p. 503-7.
96. Geiser, J.R., D. van Tuinen, S.E. Brockerhoff, M.M. Neff, and T.N. Davis, *Can calmodulin function without binding calcium?* Cell, 1991. **65**(6): p. 949-59.
97. Komeiji, Y., Y. Ueno, and M. Uebayasi, *Molecular dynamics simulations revealed Ca(2+)-dependent conformational change of Calmodulin.* FEBS Lett, 2002. **521**(1-3): p. 133-9.
98. Mori, Y., M. Wakamori, S. Oda, C.F. Fletcher, N. Sekiguchi, E. Mori, N.G. Copeland, N.A. Jenkins, K. Matsushita, Z. Matsuyama, and K. Imoto, *Reduced voltage sensitivity of activation of P/Q-type Ca2+ channels is associated with the ataxic mouse mutation rolling Nagoya (tg(rol)).* J Neurosci, 2000. **20**(15): p. 5654-62.
99. Varadi, G., P. Lory, D. Schultz, M. Varadi, and A. Schwartz, *Acceleration of activation and inactivation by the beta subunit of the skeletal muscle calcium channel.* Nature, 1991. **352**(6331): p. 159-62.
100. Berrow, N.S., V. Campbell, E.M. Fitzgerald, K. Brickley, and A.C. Dolphin, *Antisense depletion of beta-subunits modulates the biophysical and pharmacological properties of neuronal calcium channels.* J Physiol, 1995. **482 (Pt 3)**: p. 481-91.
101. Mullner, C., L.A. Broos, A.M. van den Maagdenberg, and J. Striessnig, *Familial hemiplegic migraine type 1 mutations K1336E, W1684R, and V1696I alter Cav2.1 Ca2+ channel gating: evidence for beta-subunit isoform-specific effects.* J Biol Chem, 2004. **279**(50): p. 51844-50.
102. Olcese, R., A. Neely, N. Qin, X. Wei, L. Birnbaumer, and E. Stefani, *Coupling between charge movement and pore opening in vertebrate neuronal alpha 1E calcium channels.* J Physiol, 1996. **497 (Pt 3)**: p. 675-86.
103. Helton, T.D., D.J. Kojetin, J. Cavanagh, and W.A. Horne, *Alternative splicing of a beta4 subunit proline-rich motif regulates voltage-dependent gating and toxin block of Cav2.1 Ca2+ channels.* J Neurosci, 2002. **22**(21): p. 9331-9.

104. Wakamori, M., G. Mikala, and Y. Mori, *Auxiliary subunits operate as a molecular switch in determining gating behaviour of the unitary N-type Ca2+ channel current in Xenopus oocytes.* J Physiol, 1999. **517 (Pt 3)**: p. 659-72.
105. Stotz, S.C., S.E. Jarvis, and G.W. Zamponi, *Functional roles of cytoplasmic loops and pore lining transmembrane helices in the voltage-dependent inactivation of HVA calcium channels.* J Physiol, 2004. **554**(Pt 2): p. 263-73.
106. Hoshi, T., W.N. Zagotta, and R.W. Aldrich, *Biophysical and molecular mechanisms of Shaker potassium channel inactivation.* Science, 1990. **250**(4980): p. 533-8.
107. West, J.W., D.E. Patton, T. Scheuer, Y. Wang, A.L. Goldin, and W.A. Catterall, *A cluster of hydrophobic amino acid residues required for fast Na(+)-channel inactivation.* Proc Natl Acad Sci U S A, 1992. **89**(22): p. 10910-4.
108. Stotz, S.C. and G.W. Zamponi, *Identification of inactivation determinants in the domain IIS6 region of high voltage-activated calcium channels.* J Biol Chem, 2001. **276**(35): p. 33001-10.
109. Herlitze, S., G.H. Hockerman, T. Scheuer, and W.A. Catterall, *Molecular determinants of inactivation and G protein modulation in the intracellular loop connecting domains I and II of the calcium channel alpha1A subunit.* Proc Natl Acad Sci U S A, 1997. **94**(4): p. 1512-6.
110. Berrou, L., G. Bernatchez, and L. Parent, *Molecular determinants of inactivation within the I-II linker of alpha1E (CaV2.3) calcium channels.* Biophys J, 2001. **80**(1): p. 215-28.
111. Kraus, R.L., M.J. Sinnegger, H. Glossmann, S. Hering, and J. Striessnig, *Familial hemiplegic migraine mutations change alpha1A Ca2+ channel kinetics.* J Biol Chem, 1998. **273**(10): p. 5586-90.
112. Stotz, S.C., J. Hamid, R.L. Spaetgens, S.E. Jarvis, and G.W. Zamponi, *Fast inactivation of voltage-dependent calcium channels. A hinged-lid mechanism?* J Biol Chem, 2000. **275**(32): p. 24575-82.
113. Stotz, S.C. and G.W. Zamponi, *Structural determinants of fast inactivation of high voltage-activated Ca(2+) channels.* Trends Neurosci, 2001. **24**(3): p. 176-81.
114. Spaetgens, R.L. and G.W. Zamponi, *Multiple structural domains contribute to voltage-dependent inactivation of rat brain alpha(1E) calcium channels.* J Biol Chem, 1999. **274**(32): p. 22428-36.
115. Tadross, M.R., M. Ben Johny, and D.T. Yue, *Molecular endpoints of Ca2+/calmodulin- and voltage-dependent inactivation of Ca(v)1.3 channels.* J Gen Physiol, 2010. **135**(3): p. 197-215.
116. Imredy, J.P. and D.T. Yue, *Mechanism of Ca(2+)-sensitive inactivation of L-type Ca2+ channels.* Neuron, 1994. **12**(6): p. 1301-18.
117. Peterson, B.Z., C.D. DeMaria, J.P. Adelman, and D.T. Yue, *Calmodulin is the Ca2+ sensor for Ca2+ -dependent inactivation of L-type calcium channels.* Neuron, 1999. **22**(3): p. 549-58.
118. Zuhlke, R.D., G.S. Pitt, K. Deisseroth, R.W. Tsien, and H. Reuter, *Calmodulin supports both inactivation and facilitation of L-type calcium channels.* Nature, 1999. **399**(6732): p. 159-62.
119. Lee, A., S.T. Wong, D. Gallagher, B. Li, D.R. Storm, T. Scheuer, and W.A. Catterall, *Ca2+/calmodulin binds to and modulates P/Q-type calcium channels.* Nature, 1999. **399**(6732): p. 155-9.

120. Liu, X., P.S. Yang, W. Yang, and D.T. Yue, *Enzyme-inhibitor-like tuning of Ca(2+) channel connectivity with calmodulin.* Nature, 2010. **463**(7283): p. 968-72.
121. Peterson, B.Z., J.S. Lee, J.G. Mulle, Y. Wang, M. de Leon, and D.T. Yue, *Critical determinants of Ca(2+)-dependent inactivation within an EF-hand motif of L-type Ca(2+) channels.* Biophys J, 2000. **78**(4): p. 1906-20.
122. Erickson, M.G., B.A. Alseikhan, B.Z. Peterson, and D.T. Yue, *Preassociation of calmodulin with voltage-gated Ca(2+) channels revealed by FRET in single living cells.* Neuron, 2001. **31**(6): p. 973-85.
123. Erickson, M.G., H. Liang, M.X. Mori, and D.T. Yue, *FRET two-hybrid mapping reveals function and location of L-type Ca2+ channel CaM preassociation.* Neuron, 2003. **39**(1): p. 97-107.
124. Liang, H., C.D. DeMaria, M.G. Erickson, M.X. Mori, B.A. Alseikhan, and D.T. Yue, *Unified mechanisms of Ca2+ regulation across the Ca2+ channel family.* Neuron, 2003. **39**(6): p. 951-60.
125. Zamponi, G.W., *Calmodulin lobotomized: novel insights into calcium regulation of voltage-gated calcium channels.* Neuron, 2003. **39**(6): p. 879-81.
126. McRory, J.E., J. Hamid, C.J. Doering, E. Garcia, R. Parker, K. Hamming, L. Chen, M. Hildebrand, A.M. Beedle, L. Feldcamp, G.W. Zamponi, and T.P. Snutch, *The CACNA1F gene encodes an L-type calcium channel with unique biophysical properties and tissue distribution.* J Neurosci, 2004. **24**(7): p. 1707-18.
127. Wahl-Schott, C., L. Baumann, H. Cuny, C. Eckert, K. Griessmeier, and M. Biel, *Switching off calcium-dependent inactivation in L-type calcium channels by an autoinhibitory domain.* Proc Natl Acad Sci U S A, 2006. **103**(42): p. 15657-62.
128. Griessmeier, K., H. Cuny, K. Rotzer, O. Griesbeck, H. Harz, M. Biel, and C. Wahl-Schott, *Calmodulin is a functional regulator of Cav1.4 L-type Ca2+ channels.* J Biol Chem, 2009. **284**(43): p. 29809-16.
129. Morgans, C.W., *Neurotransmitter release at ribbon synapses in the retina.* Immunol Cell Biol, 2000. **78**(4): p. 442-6.
130. Yang, P.S., B.A. Alseikhan, H. Hiel, L. Grant, M.X. Mori, W. Yang, P.A. Fuchs, and D.T. Yue, *Switching of Ca2+-dependent inactivation of Ca(v)1.3 channels by calcium binding proteins of auditory hair cells.* J Neurosci, 2006. **26**(42): p. 10677-89.
131. Oz, S., A. Benmocha, Y. Sasson, D. Sachyani, L. Almagor, A. Lee, J.A. Hirsch, and N. Dascal, *Competitive and non-competitive regulation of calcium-dependent inactivation in CaV1.2 L-type Ca2+ channels by calmodulin and Ca2+-binding protein 1.* J Biol Chem, 2013. **288**(18): p. 12680-91.
132. Yang, P.S., M.B. Johny, and D.T. Yue, *Allostery in Ca(2+) channel modulation by calcium-binding proteins.* Nat Chem Biol, 2014. **10**(3): p. 231-8.
133. Johny, M.B., P.S. Yang, H. Bazzazi, and D.T. Yue, *Dynamic switching of calmodulin interactions underlies Ca2+ regulation of CaV1.3 channels.* Nat Commun, 2013. **4**: p. 1717.
134. Dick, I.E., M.R. Tadross, H. Liang, L.H. Tay, W. Yang, and D.T. Yue, *A modular switch for spatial Ca2+ selectivity in the calmodulin regulation of CaV channels.* Nature, 2008. **451**(7180): p. 830-4.
135. Simms, B.A., I.A. Souza, and G.W. Zamponi, *A novel calmodulin site in the Cav1.2 N-terminus regulates calcium-dependent inactivation.* Pflugers Arch, 2013.

136. de Maria, C.D., T.W. Soong, B.A. Alseikhan, R.S. Alvania, and D.T. Yue, *Calmodulin bifurcates the local Ca2+ signal that modulates P/Q-type Ca2+ channels.* Nature, 2001. **411**(6836): p. 484-9.
137. Lee, A., H. Zhou, T. Scheuer, and W.A. Catterall, *Molecular determinants of Ca(2+)/calmodulin-dependent regulation of Ca(v)2.1 channels.* Proc Natl Acad Sci U S A, 2003. **100**(26): p. 16059-64.
138. Chaudhuri, D., J.B. Issa, and D.T. Yue, *Elementary mechanisms producing facilitation of Cav2.1 (P/Q-type) channels.* J Gen Physiol, 2007. **129**(5): p. 385-401.
139. Hudmon, A., H. Schulman, J. Kim, J.M. Maltez, R.W. Tsien, and G.S. Pitt, *CaMKII tethers to L-type Ca2+ channels, establishing a local and dedicated integrator of Ca2+ signals for facilitation.* J Cell Biol, 2005. **171**(3): p. 537-47.
140. Stea, A., S.J. Dubel, M. Pragnell, J.P. Leonard, K.P. Campbell, and T.P. Snutch, *A beta-subunit normalizes the electrophysiological properties of a cloned N-type Ca2+ channel alpha 1-subunit.* Neuropharmacology, 1993. **32**(11): p. 1103-16.
141. De Waard, M., M. Pragnell, and K.P. Campbell, *Ca2+ channel regulation by a conserved beta subunit domain.* Neuron, 1994. **13**(2): p. 495-503.
142. Bichet, D., V. Cornet, S. Geib, E. Carlier, S. Volsen, T. Hoshi, Y. Mori, and M. De Waard, *The I-II loop of the Ca2+ channel alpha1 subunit contains an endoplasmic reticulum retention signal antagonized by the beta subunit.* Neuron, 2000. **25**(1): p. 177-90.
143. Leroy, J., M.W. Richards, A.J. Butcher, M. Nieto-Rostro, W.S. Pratt, A. Davies, and A.C. Dolphin, *Interaction via a key tryptophan in the I-II linker of N-type calcium channels is required for beta1 but not for palmitoylated beta2, implicating an additional binding site in the regulation of channel voltage-dependent properties.* J Neurosci, 2005. **25**(30): p. 6984-96.
144. Obermair, G.J., B. Schlick, V. Di Biase, P. Subramanyam, M. Gebhart, S. Baumgartner, and B.E. Flucher, *Reciprocal interactions regulate targeting of calcium channel beta subunits and membrane expression of alpha1 subunits in cultured hippocampal neurons.* J Biol Chem, 2010. **285**(8): p. 5776-91.
145. Fang, K. and H.M. Colecraft, *Mechanism of auxiliary β-subunit-mediated membrane targeting of L-type (Cav1.2) channels.* J. Physiol. , 2011.
146. Ye, Y., Y. Shibata, C. Yun, D. Ron, and T.A. Rapoport, *A membrane protein complex mediates retro-translocation from the ER lumen into the cytosol.* Nature, 2004. **429**(6994): p. 841-7.
147. Romisch, K., *Endoplasmic reticulum-associated degradation.* Annu Rev Cell Dev Biol, 2005. **21**: p. 435-56.
148. Waithe, D., L. Ferron, K.M. Page, K. Chaggar, and A.C. Dolphin, *Beta-subunits promote the expression of Ca(V)2.2 channels by reducing their proteasomal degradation.* J Biol Chem, 2011. **286**(11): p. 9598-611.
149. DeMaria, C.D., T.W. Soong, B.A. Alseikhan, R.S. Alvania, and D.T. Yue, *Calmodulin bifurcates the local Ca2+ signal that modulates P/Q-type Ca2+ channels.* Nature, 2001. **411**(6836): p. 484-9.
150. Bourdin, B., F. Marger, S. Wall-Lacelle, T. Schneider, H. Klein, R. Sauve, and L. Parent, *Molecular determinants of the CaVbeta-induced plasma membrane targeting of the CaV1.2 channel.* J Biol Chem, 2010. **285**(30): p. 22853-63.

151. Gao, T., M. Bunemann, B.L. Gerhardstein, H. Ma, and M.M. Hosey, *Role of the C terminus of the alpha 1C (CaV1.2) subunit in membrane targeting of cardiac L-type calcium channels.* J Biol Chem, 2000. **275**(33): p. 25436-44.
152. Ravindran, A., E. Kobrinsky, Q.Z. Lao, and N.M. Soldatov, *Functional properties of the CaV1.2 calcium channel activated by calmodulin in the absence of alpha2delta subunits.* Channels (Austin), 2009. **3**(1): p. 25-31.
153. Bernatchez, G., D. Talwar, and L. Parent, *Mutations in the EF-hand motif impair the inactivation of barium currents of the cardiac alpha1C channel.* Biophys J, 1998. **75**(4): p. 1727-39.
154. Dolmetsch, R.E., U. Pajvani, K. Fife, J.M. Spotts, and M.E. Greenberg, *Signaling to the nucleus by an L-type calcium channel-calmodulin complex through the MAP kinase pathway.* Science, 2001. **294**(5541): p. 333-9.
155. Brunet, S., T. Scheuer, and W.A. Catterall, *Cooperative regulation of Ca(v)1.2 channels by intracellular Mg(2+), the proximal C-terminal EF-hand, and the distal C-terminal domain.* J Gen Physiol, 2009. **134**(2): p. 81-94.
156. Brunet, S., T. Scheuer, R. Klevit, and W.A. Catterall, *Modulation of CaV1.2 channels by Mg2+ acting at an EF-hand motif in the COOH-terminal domain.* J Gen Physiol, 2005. **126**(4): p. 311-23.
157. Wang, H.G., M.S. George, J. Kim, C. Wang, and G.S. Pitt, *Ca2+/calmodulin regulates trafficking of Ca(V)1.2 Ca2+ channels in cultured hippocampal neurons.* J Neurosci, 2007. **27**(34): p. 9086-93.
158. Kobrinsky, E., S. Tiwari, V.A. Maltsev, J.B. Harry, E. Lakatta, D.R. Abernethy, and N.M. Soldatov, *Differential role of the alpha1C subunit tails in regulation of the Cav1.2 channel by membrane potential, beta subunits, and Ca2+ ions.* J Biol Chem, 2005. **280**(13): p. 12474-85.
159. Wei, X., A. Neely, R. Olcese, W. Lang, E. Stefani, and L. Birnbaumer, *Increase in Ca2+ channel expression by deletions at the amino terminus of the cardiac alpha 1C subunit.* Receptors Channels, 1996. **4**(4): p. 205-15.
160. Liao, P. and T.W. Soong, *CaV1.2 channelopathies: from arrhythmias to autism, bipolar disorder, and immunodeficiency.* Pflugers Arch, 2010. **460**(2): p. 353-9.
161. Jeon, D., S. Kim, M. Chetana, D. Jo, H.E. Ruley, S.Y. Lin, D. Rabah, J.P. Kinet, and H.S. Shin, *Observational fear learning involves affective pain system and Cav1.2 Ca2+ channels in ACC.* Nat Neurosci, 2010. **13**(4): p. 482-8.
162. White, J.A., B.C. McKinney, M.C. John, P.A. Powers, T.J. Kamp, and G.G. Murphy, *Conditional forebrain deletion of the L-type calcium channel Ca V 1.2 disrupts remote spatial memories in mice.* Learn Mem, 2008. **15**(1): p. 1-5.
163. Lee, A.S., K.L. Gonzales, A. Lee, S. Moosmang, F. Hofmann, A.A. Pieper, and A.M. Rajadhyaksha, *Selective genetic deletion of cacna1c in the mouse prefrontal cortex.* Mol Psychiatry, 2012. **17**(11): p. 1051.
164. Bhat, S., D.T. Dao, C.E. Terrillion, M. Arad, R.J. Smith, N.M. Soldatov, and T.D. Gould, *CACNA1C (Cav1.2) in the pathophysiology of psychiatric disease.* Prog Neurobiol, 2012. **99**(1): p. 1-14.
165. Bader, P.L., M. Faizi, L.H. Kim, S.F. Owen, M.R. Tadross, R.W. Alfa, G.C. Bett, R.W. Tsien, R.L. Rasmusson, and M. Shamloo, *Mouse model of Timothy syndrome*

recapitulates triad of autistic traits. Proc Natl Acad Sci U S A, 2011. **108**(37): p. 15432-7.
166. Green, E.K., D. Grozeva, I. Jones, L. Jones, G. Kirov, S. Caesar, K. Gordon-Smith, C. Fraser, L. Forty, E. Russell, M.L. Hamshere, V. Moskvina, I. Nikolov, A. Farmer, P. McGuffin, P.A. Holmans, M.J. Owen, M.C. O'Donovan, and N. Craddock, *The bipolar disorder risk allele at CACNA1C also confers risk of recurrent major depression and of schizophrenia.* Mol Psychiatry, 2010. **15**(10): p. 1016-22.
167. He, K., Z. An, Q. Wang, T. Li, Z. Li, J. Chen, W. Li, T. Wang, J. Ji, G. Feng, H. Lin, Q. Yi, and Y. Shi, *CACNA1C, schizophrenia and major depressive disorder in the Han Chinese population.* Br J Psychiatry, 2014. **204**: p. 36-9.
168. Splawski, I., K.W. Timothy, L.M. Sharpe, N. Decher, P. Kumar, R. Bloise, C. Napolitano, P.J. Schwartz, R.M. Joseph, K. Condouris, H. Tager-Flusberg, S.G. Priori, M.C. Sanguinetti, and M.T. Keating, *Ca(V)1.2 calcium channel dysfunction causes a multisystem disorder including arrhythmia and autism.* Cell, 2004. **119**(1): p. 19-31.
169. Splawski, I., K.W. Timothy, N. Decher, P. Kumar, F.B. Sachse, A.H. Beggs, M.C. Sanguinetti, and M.T. Keating, *Severe arrhythmia disorder caused by cardiac L-type calcium channel mutations.* Proc Natl Acad Sci U S A, 2005. **102**(23): p. 8089-96; discussion 8086-8.
170. Barrett, C.F. and R.W. Tsien, *The Timothy syndrome mutation differentially affects voltage- and calcium-dependent inactivation of CaV1.2 L-type calcium channels.* Proc Natl Acad Sci U S A, 2008. **105**(6): p. 2157-62.
171. Depil, K., S. Beyl, A. Stary-Weinzinger, A. Hohaus, E. Timin, and S. Hering, *Timothy mutation disrupts the link between activation and inactivation in Ca(V)1.2 protein.* J Biol Chem, 2011. **286**(36): p. 31557-64.
172. Seisenberger, C., V. Specht, A. Welling, J. Platzer, A. Pfeifer, S. Kuhbandner, J. Striessnig, N. Klugbauer, R. Feil, and F. Hofmann, *Functional embryonic cardiomyocytes after disruption of the L-type alpha1C (Cav1.2) calcium channel gene in the mouse.* J Biol Chem, 2000. **275**(50): p. 39193-9.
173. Splawski, I., K.W. Timothy, S.G. Priori, C. Napolitano, and R. Bloise, *Timothy Syndrome.* 1993.
174. Napolitano, C. and C. Antzelevitch, *Phenotypical manifestations of mutations in the genes encoding subunits of the cardiac voltage-dependent L-type calcium channel.* Circ Res, 2011. **108**(5): p. 607-18.
175. Hermida, J.S., J.L. Lemoine, F.B. Aoun, G. Jarry, J.L. Rey, and J.C. Quiret, *Prevalence of the brugada syndrome in an apparently healthy population.* Am J Cardiol, 2000. **86**(1): p. 91-4.
176. Sinner, M.F., A. Pfeufer, S. Perz, E. Schulze-Bahr, G. Monnig, L. Eckardt, B.M. Beckmann, H.E. Wichmann, G. Breithardt, G. Steinbeck, L. Fabritz, S. Kaab, and P. Kirchhof, *Spontaneous Brugada electrocardiogram patterns are rare in the German general population: results from the KORA study.* Europace, 2009. **11**(10): p. 1338-44.
177. Miyasaka, Y., H. Tsuji, K. Yamada, S. Tokunaga, D. Saito, Y. Imuro, N. Matsumoto, and T. Iwasaka, *Prevalence and mortality of the Brugada-type electrocardiogram in one city in Japan.* J Am Coll Cardiol, 2001. **38**(3): p. 771-4.
178. Sacher, F., P. Meregalli, C. Veltmann, M.E. Field, A. Solnon, P. Bru, S. Abbey, P. Jais, H.L. Tan, C. Wolpert, G. Lande, V. Bertault, N. Derval, D. Babuty, D. Lacroix, S.

Boveda, P. Maury, M. Hocini, J. Clementy, P. Mabo, H. Lemarec, J. Mansourati, M. Borggrefe, A. Wilde, M. Haissaguerre, and V. Probst, *Are women with severely symptomatic brugada syndrome different from men?* J Cardiovasc Electrophysiol, 2008. **19**(11): p. 1181-5.

179. Antzelevitch, C., P. Brugada, M. Borggrefe, J. Brugada, R. Brugada, D. Corrado, I. Gussak, H. LeMarec, K. Nademanee, A.R. Perez Riera, W. Shimizu, E. Schulze-Bahr, H. Tan, and A. Wilde, *Brugada syndrome: report of the second consensus conference.* Heart Rhythm, 2005. **2**(4): p. 429-40.
180. Probst, V., C. Veltmann, L. Eckardt, P.G. Meregalli, F. Gaita, H.L. Tan, D. Babuty, F. Sacher, C. Giustetto, E. Schulze-Bahr, M. Borggrefe, M. Haissaguerre, P. Mabo, H. Le Marec, C. Wolpert, and A.A. Wilde, *Long-term prognosis of patients diagnosed with Brugada syndrome: Results from the FINGER Brugada Syndrome Registry.* Circulation, 2010. **121**(5): p. 635-43.
181. Kanter, R.J., R. Pfeiffer, D. Hu, H. Barajas-Martinez, M.P. Carboni, and C. Antzelevitch, *Brugada-like syndrome in infancy presenting with rapid ventricular tachycardia and intraventricular conduction delay.* Circulation, 2011. **125**(1): p. 14-22.
182. Skinner, J.R., S.K. Chung, D. Montgomery, C.H. McCulley, J. Crawford, J. French, and M.I. Rees, *Near-miss SIDS due to Brugada syndrome.* Arch Dis Child, 2005. **90**(5): p. 528-9.
183. Vatta, M., R. Dumaine, G. Varghese, T.A. Richard, W. Shimizu, N. Aihara, K. Nademanee, R. Brugada, J. Brugada, G. Veerakul, H. Li, N.E. Bowles, P. Brugada, C. Antzelevitch, and J.A. Towbin, *Genetic and biophysical basis of sudden unexplained nocturnal death syndrome (SUNDS), a disease allelic to Brugada syndrome.* Hum Mol Genet, 2002. **11**(3): p. 337-45.
184. Brugada, P. and J. Brugada, *Right bundle branch block, persistent ST segment elevation and sudden cardiac death: a distinct clinical and electrocardiographic syndrome. A multicenter report.* J Am Coll Cardiol, 1992. **20**(6): p. 1391-6.
185. Burashnikov, E., R. Pfeiffer, H. Barajas-Martinez, E. Delpon, D. Hu, M. Desai, M. Borggrefe, M. Haissaguerre, R. Kanter, G.D. Pollevick, A. Guerchicoff, R. Laino, M. Marieb, K. Nademanee, G.B. Nam, R. Robles, R. Schimpf, D.D. Stapleton, S. Viskin, S. Winters, C. Wolpert, S. Zimmern, C. Veltmann, and C. Antzelevitch, *Mutations in the cardiac L-type calcium channel associated with inherited J-wave syndromes and sudden cardiac death.* Heart Rhythm, 2010. **7**(12): p. 1872-82.
186. Delpon, E., J.M. Cordeiro, L. Nunez, P.E. Thomsen, A. Guerchicoff, G.D. Pollevick, Y. Wu, J.K. Kanters, C.T. Larsen, J. Hofman-Bang, E. Burashnikov, M. Christiansen, and C. Antzelevitch, *Functional effects of KCNE3 mutation and its role in the development of Brugada syndrome.* Circ Arrhythm Electrophysiol, 2008. **1**(3): p. 209-18.
187. Hu, D., H. Barajas-Martinez, E. Burashnikov, M. Springer, Y. Wu, A. Varro, R. Pfeiffer, T.T. Koopmann, J.M. Cordeiro, A. Guerchicoff, G.D. Pollevick, and C. Antzelevitch, *A mutation in the beta 3 subunit of the cardiac sodium channel associated with Brugada ECG phenotype.* Circ Cardiovasc Genet, 2009. **2**(3): p. 270-8.
188. Watanabe, H., T.T. Koopmann, S. Le Scouarnec, T. Yang, C.R. Ingram, J.J. Schott, S. Demolombe, V. Probst, F. Anselme, D. Escande, A.C. Wiesfeld, A. Pfeufer, S. Kaab, H.E. Wichmann, C. Hasdemir, Y. Aizawa, A.A. Wilde, D.M. Roden, and C.R. Bezzina,

Sodium channel beta1 subunit mutations associated with Brugada syndrome and cardiac conduction disease in humans. J Clin Invest, 2008. **118**(6): p. 2260-8.
189. Giudicessi, J.R., D. Ye, D.J. Tester, L. Crotti, A. Mugione, V.V. Nesterenko, R.M. Albertson, C. Antzelevitch, P.J. Schwartz, and M.J. Ackerman, *Transient outward current (I(to)) gain-of-function mutations in the KCND3-encoded Kv4.3 potassium channel and Brugada syndrome.* Heart Rhythm, 2011. **8**(7): p. 1024-32.
190. Rook, M.B., C. Bezzina Alshinawi, W.A. Groenewegen, I.C. van Gelder, A.C. van Ginneken, H.J. Jongsma, M.M. Mannens, and A.A. Wilde, *Human SCN5A gene mutations alter cardiac sodium channel kinetics and are associated with the Brugada syndrome.* Cardiovasc Res, 1999. **44**(3): p. 507-17.
191. Barajas-Martinez, H., D. Hu, T. Ferrer, C.G. Onetti, Y. Wu, E. Burashnikov, M. Boyle, T. Surman, J. Urrutia, C. Veltmann, R. Schimpf, M. Borggrefe, C. Wolpert, B.B. Ibrahim, J.A. Sanchez-Chapula, S. Winters, M. Haissaguerre, and C. Antzelevitch, *Molecular genetic and functional association of Brugada and early repolarization syndromes with S422L missense mutation in KCNJ8.* Heart Rhythm, 2012. **9**(4): p. 548-55.
192. Yatani, A., M. Wakamori, G. Mikala, and A. Bahinski, *Block of transient outward-type cloned cardiac K+ channel currents by quinidine.* Circ Res, 1993. **73**(2): p. 351-9.
193. McGregor, M. and J. Chen, *Should the implantable cardiac defibrillator be used for primary prevention of sudden death? A review of the issues relevant to hospital decision making.* Can J Cardiol, 2004. **20**(12): p. 1199-204.
194. Bennett, P.B., K. Yazawa, N. Makita, and A.L. George, Jr., *Molecular mechanism for an inherited cardiac arrhythmia.* Nature, 1995. **376**(6542): p. 683-5.
195. Levi, R. and L.J. DeFelice, *Sodium-conducting channels in cardiac membranes in low calcium.* Biophys J, 1986. **50**(1): p. 5-9.
196. Cohen, N.M. and W.J. Lederer, *Calcium current in isolated neonatal rat ventricular myocytes.* J Physiol, 1987. **391**: p. 169-91.
197. Sanguinetti, M.C., C. Jiang, M.E. Curran, and M.T. Keating, *A mechanistic link between an inherited and an acquired cardiac arrhythmia: HERG encodes the IKr potassium channel.* Cell, 1995. **81**(2): p. 299-307.
198. Romey, G., L. Garcia, F. Rieger, and M. Lazdunski, *Targets for calcium channel blockers in mammalian skeletal muscle and their respective functions in excitation-contraction coupling.* Biochem Biophys Res Commun, 1988. **156**(3): p. 1324-32.
199. Benitah, J.P., J.L. Alvarez, and A.M. Gomez, *L-type Ca(2+) current in ventricular cardiomyocytes.* J Mol Cell Cardiol, 2010. **48**(1): p. 26-36.
200. Dulhunty, A.F., *Excitation-contraction coupling from the 1950s into the new millennium.* Clin Exp Pharmacol Physiol, 2006. **33**(9): p. 763-72.
201. Barhanin, J., F. Lesage, E. Guillemare, M. Fink, M. Lazdunski, and G. Romey, *K(V)LQT1 and lsK (minK) proteins associate to form the I(Ks) cardiac potassium current.* Nature, 1996. **384**(6604): p. 78-80.
202. Nakamura, T.Y., M. Artman, B. Rudy, and W.A. Coetzee, *Inhibition of rat ventricular IK1 with antisense oligonucleotides targeted to Kir2.1 mRNA.* Am J Physiol, 1998. **274**(3 Pt 2): p. H892-900.

203. Ogawa, M., K. Kumagai, Y. Yamanouchi, and K. Saku, *Spontaneous onset of ventricular fibrillation in Brugada syndrome with J wave and ST-segment elevation in the inferior leads.* Heart Rhythm, 2005. **2**(1): p. 97-9.
204. Berne, P. and J. Brugada, *Brugada syndrome 2012.* Circ J, 2012. **76**(7): p. 1563-71.
205. Bayes de Luna, A., J. Brugada, A. Baranchuk, M. Borggrefe, G. Breithardt, D. Goldwasser, P. Lambiase, A.P. Riera, J. Garcia-Niebla, C. Pastore, G. Oreto, W. McKenna, W. Zareba, R. Brugada, and P. Brugada, *Current electrocardiographic criteria for diagnosis of Brugada pattern: a consensus report.* J Electrocardiol, 2012. **45**(5): p. 433-42.
206. Cordeiro, J.M., M. Marieb, R. Pfeiffer, K. Calloe, E. Burashnikov, and C. Antzelevitch, *Accelerated inactivation of the L-type calcium current due to a mutation in CACNB2b underlies Brugada syndrome.* J Mol Cell Cardiol, 2009. **46**(5): p. 695-703.
207. Dafi, O., L. Berrou, Y. Dodier, A. Raybaud, R. Sauve, and L. Parent, *Negatively charged residues in the N-terminal of the AID helix confer slow voltage dependent inactivation gating to CaV1.2.* Biophys J, 2004. **87**(5): p. 3181-92.
208. Pitt, G.S., R.D. Zuhlke, A. Hudmon, H. Schulman, H. Reuter, and R.W. Tsien, *Molecular basis of calmodulin tethering and Ca2+-dependent inactivation of L-type Ca2+ channels.* J Biol Chem, 2001. **276**(33): p. 30794-802.
209. Heinemann, S.H., H. Terlau, W. Stuhmer, K. Imoto, and S. Numa, *Calcium channel characteristics conferred on the sodium channel by single mutations.* Nature, 1992. **356**(6368): p. 441-3.
210. Simms, B.A. and G.W. Zamponi, *The Brugada syndrome mutation A39V does not affect surface expression of neuronal rat Cav1.2 channels.* Mol Brain, 2012. **5**: p. 9.
211. Oz, S., V. Tsemakhovich, C.J. Christel, A. Lee, and N. Dascal, *CaBP1 regulates voltage-dependent inactivation and activation of Ca(V)1.2 (L-type) calcium channels.* J Biol Chem, 2011. **286**(16): p. 13945-53.
212. Altier, C., S.J. Dubel, C. Barrere, S.E. Jarvis, S.C. Stotz, R.L. Spaetgens, J.D. Scott, V. Cornet, M. De Waard, G.W. Zamponi, J. Nargeot, and E. Bourinet, *Trafficking of L-type calcium channels mediated by the postsynaptic scaffolding protein AKAP79.* J Biol Chem, 2002. **277**(37): p. 33598-603.
213. Hudmon, A., E. Lebel, H. Roy, A. Sik, H. Schulman, M.N. Waxham, and P. De Koninck, *A mechanism for Ca2+/calmodulin-dependent protein kinase II clustering at synaptic and nonsynaptic sites based on self-association.* J Neurosci, 2005. **25**(30): p. 6971-83.
214. Perez-Reyes, E., A. Castellano, H.S. Kim, P. Bertrand, E. Baggstrom, A.E. Lacerda, X.Y. Wei, and L. Birnbaumer, *Cloning and expression of a cardiac/brain beta subunit of the L-type calcium channel.* J Biol Chem, 1992. **267**(3): p. 1792-7.
215. Hamid, J., D. Nelson, R. Spaetgens, S.J. Dubel, T.P. Snutch, and G.W. Zamponi, *Identification of an integration center for cross-talk between protein kinase C and G protein modulation of N-type calcium channels.* J Biol Chem, 1999. **274**(10): p. 6195-202.
216. Li, Q., A. Lau, T.J. Morris, L. Guo, C.B. Fordyce, and E.F. Stanley, *A syntaxin 1, Galpha(o), and N-type calcium channel complex at a presynaptic nerve terminal: analysis by quantitative immunocolocalization.* J Neurosci, 2004. **24**(16): p. 4070-81.
217. Spafford, J.D., D.W. Munno, P. Van Nierop, Z.P. Feng, S.E. Jarvis, W.J. Gallin, A.B. Smit, G.W. Zamponi, and N.I. Syed, *Calcium channel structural determinants of synaptic*

transmission between identified invertebrate neurons. J Biol Chem, 2003. **278**(6): p. 4258-67.
218. Dolphin, A.C., C.N. Wyatt, J. Richards, R.E. Beattie, P. Craig, J.H. Lee, L.L. Cribbs, S.G. Volsen, and E. Perez-Reyes, *The effect of alpha2-delta and other accessory subunits on expression and properties of the calcium channel alpha1G.* J Physiol, 1999. **519 Pt 1**: p. 35-45.
219. Haack, J.A. and R.L. Rosenberg, *Calcium-dependent inactivation of L-type calcium channels in planar lipid bilayers.* Biophys J, 1994. **66**(4): p. 1051-60.
220. Qin, N., R. Olcese, M. Bransby, T. Lin, and L. Birnbaumer, *Ca2+-induced inhibition of the cardiac Ca2+ channel depends on calmodulin.* Proc Natl Acad Sci U S A, 1999. **96**(5): p. 2435-8.
221. Kim, J., S. Ghosh, D.A. Nunziato, and G.S. Pitt, *Identification of the components controlling inactivation of voltage-gated Ca2+ channels.* Neuron, 2004. **41**(5): p. 745-54.
222. Lian, L.Y., D. Myatt, and A. Kitmitto, *Apo calmodulin binding to the L-type voltage-gated calcium channel Cav1.2 IQ peptide.* Biochem Biophys Res Commun, 2007. **353**(3): p. 565-70.
223. Nie, H.G., L.Y. Hao, J.J. Xu, E. Minobe, A. Kameyama, and M. Kameyama, *Distinct roles of CaM and Ca(2+)/CaM -dependent protein kinase II in Ca(2+) -dependent facilitation and inactivation of cardiac L-type Ca(2+) channels.* J Physiol Sci, 2007. **57**(3): p. 167-73.
224. Ohrtman, J., B. Ritter, A. Polster, K.G. Beam, and S. Papadopoulos, *Sequence differences in the IQ motifs of CaV1.1 and CaV1.2 strongly impact calmodulin binding and calcium-dependent inactivation.* J Biol Chem, 2008. **283**(43): p. 29301-11.
225. Huang, H., B.Z. Tan, Y. Shen, J. Tao, F. Jiang, Y.Y. Sung, C.K. Ng, M. Raida, G. Kohr, M. Higuchi, H. Fatemi-Shariatpanahi, B. Harden, D.T. Yue, and T.W. Soong, *RNA editing of the IQ domain in Ca(v)1.3 channels modulates their Ca(2)(+)-dependent inactivation.* Neuron, 2012. **73**(2): p. 304-16.
226. Bazzazi, H., M. Ben Johny, P.J. Adams, T.W. Soong, and D.T. Yue, *Continuously tunable Ca(2+) regulation of RNA-edited CaV1.3 channels.* Cell Rep, 2013. **5**(2): p. 367-77.
227. Evans, T.I., J.W. Hell, and M.A. Shea, *Thermodynamic linkage between calmodulin domains binding calcium and contiguous sites in the C-terminal tail of Ca(V)1.2.* Biophys Chem, 2011. **159**(1): p. 172-87.
228. Taiakina, V., A.N. Boone, J. Fux, A. Senatore, D. Weber-Adrian, J.G. Guillemette, and J.D. Spafford, *The calmodulin-binding, short linear motif, NSCaTE is conserved in L-type channel ancestors of vertebrate Cav1.2 and Cav1.3 channels.* PLoS One, 2013. **8**(4): p. e61765.
229. Benmocha, A., L. Almagor, S. Oz, J.A. Hirsch, and N. Dascal, *Characterization of the calmodulin-binding site in the N terminus of CaV1.2.* Channels (Austin), 2009. **3**(5): p. 337-42.
230. Zhou, H., K. Yu, K.L. McCoy, and A. Lee, *Molecular mechanism for divergent regulation of Cav1.2 Ca2+ channels by calmodulin and Ca2+-binding protein-1.* J Biol Chem, 2005. **280**(33): p. 29612-9.

231. Findeisen, F. and D.L. Minor, Jr., *Structural basis for the differential effects of CaBP1 and calmodulin on Ca(V)1.2 calcium-dependent inactivation.* Structure, 2010. **18**(12): p. 1617-31.
232. Dzhura, I., Y. Wu, R.J. Colbran, J.D. Corbin, J.R. Balser, and M.E. Anderson, *Cytoskeletal disrupting agents prevent calmodulin kinase, IQ domain and voltage-dependent facilitation of L-type Ca2+ channels.* J Physiol, 2002. **545**(Pt 2): p. 399-406.
233. Jiang, X., N.J. Lautermilch, H. Watari, R.E. Westenbroek, T. Scheuer, and W.A. Catterall, *Modulation of CaV2.1 channels by Ca2+/calmodulin-dependent protein kinase II bound to the C-terminal domain.* Proc Natl Acad Sci U S A, 2008. **105**(1): p. 341-6.
234. Hanson, P.I., M.S. Kapiloff, L.L. Lou, M.G. Rosenfeld, and H. Schulman, *CaM kinase was purified by chromatography on DE-52, phosphocellulose, and calmodulin-Sepharose.* ibid, 1989. **3**(59).
235. Meyer, T., P.I. Hanson, L. Stryer, and H. Schulman, *Calmodulin trapping by calcium-calmodulin-dependent protein kinase.* Science, 1992. **256**(5060): p. 1199-202.
236. Hudmon, A. and H. Schulman, *Neuronal CA2+/calmodulin-dependent protein kinase II: the role of structure and autoregulation in cellular function.* Annu Rev Biochem, 2002. **71**: p. 473-510.
237. Xiong, L., Q.K. Kleerekoper, R. He, J.A. Putkey, and S.L. Hamilton, *Sites on calmodulin that interact with the C-terminal tail of Cav1.2 channel.* J Biol Chem, 2005. **280**(8): p. 7070-9.
238. Adler, E.M., G.J. Augustine, S.N. Duffy, and M.P. Charlton, *Alien intracellular calcium chelators attenuate neurotransmitter release at the squid giant synapse.* J Neurosci, 1991. **11**(6): p. 1496-507.
239. Mruk, K., B.M. Farley, A.W. Ritacco, and W.R. Kobertz, *Calmodulation meta-analysis: predicting calmodulin binding via canonical motif clustering.* J Gen Physiol, 2014. **144**(1): p. 105-14.
240. Shipston, M.J., *Ion channel regulation by protein palmitoylation.* J Biol Chem, 2011. **286**(11): p. 8709-16.
241. Blumenstein, Y., N. Kanevsky, G. Sahar, R. Barzilai, T. Ivanina, and N. Dascal, *A novel long N-terminal isoform of human L-type Ca2+ channel is up-regulated by protein kinase C.* J Biol Chem, 2002. **277**(5): p. 3419-23.
242. Clatot, J., A. Ziyadeh-Isleem, S. Maugenre, I. Denjoy, H. Liu, G. Dilanian, S.N. Hatem, I. Deschenes, A. Coulombe, P. Guicheney, and N. Neyroud, *Dominant-negative effect of SCN5A N-terminal mutations through the interaction of Nav1.5 alpha-subunits.* Cardiovasc Res, 2012.
243. Kovalevskaya, N.V., M. van de Waterbeemd, F.M. Bokhovchuk, N. Bate, R.J. Bindels, J.G. Hoenderop, and G.W. Vuister, *Structural analysis of calmodulin binding to ion channels demonstrates the role of its plasticity in regulation.* Pflugers Arch, 2013. **465**(11): p. 1507-19.
244. Nunomura, W., D. Sasakura, K. Shiba, S. Nakamura, S. Kidokoro, and Y. Takakuwa, *Structural stabilization of protein 4.1R FERM domain upon binding to apo-calmodulin: novel insights into the biological significance of the calcium-independent binding of calmodulin to protein 4.1R.* Biochem J, 2011. **440**(3): p. 367-74.

245. Singh, A., D. Hamedinger, J.C. Hoda, M. Gebhart, A. Koschak, C. Romanin, and J. Striessnig, *C-terminal modulator controls Ca2+-dependent gating of Ca(v)1.4 L-type Ca2+ channels.* Nat Neurosci, 2006. **9**(9): p. 1108-16.
246. Bannister, J.P., C.M. Thomas-Gatewood, Z.P. Neeb, A. Adebiyi, X. Cheng, and J.H. Jaggar, *Ca(V)1.2 channel N-terminal splice variants modulate functional surface expression in resistance size artery smooth muscle cells.* J Biol Chem, 2011. **286**(17): p. 15058-66.
247. Tang, Z.Z., M.C. Liang, S. Lu, D. Yu, C.Y. Yu, D.T. Yue, and T.W. Soong, *Transcript scanning reveals novel and extensive splice variations in human l-type voltage-gated calcium channel, Cav1.2 alpha1 subunit.* J Biol Chem, 2004. **279**(43): p. 44335-43.
248. Wielowieyski, P.A., J.T. Wigle, M. Salih, P. Hum, and B.S. Tuana, *Alternative splicing in intracellular loop connecting domains II and III of the alpha 1 subunit of Cav1.2 Ca2+ channels predicts two-domain polypeptides with unique C-terminal tails.* J Biol Chem, 2001. **276**(2): p. 1398-406.
249. David, L.S., E. Garcia, S.M. Cain, E. Thau, J.R. Tyson, and T.P. Snutch, *Splice-variant changes of the Ca(V)3.2 T-type calcium channel mediate voltage-dependent facilitation and associate with cardiac hypertrophy and development.* Channels (Austin), 2010. **4**(5): p. 375-89.
250. Adams, P.J., E. Garcia, L.S. David, K.J. Mulatz, S.D. Spacey, and T.P. Snutch, *Ca(V)2.1 P/Q-type calcium channel alternative splicing affects the functional impact of familial hemiplegic migraine mutations: implications for calcium channelopathies.* Channels (Austin), 2009. **3**(2): p. 110-21.
251. Ertel, E.A., K.P. Campbell, M.M. Harpold, F. Hofmann, Y. Mori, E. Perez-Reyes, A. Schwartz, T.P. Snutch, T. Tanabe, L. Birnbaumer, R.W. Tsien, and W.A. Catterall, *Nomenclature of voltage-gated calcium channels.* Neuron, 2000. **25**(3): p. 533-5.
252. Peracchia, C., A. Sotkis, X.G. Wang, L.L. Peracchia, and A. Persechini, *Calmodulin directly gates gap junction channels.* J Biol Chem, 2000. **275**(34): p. 26220-4.
253. Moreau, B., S. Straube, R.J. Fisher, J.W. Putney, Jr., and A.B. Parekh, *Ca2+-calmodulin-dependent facilitation and Ca2+ inactivation of Ca2+ release-activated Ca2+ channels.* J Biol Chem, 2005. **280**(10): p. 8776-83.
254. Rey, O., S.H. Young, R. Papazyan, M.S. Shapiro, and E. Rozengurt, *Requirement of the TRPC1 cation channel in the generation of transient Ca2+ oscillations by the calcium-sensing receptor.* J Biol Chem, 2006. **281**(50): p. 38730-7.
255. Alseikhan, B.A., C.D. DeMaria, H.M. Colecraft, and D.T. Yue, *Engineered calmodulins reveal the unexpected eminence of Ca2+ channel inactivation in controlling heart excitation.* Proc Natl Acad Sci U S A, 2002. **99**(26): p. 17185-90.
256. Snutch, T.P., W.J. Tomlinson, J.P. Leonard, and M.M. Gilbert, *Distinct calcium channels are generated by alternative splicing and are differentially expressed in the mammalian CNS.* Neuron, 1991. **7**(1): p. 45-57.
257. Agler, H.L., J. Evans, L.H. Tay, M.J. Anderson, H.M. Colecraft, and D.T. Yue, *G protein-gated inhibitory module of N-type (ca(v)2.2) ca2+ channels.* Neuron, 2005. **46**(6): p. 891-904.
258. Zhou, J., R. Olcese, N. Qin, F. Noceti, L. Birnbaumer, and E. Stefani, *Feedback inhibition of Ca2+ channels by Ca2+ depends on a short sequence of the C terminus that*

does not include the Ca2+ -binding function of a motif with similarity to Ca2+ -binding domains. Proc Natl Acad Sci U S A, 1997. **94**(6): p. 2301-5.
259. Langwieser, N., C.J. Christel, T. Kleppisch, F. Hofmann, C.T. Wotjak, and S. Moosmang, *Homeostatic switch in hebbian plasticity and fear learning after sustained loss of Cav1.2 calcium channels.* J Neurosci, 2012. **30**(25): p. 8367-75.
260. Blaeser, F., M.J. Sanders, N. Truong, S. Ko, L.J. Wu, D.F. Wozniak, M.S. Fanselow, M. Zhuo, and T.A. Chatila, *Long-term memory deficits in Pavlovian fear conditioning in Ca2+/calmodulin kinase kinase alpha-deficient mice.* Mol Cell Biol, 2006. **26**(23): p. 9105-15.
261. Busquet, P., N.K. Nguyen, E. Schmid, N. Tanimoto, M.W. Seeliger, T. Ben-Yosef, F. Mizuno, A. Akopian, J. Striessnig, and N. Singewald, *CaV1.3 L-type Ca2+ channels modulate depression-like behaviour in mice independent of deaf phenotype.* Int J Neuropsychopharmacol, 2010. **13**(4): p. 499-513.
262. Payne, H.L., P.S. Donoghue, W.M. Connelly, S. Hinterreiter, P. Tiwari, J.H. Ives, V. Hann, W. Sieghart, G. Lees, and C.L. Thompson, *Aberrant GABA(A) receptor expression in the dentate gyrus of the epileptic mutant mouse stargazer.* J Neurosci, 2006. **26**(33): p. 8600-8.
263. Bading, H., D.D. Ginty, and M.E. Greenberg, *Regulation of gene expression in hippocampal neurons by distinct calcium signaling pathways.* Science, 1993. **260**(5105): p. 181-6.
264. Wu, G.Y., K. Deisseroth, and R.W. Tsien, *Activity-dependent CREB phosphorylation: convergence of a fast, sensitive calmodulin kinase pathway and a slow, less sensitive mitogen-activated protein kinase pathway.* Proc Natl Acad Sci U S A, 2001. **98**(5): p. 2808-13.
265. Grueter, C.E., S.A. Abiria, I. Dzhura, Y. Wu, A.J. Ham, P.J. Mohler, M.E. Anderson, and R.J. Colbran, *L-type Ca2+ channel facilitation mediated by phosphorylation of the beta subunit by CaMKII.* Mol Cell, 2006. **23**(5): p. 641-50.
266. Cens, T., M.E. Mangoni, S. Richard, J. Nargeot, and P. Charnet, *Coexpression of the beta2 subunit does not induce voltage-dependent facilitation of the class C L-type Ca channel.* Pflugers Arch, 1996. **431**(5): p. 771-4.
267. Bourinet, E., P. Charnet, W.J. Tomlinson, A. Stea, T.P. Snutch, and J. Nargeot, *Voltage-dependent facilitation of a neuronal alpha 1C L-type calcium channel.* Embo J, 1994. **13**(21): p. 5032-9.
268. Qin, N., D. Platano, R. Olcese, J.L. Costantin, E. Stefani, and L. Birnbaumer, *Unique regulatory properties of the type 2a Ca2+ channel beta subunit caused by palmitoylation.* Proc Natl Acad Sci U S A, 1998. **95**(8): p. 4690-5.
269. Yoshino, M., T. Someya, A. Nishio, K. Yazawa, T. Usuki, and H. Yabu, *Multiple types of voltage-dependent Ca channels in mammalian intestinal smooth muscle cells.* Pflugers Arch, 1989. **414**(4): p. 401-9.
270. Schmid, R., K. Seydl, W. Baumgartner, K. Groschner, and C. Romanin, *Trypsin increases availability and open probability of cardiac L-type Ca2+ channels without affecting inactivation induced by Ca2+.* Biophys J, 1995. **69**(5): p. 1847-57.
271. Hofer, G.F., K. Hohenthanner, W. Baumgartner, K. Groschner, N. Klugbauer, F. Hofmann, and C. Romanin, *Intracellular Ca2+ inactivates L-type Ca2+ channels with a*

Hill coefficient of approximately 1 and an inhibition constant of approximately 4 microM by reducing channel's open probability. Biophys J, 1997. **73**(4): p. 1857-65.
272. Berggren, P.O., S.N. Yang, M. Murakami, A.M. Efanov, S. Uhles, M. Kohler, T. Moede, A. Fernstrom, I.B. Appelskog, C.A. Aspinwall, S.V. Zaitsev, O. Larsson, L.M. de Vargas, C. Fecher-Trost, P. Weissgerber, A. Ludwig, B. Leibiger, L. Juntti-Berggren, C.J. Barker, J. Gromada, M. Freichel, I.B. Leibiger, and V. Flockerzi, *Removal of Ca2+ channel beta3 subunit enhances Ca2+ oscillation frequency and insulin exocytosis.* Cell, 2004. **119**(2): p. 273-84.
273. Wagner, S., E. Hacker, E. Grandi, S.L. Weber, N. Dybkova, S. Sossalla, T. Sowa, L. Fabritz, P. Kirchhof, D.M. Bers, and L.S. Maier, *Ca/calmodulin kinase II differentially modulates potassium currents.* Circ Arrhythm Electrophysiol, 2009. **2**(3): p. 285-94.
274. Li, J., C. Marionneau, O. Koval, L. Zingman, P.J. Mohler, J.M. Nerbonne, and M.E. Anderson, *Calmodulin kinase II inhibition enhances ischemic preconditioning by augmenting ATP-sensitive K+ current.* Channels (Austin), 2007. **1**(5): p. 387-94.
275. Cibulsky, S.M. and W.A. Sather, *Control of ion conduction in L-type Ca2+ channels by the concerted action of S5-6 regions.* Biophys J, 2003. **84**(3): p. 1709-19.
276. Kepplinger, K.J., H. Kahr, G. Forstner, M. Sonnleitner, H. Schindler, T. Schmidt, K. Groschner, N.M. Soldatov, and C. Romanin, *A sequence in the carboxy-terminus of the alpha(1C) subunit important for targeting, conductance and open probability of L-type Ca(2+) channels.* FEBS Lett, 2000. **477**(3): p. 161-9.
277. Asmara, H., E. Minobe, Z.A. Saud, and M. Kameyama, *Interactions of calmodulin with the multiple binding sites of Cav1.2 Ca2+ channels.* J Pharmacol Sci, 2010. **112**(4): p. 397-404.
278. Koch, W.J., P.T. Ellinor, and A. Schwartz, *cDNA cloning of a dihydropyridine-sensitive calcium channel from rat aorta. Evidence for the existence of alternatively spliced forms.* J Biol Chem, 1990. **265**(29): p. 17786-91.
279. Cheng, X., J. Liu, M. Asuncion-Chin, E. Blaskova, J.P. Bannister, A.M. Dopico, and J.H. Jaggar, *A novel Ca(V)1.2 N terminus expressed in smooth muscle cells of resistance size arteries modifies channel regulation by auxiliary subunits.* J Biol Chem, 2007. **282**(40): p. 29211-21.
280. Pietrobon, D., *Calcium channels and channelopathies of the central nervous system.* Mol Neurobiol, 2002. **25**(1): p. 31-50.
281. Simms, B.A. and G.W. Zamponi, *Neuronal Voltage-Gated Calcium Channels: Structure, Function, and Dysfunction.* Neuron, 2014. **82**(1): p. 24-45.
282. Pietrobon, D., *CaV2.1 channelopathies.* Pflugers Arch, 2010. **460**(2): p. 375-93.
283. Frank, C.A., *How voltage-gated calcium channels gate forms of homeostatic synaptic plasticity.* Front Cell Neurosci, 2014. **8**: p. 40.
284. Dolphin, A.C., *G protein modulation of voltage-gated calcium channels.* Pharmacol Rev, 2003. **55**(4): p. 607-27.
285. Tedford, H.W. and G.W. Zamponi, *Direct G protein modulation of Cav2 calcium channels.* Pharmacol Rev, 2006. **58**(4): p. 837-62.
286. Herlitze, S., D.E. Garcia, K. Mackie, B. Hille, T. Scheuer, and W.A. Catterall, *Modulation of Ca2+ channels by G-protein beta gamma subunits.* Nature, 1996. **380**(6571): p. 258-62.

287. Chang, B., J.R. Heckenlively, P.R. Bayley, N.C. Brecha, M.T. Davisson, N.L. Hawes, A.A. Hirano, R.E. Hurd, A. Ikeda, B.A. Johnson, M.A. McCall, C.W. Morgans, S. Nusinowitz, N.S. Peachey, D.S. Rice, K.A. Vessey, and R.G. Gregg, *The nob2 mouse, a null mutation in Cacna1f: anatomical and functional abnormalities in the outer retina and their consequences on ganglion cell visual responses.* Vis Neurosci, 2006. **23**(1): p. 11-24.
288. Mochida, S., A.P. Few, T. Scheuer, and W.A. Catterall, *Regulation of presynaptic Ca(V)2.1 channels by Ca2+ sensor proteins mediates short-term synaptic plasticity.* Neuron, 2008. **57**(2): p. 210-6.
289. Forsythe, I.D., T. Tsujimoto, M. Barnes-Davies, M.F. Cuttle, and T. Takahashi, *Inactivation of presynaptic calcium current contributes to synaptic depression at a fast central synapse.* Neuron, 1998. **20**(4): p. 797-807.
290. Leal, K., S. Mochida, T. Scheuer, and W.A. Catterall, *Fine-tuning synaptic plasticity by modulation of Ca(V)2.1 channels with Ca2+ sensor proteins.* Proc Natl Acad Sci U S A, 2012. **109**(42): p. 17069-74.
291. Magupalli, V.G., S. Mochida, J. Yan, X. Jiang, R.E. Westenbroek, A.C. Nairn, T. Scheuer, and W.A. Catterall, *Ca2+-independent activation of Ca2+/calmodulin-dependent protein kinase II bound to the C-terminal domain of CaV2.1 calcium channels.* J Biol Chem, 2013. **288**(7): p. 4637-48.
292. Cuttle, M.F., T. Tsujimoto, I.D. Forsythe, and T. Takahashi, *Facilitation of the presynaptic calcium current at an auditory synapse in rat brainstem.* J Physiol, 1998. **512 (Pt 3)**: p. 723-9.
293. Halling, D.B., P. Aracena-Parks, and S.L. Hamilton, *Regulation of voltage-gated Ca2+ channels by calmodulin.* Sci STKE, 2005. **2005**(315): p. re15.
294. Simms, B.A., I.A. Souza, R. Rehak, and G.W. Zamponi, *The Cav1.2 N-terminus contains a CaM Kinase site that modulates channel trafficking and function.* Pflugers Arch, 2014. **IN PRESS**.
295. Simms, B.A., I.A. Souza, and G.W. Zamponi, *Effect of the Brugada syndrome mutation A39V on calmodulin regulation of Cav1.2 channels.* Mol Brain, 2014. **7**(1): p. 34.
296. Canti, C., K.M. Page, G.J. Stephens, and A.C. Dolphin, *Identification of residues in the N terminus of alpha1B critical for inhibition of the voltage-dependent calcium channel by Gbeta gamma.* J Neurosci, 1999. **19**(16): p. 6855-64.
297. Page, K.M., C. Canti, G.J. Stephens, N.S. Berrow, and A.C. Dolphin, *Identification of the amino terminus of neuronal Ca2+ channel alpha1 subunits alpha1B and alpha1E as an essential determinant of G-protein modulation.* J Neurosci, 1998. **18**(13): p. 4815-24.
298. Mezghrani, A., A. Monteil, K. Watschinger, M.J. Sinnegger-Brauns, C. Barrere, E. Bourinet, J. Nargeot, J. Striessnig, and P. Lory, *A destructive interaction mechanism accounts for dominant-negative effects of misfolded mutants of voltage-gated calcium channels.* J Neurosci, 2008. **28**(17): p. 4501-11.

APPENDIX A: PUBLICATIONS OVER THE SPAN OF THIS THESIS

Papers (published):

8. **Simms BA**, Souza IA, Rehak R and Zamponi GW (2014) The amino terminus of high voltage activated calcium channels: CaM you can't you, Channels. 2014 May 29 8(4) [Epub ahead of print] Open Access License (CC-BY-NC)

7. **Simms BA**, Souza IA, Rehak R and Zamponi GW (2014) The Cav1.2 N-terminus contains a CaM Kinase site that modulates channel trafficking and function, Pflugers Arch. 2014 May 28 [Epub ahead of print]
Rightslink License # 3466000203199

6. **Simms BA,** Souza IA, Zamponi GW (2014) Effect of the Brugada syndrome mutation A39V on calmodulin regulation of Cav1.2 channels, Mol. Brain. 7(34)
Open Access License Type 4

5. **Simms BA**, Zamponi GW (2014) Neuronal voltage gated calcium channels: structure, function and dysfunction, Neuron. 82 (1): 24-45
Rightslink License # 3383140372821

4. **Simms BA**, Souza IA, Zamponi GW. (2013) A novel calmodulin site in the Cav1.2 N-terminus regulates calcium-dependent inactivation, Pflugers Arch. 466 (9): 1793-80
Rightslink License # 3384280233881

3. **Simms BA**, Zamponi GW. (2012) The Brugada syndrome mutation A39V does not affect surface expression of neuronal rat Cav1.2 channels, Mol. Brain. 5 (1): 9
Open Access License Type 4

2. **Simms BA**, Zamponi GW. (2012) Trafficking and stability of voltage-gated calcium channels, Cell. Mol. Life. Sci. 69 (6): 843-56
Rightslink License # 3384280143272

1. Altier C, Garcia-Caballero A, **Simms B**, You H, Chen L, Walcher J, Tedford HW, Hermosilla T, Zamponi GW. (2011) The CavBeta subunit prevents RFP2-mediated ubiquitination and proteasomal degradation of L-type channels. Nat. Neurosci. 14 (2): 173-80
Text/Figures not used herein

Book chapters (published):

1. **Simms BA**. (2014) Brugada syndrome and voltage-gated calcium channels. In: Weiss N, Koschak A, editors. Pathology of Calcium Channels. 1st ed. New York: Springer Publishing
Rightslink License # 3384271364750

Abstracts/Posters:

3. Asmara, H, Health NC, **Simms B**, Bartoletti TM, Rehak R, Micu I, Zhang FX, Stys P, Zamponi GW and Turner RW (2014) T-type calcium channels form a calcium-dependent complex with calmodulin. Soc. Neurosci. Abstracts.

2. **Simms BA**, Assis-Souza I, Black SA, Zamponi GW. (2013) A Novel CaMKII interaction in the N-terminus of Cav1.2 Regulates Channel Expression. Federation of European Neurosciences. Abstracts

1. Altier C, Garcia-Caballero A, **Simms B**, Walcher J, Tedford HW, Hermosilla T, Zamponi GW. (2009) The CavB subunit prevents ubiquitination and proteasomal degradation of L-type calcium channels via the Derlin-1/p97 ERAD protein complex. Biophys. Soc. Abstracts.

APPENDIX B: **THE AMINO TERMINUS OF HIGH VOLTAGE ACTIVATED CALCIUM CHANNELS: CAM YOU OR CAN'T YOU?**

Abstract

Voltage-gated calcium channels (VGCCs), calmodulin (CaM) and calmodulin kinase II (CaMKII) are essential for various physiological processes in the nervous system. CaM and CaMKII differentially regulate calcium dependent facilitation (CDF) and calcium dependent inactivation (CDI) of the Cav1 and Cav2 families of VGCCs. It is generally accepted that conserved structures in the C-terminus of these channels regulate CDF and CDI, and yet recent evidence indicates that other intracellular regions may be involved. We recently discovered that N-terminal sequences in Cav1.2 bind CaM and CaMKII and function to regulate CDI, as well as surface expression and open probability, respectively. Cav1 and Cav2 share significant portions of N-terminal sequence and therefore we explored whether homologous binding sites might exist in Cav2.1. Here, we show that like the proximal N-terminus of Cav1.2, the homologous region of Cav2.1 contains sequences which interact either directly or indirectly with CaM.

Results & Discussion

Voltage gated calcium channels (VGCCs) regulate diverse neuronal processes including synaptic vesicle release, differentiation, gene transcription, and excitability [280]. Dysfunction of the high voltage activated (HVA) Cav2.1 channel has been associated with disorders such as cerebellar ataxia, migraine, and epilepsy [280-282]. At the molecular level Cav2 channels are important for promoting neurotransmitter release [6, 283] and CREB transcription [4, 5]. These principal functions of Cav2 channels are modulated by G proteins [48, 284-287], calmodulin (CaM) [85, 288, 289], CaM related proteins [233, 290] and CaM kinase [138, 233, 291, 292]. CaM regulates two competing functional processes for Cav2.1 channels via C-terminal interactions with an IQ motif and downstream calcium binding domain (CBD) [85, 137]. The high affinity C-lobe of CaM increases Cav2.1 conductance when calcium levels are low by a process termed calcium dependent facilitation (CDF) [137], while the low affinity N-lobe of CaM reduces channel conductance by calcium dependent inactivation (CDI) when global calcium levels rise [119, 293]. CDF of Cav2.1 critically depends on the IQ motif, whereas CDI involves the IQ and CBD motifs. Cav2.2 and Cav2.3 channels also undergo N-lobe CDI, but not CDF, suggesting critical sequence variation must exist to explain this disparity[124].

Unlike Cav2, Cav1 channels show two different types of CDI: one type is regulated by the N-lobe of CaM and involves the Cav1 N- and C-terminus regions [134], and the other type is mediated by the C-lobe of CaM and depends on several subregions of the C-terminus [117, 226]. CaMKII modulates CDF of Cav1 channels [139], but only in channel constructs that contain substantial mutations in the IQ region [118], thus calling into question whether CDF is

physiologically relevant for these channels. In recent work we identified a CaM binding site in the N-terminus of Cav1.2 at cysteine 106 [135] which contributes to N-lobe CDI, and four successive residues (cysteine 117, isoleucine 118, serine 119 and isoleucine 120) downstream of the CaM site that are responsible for binding α-CaMKII [294]. We were able to show by functional analysis that the CaM binding site formed by C106 of Cav1.2 is critical for N-lobe CDI [135], while the N-terminal α-CaMKII site serves to increase the surface expression of the channel (plus an offsetting decrease in open probability)[294]. We also discovered that a point mutation (A39V) linked to Brugada syndrome reduces N-lobe CDI in the brain isoform of Cav1.2[295]. Given the importance of the N-terminus in calcium regulation of Cav1.2 we examined whether the N-terminus of other VGCCs might also possess CaM binding sites. We focused on the Cav2.1 N-terminus because of well documented calmodulin regulation of this channel subtype.

The CDI literature for VGCCs suggests that a functional CaM site does not exist in the N-terminus of Cav2 channels [134]. However close examination of the Cav2.1 N-terminus reveals that residue C71 is homologous to C106 of Cav1.2 (Appendix B Figure 1), and both residues are part of a β-fold structure [135]. To explore whether CaM can interact biochemically with the N-terminus of Cav2.1, we created a GFP-tagged fusion protein of this region and performed a a pulldown experiment using CaM sepharose beads. As shown in Appendix B Figure 2A-C, the full length N-terminus region was unable to interact with CaM in agreement with previous studies [134]. It is possible, however, that the Cav2.1 N-terminus may contain an autoinhibitory domain that prevents that association of CaM with a putative CaM interaction domain near residue C71.

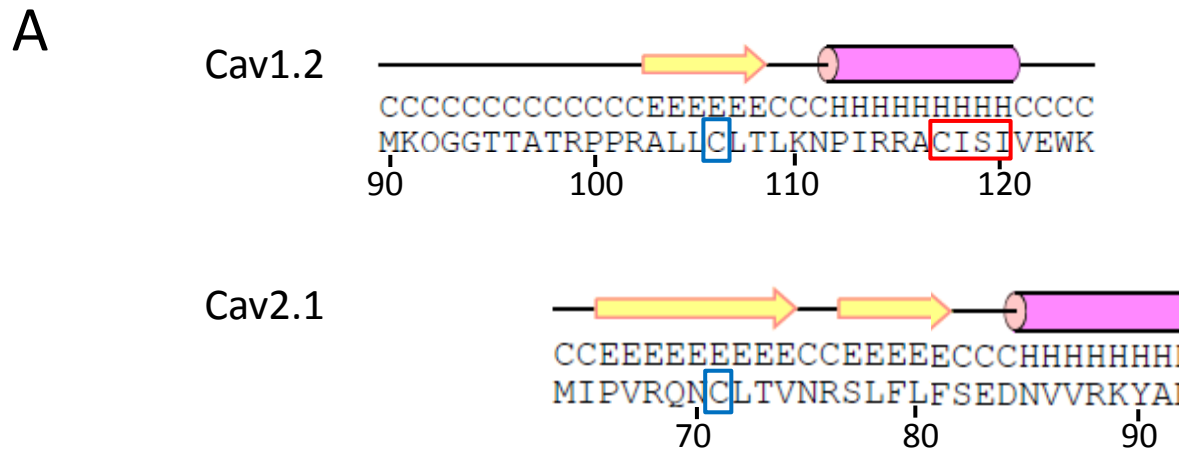

Appendix B-Figure 1

Appendix B-Figure 1: Conservation of a proximal cysteine residue in Cav1.2 and Cav2.1 N_{2B} regions, and alignment of Cav2 sequences A) Predicted secondary structure (PSIPRED http://bioinf.cs.ucl.aIt c.uk/psipred/) of the Cav1.2 proximal N-terminus. The blue box highlights the residue C106 shown previously by our group [135] to regulate N-lobe CDI of Cav1.2 channels. The red box highlights residues (C117, I118, S119 and I120) shown previously by our group [294] to bind α-CaMKII. Below Cav1.2 is the predicted secondary structure of Cav2.1 proximal N-terminus for which the blue box highlights C71, which is homologous to Cav1.2 C106. B) A sequence alignment of the short (brain) and long isoforms of Cav2.3, as well as Cav2.1 and Cav2.2. Blue residues signify sequence conservation, green residues conserved charge or hydrophobicity and black residues a lack of homology. Underlined residues in the Cav2.2 sequence (45-55 a.a.) have been shown to bind Gβγ [257] while the brain isoform of Cav2.3[33] starts at residue 61 (bolded) of the Cav2.1 sequence. Sequence alignment was constructed using CLUSTALW and numbering corresponds to the Cav2.1 sequence.

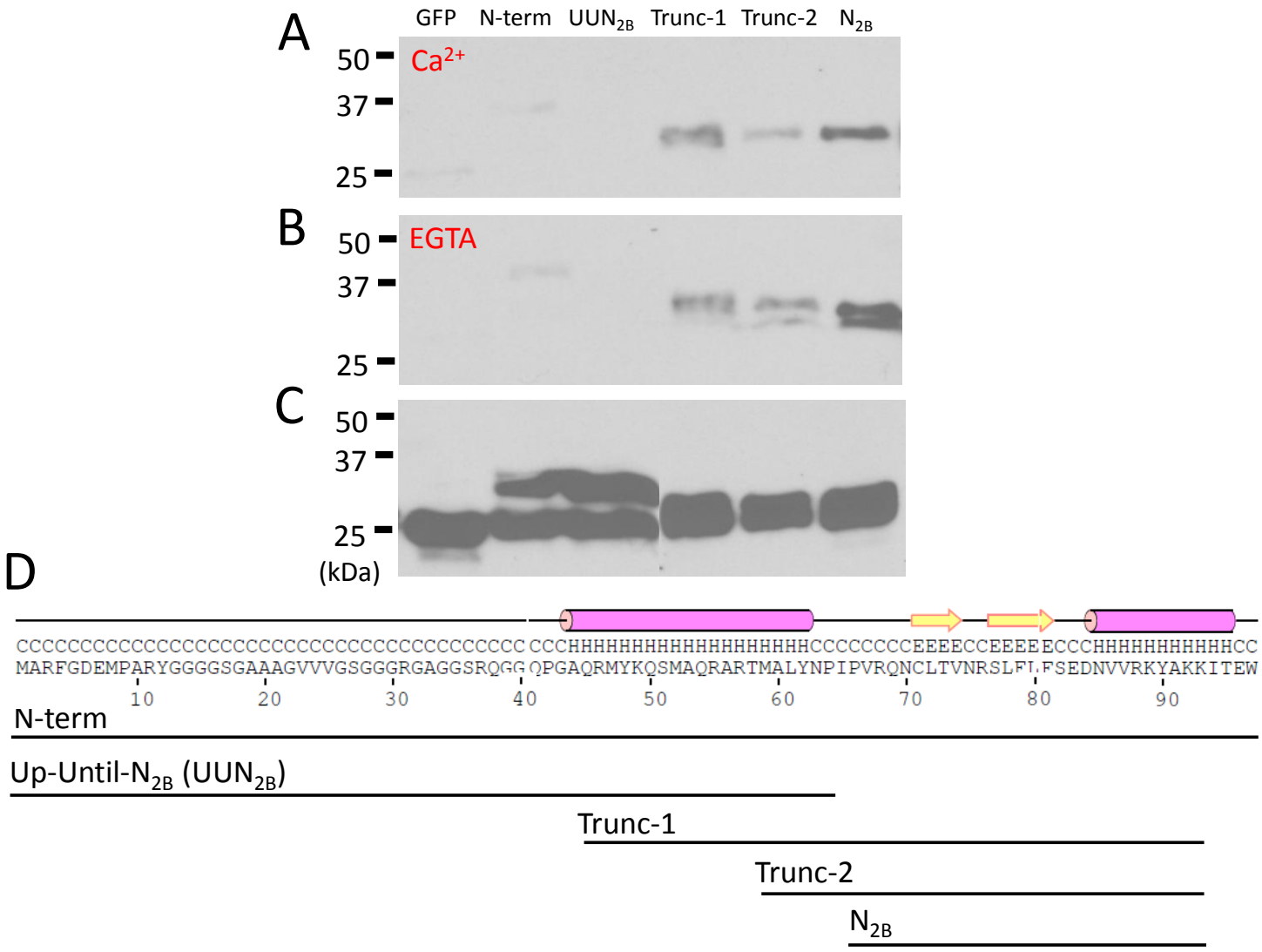

Appendix B-Figure 2

Appendix B-Figure 2: Truncating the first 42 residues permits binding of the Cav2.1 N-terminus to CaM sepharose in the absence of calcium. A) CaM sepharose pulldowns of GFP fusion proteins (0.5mM calcium washes) of the Cav2.1 N-terminus including Nterm, UUN_{2B}, Trunc-1, Trunc-2 and N_{2B}. B) Paired CaM sepharose pulldowns washed with 5mM EGTA, and corresponding lysates (C). This experiment is one of two repetitions. D) Predicted secondary structure (PSIPRED http://bioinf.cs.ucl.aIt c.uk/psipred/) of the Cav2.1 N-terminus and map of Cav1.2 N-terminal GFP fusion proteins used.

We thus created a series of truncation mutants that lacked various portions of the N-terminus region and tested their ability to interact with CaM beads. The truncation points were selected based on the functions of homologous regions in Cav2.2 and Cav2.3 calcium channels. The first truncation mutant (Trunc-1) includes an α-helical region that corresponds to a known Gβγ interaction site in Cav2.2 channels (Appendix B Figure 1B, 2D**)**. [257, 296, 297] The second truncation (Trunc-2) construct was designed to align with a short N-terminal isoform of Cav2.3 that exists in rat brain [33] (Appendix B Figure 1B, 2D). The N_{2B} fusion protein corresponds to an analogous region in Cav1.2 channels that was shown to interact with CaM in our recent work [135]. Finally, UUN_{2B} includes the N-terminus sequence up to the beginning of the N_{2B} construct (Appendix B Figure. 2D).

When we examined these GFP fusion proteins for pulldown on CaM sepharose we found that N_{2B}, Trunc-1 and Trunc-2 bound readily to CaM sepharose in both calcium and in the absence of calcium (i.e. 5mM EGTA washes), while UUN_{2B} did not bind at all (Appendix B Figure 2A-C). This calcium insensitivity of binding observed for N_{2B} and the two Trunc constructs is similar to our observation with the N_{2B} region of Cav1.2 which also bound readily to CaM sepharose in the absence of calcium, but which we later discovered to be mediated indirectly via CaMKII association [135, 294]. Hence, our results with Cav2.1 N_{2B} indicate the presence of a either a calcium insensitive CaM (i.e. apoCaM) binding site, or alternatively an α-CaMKII binding site. Successful pulldown of both Trunc-1 and Trunc-2 indicate that the portion of the Cav2.1 N-terminus which prevents association with CaM sepharose in the full length N-terminus is located upstream of the first α-helical region (Appendix B Figure 2D). Altogether, these data suggest that sequences in the distal N-terminus of Cav2.1 act as an autohibitory

domain for CaM binding sequences located more proximally. Examples of autoinhibitory domains which disrupt CaM interaction have been described in other VGCCs including Cav1.4, for which the distal C-terminus acts to disrupt interactions between CaM and upstream C-terminal sequences, which functionally ablates CDI [127, 128].

To refine the portion of the Cav2.1 N-terminus that binds CaM sepharose we further divided the N_{2B} region into four sub-regions of differing structural composition **(**Appendix B Figure 3A**)**. Appendix B Figure 3B shows that $N_{2B\text{-}I}$, $N_{2B\text{-}II}$ and $N_{2B\text{-}III}$, but not $N_{2B\text{-}IV}$ are pulled down on CaM sepharose in the presence of calcium. With EGTA washes (Appendix B Figure 3C) binding of $N_{2B\text{-}I}$ was abolished which fits with the notion that C71 is a calcium sensitive CaM interaction site, at least when isolated from adjacent CaM binding regions. In contrast, CaM binding to the $N_{2B\text{-}II}$ region was maintained upon removel of calcium (Appendix B Figure 3), suggesting that very much like in Cav1.2 channels, the $N_{2B\text{-}II}$ region contains the necessary elements for calcium-independent CaM interactions [135]. Altogether, these data indicate that $N_{2B\text{-}I}$ contains a calcium sensitive CaM interaction site, while the downstream $N_{2B\text{-}II}$ region contains an additional locus that permits CaM sepharose interactions even in the absence of calcium (and perhaps indirectly via CamKII interactions like in Cav1.2 channels).

We next used site directed mutagenesis to pinpoint the exact residues which participate in this interaction. We focused on $N_{2B\text{-}III}$ as it contains the necessary elements for calcium sensitive and insensitive binding. Appendix B Figure 4A-C shows that in order to remove all pulldown by CaM sepharose five residues must be mutated in $N_{2B\text{-}III}$ (C71, T73, S77, F79 and S82) such that the mutant construct $N_{2B\text{-}III\text{-}RARAR}$ can non longer bind to CaM sepharose.

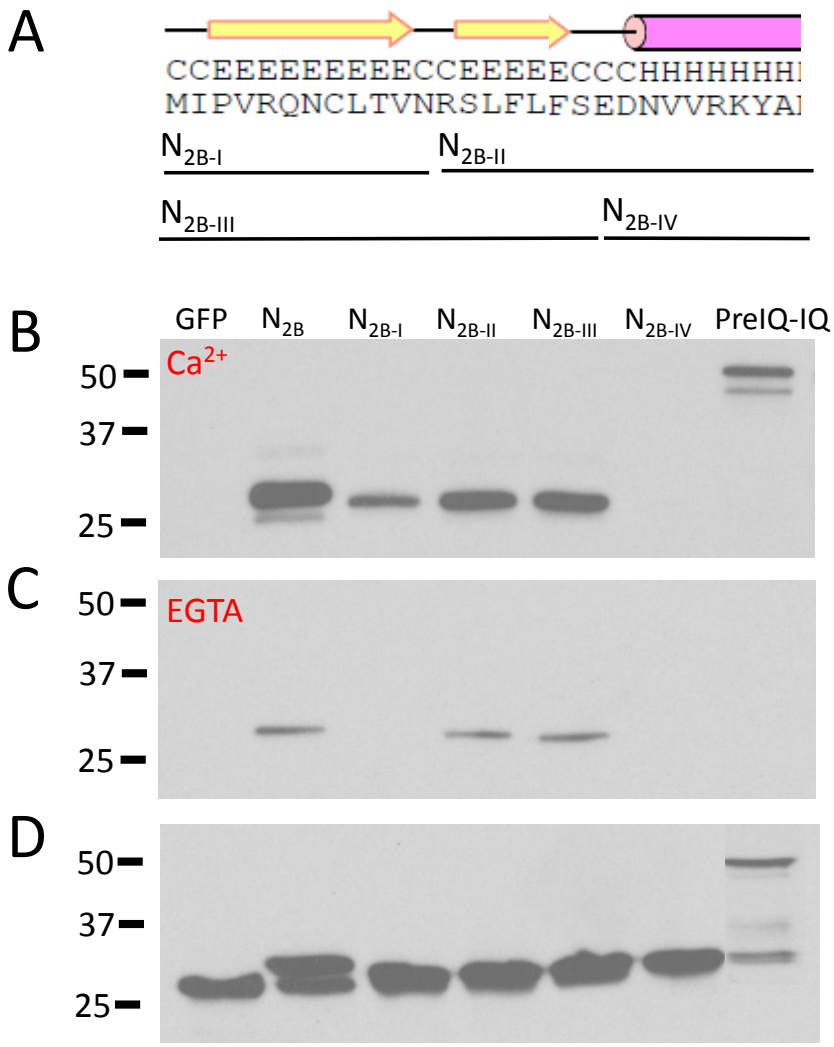

Appendix B-Figure 3

Appendix B-Figure 3: The $N_{2B\text{-}I}$, $N_{2B\text{-}II}$ and $N_{2B\text{-}III}$ portions of the Cav2.1 N-terminus pulldown on CaM sepharose. A) Predicted secondary structure (PSIPRED http://bioinf.cs.ucl.aIt c.uk/psipred/) of the Cav2.1 N_{2B} and map of N_{2B} sub-fragments. B) CaM sepharose pulldowns of GFP fusion proteins (0.5mM calcium washes) of the Cav2.1 N_{2B} region including N_{2B}, $N_{2B\text{-}I}$, $N_{2B\text{-}II}$, $N_{2B\text{-}III}$ and $N_{2B\text{-}IV}$. The PreIQ-IQ region of the Cav1.2 C-terminus is included as a control. C) Paired CaM sepharose pulldowns washed with 5mM EGTA, and corresponding lysates (D).

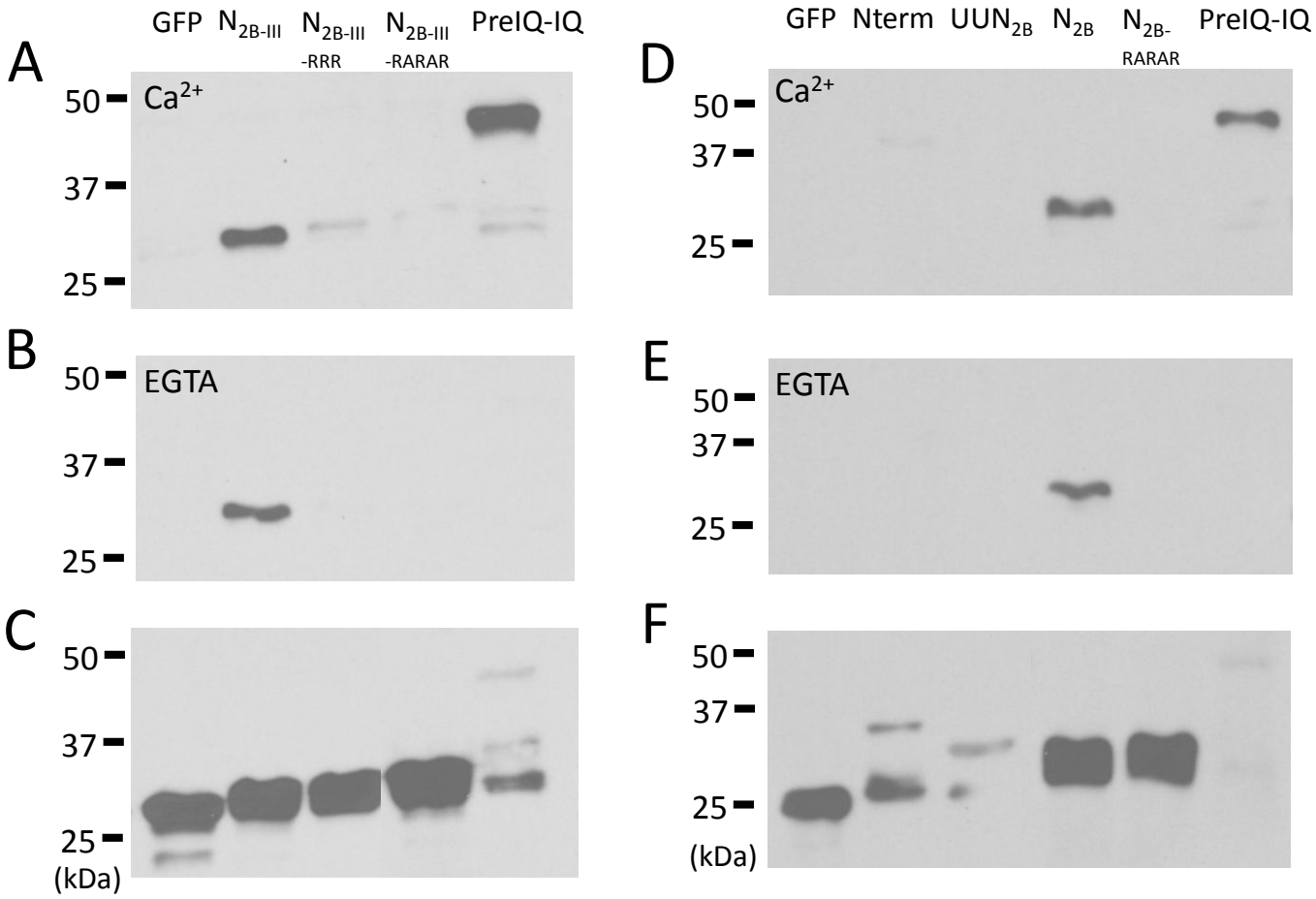

Appendix B-Figure 4

Appendix B-Figure 4: Five residues in the proximal N-terminus of Cav2.1 are required for binding to CaM sepharose A) CaM sepharose pulldowns of Cav2.1 N-terminal GFP fusion proteins (0.5mM calcium washes) of $N_{2B\text{-}III}$ and the mutants, $N_{2B\text{-}III\text{-}RRR}$ and $N_{2B\text{-}III\text{-}RARAR}$, as well as the control construct from Cav1.2, PreIQ-IQ-GFP. B) Paired CaM sepharose pulldowns washed with 5mM EGTA, and corresponding lysates (C). D) CaM sepharose pulldowns of GFP fusion proteins (0.5mM calcium washes) of the Cav2.1 N-terminus including Nterm, UU-N_{2B}, N_{2B}, $N_{2B\text{-}RARAR}$ and the control construct from Cav1.2 PreIQ-IQ. E) Paired CaM sepharose pulldowns washed with 5mM EGTA, and corresponding lysates (F).

Appendix B Figure 4D-F verifies that this same sequence of mutations eliminates binding for the entire N_{2B} region as well, suggesting that discruption of CaM interactions with the N_{2B} region are sufficient to abolish all N-terminus CaM interactions including the calcium insensitve interaction in the $N_{2B\text{-}II}$ region.

How do our data with Cav2.1 fit with the literature? It may be possible for the N-terminus of Cav2 channels to participate in N-lobe CDI despite the absence of a region that corresponds to the Cav1 specific, NSCaTE element [134]. Like with Cav1 channels, CaM is anchored to the Cav2.1 C-terminus (i.e. IQ and possibly CBD domain) at rest and upon calcium rise changes comformation to induce N-lobe CDI. Current literature suggests that this is an exclusively C-terminal process for Cav2.1 channels. However, if the β-fold structure (i.e. $N_{2B\text{-}I}$) which contains C71 were to function as a Ca^{2+}/CaM binding site in the holochannel, it is possible that this residue may serve as an interaction site for the N-lobe of CaM during CDI. If so, the cysteine residues present in Cav1.2 (C106), Cav1.3 (C136), Cav2.1 (C71) and other HVA VGCCs, could potentially function to regulate N-lobe CDI in a similar fashion, while the upstream tryptophan residues present in the N-terminus of Cav1 channels, (i.e.W52 for Cav1.2 and W82 for Cav1.3) combined with differential C-terminal sequences [133, 137, 237, 277], CaM stoichiometry (i.e. 2:1 for Cav1 channels) and orientation [84, 87, 123], may give NSCaTE its Cav1 specific function[134]. Hence, it is possible that N-lobe CDI of Cav2.1 may involve the N-terminus like it does in Cav1.2 channels, but this will need to be explored at the functional level.

Much like for CaM, the CaMKII/Cav2.1 literature describes C-terminal, but not N-terminal associations with the channel. Jiang and colleagues showed that ablating either the IQ or CBD domains of Cav2.1 is sufficient to prevent binding to CaMKII, the functional consequence of which is an accelaration in the rate of inactivation and a shift in the voltage dependence of inactivation [233]. This C-terminal association with CaMKII was later shown to modulate short term synaptic plasticity in superior cervical ganglion neurons illustrating its physiological relevance [291]. Here, we observe calcium insensitive pulldown of the Cav2.1 N_{2B} region (Appendix B Figure 2, 3B-D & 4D-F), which may be consistent with the exitence of a CaM kinase site in the amino terminus of Cav2.1. Hudmon and colleagues found that all intracellular domain linkers of Cav1.2 could bind α-CaMKII in the presence of Ca^{2+}/CaM, and it is thus conceivable that Cav2.1 channels may also contain CaMKII interaction sites in more than one intracellular region [139].

In summary, we show that CaM sepharose can bind proximal regions of the Cav2.1 N-terminus in both calcium sensitive and insensitive manners. Five residues (C71, T73, S77, F79 & S82) are important for these associations, all of which are conserved in Cav2.2, and four of which are conserved in Cav2.3 channels (see Appendix B Figure 1B). Truncation of the Cav2.1 N-terminus demonstrates that binding to CaM sepharose is regulated by distal N-terminus sequences. Overall our data suggest that conserved sequence in the proximal N-terminus of Cav2 channels interact with CaM, and either apoCaM, or CaMKII. The functions of these novel interaction sites remain to be determined, and whether autoinhibtion of CaM binding to the N-terminus can be dynamically regulated in intact channels needs to be explored.

Methods

cDNA Constructs

Wild type (WT) rat calcium channel subunit cDNAs encoding Cavβ2a and Cavα2δ1 subunits were donated by Dr. Terry Snutch (University of British Columbia, Vancouver, BC). The WT human calcium channel subunit cDNA encoding Cav2.1-HA was a gift from Dr. Philippe Lory (University of Montpellier, France). The origins of the clones used or GenBank™ accession numbers where available are as follows: Cavβ2a [214], Cavα2δ1 [AF286488], and Cav2.1-HA[298]. $Cav2.1_{-RARAR}$ channels were created by cloning their respective synthesized sequences (Genscript) into NheI/NotI. The Cav1.2 PreIQ-IQ GFP fusion protein has been previously described [135]. Cav2.1 N-terminal GFP fusion proteins were constructed by PCR, or annealing reaction (described previously [135]) followed by cloning into N1-GFP (Clontech) using BamHI/XhoI included (primers used):

Nterm

(ATACTCGAGATGGCCCGCTTCGG/TATAGGATCCCCGGCGTATTTTCTCACCACG),

Up-Until-N_{2B} or UUN_{2B}

(ATATCTCGAGATGGCCCGCTTCGG/TATAGGATCCCCGGGGTTGTAGAGTGC),

N_{2B}

(ATATCTCGAGATGATCCCCGTCC/ TATAGGATCCCCGGCGTATTTTCTCACC),

$N_{2B-RARAR}$

(TCGAGATGATCCCCGTCCGACAGAACCGCCTCGCGGTTAACCGGCGTCTCGCCCTC

TTCAGGGAAGACAACGTGGTGAGAAAATACGCCGGG/GATCCCCGGCGTATTTTCTC

ACCACGTTGTCTTCCCTGAAGAGGGCGAGACGCCGGTTAACCGCGAGGCGGTTCTGT
CGGACGGGGATCATC),

$N_{2B\text{-}I}$

(TCGAGATGATCCCCGTCCGACAGAACTGCCTCACGGTTAACGGG/GATCCCCGTTAA
CCGTGAGGCAGTTCTGTCGGACGGGGATCATC)

$N_{2B\text{-}II}$

(TCGAGATGCGGTCTCTCTTCCTCTTCAGCGAAGACAACGTGGTGAGAAAATACGCC
GGG/GATCCCCGGCGTATTTTCTCACCACGTTGTCTTCGCTGAAGAGGAAGAGAGAC
CGCATC)

$N_{2B\text{-}III}$

(TCGAGATGATCCCCGTCCGACAGAACTGCCTCACGGTTAACCGGTCTCTCTTCCTCT
TCAGCGGG/GATCCCCGCTGAAGAGGAAGAGAGACCGGTTAACCGTGAGGCAGTTCT
GTCGGACGGGGATCATC),

$N_{2B\text{-}III\text{-}RRR}$

(TCGAGATGATCCCCGTCCGACAGAACCGCCTCACGGTTAACCGGCGTCTCTTCCTCT
TCAGGGGG/GATCCCCCCTGAAGAGGAAGAGACGCCGGTTAACCGTGAGGCGGTTCT
GTCGGACGGGGATCATC),

$N_{2B\text{-}III\text{-}RARAR}$

(TCGAGATGATCCCCGTCCGACAGAACCGCCTCGCGGTTAACCGGCGTCTCGCCCTC
TTCAGGGGG/GATCCCCCCTGAAGAGGGCGAGACGCCGGTTAACCGCGAGGCGGTTC
TGTCGGACGGGGATCATC).

$N_{2B\text{-}IV}$

(TCGAGATGGAAGACAACGTGGTGAGAAAATACGCCGGG/GATCCCCGGCGTATTTT CTCACCACGTTGTCTTCCATC)

All cDNAs were sequenced after cloning to verify fidelity.

Tissue culture and transient transfection of tsA-201 cells

Human embryonic kidney tsA-201 cells were cultured and transiently transfected using the calcium phosphate method as described previously [215]. For CaM pulldown experiments 3ug of each GFP fusion protein construct was transfected in 100mm plates. Cells were grown at 37°C for 48h after transfection to 75-85% confluence.

CaM sepharose pulldown and western blotting

Cultured tsA-201 cells were transiently transfected as described above and were lysed with a modified RIPA buffer (in mM; 50 Tris, 130 NaCl, 0.2% triton X-100, 0.2% NP-40, 0.5 Ca^{2+}, pH 7.4). For conditions without calcium, 5mM EGTA was substituted. Detailed methods for cell preparation, CaM sepharose pulldowns and immunoblots have been described previously [135]. Western blot analysis was performed using 1/1000 anti-GFP (Santa-Cruz-8334) followed by 1/5000 GE Healthcare horseradish peroxidase-linked secondary antibody (rabbit).